LA-11534-T
Thesis

UC-413
Issued: April 1989.

LA--11534-T

DE89 009586

Evaluation and Application of Delayed Neutron Precursor Data

*Michaele Clarice Brady**

**Collaborator/Graduate Research Assistant at Los Alamos.*
Oak Ridge National Laboratory, Oak Ridge, TN 37831.

Los Alamos National Laboratory
Los Alamos,New Mexico 87545

ACKNOWLEDGEMENTS

The author wishes to take this opportunity to acknowledge the many people and organizations who helped to make this work possible. The research presented here was funded in part by Associated Western Universities under a Department of Energy (DOE) contract and also by the DOE Office of Basic Energy Sciences. These organizations are gratefully acknowledged and their assistance in this endeavor is highly appreciated.

A special thanks to Dr. T. R. England from whom I have received many benefits based on his expertise, experience, and good nature. I am indebted to him for his guidance and inspiration in performing the work presented here. I would also like to express my appreciation to Dr. T. A. Parish for his encouragement throughout the course of this work and particularly his assistance in the preparation of this manuscript.

Prof. K. -L. Kratz of the University of Mainz; Prof. Gösta Rudstam of the Swedish Research Council's Laboratory at Studsvik; P. Reeder and R. Warner of Pacific Northwest Laboratory; and Prof. G. Couchell of the University of Lowell are gratefully acknowledged for providing their experimental delayed neutron spectral data. A special note of appreciation is expressed to Drs. F. M. Mann and R. E. Schenter of Hanford Engineering Development Laboratory for providing their evaluation of delayed neutron emission probabilities as well as several fruitful discussions.

Finally, to the staff of the Applied Nuclear Science Group (T-2) at Los Alamos National Laboratory, I extend my sincere appreciation for their support and encouragement over the three years this work progressed.

TABLE OF CONTENTS

TABLE OF CONTENTS (Continued)

LIST OF TABLES

LIST OF FIGURES

LIST OF FIGURES (Continued)

LIST OF FIGURES (Continued)

LIST OF FIGURES (Continued)

ABSTRACT

Evaluation and Application of Delayed Neutron

Precursor Data. (December 1988)

Michaele Clarice Brady, B.S., M.S.,

Texas A&M University

Co-Chair of Advisory Committee: Dr. Talmadge R. England
Dr. Theodore A. Parish

Up to 1300 nuclides are yielded in fission. Of these, 271 have been identified as precursors for delayed neutron emission. An extensive reference library of delayed neutron data has been compiled which contains fission yields and branchings, delayed neutron emission probabilities and spectra for each of these 271 precursor nuclides. The emphasis of the present work has been in improving the spectral data. Experimental spectra from laboratories in the United States, Germany, and Sweden have been incorporated in this evaluation. The experimental spectra have been augmented with model calculations such that the spectra included in the final library extend over the full theoretical energy range for delayed neutron emission. Models were also used to predict spectra for nuclides with no measured data.

The data compiled in the precursor library have been used to calculate the aggregate behavior of delayed neutrons for the 43 fissioning systems having evaluated fission yields. Delayed neutron activities predicted using the explicit precursor data have also been approximated by three, six, nine and twelve time-groups using least squares techniques. The fitted six group data, being the more conventional representation, were also used to predict a consistent set of six-group spectra. Comparisons with the University of Lowell's recently published measurements of ^{235}U delay interval spectra were also made. Beta-effective calculations for a simple Godiva system were performed and were compared to the experimental value.

The point reactor kinetics equations were modified to accommodate the data in the precursor library. Both the explicit data and the group data were used to calculate the kinetic response of a reactor to step changes in reactivity.

The precursor data and the six-group data are intended for inclusion in the next version of the Evaluated Nuclear Data Files, ENDF/B-VI.

CHAPTER I.

INTRODUCTION

The first evidence for the emission of neutrons with an appreciable time delay after fission was reported in 1939, less than a month after the discovery of nuclear fission.[1] These "delayed neutrons", although small in number (~1% of the total neutrons emitted from fission) were quickly recognized for their importance in controlling the rate of fission in a chain-reacting assembly.[1,2]

Delayed neutrons originate from the decay of nuclei formed following the beta decay of certain fission products known as delayed neutron precursors.[3] Early methods of isotope separation did not facilitate the study of the precursor nuclides individually (many with half-lives on the order of tenths of a second); it was soon found to be convenient to study them in "groups" characterized by their half-lives. By the mid-1950s researchers determined that delayed neutron decay data (activity following an irradiation) could be satisfactorily represented using six delayed neutron groups.[4]

The delayed neutron data set that is widely used today is a part of the Evaluated Nuclear Data Files (ENDF/B) which are maintained by the National Nuclear Data Center (NNDC) at Brookhaven National Laboratory. The current version, ENDF/B-V, contains delayed neutron yields, half-lives, and energy spectra in the six-group formalism.[5] Recent advancements in on-line isotope separation techniques and improved sensitivity in neutron detection methods have made it possible to obtain detailed information for the individual delayed neutron precursors.[6]

Calculating the production of delayed neutrons from fission using individual precursor data has several advantages. The primary advantage is that a single set of precursor data (emission probabilities and spectra) may be used to predict delayed neutron production for any fissioning system provided fission yields are available. Current methods based on temporal group representations require

---

The style and format of this dissertation are patterned after those used in *Nuclear Technology*.

separate data sets for each fissioning system. The use of individual precursor data to calculate time-dependent delayed neutron spectra is straightforward. Also, the precursor data are readily applicable to the calculation of delayed neutron production for both pulse and equilibrium irradiations. The work presented here includes a compilation and evaluation of precursor data, particularly the energy spectra, as of mid-1986. The objectives of this work as paraphrased from the original research proposal include:

1. the review and comparison of spectral data for individual precursor nuclides,

2. to select or produce a calculational model that will provide delayed neutron spectra for nuclides with no measured data as well as augment existing measurements that lack data at lower energies and/or very high energies.

3. utilizing a non-linear least-squares fitting procedure, study the temporal grouping of delayed neutrons and thus determine group yields and decay constants, and attempt to calculate group spectra consistent with the fitted-group yields and half-lives, as well as the individual precursor data.

In this evaluation, experimental data have been augmented from theory and systematics to create a comprehensive data base for 271 precursor nuclides. Spectral data compiled in this evaluation include major data sets from experimentalists in the United States, Sweden, and Germany. Two different calculational models were used in this evaluation. The BETA code model[7] developed at Hanford Engineering Development Laboratory (HEDL) was used to augment the existing experimental data. However, its requirements for detailed nuclear level information for each precursor, its daughter and granddaughter, made it impractical for predicting delayed neutron spectra for the nuclides with no measured data. A simpler single-parameter model was developed for this purpose.

The compilation of precursor data, while strongly emphasizing spectral data, must also include delayed neutron emission probabilities (P_n values) and fission

yields. Values based on measurements for 89 precursors are taken from the 1986 evaluation by F. M. Mann.[8] Model P_n-values for an additional 182 nuclides were calculated based on a semi-empirical relationship and using fitting parameters recommended by Mann. The fission product yields used in this evaluation were taken from a preliminary version of ENDF/B-VI and were extended to include additional nuclides.

The precursor data have been used to calculate aggregate quantities such as the delayed neutron yield from fission (ν_d), total spectra and average energies, and have also been analyzed in terms of the more common few-group representation. A non-linear least-squares code was used to study the temporal grouping of delayed neutrons into three, six, nine, and twelve groups. Final fits were made using the traditional six-group representation. A method of deriving consistent six-group spectra is also developed.

Further steps were taken to apply the newly derived six-group data in both β-effective and point reactor kinetics calculations. The six-group spectra for fast fission in ^{235}U were used to calculate delay interval spectra for comparison with recent measurements at the University of Lowell.[9]

The history and status of delayed neutron data prior to this work are discussed based on a review of the literature represented in the general bibliography given as Appendix A.

CHAPTER II.

BACKGROUND AND LITERATURE REVIEW

In the process called nuclear fission a heavy nucleus is split into two fragments accompanied by the release of considerable energy and the emission of neutrons, gamma rays, beta rays, and neutrinos. These particles may be emitted at the instant of fission or later as the fission fragments undergo radioactive decay. As illustrated in Fig. 1, neutrons that are released at the instant of fission (within $\sim 10^{-14}$ sec) are called prompt neutrons and account for approximately 99% of the total number of neutrons emitted from fission. Certain of the fission products will be neutron rich and therefore beta unstable. The decay of these fission products by beta emission will produce daughter nuclei which have the potential to de-excite by emitting a neutron. These neutrons will appear with a half-life equal to that of the beta decay of its parent (precursor) nuclide; as this is comparatively long after the fission event these neutrons are referred to as "delayed neutrons" and comprise the other $\sim 1\%$ of neutrons released in fission.

HISTORICAL TREATMENT OF DELAYED NEUTRONS FROM FISSION

Two hypotheses were initially put forth to explain the presence of these "delayed" neutrons that were observed following the fission event. The first was that they were photoneutrons produced as a result of gamma activity of fission products and the second, suggested by Enrico Fermi, was that they were produced directly from fission products that had undergone one or more beta transitions.[2] The photoneutron hypothesis was easily dismissed as a result of subsequent yield measurements. The second received support when Bohr and Wheeler[10] advanced the liquid-drop model showing cases where the energy released on beta decay could exceed the binding energy of the last neutron in the residual nucleus, thus leading to the emission of a delayed neutron.

Early investigations of aggregate delayed neutron production rates reported a single half life of 12.5 seconds.[11] Further experiments found additional delayed

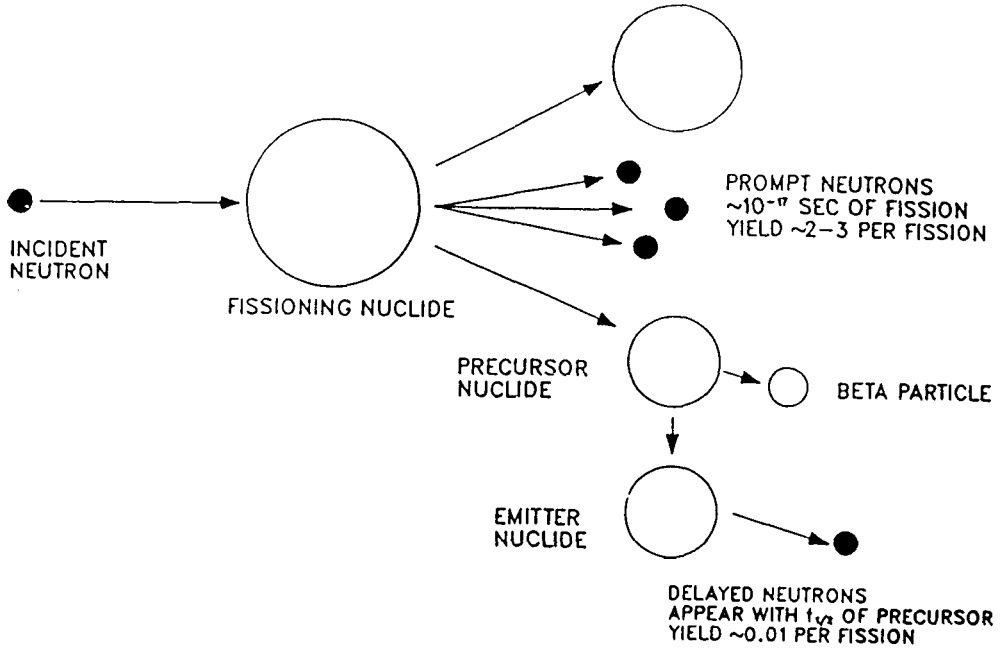

Fig. 1. Delayed neutrons from fission.

neutron periods, first two, then five and, by 1948, six delayed periods and abundances had been reported.[4] Reference 2 is an excellent review of delayed neutron measurements and data prior to 1956.

A comprehensive study of delayed neutrons from fast and thermal fission was carried out at Los Alamos during the years 1954–1957.[3,4,12] The major result of this study was to define the "six-group" representation of delayed neutrons from fission now in nearly universal use. It is because of the overwhelming influence of this study that it is reviewed here.

The Los Alamos measurements involved delayed neutrons from fast fission of six nuclides; ^{232}Th, ^{233}U, ^{235}U, ^{238}U, ^{239}Pu, and ^{240}Pu, and the thermal fission of ^{233}U, ^{235}U, and ^{239}Pu. In all cases the bare, spherical, ^{235}U metal assembly, Godiva, was used as the neutron source. The Godiva central spectrum (a slightly degraded fission neutron spectrum) was used for the "fast" irradiations. In

order to achieve a "thermal" spectrum, an eight-inch cubic polyethylene block was cadmium shielded and mounted near Godiva and the fission samples passed through it via a pneumatic transfer system. Infinite (i.e., long compared to the longest delayed neutron period) irradiations were used to emphasize the longer lived delayed neutron groups and instantaneous (short compared to the shortest delayed neutron period) irradiations were performed to accentuate the contribution of the short lived delayed neutron groups. Both the instantaneous and infinite irradiations consisted of 10^{16} total fissions; produced via super-prompt-critical bursts of 0.25 milliseconds for the instantaneous irradiations, and by delayed critical operation for the infinite irradiations.

The analysis of the delayed neutron activity curves, such as those shown in Fig. 2, was performed based on the assumption that delayed neutron activity as a function of time can be represented by a linear superposition of exponential decay periods. This assumption may be represented as:

$$n_d(t) = \sum_{i=1}^{k} A_i \, e^{-\lambda_i t} \tag{1}$$

where $n_d(t)$ is the delayed neutron activity as a function of time, k is the number of periods or "groups" to be determined, A_i and λ_i are parameters to be determined from a least squares fit. The initial delayed neutron activity is proportional to $a_i\lambda_i$ following an instantaneous irradiation, and proportional to a_i for an infinite irradiation; where a_i and λ_i are the abundance and decay constant, respectively, for the i^{th} delayed neutron group. Therefore, in fitting the instantaneous (pulse) irradiation data, $A_i = a_i\lambda_i$; and in the case of the infinite irradiation data, A_i, is simply taken as a_i.

Two approaches to the analysis of the data were taken; (1) simultaneous solution of all periods and abundances from the pulse irradiation data, and (2) determination of four long-period groups from the infinite irradiation data and four short-period groups from the prompt data, later renormalizing the two sets of yields at the second delayed neutron group. The second method was found to give values of a_i and λ_i with the smallest calculated errors. The final values

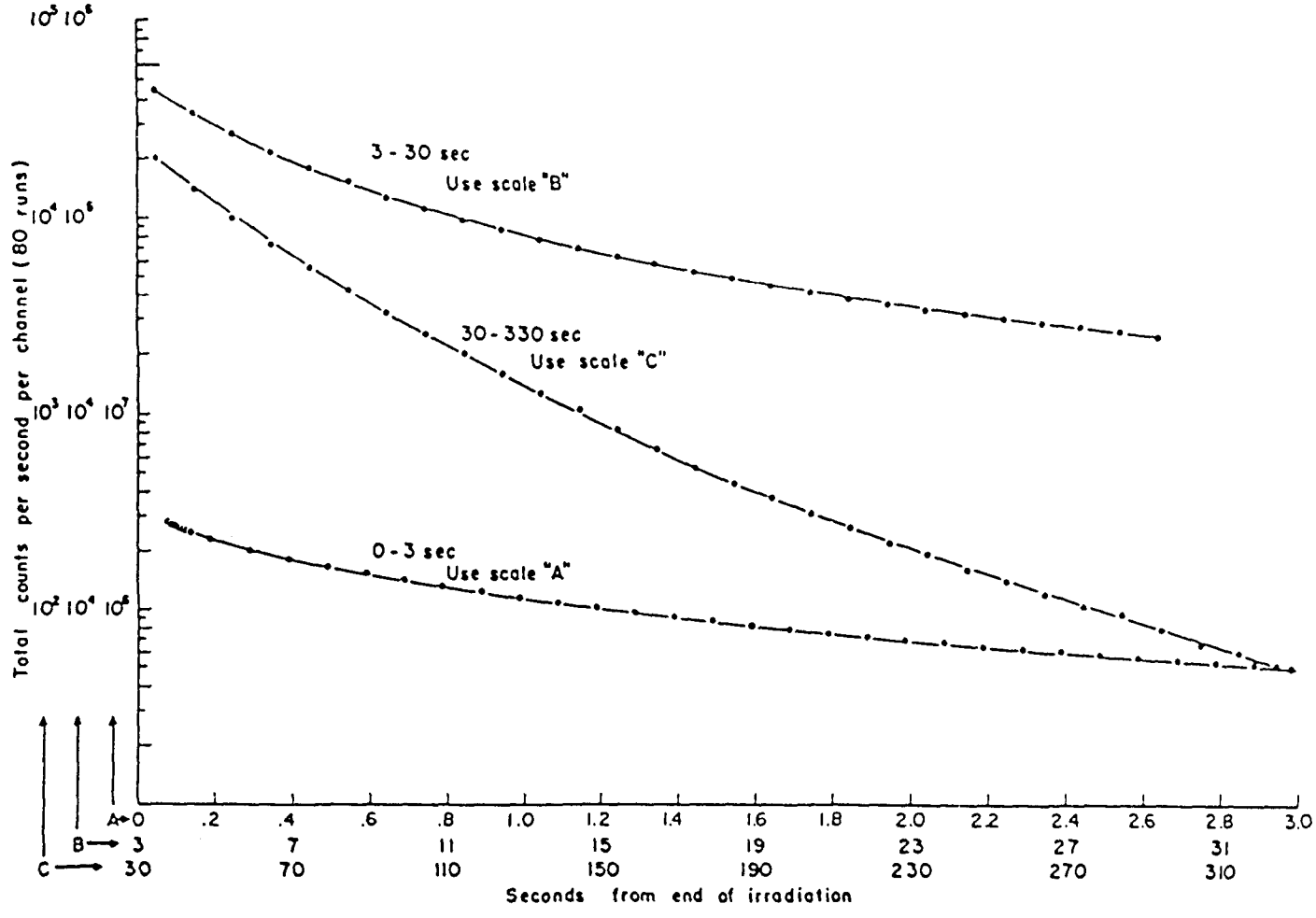

Fig. 2. Delayed-neutron decay following instantaneous irradiations of ^{235}U (fast fission). Ref. 3.

for λ_1, λ_2 and the ratio of a_1/a_2 were taken from the infinite irradiation data and all other values were taken from the pulse irradiation data.

The instantaneous irradiation data also provided an independent method of determining absolute total delayed neutron yields from the nine fissioning systems via standard counting of the 67-hour beta activity from ^{99}Mo.

It is important to note that the number of periods, k, was not preselected as six, rather that six periods led to rapid convergence and were found to give the best least squares fit to the data. This being the case, the Los Alamos researchers concluded that six main precursors (or precursor combinations) predominate delayed neutron activity following fission; however it was clearly recognized that more than six precursors existed. The six-group representation has become so commonly used today that the groups are often thought of as "precursors" themselves. Details and numerical results of the Los Alamos experiments and data analysis can be found in Refs. 3 and 4.

Shortly after the Los Alamos measurements, a group of researchers at Argonne National Laboratory measured abundances and half-lives from groups one through five for thermal fission in ^{241}Pu and for the three longer lived delayed neutron groups for the spontaneous fission of ^{252}Cf.[3] This brought the number of different fissioning systems with measurements of six-group data to 11. (^{252}Cf(S) was not included in ENDF/B-V.)

The six-group representation of delayed neutrons can be illustrated schematically as in Fig. 3. There is a fundamental characteristic inherent in the six-group notation that is evident in this figure. Any nuclide placed into one of these "groups" must decay by delayed neutron emission, no alternative decay paths are permitted. This also means that there is no coupling among any of the six groups; i.e., the activity in any one group does not affect that in another. As discussed earlier, the decay constants, λ_i, and abundances, a_i, describing the production and decay of the six groups are simply derived from a fit to the mathematical relationship given as Eq. (1). Although there is no true physical basis for the six groups, they are often regarded as fictitious nuclides whose

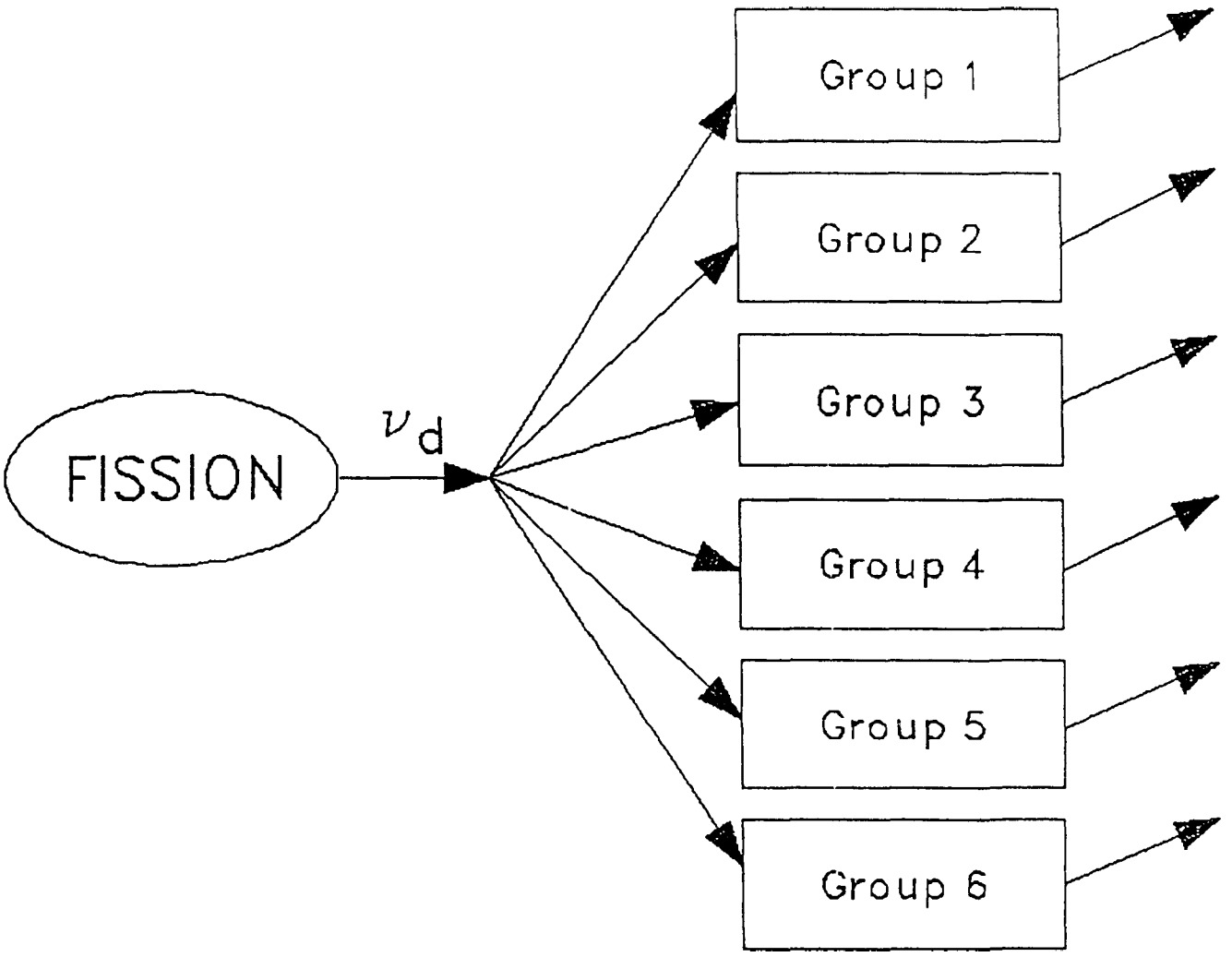

Fig. 3. Six-group precursor representation.

probability of delayed neutron emission is unity, and whose production rates are proportional to the group abundance.[13]

Much effort has been expended in the measurement of total delayed neutron yields. For a review of these measurements see Refs. 14–16, and more recently Refs. 17–20. The majority of these measurements have been made for one or more of three incident neutron energies (or groups of incident neutron energy). These include fission induced by thermal neutrons, fission induced by fission spectrum neutrons (0.5–2.0 MeV) and fission induced by high-energy (14 MeV) neutrons.

Early investigations into the energy of delayed neutrons were quite sparse. Roberts and co-workers[1] in 1939 estimated the mean energy of delayed neutrons from ^{235}U to be 0.5 MeV. That value was based on observations of recoil nuclei in a cloud chamber. Several years later workers at Argonne[21] (1948) and Oak Ridge[22] (1946) measured the mean energies of the individual groups. Bonner and co-workers at Los Alamos[23] (1956) performed cloud chamber experiments to measure the group four spectrum. The most accurate and comprehensive of these early spectral measurements were those reported by Batchelor and McK. Hyder[24] (1956) using a ^{3}He spectrometer to measure energies of delayed neutrons from a slug of natural uranium. The irradiation and counting times were varied to accentuate the different group spectra, and although the energy resolution and counting statistics were considered relatively poor, these spectra comprised the principal delayed neutron spectral data until the early 1970s.

In 1972, G. Fieg[25] reported measurements of delayed neutron spectra from thermal and 14 MeV fission in ^{235}U, and 14 MeV fission of ^{238}U and ^{239}Pu. These experiments used proton-recoil proportional counters and were carried out at different time intervals after fission in order to accentuate the first four delayed neutron groups. Group five was measured only for the 14 MeV fission of ^{238}U. Fieg demonstrated that his results were in agreement, within error limits, with those of Batchelor and McK. Hyder. The aggregate results from thermal and 14 MeV fission in ^{235}U were also compared and led Fieg to conclude (from the similar shapes) that the same precursors were responsible for the different neutron groups.[25]

Shalev and Cuttler[26] (1973) using the Israel Research Reactor-1 and a ^{3}He proportional counter measured the group two and group four spectra for ^{232}Th, ^{233}U, ^{235}U, ^{238}U, and ^{239}Pu. The ^{3}He counter used by Shalev and Cuttler had much better resolution than the proton-recoil detector of Fieg, however the Fieg measurements extended to much lower energies (~80 keV) than did the ^{3}He measurements (~150 keV).

At the time of the ENDF/B-IV evaluation performed by S. Cox[14] (1974), Fieg's data was taken to be the most complete set of spectra data. It was recommended that Fieg's data be used in ENDF/B-IV for groups 1, 3, 4 and 5. In the cases where group five and/or six measured data did not exist, it was assumed that the group four data could be used without introducing any appreciable error.[14] The group two data recommended for ENDF/B-IV was that of Shalev and Cuttler. Cox also concluded, based on Fieg's observations for the thermal and 14 MeV spectra of ^{235}U, that it was reasonable to apply the 14 MeV spectra to lower energy regions as well.

In Kaiser and Carpenter's evaluation of delayed neutron data for ENDF/B-V (1975),[27] it was noted that the status of delayed neutron spectral data had remained virtually unchanged since Cox's ENDF/B-IV evaluation. The only recommended change for ENDF/B-V was that Fieg's data also be used for group two for internal consistency and because his data extended down to ~80 keV and should therefore be more representative of the low energy end of the spectra.

ENDF/B-V CONTENT

The most widely used, comprehensive set of delayed neutron data is that contained within the massive ENDF/B-V nuclear data files. Table I summarizes the ENDF/B-V evaluation for delayed neutrons.[28] Six-group decay constants and relative abundances are also contained in the data files for the seven nuclides listed in Table I. These group constants and their respective group spectra are presented independent of the incident neutron energy (i.e., thermal fission, fast fission or 14 MeV fission). However, the average delayed neutron yield per fission (ν_d), as shown in Table I, is given as a function of the fission energy. Typically, ν_d is constant to about 4 MeV, then decreases linearly until ~7 MeV where is

TABLE I

Summary of ENDF/B-V Evaluation for Delayed Neutrons

Fissionable Nuclide	$\bar{\nu}_d$ per 100 Fissions	Energy Range (MeV)		Spectra
^{232}Th	5.27	Constant	0 to 4	Same as ^{235}U
	5.27 to 3.00	Linear	4 to 7	
	3.00	Constant	7 to 20	
^{233}U	0.740	Constant	0 to 4.5	Same as ^{235}U
	0.740 to 0.470	Linear	4.5 to 6	
	0.470	Constant	6 to 14	
	0.470 to 0.420	Linear	14 to 15	
	0.420	Constant	15 to 20	
^{235}U	1.67	Constant	0 to 4	Group 4 spectra used
	1.67 to 0.900	Linear	4 to 7	for groups 5 and 6
	0.900	Constant	7 to 20	
^{238}U	4.40	Constant	0 to 4	Group 5 spectra used
	4.40 to 2.60	Linear	4 to 9	for group 6
	2.60	Constant	9 to 20	
^{239}Pu	0.645	Constant	0 to 4	Group 4 spectra used
	0.645 to 0.430	Linear	4 to 7	for groups 5 and 6
	0.430	Constant	7 to 20	
^{240}Pu	0.900	Constant	0 to 4	Same as ^{239}Pu
	0.900 to 0.615	Linear	4 to 7	
	0.615	Constant	7 to 20	
^{241}Pu	1.62	Constant	0 to 4	Same as ^{239}Pu
	1.62 to 0.840	Linear	4 to 7	
	0.840	Constant	7 to 20	

again constant to 20 MeV. Six-group spectra are given in ENDF/B-V for all seven nuclides listed in Table I, however, only the spectra for ^{235}U, ^{238}U and ^{239}Pu are unique evaluations based on measurements. As noted in Table I, the spectra given for ^{232}Th and ^{233}U are simply the ^{235}U spectra, and those for ^{240}Pu and ^{241}Pu are the same as the ^{239}Pu spectra. Even for the three nuclides with uniquely measured spectra, none have measured group six spectra and only ^{238}U has a measured group five spectrum. The group four spectra (or in the case of ^{238}U, the group five spectrum) are substituted for the missing group spectra.

It is evident from Table I that the greatest deficiency in the ENDF/B-V delayed neutron data is in the spectra. Figure 4 further illustrates the need for more accurate spectral data as it depicts an additional shortcoming of the ENDF/B-V delayed neutron spectra, namely their limited energy range. The evaluated data presented in ENDF/B-V extend from ~76 keV to approximately 1.2 MeV. There is experimental evidence of the emission of delayed neutrons in excess of 3 and 4 Mev.[6,29] Also, a straight line extrapolation from 76 keV to zero at zero energy was used in ENDF/B-V to estimate the spectra at the lower energies. This is contradicted by recent experimental data exhibiting detailed structure at energies below 76 keV.[30–33] These facts provide much of the motivation for the emphasis given in this dissertation to improve the representation of delayed neutron spectral data.

The theory of delayed neutron emission and the data required to describe delayed neutron activity from individual precursor nuclides are discussed in sufficient detail to introduce and define terms specific to the topic of concern.

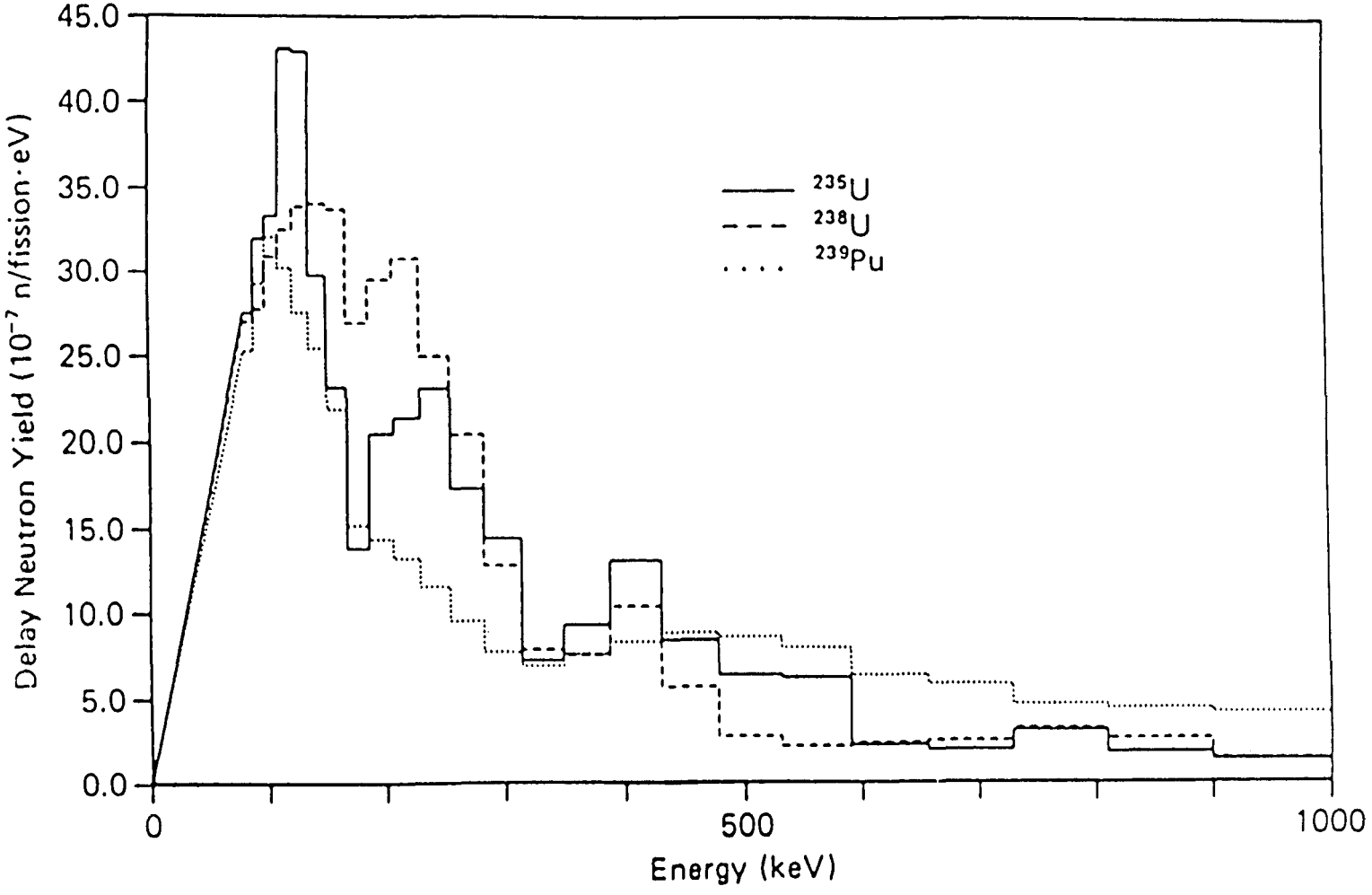

Fig. 4. ENDF/B-V group-one spectra.

CHAPTER III.

THEORY OF DELAYED NEUTRON EMISSION

A schematic representation of the delayed neutron emission process is given in Fig. 5. The beta unstable fission product (Z, N) known as the delayed neutron precursor has a characteristic maximum beta decay energy, Q_β. This Q_β is the energy difference between the ground state of the precursor nuclide and the ground state of its $(Z+1, N-1)$ beta decay daughter. It is this daughter nucleus which, under certain conditions, actually decays by neutron emission and is therefore known as the delayed neutron emitter. This emitter nucleus is usually formed in an excited state occupying any one of the energy levels above its ground state shown in Fig. 5. If the excitation energy of the nucleus exceeds its characteristic neutron binding energy, $S(n)$, a neutron may be emitted producing a $(Z+1, N-2)$ granddaughter. There is also experimental evidence that in some cases the excitation energy exceeds not only the binding energy of the first neutron, $S(n)$, but also that of the second neutron, $S(2n)$. In this situation, the emission of two delayed neutrons is possible. The $(\beta-, 2n)$ process has been observed experimentally in light nuclei as well as nuclei with $A > 50$.[34,35] The high density of nuclear levels above the neutron binding energy indicates that a continuous energy spectrum of delayed neutrons exists as has been experimentally observed.[3] As can be seen in Fig. 5, a competing process is for the daughter nucleus to simply decay by gamma emission to its ground state.

The de-excitation of the emitter nucleus is nearly instantaneous. Therefore, the probability of delayed neutron emission, P_n, and the time constant associated with delayed neutron production are properties attributed to the precursor nuclide rather than the emitter. The production rate of delayed neutrons from a particular precursor nuclide is proportional to its own rate of decay. The P_n value may be described as the number of neutrons produced per decay of the precursor, and is sometimes loosely termed the neutron-to-beta branching ratio for the precursor.[3]

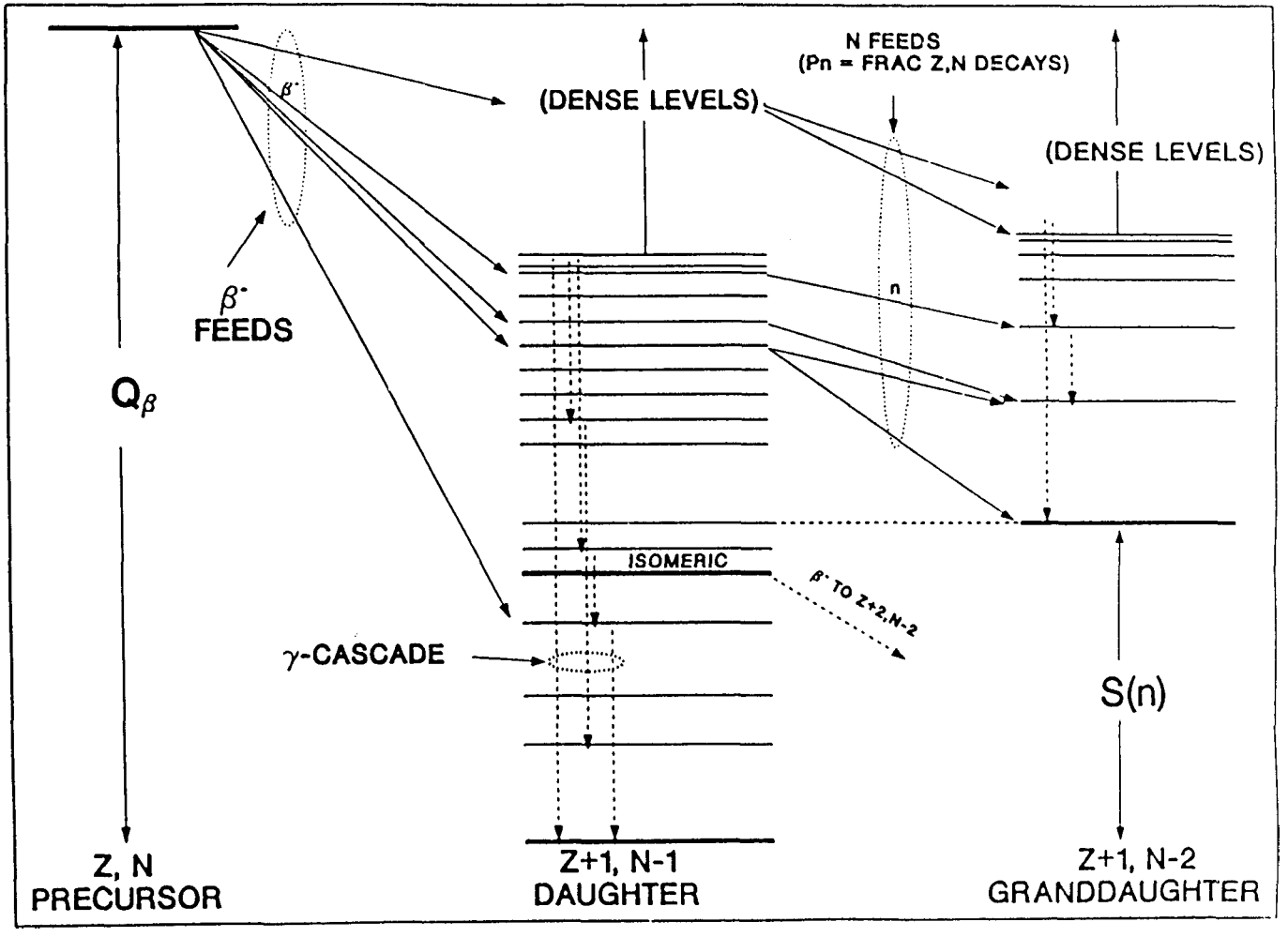

Fig. 5. Schematic of beta decay plus delayed neutron emission.

There are three basic quantities which must be known for each precursor in order to calculate delayed neutron yields and spectra from fission. These quantities are:

1. delayed neutron emission probabilities, P_n values,
2. fission yields;
    a. cumulative yield for equilibrium calculations,
    b. direct (independent) yield for pulse calculations, and
3. energy spectra.

DELAYED NEUTRON EMISSION PROBABILITIES

Theory

Early attempts to calculate theoretical neutron emission probabilities were formulated using conventional (Fermi) beta decay theory and energetics. The Fermi theory of beta decay is based on the neutrino hypothesis in which the disintegration energy released in the beta decay process is carried away by the beta particle, the recoil nucleus and a third particle, the neutrino.[36] When a nucleus emits an electron (beta-minus emission), as is the case leading to delayed neutron emission, the number of protons in the nucleus is increased by one and the number of neutrons is decreased by one, with the mass number remaining the same. This process may be regarded as the transformation of a neutron into a proton, an electron and an antineutrino.[37]

Consistent with the Fermi theory of beta decay the number of beta transitions from the precursor nuclide to excited states of the emitter (daughter) in the energy interval dE about $E, W(E)$ may be written as:

$$W(E)dE = C \mid M_{if} \mid^2 f(Z+1, Q_\beta - E)\omega(E)dE \qquad (2)$$

where C is a constant, $\mid M_{if} \mid^2$ is the square matrix element of the beta transition (between initial and final states), $f(Z+1, Q_\beta - E)$ gives the charge and energy dependence of the transition (known as the Fermi function; a statistical rate

function describing the effect of the Coulomb field on the transition), and $\omega(E)$ represents the level density of the daughter nuclide.[3] The matrix elements show no systematic relation to the energy of the final (emitter nucleus) state, therefore $\mid M_{if} \mid^2$ is usually assumed to be a constant. Alternatively, the probability of neutron emission from an energy state E may be written in terms of the partial widths for neutron (Γ_n) and gamma (Γ_g) emission;[38]

$$\frac{\Gamma_n}{\Gamma_n + \Gamma_g} \tag{3}$$

Using Eqs. (2) and (3), the neutron emission probability is obtained from the ratio of the number of neutron emitting states to the total number of excited states in the emitter nuclide may be written as

$$P_n = \frac{\int_{S(n)}^{Q_\beta} f(Z+1, Q_\beta - E)\omega(E)\, \frac{\Gamma_n}{\Gamma_n + \Gamma_g}\, dE}{\int_0^{Q_\beta} f(Z+1, Q_\beta - E)\,\omega(E)\, dE} \tag{4}$$

The above equation does not include the effects of angular momentum and parity on the energy path. To include these effects, contributions from all possible spin states are summed as in Eq. (5).

$$P_n = \frac{\int_{S(n)}^{Q_\beta} \sum_J \sum_j \mid M_{if} \mid^2 \; f(Z+1, Q_\beta - E)\omega(E, J^\pi)\, \frac{\Gamma_n^j(E_n)dE}{\Gamma_n^j(E_n) + \Gamma_g}}{\int_0^{Q_\beta} \sum_J \sum_j \mid M_{if} \mid^2 \; f(Z+1, Q_\beta - E)\omega(E, J^\pi)dE} \tag{5}$$

where:

$\omega(E, J^\pi)$ = density of levels with spin, J, and parity, π, in the emitter at energy, E

$\Gamma_n^j(E_n)$ = neutron width for l-wave neutrons with total angular momentum j and energy E_n emitted from the emitter,

and the remaining terms are as previously defined.[39,40] The spacing between levels with the same spin and parity at the higher excitation energies of the

level scheme is quite small (of the order of 10 eV). This upper part is the region of interest for delayed neutron emission and it suggests that due to the large number of possible states of the emitter nucleus beta decay can be discussed in statistical terms.[41] The appropriate parameter in this treatment becomes the beta strength function,[10] which is defined as the product of the level density and the average transition probability to a single final level:[39]

$$S_\beta(E) = \mid M_{if} \mid^2 \frac{\omega(E)}{6220} \text{ sec}^{-1} \text{ MeV}^{-1} \tag{6}$$

The strength function may also be thought of as the average transition rate per unit energy interval.[42] Theoretical studies of the beta strength function have been carried out under two general assumptions:

i. the beta strength function is proportional to the level density, i.e., $\mid M_{if} \mid^2 = \text{constant}$,

ii. the beta strength function is constant above and zero below a given cutoff energy, thus;

$$E > Ec \quad \mid M_{if} \mid^2 \omega(E) = \text{ constant, and}$$

$$E < Ec \quad \mid M_{if} \mid^2 \omega(E) = 0.$$

The results of these studies in relation to measured delayed neutron emission probabilities suggests the beta strength function is energy dependent but not as strongly energy dependent as assumption (i.) would indicate.[39] A constant beta strength function above a certain cutoff energy was found to be unfeasible as it requires a very high excitation energy to be the cutoff and thus implies unphysical conditions concerning the beta decay of the precursor nuclide.[39]

Systematics

Predictions of neutron emission probabilities based on theoretical calculations have been hampered by the paucity of knowledge of level densities, spins, parities, and nuclear spectroscopic data. As a result several semi-empirical and systematic treatments have been proposed.

Amiel and Feldstein[43] presented a semi-empirical treatment of neutron emission probabilities that related the P_n value to the energy window, $(Q_\beta - S(n))$, for neutron emission;

$$P_n = c(Q_\beta - S(n))^m \tag{7}$$

where c and m are free parameters determined from a fit to experimental data. They reported a value of 1.65 ± 0.241 as the best value obtained for m. The above relationship suggests that the beta strength function may be taken as constant for small changes of transition energy and that gamma competition may be neglected. This assumption is especially valid for higher excitation energies. Analysis of delayed proton spectra support the assumption of a uniform beta strength function for positron emission.[43] However, some researchers remain cautious and are uncertain of the implications of these results for the beta strength function in the case of electron emission.[39,44]

Kratz and Herrmann studied the systematics of delayed neutron emission probabilities in an effort to relate the P_n value not only to the magnitude of the energy window, but also to its position in the energy scale.[45] Expressing Eq. (4) in terms of the beta strength function [Eq. (6)] yields the expression:

$$P_n = \frac{\int_{S(n)}^{Q_\beta} f(Z+1, Q_\beta - E) S_\beta(E) \frac{\Gamma_n}{\Gamma_n + \Gamma_g} dE}{\int_0^{Q_\beta} f(Z+1, Q_\beta - E) S_\beta(E) dE} \tag{8}$$

As a first order approximation, competition with gamma decay may be neglected,[45] $\Gamma_n/(\Gamma_n + \Gamma_g) = \sim 1$, and the statistical rate function becomes;

$$f(Z+1, Q_\beta - E) \propto (Q_\beta - S(n))^n \tag{9}$$

where $n = 5$ for beta decaying nuclei.[38,41,45] The beta strength function was taken as a constant above a cutoff energy K, and zero below it, and was chosen according to the even and oddness of the precursor nucleus;[45]

$$\begin{aligned} K &= 0 \quad \text{even-even} \\ &= 13/\sqrt{A} \quad \text{odd} \\ &= 26/\sqrt{A} \quad \text{odd-odd} \end{aligned}$$

Substituting into Eq. (8) yields;

$$P_n = \frac{\int_{S(n)}^{Q_\beta} (Q_\beta - E)^n dE}{\int_0^{Q_\beta} (Q_\beta - E)^n dE} \tag{10}$$

and performing the integration gives;

$$P_n \simeq a \left(\frac{Q_\beta - S(n)}{Q_\beta - K} \right)^b \tag{11}$$

where a and b are free parameters. Values for a and b are determined by a fit of experimental P_n values to Eq. (11),[8,45,46] which is commonly referred to as the Kratz-Herrmann equation.

FISSION YIELDS

An additional requirement for calculating delayed neutrons from individual precursor data is to have an accurate estimate of the yield from fission of the particular precursor nuclides. The current Evaluated Nuclear Data Files (ENDF/B version V) contain tabulations for two types of fission yields; direct (or independent) yields and cumulative yields.

The direct fission yield is a "prompt" yield, i.e., it is the yield directly from fission before any subsequent decay and production scheme. The cumulative fission yields represent more of an "equilibrium" yield, it includes the direct yields from fission as well as the yield (production) of that nuclide as a result of the radioactive decay of other fission product nuclides.

The current ENDF/B-V yields are based on the compilations of Meek and Rider[47] and are considered to be outstanding within their applicable range of data. A preliminary yield set for incorporation in ENDF/B-VI is primarily the result of a more recent compilation by England and Rider.[48] The philosophy in the U.S. and particularly at Los Alamos, where many of the fission product yield evaluations are currently being performed, is to include all measured data and to expand each mass chain to include each nuclide and isomeric state in the ENDF/B decay files (~879 nuclides) or to cover at least four charge units on

either side of the most probable charge ($\pm 4Z$).[48] In order to perform these tasks it is necessary to model the yield distributions, including the effects of neutron and proton pairing,[49] as well as branchings to isomeric states,[50] (when such data do not exist).

The yield distribution model most commonly used is referred to as the Z_p-model[51,52] and is shown schematically in Fig. 6. The term Z_p represents the most probable charge along a mass chain and is the value of charge where the direct yield from fission is a maximum. The Z_p-model uses a Gaussian distribution about this point to distribute the measured mass chain yield. The models currently in use at Los Alamos are based on this Z_p model with modifications to incorporate the influence of neutron and proton pairing.[49] This has been done by introducing fractional quantities, X (proton pairing), and Y (neutron pairing) to modify the fractional independent yield (FIY), as calculated by the Z_p-model, as shown in Eq. (12).

$$FIY(Z,A) = \frac{(1 \pm X)(1 \pm Y)}{NORM} \int_{Z-1/2}^{Z+1/2} \frac{1}{(2\pi\sigma^2)^{1/2}} e^{-\frac{(Z-Z_p)}{2\sigma^2}} dZ \qquad (12)$$

The integrand in the above equation represents the Z_p model for yield distributions where σ is the Gaussian width. The term to the right of the integral sign represents modifications to the model to include the effects of pairing. The "+" sign is used for products with an even number of protons (Z) or neutrons (N) and the "−" sign is for those with odd Z or N. $NORM$ is a quantity used to renormalize the fractional mass chain yield to unity. Particular values for X and Y used in the current yield evaluation are found in Ref. 49.

Once the expansions along the mass chains to include all $Z_p \pm 4$ nuclides had been made, various integral tests were performed on each of the yield sets to check for errors and ultimately provide a set of independent yields normalized to 200%. These tests included calculating the average neutron number [Eq. (13a)] and average charge based on the independent yields, YI, [Eq. (13b)] and the average charge's deviation from the fission nuclide charge, the prompt neutron

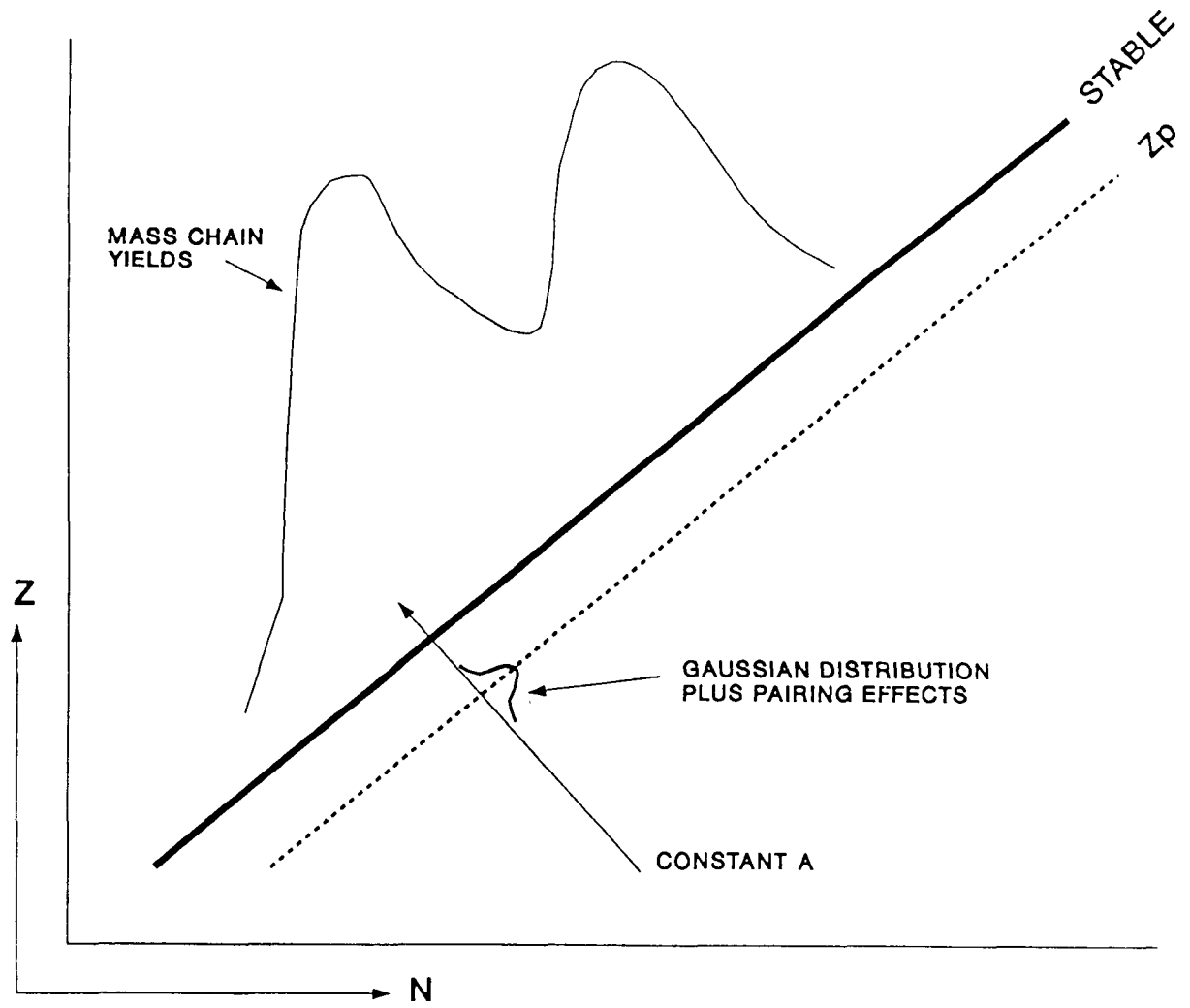

Fig. 6. Schematic of yield distribution.

yield [Eq. (13c)], and the delayed neutron yield [Eq. (13d)] which is based on cumulative fission yields, YC.[48]

$$N_{ave} = \sum_i YI(Z,A)_i N_i \tag{13a}$$

$$Z_{ave} = \sum_i YI(Z,A)_i Z_i \tag{13b}$$

$$\nu_p = A_f + k - (Z_{ave} + N_{ave}) \tag{13c}$$

$$k = 0 \text{ spontaneous fission}$$

$$= 1 \text{ other}$$

$$\nu_d = \sum_i YC(Z,A)_i P_n^i \tag{13d}$$

It is also worth pointing out that the delayed neutron precursor data can be used to provide an accurate test of the cumulative yield data. The current yield evaluation is a preliminary version of what is to be ENDF/B-VI and contains data for 34 fissioning nuclides at one or more incident neutron energies and/or spontaneous fission. Results of the integral tests on these preliminary yield sets have been published.[48] However, at the time of that publication the yields had not been expanded to include all of the 879 nuclides in the decay files (or $Z_p \pm 4$ charge units). The neutron and proton pairing factors for ^{238}U(F) (fast fission of ^{238}U) have also been changed from Ref. 48. Currently the values being used for neutron and proton pairing for ^{238}U(F) are the same as those used for ^{235}U(F). A summary of the fission product yield evaluations in ENDF/B-IV and -V as well as this preliminary ENDF/B-VI set are given in Table II.

SPECTRA

The study of delayed neutron spectra has historically had a dual purpose: to better understand and evaluate the importance of delayed neutrons in reactor control, particularly in the case of fast breeder reactors, and to examine various aspects of the nuclear structure of excessively neutron-rich nuclei.[53] The work described in this thesis was performed with the first of these goals in mind. Batchelor and McK. Hyder[24] made the first attempt to calculate the energy distribution of delayed neutrons choosing group one, (assumed to be primarily

TABLE II

Evolution of ENDF/B Fission Yield Evaluations

Evaluation	Pre-ENDF	ENDF/B-IV	ENDF/B-V	ENDF/B-VI
Report NEDO-	12154	12154-1	12154-2E	12154-3F
Year	1972	1974	1978	1987
Nuclides	10	10	20	50
Cumulative yields	Yes	Yes*	Yes	Yes
Ind. yields	No	Yes	Yes	Yes
Isomer ratios	No	No	Yes	Yes
Odd-Even pairing	No	Yes	Yes	Yes
Delayed neutron	No	No	Yes	Yes
Charge balance	No	Yes	Yes	Yes
Ternary fission	No	No	Yes	Yes
References	812	956	1119	1371
Input values	6000	12400	18000	28400
Final yields	11000	22000	44000	110000

*Evaluated but not in ENDF/B-IV.

^{87}Br), for their effort. Comparison between their prediction and experiment was poor owing, partly, to the quality of data at that time, particularly the mass values used to calculate Q_β. Two attempts were made in the late 1960s to calculate spectra using spin dependent level densities,[54] and in one case, spin and parity selection rules and a more precise form for the level density.[55] Spectra predicted in the first of these studies were found to be in poor agreement with experimental spectra, whereas the group two spectrum (^{88}Br and ^{137}I were assumed to be the major contributors) calculated in the latter of these two efforts, agreed well with experiment.[56] However, this agreement was later found to be largely coincidental in that the 400 keV – 500 keV dominant peak in the group two spectrum attributed to ^{88}Br by Gauvin and Tourreil was later shown to be the result of ^{137}I, yielding the results of the study inconclusive.[56]

In 1972 Takahashi[53] published calculated spectra for ^{87}Br and ^{137}I obtained by applying the "gross theory" of beta decay to delayed neutron emission. This theory developed by Takahashi and Yamada[57,58] is a simple analogy to the liquid-drop model of nuclear masses[59] that is appropriated for dealing with average properties of beta decay. The decay properties are averaged over many transitions to different final states rather that being treated as individual transitions to particular final states.[58] In this representation the total strength is represented as a sum of the single particle strength functions for (1) Fermi allowed transitions, (2) Gamow-Teller allowed transitions, and (3) first forbidden transitions, the net effect being that the total strength is reduced to a function of one free parameter, the spreading width of the collective states. (See Refs. 60–62, or any basic nuclear physics text for a review of the classical theory of beta decay.) Takahashi's[53] calculated spectrum for ^{87}Br was found to have some similarity to the Batchelor and McK. Hyder[24] measured group one spectrum and his ^{137}I spectrum compared favorably with that measured by Shalev and Rudstam.[63] The agreement was "regarded as reasonable in view of the nature of the gross theory." The gross theory is useful in predicting spectral shapes (envelopes) but yields little insight into the detailed structure of delayed neutron spectra.

Pappas and Sverdrup (1972) calculated the envelopes of delayed neutron spectra using a combined energy-angular momentum (spin and parity dependent) approach.[39] Using two forms of the beta strength function and different mass formulae to predict Q_β and $S(n)$ comparisons were made with measured spectra for ^{87}Br, ^{83}As, and ^{137}I but the results were inconclusive in that, again, the theory only predicted the general shape of the spectra and no fine structure. Generally, the energy dependent beta strength appeared to calculate the low energy parts of the spectra well and the energy-independent beta strength seemed better at predicting the high energy parts of the spectra.[39]

A more comprehensive approach was taken by Shalev and Rudstam[56] in which they used measured spectra for ^{87}Br and ^{137}I to obtain a set of level density parameters which were then used to predict spectra for ^{85}As, ^{134}Sn, ^{135}Sb, and ^{136}Te. Their goal was to "find a logical and consistent set of parameters (level density parameter, a; Q-values; binding energies; neutron and gamma widths; etc.) such that experimental and calculated data are in reasonable agreement for as many precursors as possible."[56] Unfortunately they could not find a single data set to give satisfactory results for the spectra shape for all the isotopes under consideration , but in view of their simple approach were quite satisfied with the modest agreement they did obtain.

Rudstam[64] (1978) later superimposed fine structure extracted from published spectra onto calculated spectral envelopes for 25 precursor nuclides in an effort to characterize the spectra. An extrapolation procedure was then used to deduce the spectra for another five precursors. The spectra for the 30 precursors were then used to predict total delayed neutron spectra for ^{235}U and ^{239}Pu which compared fairly well in overall shape with experiment. These early spectra calculations used various representations for level density, nuclear masses and gamma and neutron branchings, and nearly all made the simplifying assumption that any decay resulted in the ground state of the final nucleus being occupied. An attempt to improve theoretical spectra by including transitions to excited states in the final nucleus was made by Gjotterud, Hoff, and Pappas[65] (1978) which was generally successful in terms of the spectral envelopes. This same group,[44] using a Monte Carlo method based on a statistical model, made

the first attempt to actually calculate the observed structure of delayed neutron spectra. A qualitative comparison was made with the measured spectra of Shalev and Rudstam,[56,63,66] and appeared to be satisfactory for all precursor nuclides except ^{135}Sb which seemed to require a more refined model.[66]

With the exception of the work of Takahashi and colleagues, the methods used to predict delayed neutron spectra relied primarily on statistical models and simple assumptions of the energy dependence of the beta strength function. Recent work of Klapdor and colleagues[67,68] utilizes microscopic calculations to model and account for structure in the beta strength function used to predict the beta decay properties of nuclei far from stability. The results of this microscopic theory have for the most part been shown to be an improvement over the predictions based on the gross theory of beta decay.

Mann and associates[7,69,70] have shown that beta decay properties for some important fission products may be accurately calculated using a statistical approach with one free global parameter. Their model treats the delayed neutron emitter (daughter) as a compound nucleus that statistically decays as in the Hauser-Feshbach approach.[7] The efforts of Mann and co-workers culminated in the production of the BETA code[7] which has been used in this dissertation. Appendix B contains a description of the BETA code and its subroutines, a block diagram describing the BETA code, and a detailed description of the required input.

CHAPTER IV.

THE PRECURSOR DATA BASE

A "data evaluation" usually involves a review of the available measured data, experimental methods and their influence on the data; comparison with theory and/or systematic arguments; and the manipulation of both the data and theory (including systematics) in order to recommend a creditable, comprehensive data set. ENDF/B-IV (1974) and ENDF/B-V (1978) contain delayed neutron data in the six-group format and are based primarily on an evaluation by Cox[14] (1974), with minor changes to spectra for delay group two being made for ENDF/B-V as a result of an evaluation by Kaiser and Carpenter[27] at Argonne National Laboratory as discussed in Chapter II.

Interest in breeder reactors and improvements in on-line isotope separation techniques have been the primary incentives for the efforts to improve precision in delayed neutron data that have resulted in measurements of the properties of individual precursor nuclides, especially their spectra.[6] This precursor data forms the bulk of the new delayed neutron data (since the 1978 ENDF/B-V evaluation), although Refs. 17–20 do report new measurements of total delayed neutron yields and six group parameters for one or more of the following nuclides; ^{232}Th, ^{232,233,235,238}U, ^{237}Np, ^{238,239,240,241,242}Pu, ^{241,242m}Am, ^{245}Cm, and ^{249}Cf.

As described in Chapter II, it has been common practice to use a mathematical six-group approximation to describe the time-dependent production of delayed neutrons. With the data now available for individual precursors, it is possible to calculate delayed neutron production by tracing the formation and decay of each of the precursor nuclides along explicit fission product chains. This method is illustrated by Fig. 7. In contrast with the equivalent scheme for the six-group representation (Fig. 3), this approach couples not only the delayed neutron precursors along a particular mass chain but also the different mass chains themselves. The importance of this coupling will be described later in the discussion on reactor kinetics. This method follows the physical production and decay paths, the error in this approach is limited to that introduced by the

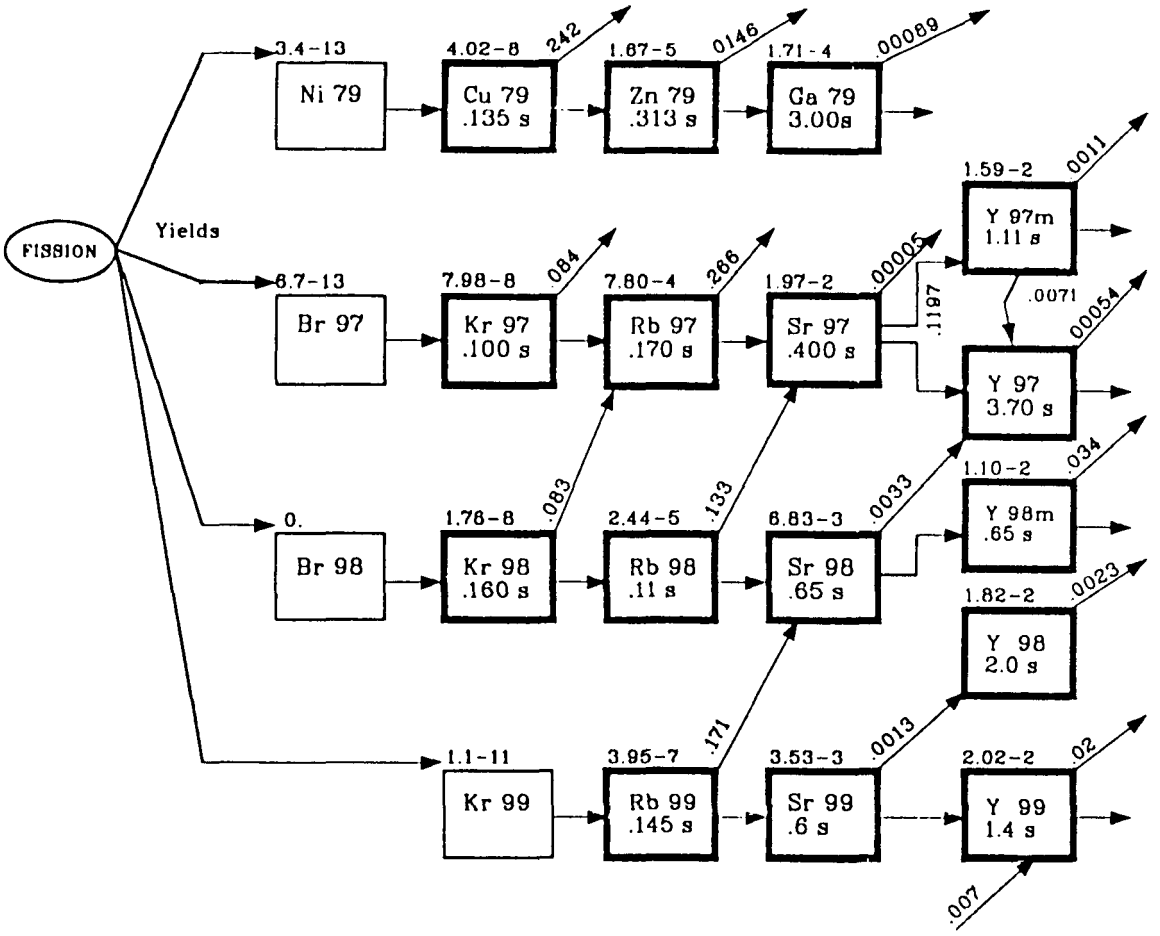

Fig. 7. Some explicit fission product chains.

uncertainty of the data. This precursor approach may be used to describe delayed neutron activity resulting from either pulse or extended irradiations. The case of an extended or "infinite" irradiation can be applied to reactors (while pulse irradiations are usually important to critical assemblies) and will be the emphasis of this work.

PRECURSOR IDENTIFICATION

Before proceeding to the data evaluation itself, it is convenient to discuss the basic contents of such a data base. The first requirement is simply to identify the precursor nuclides. Early methods of radiochemical separation and methods to determine nuclear masses made it difficult to identify precursors; at the time of Keepin's work[4] in 1956, ~16 precursors had been identified. By the time of his book,[3] *Physics of Nuclear Kinetics* (1965), the number had increased to 29. Tomlinson's review[71] (1973) contained data for 57 precursor nuclides produced in fission. By 1983 T. R. England, et al.[28] had identified 105 precursors and were incorporating these nuclides in their calculations.

Identification of precursor nuclides (other than those observed experimentally) is usually based on energetics arguments; if Q_β is larger than $S(n)$ (the neutron separation energy) delayed neutron emission is possible. Such arguments require accurate nuclear masses to calculate Q_β [Eq. (14)] and $S(n)$ [Eq. (15)];

$$Q_\beta = {}^{Z}_{A}M - {}^{Z+1}_{A}M \tag{14}$$

$$S(n) = {}^{Z+1}_{A}M - \left({}^{Z+1}_{A-1}M + {}^{0}_{1}M_n\right) \tag{15}$$

where ${}^{Z}_{A}M$ is the mass of the precursor, ${}^{Z+1}_{A}M$ is the mass of the emitter, ${}^{Z+1}_{A-1}M$ is the mass of the granddaughter, and ${}^{0}_{1}M_n$ is the rest mass of a neutron. The mass tables of Wapstra and Audi[72] were used in this dissertation when possible, masses for nuclides not contained in Ref. 72 were taken from the work of Möller and Nix.[73] Table III, which contains much of the information pertaining to the final data set and will be described later in detail, indicates which source was used for the masses of the precursor, emitter and granddaughter. Based on these

TABLE III

Precursor Emission Probabilities (P_n), Sources of Data, and Type of Spectral Modifications

CS	ID	HL	Pn	dPn	GP	Pn Source		Spectra Source	QB	S(n)	Mass Tables M1	M2	M3	Norm Area 1	Norm Area 2
Co	270720	0.1235	11.5322	0.0000	6	sys.		EVAP(398.9)	15.030	7.391	MN	MN	MN		
Cu	290720	6.4891	<0.0001	0.0000	3	sys.		EVAP(41.8)	8.964	8.880	MN	W81	W81		
Co	270730	0.1290	25.1220	0.0000	6	sys.		EVAP(430.7)	12.800	3.771	MN	MN	MN		
Ni	280730	0.4906	0.0047	0.0000	5	sys.		EVAP(95.0)	8.170	7.731	MN	MN	MN		
Cu	290730	5.1136	0.5588	0.0000	3	sys.		EVAP(159.1)	6.174	4.942	MN	W81	W81		
Co	270740	0.0920	17.4326	0.0000	6	sys.		EVAP(442.5)	16.440	6.781	MN	MN	MN		
Ni	280740	0.9002	0.3560	0.0000	4	sys.		EVAP(167.8)	5.980	4.591	MN	MN	MN		
Cu	290740	0.6482	0.2949	0.0000	5	sys.		EVAP(179.1)	10.221	8.638	MN	W81	W81		
Co	270750	0.0817	31.3124	0.0000	6	sys.		EVAP(476.6)	14.810	3.451	MN	MN	MN		
Ni	280750	0.2312	1.0022	0.0000	6	sys.		EVAP(224.9)	9.560	7.031	MN	MN	MN		
Cu	290750	0.9274	3.4700	0.6300	4	meas.		EVAP(252.5)	8.055	4.866	MN	W81	W81		
Ni	280760	0.3046	3.5113	0.0000	5	sys.		EVAP(262.0)	7.700	4.221	MN	MN	MN		
Cu	290760	0.2602	2.8418	0.0000	6	sys.		EVAP(275.0)	12.004	8.171	MN	W81	W81		
Ni	280770	0.1033	4.7115	0.0000	6	sys.		EVAP(302.9)	11.050	6.341	MN	MN	MN		
Cu	290770	0.3052	12.3119	0.0000	5	sys.		EVAP(332.1)	10.185	4.522	MN	W81	W81		
Ni	280780	0.1318	9.2984	0.0000	6	sys.		EVAP(323.4)	9.070	3.631	MN	MN	MN		
Cu	290780	0.1179	9.9093	0.0000	6	sys.		EVAP(355.0)	13.673	7.119	MN	W81	W81		
Zn	300780	1.9855	0.0041	0.0000	4	sys.		EVAP(85.6)	6.010	5.629	W81	W81	W81		
Cu	290790	0.1351	24.2057	0.0000	6	sys.		EVAP(374.1)	10.770	3.399	MN	MN	W81		
Zn	300790	0.3130	1.1459	0.0000	5	sys.		EVAP(222.7)	9.465	6.854	MN	W81	W81		
Ga	310790	3.0000	0.0890	0.0200	4	meas.	(m)	BO.11R	6.770	5.740	W83	W83	W83	0.11,0.21	
Cu	290800	0.0899	15.0430	0.0000	6	sys.		EVAP(422.0)	16.680	7.181	MN	MN	MN		
Zn	300800	0.4873	1.0983	0.0000	6	sys.		EVAP(206.9)	7.087	4.803	MN	W81	W81		
Ga	310800	1.6600	0.8300	0.0700	4	meas.	(m)	BO.11R1.06B	10.000	7.920	W83	W83	W83	0.11,0.21	0.90,1.00
Cu	290810	0.0742	52.9504	0.0000	6	sys.		EVAP(497.8)	14.900	1.521	MN	MN	MN		
Zn	300810	0.1227	5.7372	0.0000	6	sys.		EVAP(321.1)	12.125	6.559	MN	W81	W81		
Ga	310810	1.2300	11.9000	0.9400	4	meas.	(m)	BO.07R1.69B	8.320	4.990	W83	W83	W83	0.07,0.17	1.45,1.65
Zn	300820	0.1268	21.2264	0.0000	6	sys.		EVAP(381.2)	10.420	2.477	MN	MN	W81		
Ga	310820	0.6000	21.1000	1.8300	5	meas.		EVAP(327.0)	12.993	7.149	MN	W81	W81		
Zn	300830	0.0836	22.8749	0.0000	6	sys.		EVAP(415.9)	13.710	4.141	MN	MN	MN		
Ga	310830	0.3100	56.2000	9.9000	5	meas.		EVAP(399.9)	11.970	3.119	MN	MN	W81		
Ge	320830	1.9000	0.0235	0.0000	4	sys.		EVAP(117.2)	8.640	7.880	W83	W83	W83		
Ga	310840	0.0984	28.0232	0.0000	6	sys.		EVAP(425.9)	15.130	4.971	MN	MN	MN		
Ge	320840	1.2000	5.2055	0.0000	4	sys.		EVAP(283.0)	8.855	4.369	MN	W81	W81		
As	330840	5.3000	0.0860	0.0430	3	meas.		EVAP(145.8)	9.872	8.681	W83	W83	W83		
Ga	310850	0.0870	44.9654	0.0000	6	sys.		EVAP(447.7)	13.390	2.031	MN	MN	MN		
Ge	320850	0.2500	16.4540	0.0000	6	BETA		EVAP(347.0)	11.050	4.226	MN	MN	W81		
As	330850	2.0300	70.9250	7.7026	4	meas.	(m)	M2.8B	8.910	4.540	W83	W83	W83	1.30,1.60	2.30,2.80
Ge	320860	0.2470	15.2148	0.0000	6	sys.		EVAP(337.7)	9.450	2.911	MN	MN	MN		

(Continued)

TABLE III (Continued)

CS	ID	HL	Pn	dPn	GP	Pn Source		Spectra Source	QB	S(n)	Mass Tables M1	M2	M3	Norm Area 1	Norm Area 2
As	330860	0.9000	8.5030	1.6104	4	meas.		EVAP(353.8)	13.372	6.196	MN	W81	W81		
Ge	320870	0.1339	15.1329	0.0000	6	sys.		EVAP(365.5)	12.610	4.861	MN	MN	MN		
As	330870	0.3000	44.3600	20.2170	6	meas.		EVAP(383.0)	10.730	2.220	MN	MN	W81		
Se	340870	5.6000	0.1880	0.0210	3	meas.		EVAP(121.8)	7.170	6.310	W83	W83	W83		
Br	350870	55.7000	2.5400	0.1600	1	meas.	(m)	MAINZ	6.826	5.515	W83	W83	W83		
Ge	320880	0.1290	21.6551	0.0000	6	sys.		EVAP(376.6)	10.850	2.531	MN	MN	MN		
As	330880	0.1348	19.9068	0.0000	6	sys.		EVAP(373.8)	13.730	5.531	MN	MN	MN		
Se	340880	1.5000	0.9660	0.0210	4	meas.		EVAP(249.6)	8.567	4.912	MN	W81	W81		
Br	350880	16.0000	6.2600	0.3800	2	meas.	(m)	RUDSTAM	8.967	7.053	W83	W83	W83		
As	330890	0.1212	33.2722	0.0000	6	sys.		EVAP(392.7)	11.910	2.761	MN	MN	MN		
Se	340890	0.4270	7.7000	2.4000	5	meas.		EVAP(312.8)	11.378	5.573	MN	W81	W81		
Br	350890	4.3800	14.0000	0.8400	3	meas.	(m)	B.05M2.59B	8.300	5.110	W83	W83	W83	0.05,0.15	1.90,2.20
As	330900	0.0911	24.3493	0.0000	6	sys.		EVAP(403.9)	15.080	5.291	MN	MN	MN		
Se	340900	0.5550	9.1321	0.0000	5	sys.		EVAP(318.5)	10.204	4.117	MN	W81	W81		
Br	350900	1.8000	24.6000	1.8500	4	meas.	(m)	B.05M2.83B	10.700	6.310	W83	W83	W83	0.05,0.15	2.30,2.80
Se	340910	0.2700	24.4382	0.0000	6	sys.		EVAP(359.8)	11.250	3.398	MN	MN	W81		
Br	350910	0.6000	18.1000	1.4800	5	meas.	(m)	B.05M2.94B	11.795	4.493	MN	W81	W81	0.05,0.15	2.40,2.90
Rb	370910	58.2000	<0.0001	0.0000	1	sys.		EVAP(32.2)	5.859	5.796	W81	W81	W81		
Se	340920	0.1682	13.2333	0.0000	6	sys.		EVAP(320.5)	9.480	3.181	MN	MN	MN		
Br	350920	0.3600	42.7344	9.7464	5	meas.	(m)	B.05M3.0B	13.963	5.350	MN	W81	W81	0.05,0.15	2.45,2.95
Kr	360920	0.3600	0.0332	0.0031	5	meas.		EVAP(130.4)	6.156	5.113	W83	W83	W83		
Rb	370920	4.5300	0.0099	0.0005	3	meas.	(m)	MAINZ	8.120	7.366	W83	W83	W83		
Se	340930	0.0968	12.0321	0.0000	6	sys.		EVAP(340.0)	12.440	5.271	MN	MN	MN		
Br	350930	0.1760	25.0885	0.0000	6	sys.		EVAP(374.4)	12.211	3.518	MN	W81	W81		
Kr	360930	1.2900	2.0100	0.1600	4	meas.		EVAP(205.4)	8.529	5.914	W83	W83	W83		
Rb	370930	5.8600	1.3500	0.0700	3	meas.	(m)	GO.2M1.8B	7.442	5.237	W83	W83	W83	0.10,0.30	1.40,1.80
Br	350940	0.1108	29.8035	0.0000	6	sys.		EVAP(382.5)	13.580	4.411	MN	MN	W81		
Kr	360940	0.2100	6.1300	2.4100	6	meas.		EVAP(256.4)	8.199	4.080	MN	W81	W81		
Rb	370940	2.7600	10.0000	0.5000	4	meas.	(m)	GO.2M2.46B	10.307	6.786	W83	W83	W83	0.10,0.30	2.10,2.40
Br	350950	0.1069	27.0797	0.0000	6	sys.		EVAP(371.0)	11.990	3.271	MN	MN	MN		
Kr	360950	0.7800	7.5051	0.0000	5	BETA		EVAP(278.9)	10.078	5.151	MN	W81	W81		
Rb	370950	0.3800	8.6200	0.4200	5	meas.	(m)	GO.2M1.8B	9.282	4.330	W83	W83	W83	0.10,0.30	1.40,1.80
Br	350960	0.0888	21.9195	0.0000	6	sys.		EVAP(384.6)	14.960	5.491	MN	MN	MN		
Kr	360960	0.2931	7.7473	0.0000	6	sys.		EVAP(267.7)	8.066	3.479	MN	W81	W81		
Rb	370960	0.2040	14.0000	0.7100	6	meas.	(m)	GO.2M2.22B	11.750	5.860	W83	W83	W83	0.10,0.30	2.00,2.40
Sr	380960	1.1000	0.0011	0.0000	4	sys.		EVAP(60.9)	5.413	5.176	W81	W81	W81		
Kr	360970	0.1000	8.3925	0.0000	6	sys.		EVAP(284.8)	10.331	5.086	MN	W81	W81		
Rb	370970	0.1700	26.6000	1.4800	6	meas.	(m)	GO.2M2.11B	10.520	3.980	W83	W83	W83	0.10,0.30	1.90,2.30
Sr	380970	0.4000	0.0054	0.0021	5	meas.		EVAP(148.7)	7.470	6.040	W83	W83	W83		
Y	390970	3.7000	0.0540	0.0028	3	meas.		EVAP(130.5)	6.680	5.579	W83	W83	W83		
Y	390971	1.1100	0.1090	0.0300	4	meas.		Y97	0.000	0.000	Y97				
Kr	360980	0.1602	8.2989	0.0000	6	sys.		EVAP(290.1)	9.480	3.980	MN	W81	W81		
Rb	370980	0.1100	13.3000	1.2000	6	meas.	(m)	M2.45B	12.430	5.760	W83	W83	W83	1.90,2.20	
Sr	380980	0.6500	0.3260	0.0340	5	meas.		EVAP(161.3)	5.880	4.180	W83	W83	W83		
Y	390980	2.0000	0.2280	0.0120	4	meas.		EVAP(196.0)	8.918	6.409	W83	W83	W83		
Y	390981	0.6500	3.4100	0.9600	5	meas.		Y98	0.000	0.000	Y98				

(Continued)

TABLE III (Continued)

CS	ID	HL	Pn	dPn	GP	Pn Source	Spectra Source	QB	S(n)	Mass Tables M1	M2	M3	Norm Area 1	Norm Area 2
Rb	370990	0.1450	17.1000	4.2000	6	meas.	EVAP(338.4)	11.320	3.760	W83	W83	W83		
Sr	380990	0.6000	0.1290	0.1110	5	meas.	EVAP(179.6)	7.950	5.820	W83	W83	W83		
Y	390990	1.4000	2.0200	1.4500	4	meas.	EVAP(213.8)	7.570	4.552	W81	W81	W81		
Rb	371000	0.0984	4.9500	1.0200	6	meas.	EVAP(339.4)	13.733	6.053	MN	W81	W81		
Sr	381000	0.6180	0.7430	0.0860	5	meas.	EVAP(174.9)	6.700	4.660	W83	W83	W83		
Y	391000	0.8000	0.8420	0.0990	5	meas.	EVAP(210.4)	9.900	6.950	W83	W83	W83		
Rb	371010	0.0939	28.3215	0.0000	6	sys.	EVAP(368.3)	12.310	3.178	MN	MN	W81		
Sr	381010	0.1941	2.4700	0.2800	6	meas.	EVAP(225.4)	9.026	5.605	MN	W81	W81		
Y	391010	0.6071	2.0500	0.2300	5	meas.	EVAP(249.6)	8.720	4.525	W81	W81	W81		
Sr	381020	0.2871	4.7600	2.2900	6	meas.	EVAP(237.2)	8.830	5.005	MN	MN	W81		
Y	391020	0.9000	5.9400	1.7100	4	meas.	EVAP(233.7)	10.442	6.727	MN	W81	W81		
Sr	381030	0.1196	8.8758	0.0000	6	sys.	EVAP(298.0)	11.590	5.491	MN	MN	MN		
Y	391030	0.2604	12.3656	0.0000	6	sys.	EVAP(268.5)	8.879	3.929	MN	W81	W81		
Zr	401030	1.3377	0.0242	0.0000	4	sys.	EVAP(98.1)	7.500	6.839	W81	W81	W81		
Nb	411030	1.5000	0.0137	0.0000	4	sys.	EVAP(74.4)	5.500	5.120	W83	W83	W83		
Sr	381040	0.1629	13.4698	0.0000	6	sys.	EVAP(312.7)	10.150	3.371	MN	MN	MN		
Y	391040	0.1283	8.7769	0.0000	6	sys.	EVAP(281.9)	11.890	6.382	MN	MN	W81		
Zr	401040	2.5730	0.1824	0.0000	4	sys.	EVAP(127.0)	5.846	4.728	MN	W81	W81		
Nb	411040	4.8000	0.0406	0.0000	3	sys.	EVAP(104.7)	8.700	7.940	W83	W83	W83		
Y	391050	0.1469	19.7529	0.0000	6	sys.	EVAP(312.6)	10.430	3.591	MN	MN	MN		
Zr	401050	0.4930	1.0879	0.0000	5	BETA	EVAP(179.5)	8.285	6.030	MN	W81	W81		
Nb	411050	2.8000	2.2322	0.0000	4	sys.	EVAP(180.1)	7.000	4.730	W83	W83	W83		
Y	391060	0.0894	15.6613	0.0000	6	sys.	EVAP(323.1)	13.100	5.721	MN	MN	MN		
Zr	401060	0.9071	1.5242	0.0000	4	sys.	EVAP(190.4)	7.230	4.667	MN	MN	W81		
Nb	411060	1.0000	0.9402	0.0000	4	sys.	EVAP(181.7)	10.099	7.766	MN	W81	W81		
Y	391070	0.0923	25.9442	0.0000	6	sys.	EVAP(344.0)	11.700	3.261	MN	MN	MN		
Zr	401070	0.2430	3.7127	0.0000	6	sys.	EVAP(235.9)	9.900	5.931	MN	MN	MN		
Nb	411070	0.7660	8.7806	0.0000	5	sys.	EVAP(241.7)	8.324	4.156	MN	W81	W81		
Zr	401080	0.3781	7.0302	0.0000	5	sys.	EVAP(256.8)	8.590	3.841	MN	MN	MN		
Nb	411080	0.2423	6.4669	0.0000	6	sys.	EVAP(249.5)	10.810	6.327	MN	MN	W81		
Mo	421080	1.5000	<0.0001	0.0000	4	sys.	EVAP(17.9)	5.251	5.228	MN	W81	W81		
Zr	401090	0.1300	7.3940	0.0000	6	sys.	EVAP(273.6)	10.940	5.501	MN	MN	MN		
Nb	411090	0.3154	12.6533	0.0000	5	sys.	EVAP(270.3)	9.340	4.031	MN	MN	MN		
Mo	421090	1.4090	0.1359	0.0000	4	sys.	EVAP(129.5)	8.189	6.970	MN	W81	W81		
Tc	431090	1.4000	0.0879	0.0000	4	sys.	EVAP(99.5)	5.900	5.180	W83	W83	W83		
Nb	411100	0.1298	10.0525	0.0000	6	sys.	EVAP(280.7)	11.900	6.121	MN	MN	MN		
Mo	421100	2.7720	1.3758	0.0000	4	sys.	EVAP(167.9)	6.010	3.942	MN	MN	W81		
Tc	431100	0.8300	0.6210	0.0000	4	sys.	EVAP(163.4)	9.646	7.689	MN	W81	W81		
Nb	411110	0.1718	18.3948	0.0000	6	sys.	EVAP(306.0)	10.710	3.781	MN	MN	MN		
Mo	421110	0.4664	1.0303	0.0000	5	sys.	EVAP(173.6)	8.280	6.051	MN	MN	MN		
Tc	431110	1.9824	5.6954	0.0000	4	sys.	EVAP(220.4)	8.147	4.552	MN	W81	W81		
Mo	421120	0.9754	2.0788	0.0000	4	sys.	EVAP(191.5)	7.060	4.321	MN	MN	MN		
Tc	431120	0.4314	5.2031	0.0000	5	sys.	EVAP(226.4)	10.010	6.184	MN	MN	W81		
Mo	421130	0.2287	3.7966	0.0000	6	sys.	EVAP(231.3)	9.940	5.911	MN	MN	MN		
Tc	431130	0.6524	7.1864	0.0000	5	sys.	EVAP(233.3)	8.590	4.491	MN	MN	MN		
Ru	441130	3.0000	0.0005	0.0000	4	sys.	EVAP(52.3)	7.391	7.185	MN	W81	W81		

(Continued)

TABLE III (Continued)

CS	ID	HL	Pn	dPn	GP	Pn Source		Spectra Source	QB	S(n)	Mass Tables M1	M2	M3	Norm Area 1	Norm Area 2
Tc	431140	0.2023	6.5358	0.0000	6	sys.		EVAP(251.5)	11.320	6.511	MN	MN	MN		
Ru	441140	8.1365	0.1039	0.0000	3	sys.		EVAP(107.6)	5.420	4.540	MN	MN	W81		
Rh	451140	1.7000	0.0020	0.0000	4	sys.		EVAP(62.8)	8.263	7.963	MN	W81	W81		
Tc	431150	0.2704	14.3371	0.0000	6	sys.		EVAP(278.1)	9.930	4.001	MN	MN	MN		
Ru	441150	0.8784	0.2276	0.0000	4	sys.		EVAP(136.0)	8.170	6.751	MN	MN	MN		
Rh	451150	8.3154	0.7746	0.0000	3	sys.		EVAP(140.4)	6.405	4.893	MN	W81	W81		
Tc	431160	0.1155	12.2226	0.0000	6	sys.		EVAP(293.4)	12.670	6.011	MN	MN	MN		
Ru	441160	1.7004	1.0811	0.0000	4	sys.		EVAP(167.1)	6.730	4.571	MN	MN	MN		
Rh	451160	0.9492	0.5379	0.0000	4	sys.		EVAP(154.0)	9.417	7.583	MN	W81	W81		
Tc	431170	0.1518	21.2499	0.0000	6	sys.		EVAP(309.7)	11.010	3.531	MN	MN	MN		
Ru	441170	0.3428	2.0509	0.0000	5	sys.		EVAP(202.5)	9.480	6.281	MN	MN	MN		
Rh	451170	1.2174	4.8201	0.0000	4	sys.		EVAP(200.5)	7.530	4.395	MN	MN	W81		
Ru	441180	0.6623	4.1092	0.0000	5	sys.		EVAP(216.6)	7.800	4.111	MN	MN	MN		
Rh	451180	0.3156	2.9167	0.0000	5	sys.		EVAP(208.5)	10.380	6.961	MN	MN	MN		
Ru	441190	0.1950	4.3580	0.0000	6	sys.		EVAP(237.1)	10.460	6.001	MN	MN	MN		
Rh	451190	0.4654	8.2971	0.0000	5	sys.		EVAP(234.9)	8.740	4.361	MN	MN	MN		
Pd	461190	1.7587	<0.0001	0.0000	4	sys.		EVAP(35.5)	7.160	7.060	MN	W81	W81		
Ag	471190	2.1000	<0.0001	0.0000	4	sys.		EVAP(29.7)	5.370	5.300	W81	W81	W81		
Ru	441200	0.3503	7.5652	0.0000	5	sys.		EVAP(251.2)	8.940	3.891	MN	MN	MN		
Rh	451200	0.1725	5.9282	0.0000	6	sys.		EVAP(246.2)	11.590	6.741	MN	MN	MN		
Pd	461200	3.9065	0.0068	0.0000	3	sys.		EVAP(72.3)	5.687	5.269	MN	W81	W81		
Ag	471200	1.1700	0.0015	0.0000	4	m .003		EVAP(35.5)	8.210	8.109	W81	W81	W81		
Rh	451210	0.2496	13.5677	0.0000	6	sys.		EVAP(272.9)	10.160	4.151	MN	MN	MN		
Pd	461210	0.6437	0.2722	0.0000	5	sys.		EVAP(138.0)	8.331	6.795	MN	W81	W81		
Ag	471210	0.8000	0.0753	0.0048	5	meas.		EVAP(129.4)	6.400	5.050	W83	W83	W83		
Rh	451220	0.1071	8.3012	0.0000	6	sys.		EVAP(274.3)	12.900	6.781	MN	MN	MN		
Pd	461220	1.4112	0.4377	0.0000	4	sys.		EVAP(138.0)	6.280	4.731	MN	MN	W81		
Ag	471220	1.5000	0.1840	0.0110	4	meas.		EVAP(142.8)	9.427	7.768	MN	W81	W81		
Rh	451230	0.1343	17.1070	0.0000	6	sys.		EVAP(292.8)	10.990	3.961	MN	MN	MN		
Pd	461230	0.3004	0.6897	0.0000	5	sys.		EVAP(168.2)	9.410	7.091	MN	MN	MN		
Ag	471230	0.3900	0.5450	0.0340	5	meas.		EVAP(168.8)	7.730	5.394	MN	MN	W81		
Pd	461240	0.5140	2.6986	0.0000	5	sys.		EVAP(194.9)	7.500	4.361	MN	MN	MN		
Ag	471240	0.2495	2.2881	0.0000	6	sys.		EVAP(201.9)	10.780	7.411	MN	MN	MN		
Pd	461250	0.1660	2.2664	0.0000	6	sys.		EVAP(209.0)	10.310	6.671	MN	MN	MN		
Ag	471250	0.3335	6.3167	0.0000	5	sys.		EVAP(222.0)	8.830	4.721	MN	MN	MN		
Pd	461260	0.2520	5.0310	0.0000	6	sys.		EVAP(227.8)	8.690	4.331	MN	MN	MN		
Ag	471260	0.1398	4.6380	0.0000	6	sys.		EVAP(231.4)	11.500	7.001	MN	MN	MN		
Ag	471270	0.1753	9.8629	0.0000	6	sys.		EVAP(250.2)	9.840	4.541	MN	MN	MN		
Cd	481270	0.5719	0.0101	0.0000	5	sys.		EVAP(80.0)	7.720	7.178	MN	W81	W81		
In	491270	3.7600	0.6600	0.0630	3	meas.		EVAP(105.3)	6.494	5.555	W83	W83	W83		
In	491271	1.3000	<0.0001	0.0000	4	In127		In127	0.000	0.000	In127				
Ag	471280	0.0943	6.8861	0.0000	6	sys.		EVAP(250.6)	12.050	6.691	MN	MN	MN		
Cd	481280	1.0530	0.1215	0.0000	4	sys.		EVAP(109.8)	6.049	5.021	MN	W81	W81		
In	491280	0.8400	0.0610	0.0370	4	meas.		EVAP(129.5)	9.310	7.880	W83	W83	W83		
Cd	481290	0.2987	0.1519	0.0000	6	sys.		EVAP(124.3)	8.468	7.140	MN	W81	W81		
In	491290	0.9900	2.9200	0.3700	4	meas.	(m)	BO.1R	7.600	5.390	W83	W83	W83	0.10,0.20	

(Continued)

TABLE III (Continued)

CS	ID	HL	Pn	dPn	GP	Pn Source		Spectra Source	QB	S(n)	Mass Tables M1 M2 M3	Norm Area 1	Norm Area 2
In	491291	2.5000	0.7600	2.5000	4	meas.		In129	0.000	0.000	In129		
Cd	481300	0.4767	0.9676	0.0000	5	sys.		EVAP(161.7)	7.295	5.029	MN W81 W81		
In	491300	0.5800	1.0400	0.9500	5	meas.	(m)	BO.12R	10.200	7.630	W83 W83 W83	0.12,0.22	
In	491301	0.5100	1.4800	0.1050	5	meas.		In130	0.000	0.000	In130		
Cd	481310	0.1062	4.8728	0.0000	6	sys.		EVAP(249.4)	12.068	6.635	MN W81 W81		
In	491310	0.2800	1.8400	1.0700	6	meas.		EVAP(202.2)	8.820	5.250	W83 W83 W83		
In	491311	0.1110	1.7300	0.2400	6	meas.		In131	0.000	0.000	In131		
Cd	481320	0.1357	20.5597	0.0000	6	sys.		EVAP(318.5)	11.820	2.893	MN MN W81		
In	491320	0.1200	5.3600	0.8300	6	meas.		EVAP(259.5)	13.235	7.308	MN W81 W81		
In	491330	0.1116	31.6560	0.0000	6	sys.		EVAP(332.8)	12.600	2.777	MN MN W81		
Sn	501330	1.4700	0.2549	0.0000	4	sys.		EVAP(137.2)	9.050	7.380	W83 W83 W83		
In	491340	0.0806	33.7565	0.0000	6	sys.		EVAP(349.3)	14.740	3.841	MN MN MN		
Sn	501340	1.0400	18.3000	13.9000	4	meas.	(m)	BO.1R1.62B	6.925	3.091	MN W81 W81	0.10,0.20	1.40,1.60
Sb	511340	10.2000	0.1040	0.0350	2	meas.		EVAP(100.9)	8.410	7.500	W83 W83 W83		
Sn	501350	0.4180	9.2929	0.0000	5	sys.		EVAP(237.4)	9.580	4.507	MN MN W81		
Sb	511350	1.8200	17.8700	2.1600	4	meas.	(m)	M2.075B	7.540	3.510	W83 W83 W83	1.575,2.075	
Sn	501360	0.7172	16.3918	0.0000	5	sys.		EVAP(254.4)	8.300	2.431	MN MN MN		
Sb	511360	0.8200	28.9788	3.1138	4	meas.		EVAP(234.1)	9.611	4.642	MN W81 W81		
Te	521360	19.0000	1.1400	0.4300	2	meas.	(m)	BO.07R	5.100	3.760	W83 W83 W83	0.07,0.17	
Sb	511370	0.4780	18.0322	0.0000	5	sys.		EVAP(250.9)	9.020	3.270	MN MN W81		
Te	521370	3.5000	2.6900	0.6300	3	meas.		EVAP(146.1)	7.020	5.070	W83 W83 W83		
I	531370	24.5000	6.9700	0.4200	2	meas.	(m)	M1.5R1.75B	5.885	4.025	W83 W83 W83	1.20,1.50	1.35,1.75
Sb	511380	0.1734	22.0114	0.0000	6	sys.		EVAP(280.5)	11.610	4.371	MN MN MN		
Te	521380	1.6000	6.7800	2.2600	4	meas.		EVAP(165.5)	6.432	3.913	MN W81 W81		
I	531380	6.5000	5.3800	0.4300	3	meas.	(m)	R1.92B	7.820	5.820	W83 W83 W83	1.42,1.92	
Sb	511390	0.2178	41.6934	0.0000	6	sys.		EVAP(292.3)	9.640	1.721	MN MN MN		
Te	521390	0.5800	7.9624	0.0000	5	sys.		EVAP(225.5)	9.321	4.610	MN W81 W81		
I	531390	2.3800	9.8100	0.6200	4	meas.	(m)	R1.61B	6.820	3.640	W83 W83 W83	1.30,1.60	
Te	521400	0.8938	15.4961	0.0000	4	sys.		EVAP(234.2)	7.360	2.240	MN MN W81		
I	531400	0.8600	9.2700	0.7900	4	meas.	(m)	BO.09R1.76B	9.967	5.392	MN W81 W81	0.09,0.19	1.40,1.70
Te	521410	0.2726	10.4723	0.0000	6	sys.		EVAP(243.2)	10.050	4.491	MN MN MN		
I	531410	0.4600	21.3000	3.2000	5	meas.	(m)	R1.68B	8.892	3.417	MN W81 W81	1.00,1.60	
Xe	541410	1.7200	0.0353	0.0061	4	meas.		EVAP(82.8)	6.155	5.510	W83 W83 W83		
Cs	551410	24.9000	0.0474	0.0550	2	meas.	(m)	MAINZ	5.256	4.548	W83 W83 W83		
Te	521420	0.5901	15.0790	0.0000	5	sys.		EVAP(246.4)	8.330	2.581	MN MN MN		
I	531420	0.2000	13.8601	0.0000	6	sys.		EVAP(258.2)	11.553	5.242	MN W81 W81		
Xe	541420	1.2200	0.4040	0.0380	4	meas.		EVAP(97.2)	5.040	4.146	W83 W83 W83		
Cs	551420	1.6900	0.0949	0.0940	4	meas.	(m)	MO.93B	7.320	6.210	W83 W83 W83	0.63,0.93	
I	531430	0.4010	38.4989	0.0000	5	sys.		EVAP(272.5)	8.900	1.819	MN MN W81		
Xe	541430	0.9600	3.0557	0.0000	4	sys.		EVAP(183.8)	8.510	5.289	MN W81 W81		
Cs	551430	1.7800	1.6000	0.0800	4	meas.	(m)	GO.2M1.1B	6.280	4.240	W83 W83 W83	0.10,0.30	0.80,1.10
I	531440	0.1460	15.2394	0.0000	6	sys.		EVAP(256.4)	11.280	4.971	MN MN MN		
Xe	541440	1.1000	4.6118	0.0000	4	sys.		EVAP(192.0)	7.236	3.697	MN W81 W81		
Cs	551440	1.0010	3.1300	0.1700	4	meas.	(m)	GO.2M1.175B	8.460	5.870	W83 W83 W83	0.10,0.30	0.875,1.175
I	531450	0.1934	24.0859	0.0000	6	sys.		EVAP(269.1)	9.930	2.931	MN MN MN		
Xe	541450	0.9000	6.1090	0.0000	4	sys.		EVAP(211.0)	9.191	4.886	MN W81 W81		

(Continued)

TABLE III (Continued)

CS	ID	HL	Pn	dPn	GP	Pn Source		Spectra Source	QB	S(n)	Mass Tables M1	M2	M3		Norm Area 1	Norm Area 2
Cs	551450	0.5900	13.5900	0.9000	5	meas.	(m)	GO.2M1.1B	7.800	4.240	W83	W83	W83		0.10,0.30	0.80,1.10
Xe	541460	0.5627	6.5048	0.0000	5	sys.		EVAP(212.4)	8.122	3.732	MN	W81	W81			
Cs	551460	0.3400	13.3000	1.7200	5	meas.	(m)	M1.3B	9.410	5.130	W83	W83	W83		1.00,1.30	
Ba	561460	2.0000	0.0100	0.0000	4	m .02		EVAP(65.4)	4.270	3.770	**					
La	571460	11.0000	0.0035	0.0000	2	m .007		EVAP(22.5)	6.650	6.591	MN	MN	MN			
Xe	541470	0.1991	8.7056	0.0000	6	sys.		EVAP(233.5)	10.151	4.810	MN	W81	W81			
Cs	551470	0.5460	26.1000	2.5000	5	meas.	(m)	M1.8B	8.880	4.240	W83	W83	W83		1.40,1.80	
Ba	561470	1.7550	0.0210	0.0020	4	meas.		EVAP(20.2)	5.710	5.670	W83	W83	W83			
La	571470	5.0000	0.0330	0.0060	3	meas.		EVAP(85.1)	5.190	4.480	W83	W83	W83			
Cs	551480	0.2056	25.1000	2.8000	6	meas.		EVAP(246.8)	11.777	5.766	MN	W81	W81	#		
Ba	561480	3.3250	0.0060	0.0020	3	meas.		EVAP(62.9)	5.400	5.010	W83	W83	W83			
La	571480	1.3000	0.1330	0.0100	4	meas.		EVAP(42.7)	6.500	6.320	W83	W83	W83			
Cs	551490	0.2442	32.7567	0.0000	6	sys.		EVAP(269.7)	9.420	2.195	MN	MN	W81			
Ba	561490	0.6950	0.5750	0.0840	5	meas.		EVAP(157.0)	7.800	5.350	W83	W83	W83			
La	571490	2.4080	1.0600	0.1400	4	meas.		EVAP(107.6)	6.100	4.950	W83	W83	W83			
Cs	551500	0.1238	15.0881	0.0000	6	sys.		EVAP(254.1)	11.480	5.021	MN	MN	MN			
Ba	561500	0.9620	10.9278	0.0000	4	sys.		EVAP(205.8)	6.740	2.504	MN	MN	W81			
La	571500	0.6080	0.3991	0.0000	5	sys.		EVAP(114.9)	7.620	6.300	W83	W83	W83			
Ba	561510	0.3327	3.7569	0.0000	5	sys.		EVAP(187.8)	8.760	5.211	MN	MN	MN			
La	571510	0.7194	6.5495	0.0000	5	sys.		EVAP(188.6)	7.670	4.089	MN	MN	W81			
Ba	561520	0.4205	5.7209	0.0000	5	sys.		EVAP(198.7)	7.680	3.681	MN	MN	MN			
La	571520	0.2850	6.0393	0.0000	6	sys.		EVAP(198.4)	9.650	5.661	MN	MN	MN			
La	571530	0.3258	10.6885	0.0000	5	sys.		EVAP(215.5)	8.640	3.901	MN	MN	MN			
Ce	581530	1.4688	0.6219	0.0000	4	sys.		EVAP(126.6)	7.040	5.404	MN	MN	W81			
La	571540	0.1493	10.2702	0.0000	6	sys.		EVAP(227.2)	10.680	5.381	MN	MN	MN			
Ce	581540	2.0161	0.6373	0.0000	4	sys.		EVAP(127.1)	6.030	4.371	MN	MN	MN			
Pr	591540	1.0614	0.1110	0.0000	4	sys.		EVAP(94.0)	7.575	6.668	MN	W81	W81			
La	571550	0.1540	16.7592	0.0000	6	sys.		EVAP(242.7)	9.600	3.511	MN	MN	MN			
Ce	581550	0.5278	1.6004	0.0000	5	sys.		EVAP(156.1)	8.050	5.531	MN	MN	MN			
Pr	591550	1.1224	1.5427	0.0000	4	sys.		EVAP(140.6)	6.790	4.746	MN	MN	W81			
Ce	581560	0.5963	2.9922	0.0000	5	sys.		EVAP(170.4)	7.000	3.981	MN	MN	MN			
Pr	591560	0.3793	2.7170	0.0000	5	sys.		EVAP(164.3)	8.780	5.971	MN	MN	MN			
Ce	581570	0.2144	4.4528	0.0000	6	sys.		EVAP(192.5)	9.050	5.171	MN	MN	MN			
Pr	591570	0.3800	6.3874	0.0000	5	sys.		EVAP(185.7)	7.750	4.141	MN	MN	MN			
Pr	591580	0.1685	6.4230	0.0000	6	sys.		EVAP(198.9)	9.810	5.641	MN	MN	MN			
Nd	601580	2.6949	0.0053	0.0000	4	sys.		EVAP(56.7)	4.960	4.621	MN	MN	MN			
Pr	591590	0.1806	12.3634	0.0000	6	sys.		EVAP(217.4)	8.720	3.711	MN	MN	MN			
Nd	601590	0.6146	0.2361	0.0000	5	sys.		EVAP(108.6)	7.090	5.841	MN	MN	MN			
Pm	611590	3.0005	0.0185	0.0000	3	sys.		EVAP(62.9)	5.290	4.871	MN	MN	W81			
Nd	601600	0.7886	0.9469	0.0000	5	sys.		EVAP(131.7)	5.990	4.141	MN	MN	MN			
Pm	611600	0.7289	0.2676	0.0000	5	sys.		EVAP(103.8)	7.430	6.281	MN	MN	MN			
Nd	601610	0.3113	1.6982	0.0000	5	sys.		EVAP(154.4)	8.020	5.461	MN	MN	MN			
Pm	611610	0.7899	1.7504	0.0000	5	sys.		EVAP(135.4)	6.360	4.391	MN	MN	MN			
Pm	611620	0.3243	2.1452	0.0000	5	sys.		EVAP(151.8)	8.400	5.911	MN	MN	MN			
Sm	621640	1.3850	0.0124	0.0000	4	sys.		EVAP(63.4)	5.010	4.571	MN	MN	MN			

(Continued)

TABLE III (Continued)

CS	ID	HL	Pn	dPn	GP	Pn Source	Spectra Source	QB	S(n)	Mass Tables M1	M2	M3	Norm Area 1	Norm Area 2
Eu	631640	1.5327	<0.0001	0.0000	4	sys.	EVAP(13.2)	6.590	6.571	MN	MN	MN		
Sm	621650	0.4536	0.2491	0.0000	5	sys.	EVAP(106.1)	6.930	5.691	MN	MN	MN		
Eu	631650	1.3546	0.1911	0.0000	4	sys.	EVAP(90.4)	5.650	4.751	MN	MN	MN		

General Notes
This table contains the latest evaluated Pn values (10/86). Values indicicated as derived from systematics are based on a least squares fit of the evaluated Pn values to the parameters in the Herrmann-Kratz equation. (The current spectral file is labeled tp3final.)

CS - chemical symbol
ID - nuclide ID=10000*Z+10*A+S
HL - half life in seconds, for nuclides with EVAP spec taken from ENDF/B-V summary
Pn - probability of delayed neutron emission in percent
dPn - uncertainty in Pn value (0.0 for calculated values)

GP - indicates which of the six temporal groups the nuclide probably belongs in.

QB and S(n) are in MeV

Norm Area 1 and Norm Area 2 give the energy bounds in MeV that were used in normalizing the spectra that were joined at the energies indicated under spectra source where energies are also in MeV and

B - BETA Code
G - Greenwood and Caffrey experimental data
M - Mainz group experimental data (K. Kratz and progress reports)
R - Rudstam (Studsvik) experimental data
E - Evaporation model

M1 source of mass of Z,A
M2 source of mass of Z+1,A
M3 source of mass of Z+1,A-1

MN - Moller-Nix
W81 - Wapstra81
W83 - Wapstra83

If the spectrum source is "EVAP" the temperature parameter in KeV is given in parentheses.

** A fictitious S(n) was given this nuclide to obtain a positive energy window. Moller-Nix masses give negative energy window, however this precursor has a measured Pn value.

Most evaporation spectra were calculated using W81 or MN masses; some nuclides do have Wapstra83 masses available. W83 masses agree with those used to calculate this evaporation spectra (in terms of energy difference) with the exception of those indicated by #. [For #Cs148 the W81 values give an energy window 0.411 MeV larger than the W83 masses (QB=10.92,S(n)=5.6,Pn=6.9075)]

The systematic Pn values are from the Kratz-Herrmann equation using Fred Mann's fit for a and b from the Birmingham meeting Sept. 1986 a=54.0 b=3.44 .

masses 271 of the ~1300 fission product nuclides have been identified as delayed neutron precursors and are included in this evaluation.

Several (~33) low mass nuclides have also been identified as delayed neutron precursors (see Ref. 71) but are not of interest here because we are concerned only with delayed neutrons produced from the decay of fission products.

Recall that the precursor approach to calculating delayed neutrons requires fission yields, emission probabilities, and energy spectra for each precursor nuclide. The fission yields used in this work have been taken from a preliminary ENDF/B-VI evaluation as discussed in Chapter III.

DELAYED NEUTRON EMISSION PROBABILITIES

Methods to determine P_n values from systematics have also been discussed in Chapter III. This section will discuss experimentally measured P_n values and will describe a recent evaluation performed by F. M. Mann of the Hanford Engineering Development Laboratory in Richland, Washington.[8,46] The Mann evaluation[8] is the source of experimental P_n values used in the final compilation, as well as the fitted parameters used to calculate P_n values from the Kratz-Herrmann equation [Eq. (11)]. Reference 8 also provides an excellent review of measured P_n values as of the end of 1985. These data along with some revisions and additions to include all data published as of mid 1986 are given in Appendix C.

The procedure used by Mann to evaluate the P_n's involves more than simply calculating a weighted average of the experimental values as is the more common practice.[74,75,76] In the cases that the measured P_n was reported in the literature as an upper limit, the value used in the Mann evaluation was taken as one-third the limit and its uncertainty, two-thirds the limit. An attempt was made to include correlations among experiments by introducing a normalization factor for each laboratory as in the following equations;

$$\begin{aligned} \lambda_i P_n^j &= M_{ij} \pm \Delta M_{ij} \\ \lambda_i &= 1 \pm \Delta_i \ , \end{aligned} \tag{16}$$

where

$$\begin{aligned}
\lambda_i &= \text{normalization factor for laboratory } i \\
P_n^j &= \text{emission probability for precursor } j \\
M_{ij} &= \text{measured } P_n \\
\Delta M_{ij} &= \text{uncertainty in measured } P_n \\
\Delta_i &= \text{estimate of the normalization uncertainty.}
\end{aligned}$$

The first of these equations introduces the normalization factor, λ_i, indicating the possibility of systematic error; as represented by the second equation, these normalization factors are unity within some uncertainty, Δ_i, reflecting a laboratory bias. The model equations given as Eq. (16) were then linearized and values for log P_n and log λ_i were determined using least squared techniques for the 62 precursors with more than one measurement (see Appendix C for experimental data).[46] Mann states that this procedure is very sensitive to values far from the average so experimental values more than five standard deviations from the fitted log P_n have had their uncertainties increased by a factor of ten to reduce the sensitivity of the analysis to these outlying values.[8,46] These values are noted in Appendix C.

Appendix C also indicates which measurements are relative values; i.e. measurements of delayed neutrons per fission must be divided by a "known" fission yield to derive a P_n value, some values are normalized to other emission probabilities and others are normalized to gamma activity. These relative measurements were updated using preliminary ENDF/B-VI yields,[48] the updated weighted average emission probability for the reference precursor and ENDF/B-V branching ratios, respectively. Isotopes having P_n values derived only from measurements of delayed neutrons per fission (^{85,86,87}As, ^{92}Br, and ^{136}Sb) were fit as delayed neutrons per fission and then converted to emission probabilities. In those cases where measurements were mixed (some measured relative to a yield, P_n value, or gamma activity and one or more direct determinations), all values were converted to emission probabilities prior to the fit.

The resultant, or "recommended", P_n values and laboratory bias factors from Ref. 8 are also reproduced in Appendix C. Two minor errors have been corrected in the table of recommended emission probabilities:

1. The data for ^{89}Se should not have been denoted as neutrons per fission since the value given ($7.7 \pm 2.4\%$) is itself a P_n value.

2. Footnote (a) was changed to read "values given as neutrons per 10000 fissions."

The evaluation described above provided the 89 P_n values based on measurements that are included in the current precursor data base. The Mann evaluation of delayed neutron emission probabilities also included a fit to the Kratz-Herrmann equation [Eq. (11)] to determine the free parameters "a" and "b". In this parameter determination, Mann used only the "recommended" P_n values whose uncertainties were less than ten percent, the resulting values given below were applied in conjunction with the mass values discussed earlier to calculate the remaining 182 emission probabilities contained in the current data base as given in Table III.

$$a = 54.0^{+31.0}_{-20.0}$$
$$b = 3.44 \pm 0.51$$

The uncertainties for these calculated emission probabilities were arbitrarily set to 100%.

CHAPTER V.

EVALUATION OF PRECURSOR SPECTRA

One of the major objectives in this dissertation was to improve the spectral data for the individual precursors. Methods for calculating delayed neutron spectra from theory, as well as systematics have already been discussed. (See Chapter III.) This chapter is concerned with the various aspects of the evaluation procedure that pertain to the spectra. A review of measurement techniques, the principal groups involved in the measurements, as well as arguments and techniques involved in determining the final set of experimental spectra for the thirty-four precursor nuclides will be presented. The next step in the spectra evaluation involves augmentation with theoretical models and this will be discussed next. A detailed synopsis of experimental spectra used for individual precursor nuclides is included in Appendix D.

MEASUREMENT TECHNIQUES

There are three primary neutron detection techniques used to study delayed neutron spectra. These are ^{3}He spectrometry, proton-recoil detectors and neutron time-of-flight measurements. A brief review and quantitative intercomparison of each of these in terms of understanding and interpreting the quality of the data follows.

^{3}He Spectrometry

The majority of the delayed neutron spectral measurements have been made using ^{3}He gas-filled ionization chambers, where the basic reaction used to detect neutrons is:[77]

$$ {}^3_2He + {}^1_0n \longrightarrow {}^3_1H + {}^1_1p + 763.8\,\text{keV} \ . \tag{17} $$

This type of detector and its application to the measurement of delayed neutron spectra has been discussed extensively in the literature.[6,26,77–82] The primary advantages of these detectors are their overall efficiency and energy resolution

over a broad energy range (above ~400 keV they have the best available energy resolution)[77] as seen in Fig. 8. Another characteristic of these detectors is that monoenergetic neutrons will appear as peaks in the spectra, occurring at energies equal to the neutron energy plus the Q-value of the reaction (763.8 keV). The relatively high Q-value provides yet another bonus in that the gamma background will appear at a lower energy (< 763.8 keV) than the neutron distribution.

Of course, there are also disadvantages to this detection method. The $^3\mathrm{He}(n,p)^3\mathrm{H}$ reaction has a large thermal cross section, ~5330 barns, which makes these detectors quite sensitive to thermal neutrons resulting in an inevitable thermal neutron background peak which obscures the low energy portion of the delayed neutron spectrum.[77] Typically this background peak has a full width at half maximum (FWHM) of ~12 keV.[80] Another disadvantage is the effect of competing reactions like elastic scattering of the neutrons from the helium nuclei. This competition becomes more prominent at the higher neutron energies. For example, at a neutron energy of 150 keV, the cross sections are equal, but at 2 MeV elastic scattering is about three times more probable than the (n,p) reaction.[77] There is also a competing (n,d) reaction possible for neutron energies above ~4.3 MeV; however the cross section is low for neutron energies less than ~10 MeV, and therefore, is not considered in this application. There are also the usual wall effects. These "disadvantages" can be overcome by the use of pulse shape discrimination techniques and simply careful experimental procedure.[83] The net effect being that the quality of the neutron spectrum relies heavily on the accurate determination of the detector efficiency and the response function used to unfold the pulse height spectrum.

Proton-Recoil Counters

Proton-recoil proportional counters have also been used to determine the energy spectra of delayed neutrons from fission.[32,84–86] These spectrometers measure the energy of recoil protons which result from neutron elastic scattering from ordinary hydrogen. By definition, the Q-value for elastic scattering is zero, and therefore, the total kinetic energy after the reaction is the same as before.

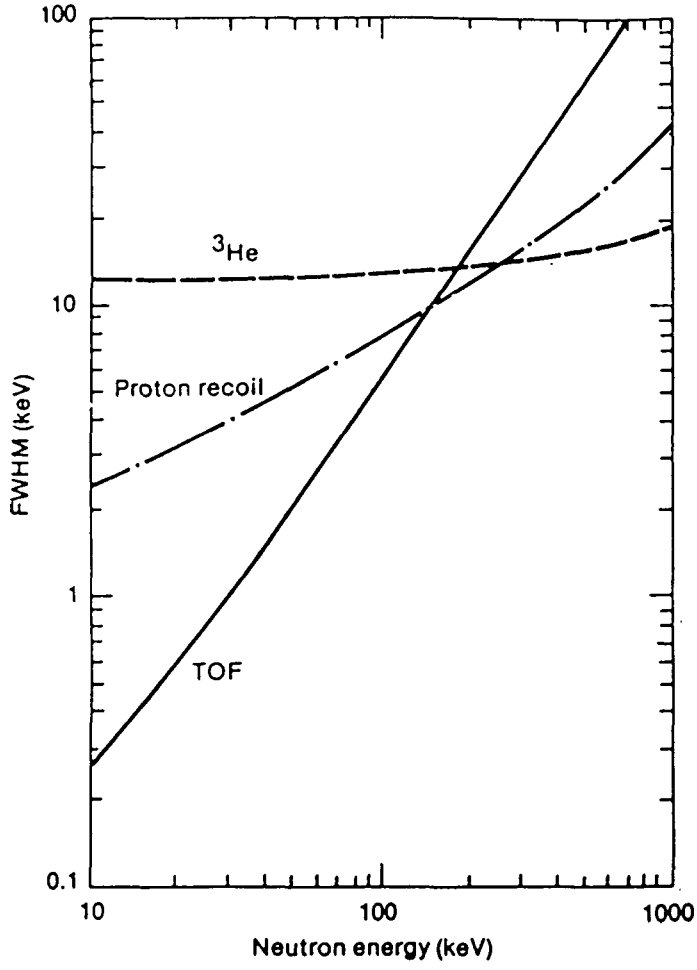

Fig. 8. Energy resolution for neutron detection methods. Ref. 80.

The target nuclei are considered at rest, thus the kinetic energy of the incident neutron must be shared between the recoil nucleus (proton) and the scattered neutron; the fraction given to the recoil nucleus being uniquely determined by the scattering angle. Over the energy range of interest, the recoil protons have an isotropic angular distribution in the center-of-mass system. One advantage of this type of detection system is its superior energy resolution compared to ^{3}He spectrometers at energies < 200 keV (Fig. 8). Insensitivity to thermal neutrons is a second positive attribute in β-delayed neutron spectroscopy. Also, in this case, knowledge of the response correction is not critical for neutron energies where the wall and end effects are not excessive.[77] Detection efficiency can be more accurately calculated because the elastic scattering cross section for neutrons on ^{1}H is precisely known ($\pm 1\%$) over the energy range of interest.[80]

The main reason that proton-recoil detectors are not more commonly used in delayed neutron spectroscopy is their low efficiency.[6] It is also known that gamma background can obscure the lower end of the energy spectrum. Lead shielding and pulse shape discrimination must be used in order to obtain the spectral distribution below $\sim$30 keV.[32,80]

These detectors sometimes rely on reactions such as $^{14}\mathrm{N}(n,p)^{14}\mathrm{C}$ to provide data for energy calibration and the detector response must be corrected for these heavy atom recoils in obtaining the neutron spectrum. Also, it has been experimentally determined that these detectors do not provide reliable results above $\sim$2–3 MeV.[6]

Time-of-Flight Measurements

The third measurement technique, time-of-flight (TOF), is still in a relatively early stage of development with respect to its use for delayed neutron measurements. In principle the method is simple; the time of flight of a neutron ejected from a target is measured over a specified distance, giving its velocity and thus also its energy. The timing begins with the detection of the beta particle as it is emitted (which coincides within $\sim 10^{-15}$ seconds of delayed neutron emission) and stops with the detection of the neutron at the end of the flight

path. The TOF technique is the only spectrometer type where the experimentalist can essentially define the energy resolution of the system by optimizing the flight path, timing uncertainty, target thickness and the other parameters in the experimental arrangement.[6] However, the system resolution and efficiency are inversely related and generally a TOF system with acceptable energy resolution will have the poorest efficiency of the three techniques.[80] An advantage, illustrated in Fig. 8, is that these systems are capable of achieving the best energy resolution; also the measured TOF spectra are straight forwardly related to delayed neutron energy distributions making the technique very attractive for future study. From Fig. 8 it is seen that the energy resolution deteriorates rapidly with increasing neutron energy (while maintaining an acceptable detector efficiency). The published TOF spectral data identify peak energies and intensities primarily as line structure[87,88] and are for the most part, preliminary results.[89]

THE PRINCIPAL EXPERIMENTAL SPECTRA

Until recently, three groups have been involved in the measurement of delayed neutron spectra from fission product nuclides. These are the group at Studsvik headed by Gösta Rudstam, the group at the University of Mainz led by K.-L. Kratz, and the P. Reeder group at Pacific Northwest Laboratory (PNL). (Specific references are given by nuclide in Appendix D.)

The first extensive set of precursor spectra was that measured at the OSIRIS separator at Studsvik, Sweden. That work began in the early 1970s[90] and, by 1981, had resulted in the measurement of delayed neutron spectra for ~25 precursor nuclides.[64] As of 1985, the Mainz group had measured the neutron energy distributions for ~23 fission product precursors,[6,31,91] including many of the same precursors measured at OSIRIS. Using the Spectrometer for On-Line Analysis of Radionuclides (SOLAR) facility, the PNL[33] group measured spectra for only four nuclides, $^{93-95}$Rb and ^{143}Cs; all of which had been previously measured by both the Studsvik and Mainz groups.[6,64,90,92]

These three sets of measurements all utilized ^{3}He spectrometry. However, there are some significant differences in the spectra (particularly at energies less

that a few hundred keV) and in the quoted uncertainties. The Mainz measurements are considered to have the best resolution and statistical accuracy and are deferred to by the PNL group.[82]

In 1985, researchers R. C. Greenwood and A. J. Caffrey from INEL (Idaho National Engineering Laboratory), using proton-recoil proportional counters, measured neutron spectra for eight precursor nuclides.[32] The energy resolution that they obtained for energies less than 200 keV was much better than obtained using ^{3}He detectors as expected from Fig. 8. This is reflected in the small uncertainty given at these energies. The primary data sets, based on quality, quantity and uniqueness, used in this dissertation are those from Studsvik, Mainz, and INEL. The basic characteristics of each of these are summarized in Table IV. The remainder of this chapter describes the procurement and preparation of these data sets for use in this evaluation.

Studsvik Data

Professor Gösta Rudstam, one of the principal investigators at Studsvik, graciously provided a magnetic tape with normalized emission spectra, complete with uncertainties, for twenty-nine nuclides for use by T. R. England of Los Alamos National Laboratory.[28] These spectra agreed with those reported by Rudstam in Ref. 93. As noted in that reference (also in Appendix D), the spectra for ^{85}As, ^{92}Rb, and $^{96-98}$Rb have only been measured by the Mainz group[6] and are therefore referred to as Mainz spectra even though they were supplied by Prof. Rudstam. The other twenty-four spectra were from measurements made at the OSIRIS separator at Studsvik that had been reanalyzed using the method outlined in Ref. 64. These spectra typically extend over an energy range from ~100 keV to 1–2 MeV, the specific energy range of each spectrum is noted in Appendix D. Figures 9 and 10 are typical examples of these spectra with uncertainties as they were provided by Prof. Rudstam.[30] There are several data points at the ends of these spectra that do not have error bars. These points are extensions[64,78] and not experimental data. All of these data were obtained using ^{3}He spectrometry and were formatted using a 10-keV bin structure.

TABLE IV

Summary of Experimental Spectra

Studsvik measurements:

^{3}He spectrometers
On-line isotope separator
Measurements for ~25 precursor nuclides
Energy range ~ 100 keV – 2 MeV

Mainz measurements:

^{3}He spectrometers
One-line isotope separator
Measurements for ~23 precursor nuclides
Energy range ~40 keV – 3 MeV

INEL measurements:

Proton-recoil spectrometer
On-line isotope separator (TRISTAN-ISOL)
Measurements for 8 precursor nuclide
Energy range ~10 keV – 1300 keV

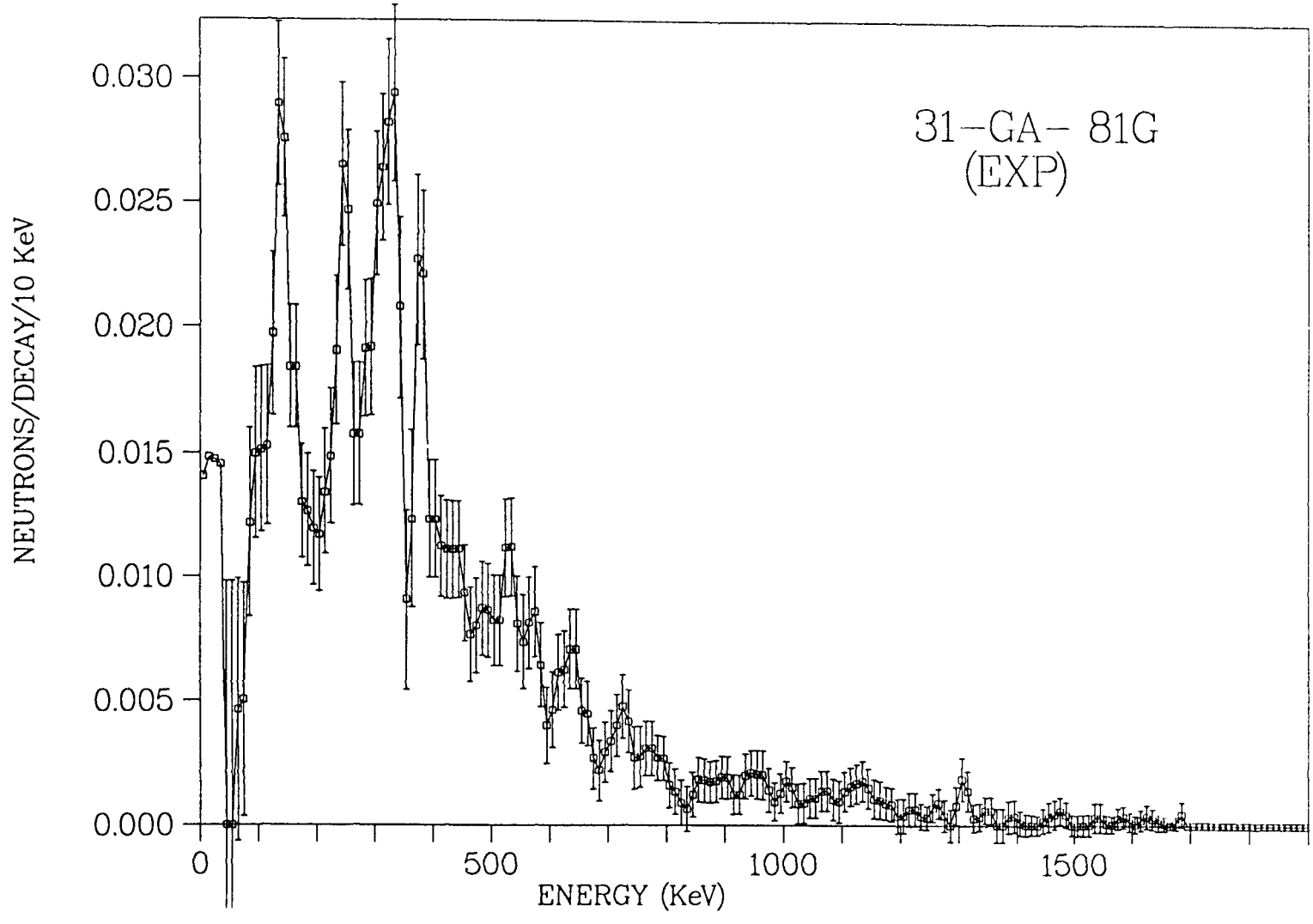

Fig. 9. Delayed neutron spectrum for ^{81}Ga (Studsvik).

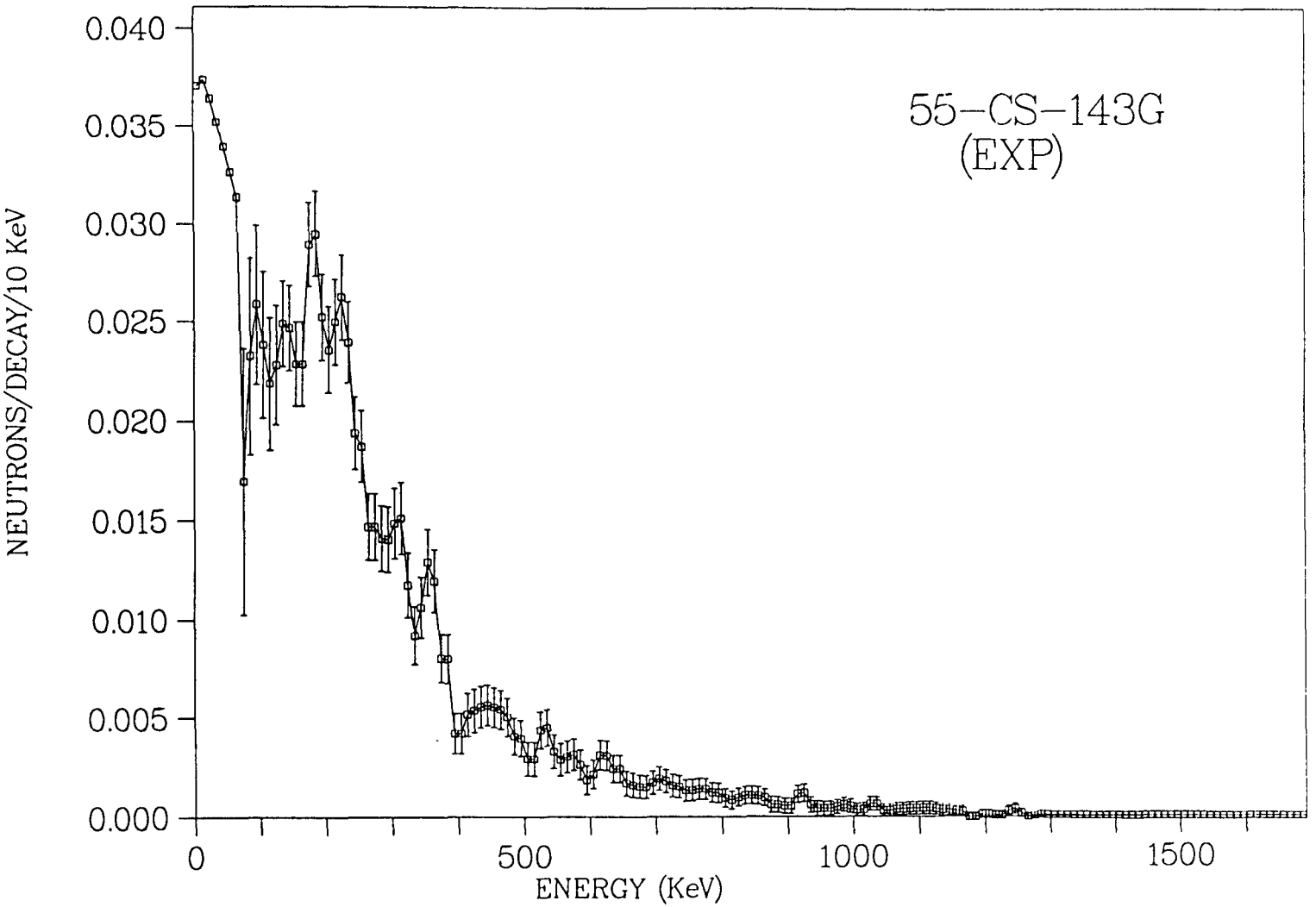

Fig. 10. Delayed neutron spectrum for ^{143}Cs (Studsvik).

Mainz Spectra

Shortly after the publication of England's 1983 article,[28] Professor K.-L. Kratz of the University of Mainz provided measured spectra for ten precursor nuclides; ^{87}Br, $^{89-92}$Br, ^{92}Rb, ^{94}Rb, and $^{96-98}$Rb. Of these, only the spectrum for ^{92}Br was unique from those reported by the Studsvik group. The spectra of $^{89-92}$Br are suspected to be the same as those reported by the ISOLDE collaboration, CERN,[91] of which Prof. Kratz was a participant.[94] As was the case with the Studsvik data, all spectra were obtained using ^{3}He spectrometry.

The data were received from Prof. Kratz as intensity (or counts) per channel with no stated uncertainties, and an energy calibration value of four keV per channel was quoted. The first task was to convert the spectra to an energy scale. This was accomplished by identifying the channel containing zero energy either by the presence of the thermal peak or as indicated by Prof. Kratz and then applying the calibration value of 4 keV/channel. The ISOLDE spectra ($^{89-92}$Br) had not been corrected for the thermal peak; for these spectra the thermal peak was used to identify the zero energy channel and in lieu of an accurate method of correcting for this peak, and on the advice of Prof. Kratz, the data below ~50 keV was ignored.

Once the ten spectra were converted to an energy scale, the data were re-binned into a normalized 10-keV structure comparable to the Studsvik data. The energy scales were checked by comparing peak energies with those found in the literature.[6,91] A typical energy range for these spectra was from ~50 keV to 2–3 MeV (depending in the precursor's energy window); specific values for the energy range of each of these spectra are also contained in Appendix D.

A few other modifications to the data were made. The spectrum for ^{97}Rb had an apparent background of ~160 counts and this was consequently subtracted from the spectrum. Also, the original data provided by Prof. Kratz did not include uncertainties. Therefore, uncertainty assignments were made based on the following information taken from a review article by K.-L. Kratz:[6]

> The errors introduced by this unfolding procedure, including all possible uncertainties in response function, efficiency, correction for scattered and

> thermal neutrons and gamma-ray pile-up, were estimated by Weaver et al. to be about 7% in the region 100 keV to 1 MeV. Below 100 keV the error is expected to be about 10%, and above 1 MeV where the counting statistics are poorer about 10 to 20%.

In the region above 1 MeV the uncertainty was taken as 15%.

A second set of Mainz spectra for thirteen nuclides was compiled from data reported in the literature. Spectra for ^{85}As, ^{93}Rb, ^{95}Rb, $^{137-138}$I, ^{135}Sb, and $^{141-147}$Cs were taken directly from the references cited in Appendix D using a digitizer in conjunction with an IBM Personal Computer. The data were then binned into the 10-keV structure and normalized to sum to 1.0.

Uncertainty assignments were made in a manner similar to those made for the set of spectra received directly from Prof. Kratz. The uncertainty in each of the three energy ranges was increased slightly (2-5%) to account for additional errors that could have resulted from digitizing. The uncertainties used are given below:

$$E < 100 \text{ keV} \quad 12\%$$

$$100 \text{ keV} < E < 1 \text{ MeV} \quad 10\%$$

$$E > 1 \text{ MeV} \quad 17\%$$

Of these thirteen spectra, four are unique from those provided by Professor Rudstam, bringing the total number of individual precursors with spectral measurements to thirty-four.

INEL (Proton-Recoil) Data

The most recently published spectra are those by R. C. Greenwood and A. J. Caffrey of INEL (Idaho National Engineering Laboratory) using proton-recoil detectors. For use here, the spectra for $^{93-97}$Rb and $^{143-145}$Cs were digitized directly from Figs. 9–16 of Ref. 32. The digitized spectra were refined to the broad group structures given in "TABLE V" (for the rubidium isotopes) and "TABLE VI" (for the cesium isotopes) of Ref. 32 for comparison and validation. Uncertainties for the spectra were inferred from the values given in Ref. 32.

EVALUATING THE PRINCIPAL EXPERIMENTAL SPECTRA

Reducing Multiple Measurements

The principal experimental spectra discussed in the previous section are indicated in bold face type in Appendix D and are the spectra referred to in the following discussion. The sixty experimental spectra collected for use in this dissertation provide data for only thirty-four precursor nuclides. Seven precursors have measured spectra from each of the three primary sources, and another twelve have spectra from two of these sources (usually Mainz and Studsvik).

The Mainz and Studsvik data sets are considered to be in fair agreement at neutron energies above a few hundred kilovolts.[6,33,95] However, the Mainz data, typically having smaller uncertainties and a broader energy range, are usually favored in this evaluation. The only notable exception to this is in the case of ^{138}I where Rudstam reports smaller uncertainties and the Mainz data is hampered by additional error introduced as a result of the digitizing procedure. The proton-recoil measurements of INEL for $^{93-97}$Rb and $^{143-145}$I are considered the most accurate of all the measurements at energies less than a few hundred keV[32] (see Fig. 8). Therefore, the primary experimental spectra (taken from the Mainz data) for these eight nuclides were combined with the proton-recoil data. This was accomplished by normalizing the INEL spectrum to the Mainz experiment over an arbitrary energy range of 100–300 keV and replacing the Mainz data from 0 to 200 keV with the normalized INEL data. The spectrum was then renormalized over the entire energy range to sum to unity.

Thus, the sixty raw spectra were reduced to thirty-four evaluated experimental spectra, one for each precursor. Of these final thirty-four, twelve are based primarily on Studsvik data and twenty-one are basically Mainz data (eight of which include the INEL data). The exception is the spectrum for ^{137}I which is a combination of both Mainz and Studsvik data. The Mainz data was used to 1.5 MeV because of its smaller uncertainties and combined with the Studsvik spectrum from 1.5–1.75 MeV due to its broader energy range. In combining the two experiments the Studsvik data was normalized to the Mainz data over the range 1.2–1.5 MeV prior to joining the two spectra at 1.5 MeV.

Augmentation With Model Spectra

Appendix D lists the theoretical energy window for each of the thirty-four nuclides with experimental spectra, as well as the energy range of the measurements. At the time of this evaluation no measured data had been reported above 3.25 MeV (^{92}Br; Ref. 91) even though the theoretical energy windows ($Q_\beta - S(n)$) were found to be as great as 8.613 MeV. Figure 11 illustrates the failure of the experimental spectra to span the energy window for delayed neutron emission. Twenty-six of the final experimental spectra (^{80,81}Ga, ^{85}As, $^{89-92}$Br, $^{93-98}$Rb, ^{134}Sn, ^{135}Sb, $^{137-141}$I and $^{142-147}$Cs) fall short of the theoretical energy window. Eight of these (^{80,81}Ga, $^{89-92}$Br, ^{134}Sn, ^{140}I) as well as the spectra for an additional four precursors (^{79}Ga, ^{129,130}In and ^{136}Te) are deficient at low energies. The gaps in the measurements for these 30 nuclides (as well as the need for spectral data for the 237 nuclides with no measured data) demonstrate the need for model calculations.

The BETA code,[7] discussed in Chapter III and Appendix B, provides a statistical model calculation of the delayed neutron spectrum given the appropriate nuclear level information for the precursor, its daughter, and granddaughter. These data were generally available from the Nuclear Data Sheets for those nuclides with measured spectral data. In the event that specific data for one of these nuclides was not available, data for a nuclide of a near mass and similar evenness or oddness were used. Appendix B contains a description and listing of the input to the BETA code for the thirty nuclides requiring extensions (at either or both the low and high energy ends) of their measured spectra.

The extensions were made as discrete steps in the evaluation process. First the experimental spectra were joined to the model at low energies and then at high energies. In each step an arbitrary area for normalization was chosen near the juncture point which was taken from the experimental data as the point at which the measured spectrum either began (low-energy extensions) or ended (high-energy extensions). The BETA model spectrum was normalized to the experiment over this range and joined to the experimental spectrum at the point defined above as the juncture. If an experiment required extensions at both low and high energies (as was the case for eight nuclides) the process

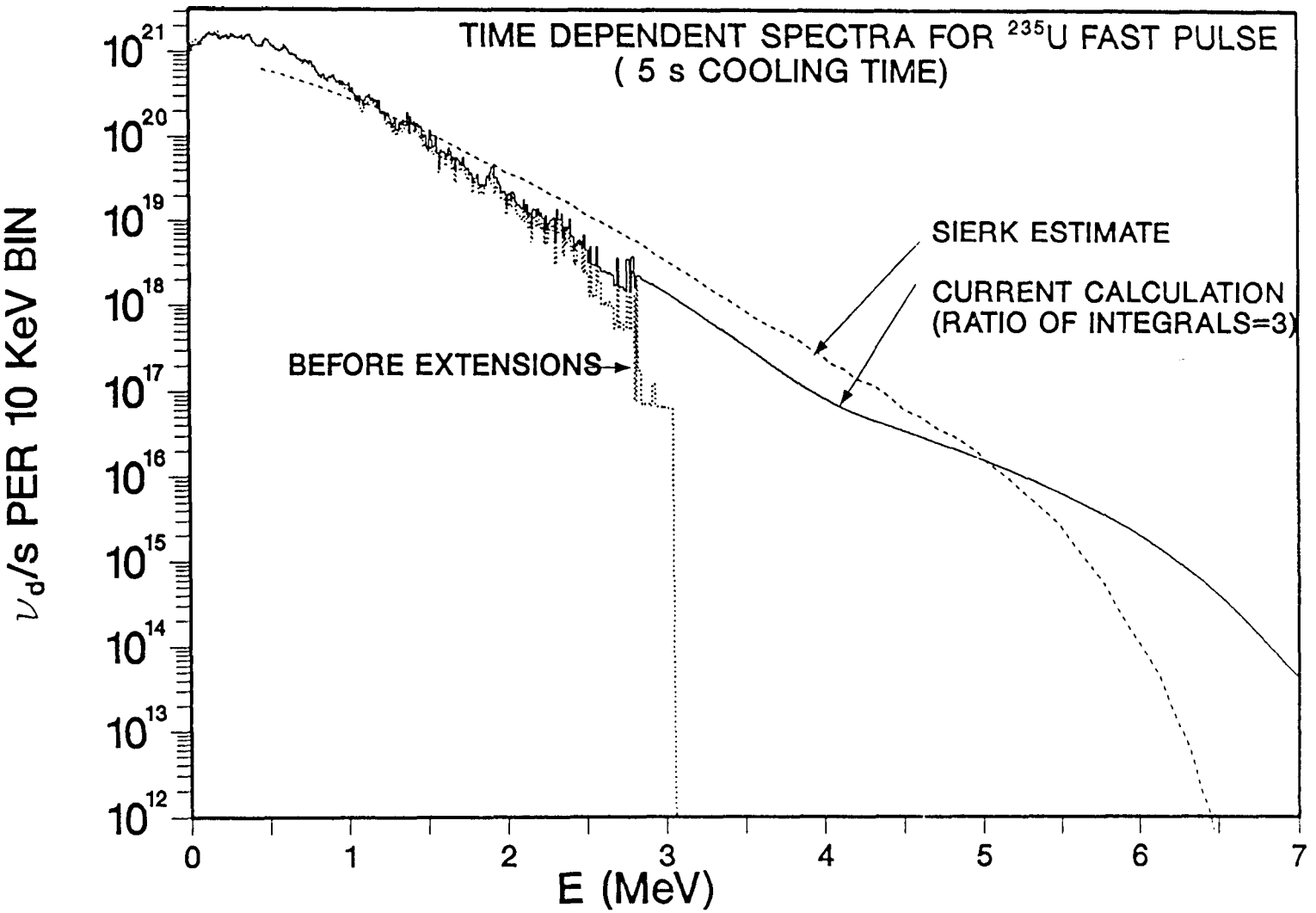

Fig. 11. ^{235}U ν_d spectra comparisons at 5 s.

was repeated at the other end of the spectrum using another normalization area associated with that juncture. After each augmentation the composite spectrum was renormalized to sum to one over the adjusted energy range.

In Table III under the column heading "Spectra Source" the information described in this chapter is given in an abbreviated form. The entry for ^{94}Rb is "(m) G0.2M2.46B" which may be interpreted as indicating a measured spectrum "(m)", which includes data from the INEL (Greenwood and Caffrey) measurements from 0 to 0.2 MeV ("G0.2"), the primary experiment is that of the Mainz group extending from 0.2 to 2.46 MeV ("M2.46") and the high energy extension was provided by data from the BETA code ("B"). The high energy tail extends to the end of the theoretical energy window which may be calculated from the Q-value for beta decay (Q_β) and neutron binding energy ($S(n)$) which are also given in Table III. A symbol "R" in the description of the spectrum source represents the data of the Studsvik group (as was supplied by Rudstam). The last two columns of Table III indicate the normalization areas used for combining the spectra. In the case of ^{94}Rb, when the INEL data was joined at 0.2 MeV it was first normalized to the Mainz data over the range given as "Norm Area 1", 0.1–0.3 MeV. Later when the high energy end of the spectrum was augmented with the BETA calculated spectrum starting at 2.46 MeV, the model spectrum was normalized to the experiment over "Norm Area 2", 2.1–2.4 MeV.

The effects of the augmentations and renormalizations of the thirty-four experimental spectra are illustrated in Figs. 12 to 45. The solid lines are the evaluated spectra as defined in Table III, and the dashed line represents the dominant experiment before any adjustments were made (also noted in Table III). In general, the effect of the augmentation and renormalization are most apparent in cases where a large (~100 keV) region at the low energy end of the spectrum had to be replaced by the model calculation, or in the eight cases where the INEL measurements were used at low energies. Use of the model spectra to extend the data to the theoretical energy window for delayed neutron emission appears to have very little effect on the overall normalization even in cases where the range is increased two-fold (for example ^{81}Ga). There are some peculiarities of the original experimental spectra that are evident from these

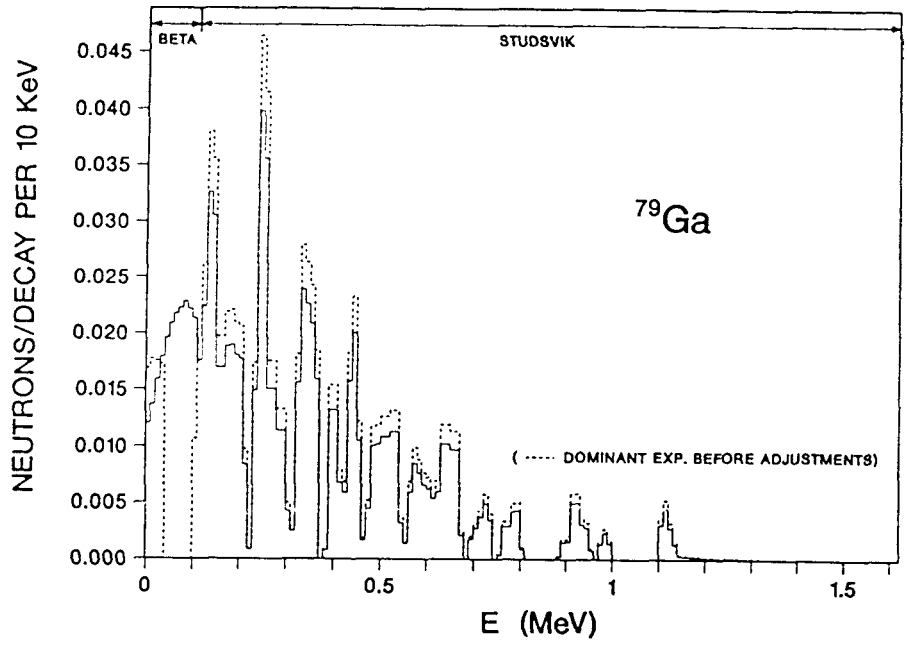

Fig. 12. Normalized delayed neutron spectra for ^{79}Ga.

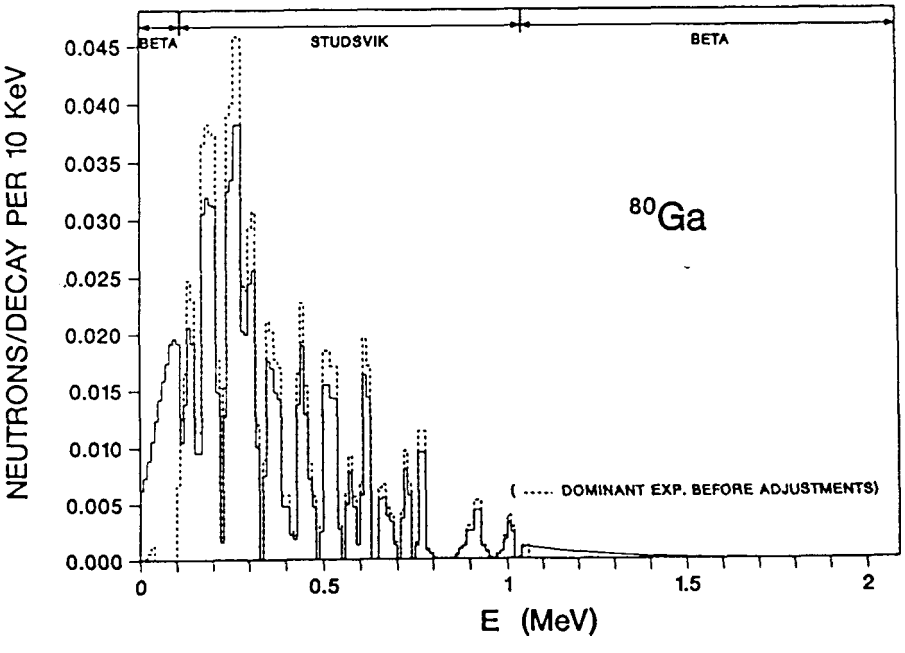

Fig. 13. Normalized delayed neutron spectra for ^{80}Ga.

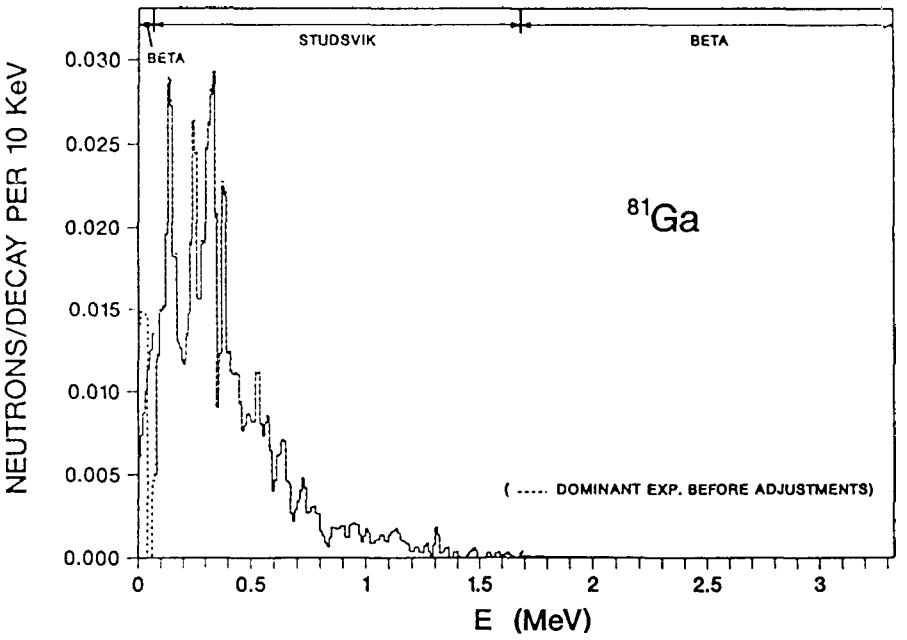

Fig. 14. Normalized delayed neutron spectra for ^{81}Ga.

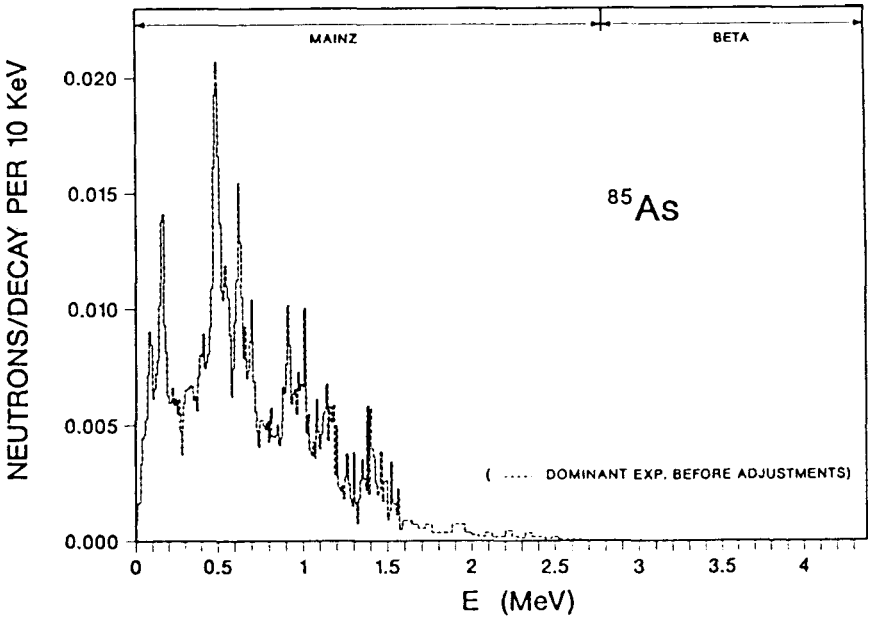

Fig. 15. Normalized delayed neutron spectra for ^{85}As.

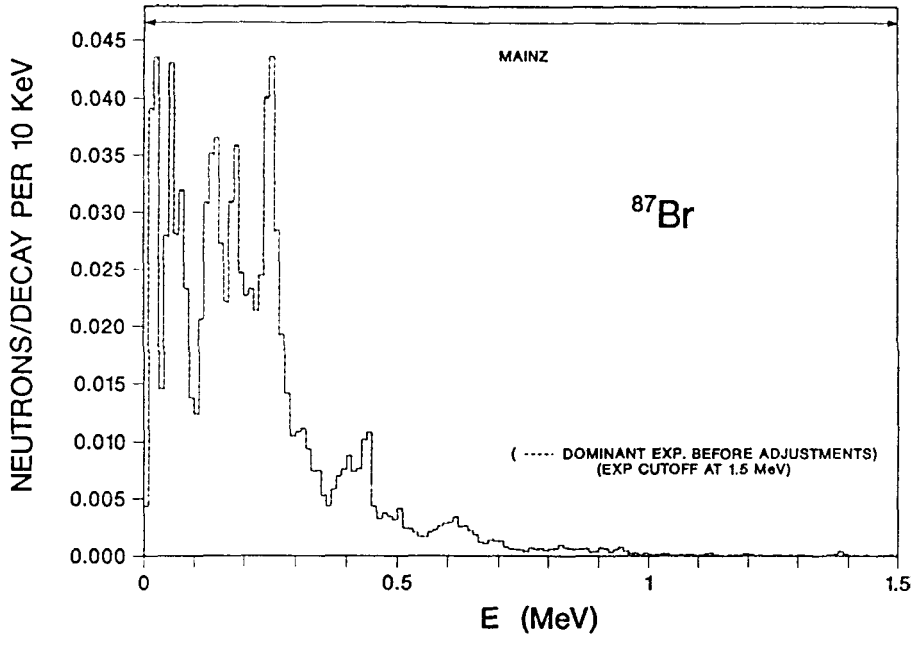

Fig. 16. Normalized delayed neutron spectra for ^{87}Br.

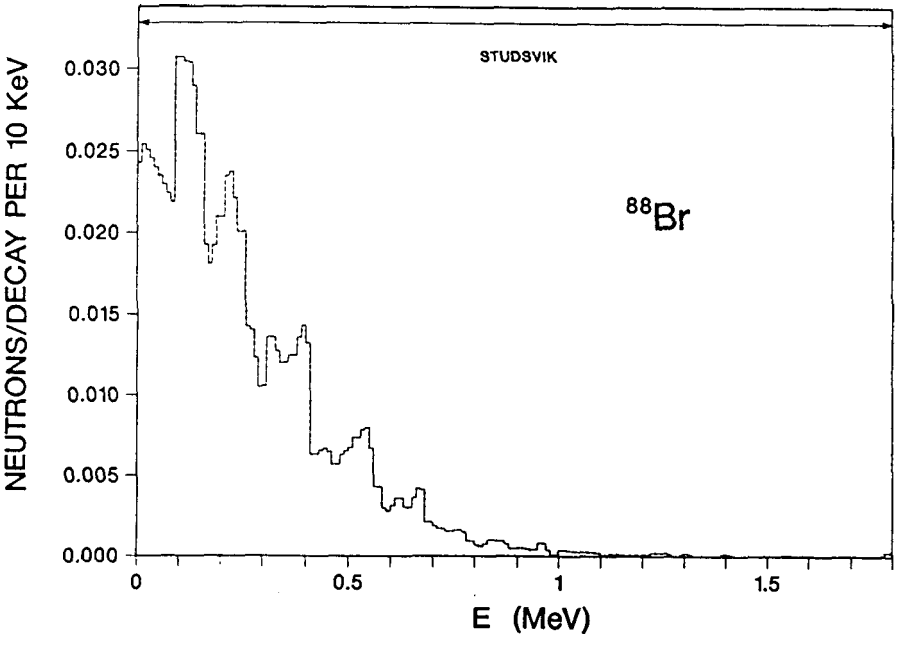

Fig. 17. Normalized delayed neutron spectra for ^{88}Br.

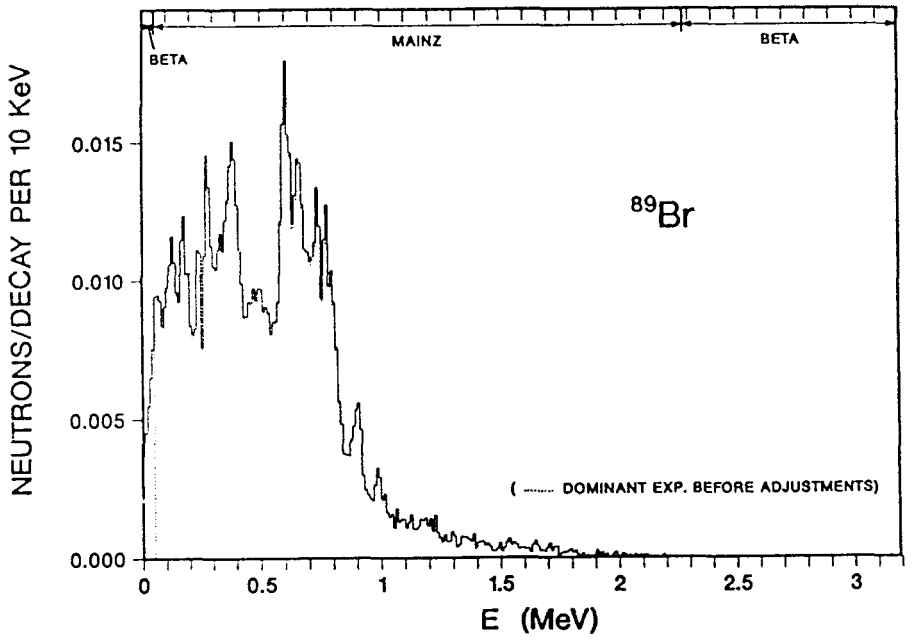

Fig. 18. Normalized delayed neutron spectra for ^{89}Br.

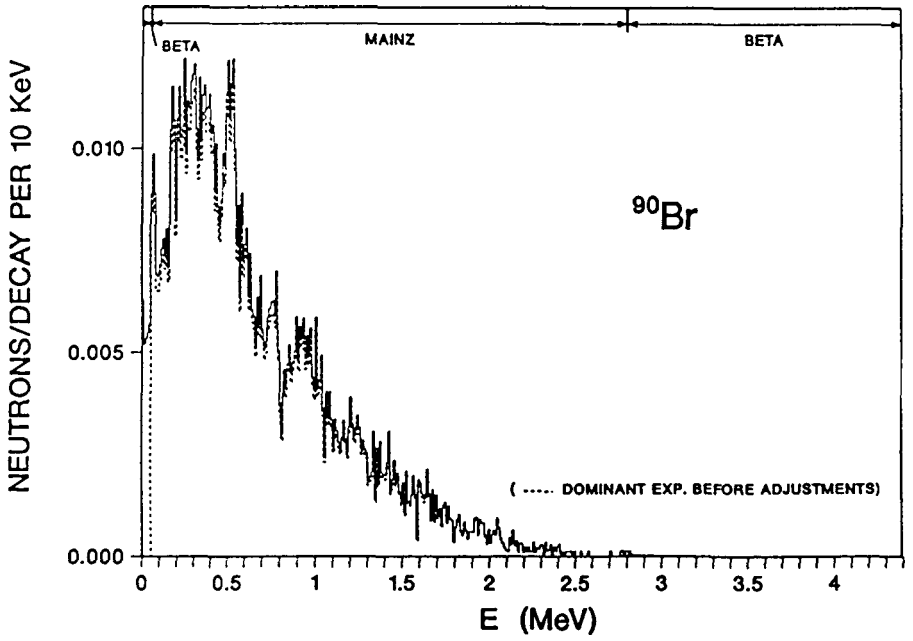

Fig. 19. Normalized delayed neutron spectra for ^{90}Br.

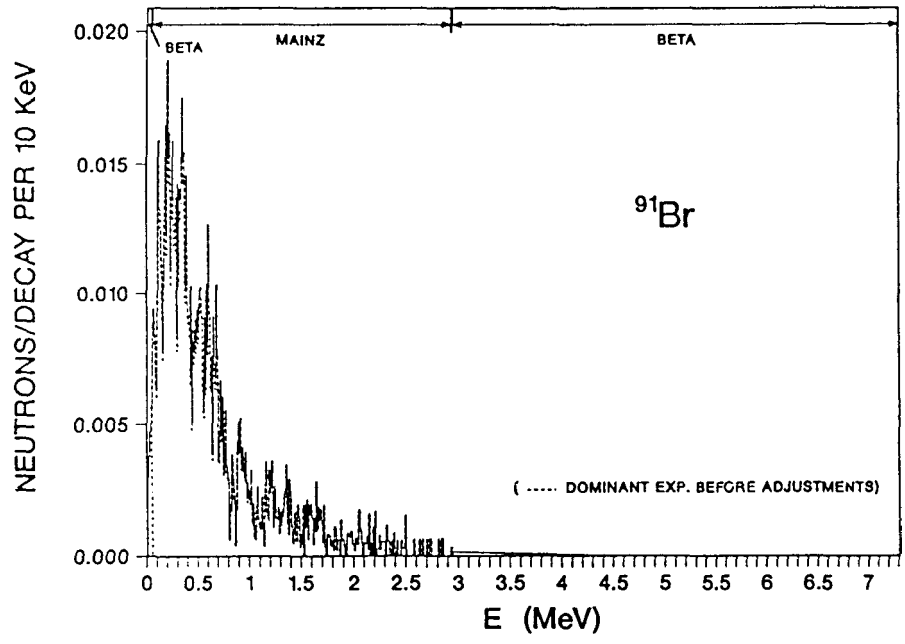

Fig. 20. Normalized delayed neutron spectra for ^{91}Br.

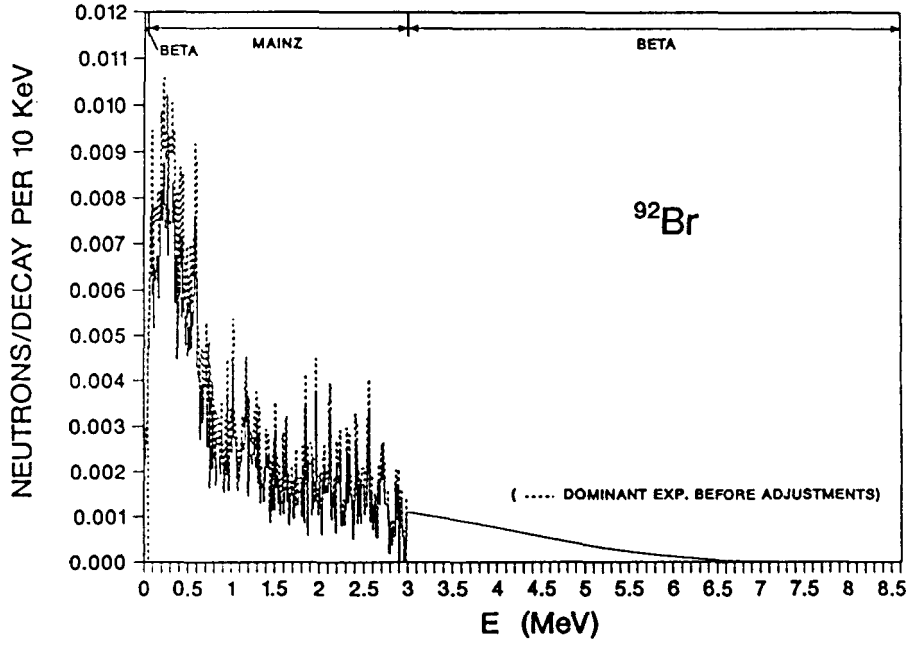

Fig. 21. Normalized delayed neutron spectra for ^{92}Br.

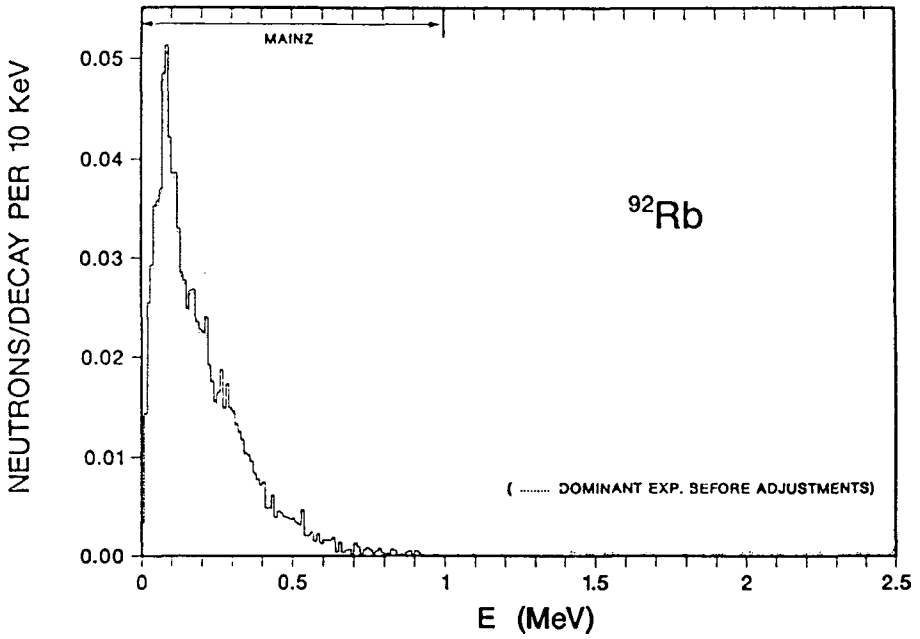

Fig. 22. Normalized delayed neutron spectra for ^{92}Rb.

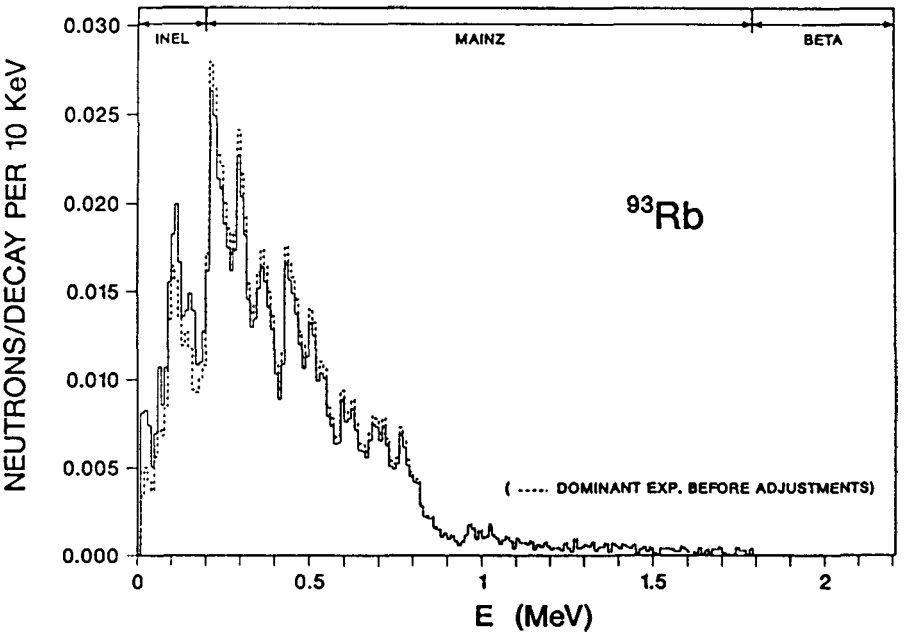

Fig. 23. Normalized delayed neutron spectra for ^{93}Rb.

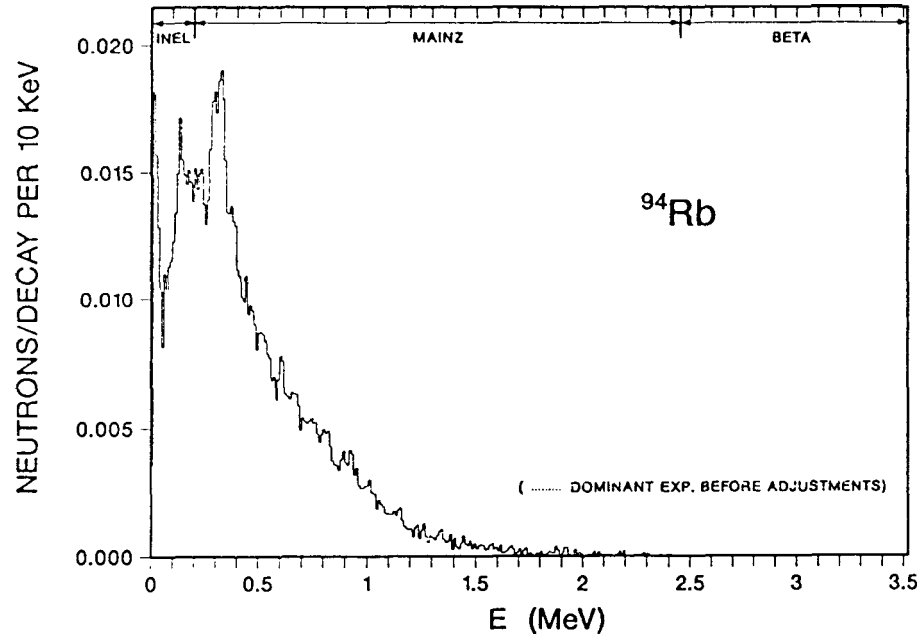

Fig. 24. Normalized delayed neutron spectra for ^{94}Rb.

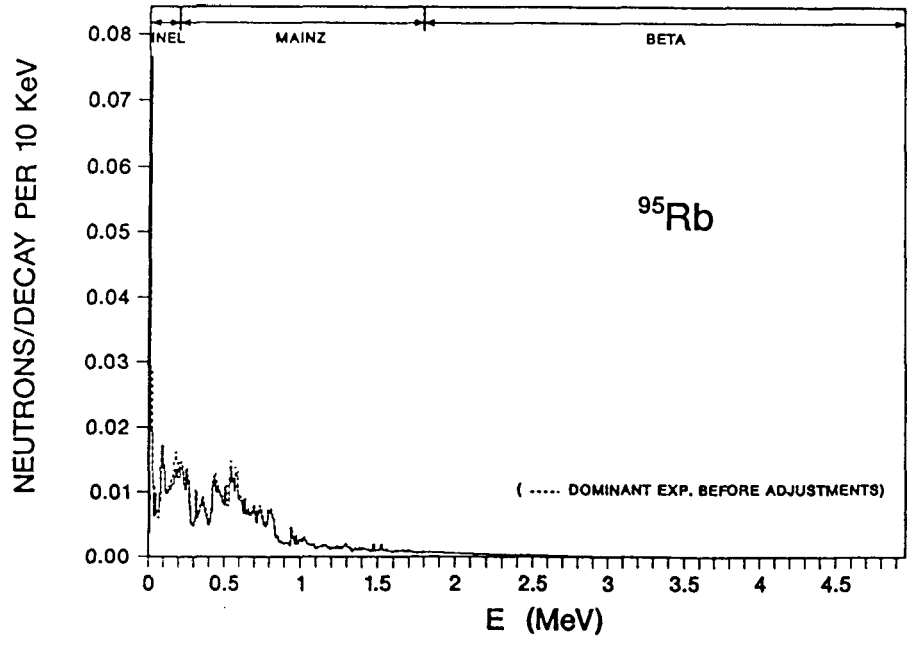

Fig. 25. Normalized delayed neutron spectra for ^{95}Rb.

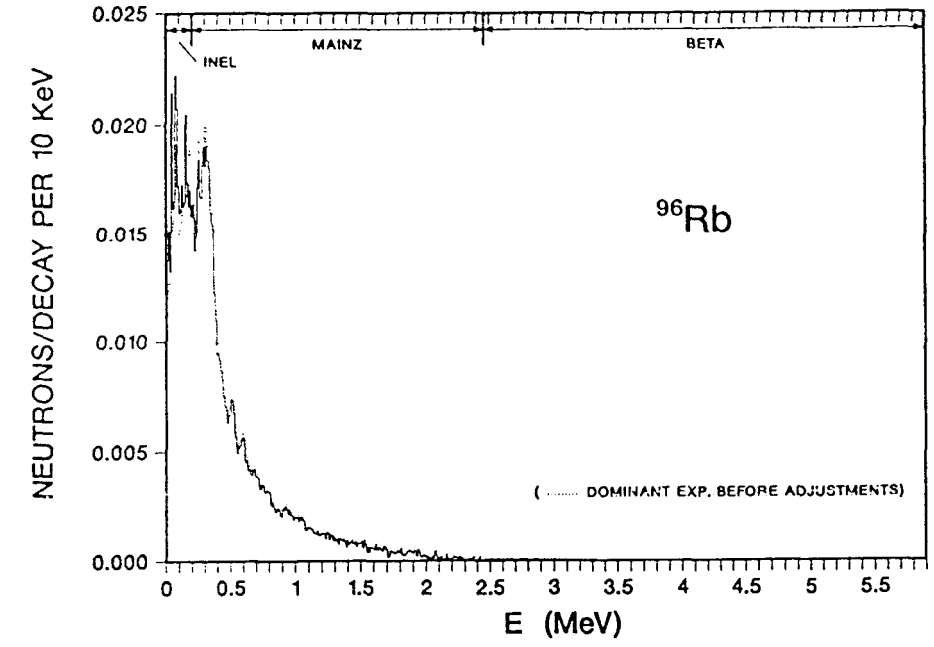

Fig. 26. Normalized delayed neutron spectra for ^{96}Rb.

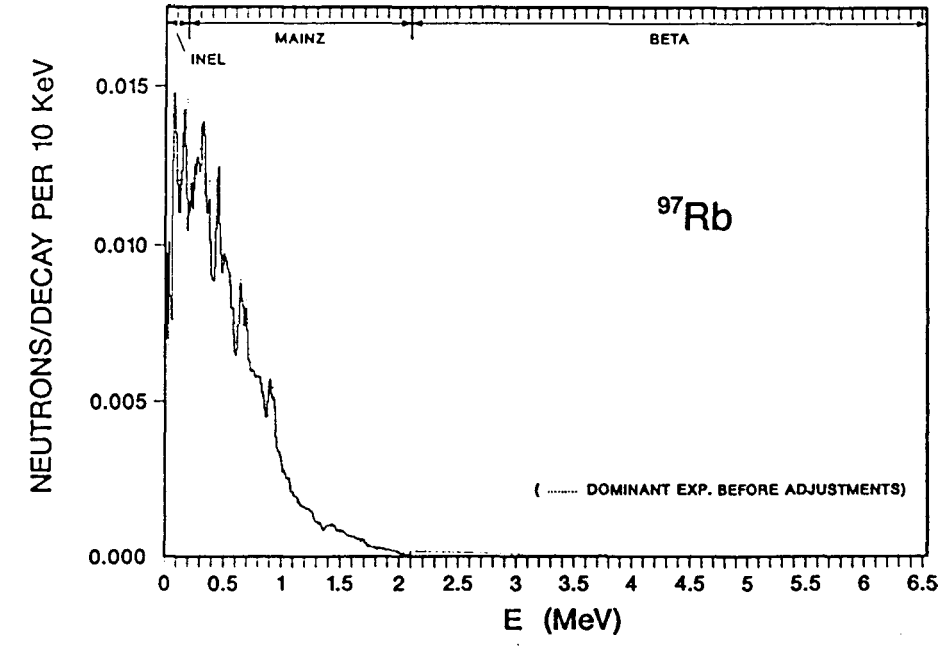

Fig. 27. Normalized delayed neutron spectra for ^{97}Rb.

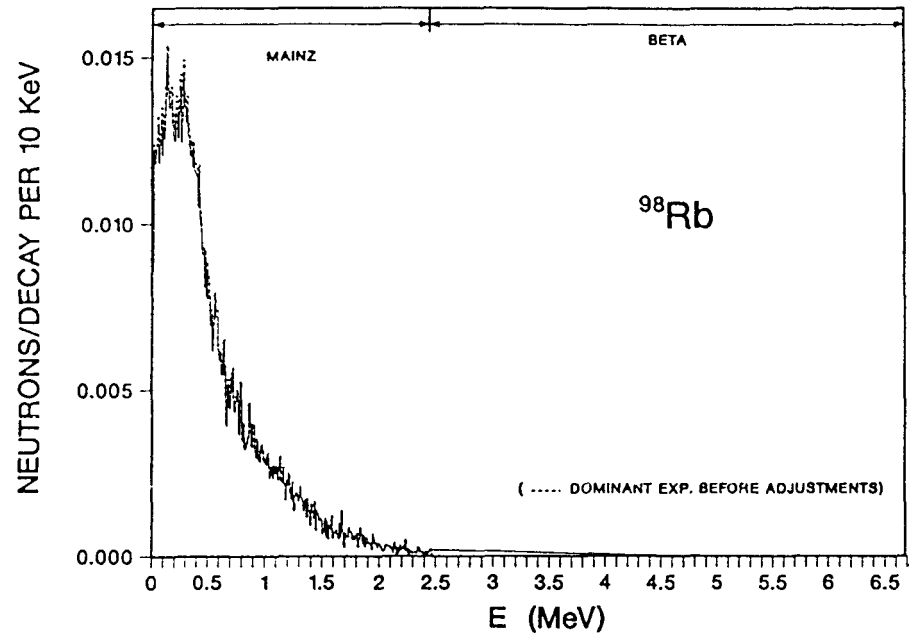

Fig. 28. Normalized delayed neutron spectra for ^{98}Rb.

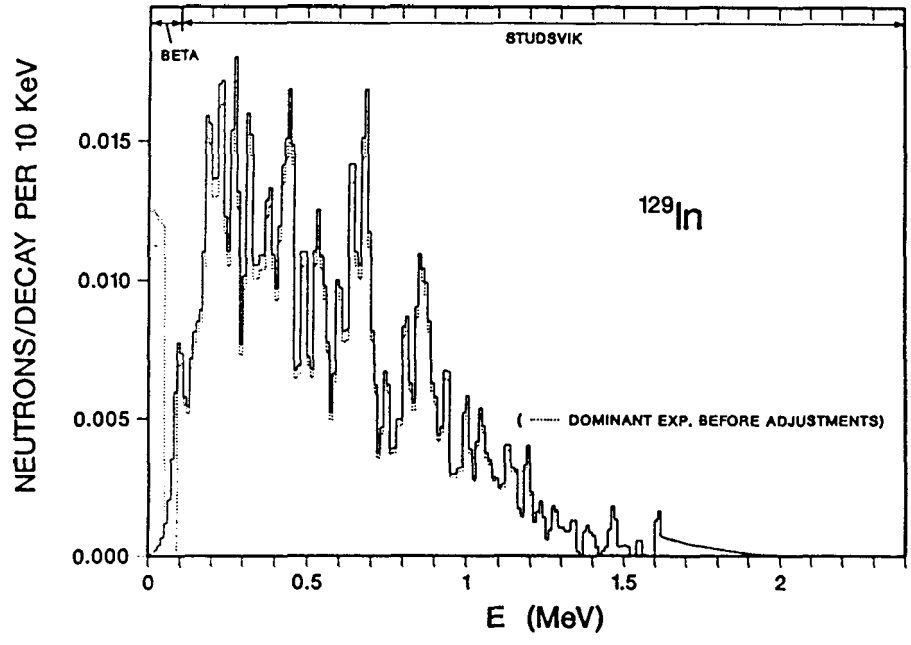

Fig. 29. Normalized delayed neutron spectra for ^{129}In.

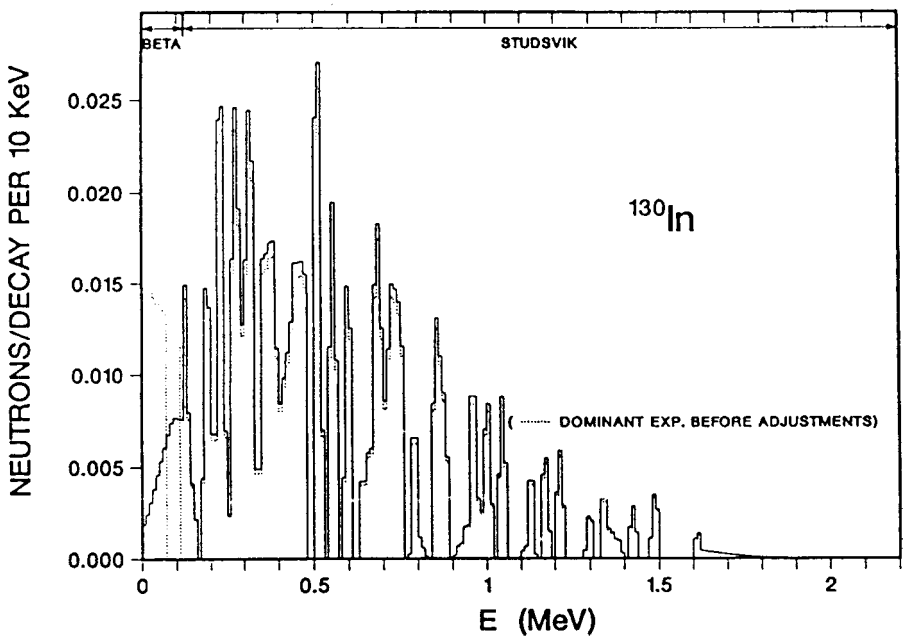

Fig. 30. Normalized delayed neutron spectra for ^{130}In.

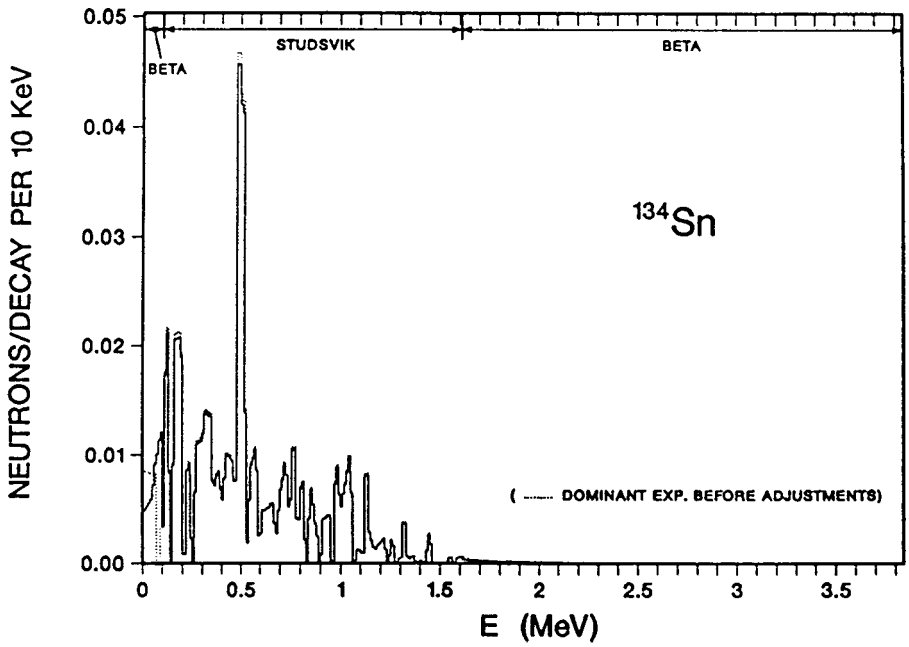

Fig. 31. Normalized delayed neutron spectra for ^{134}Sn.

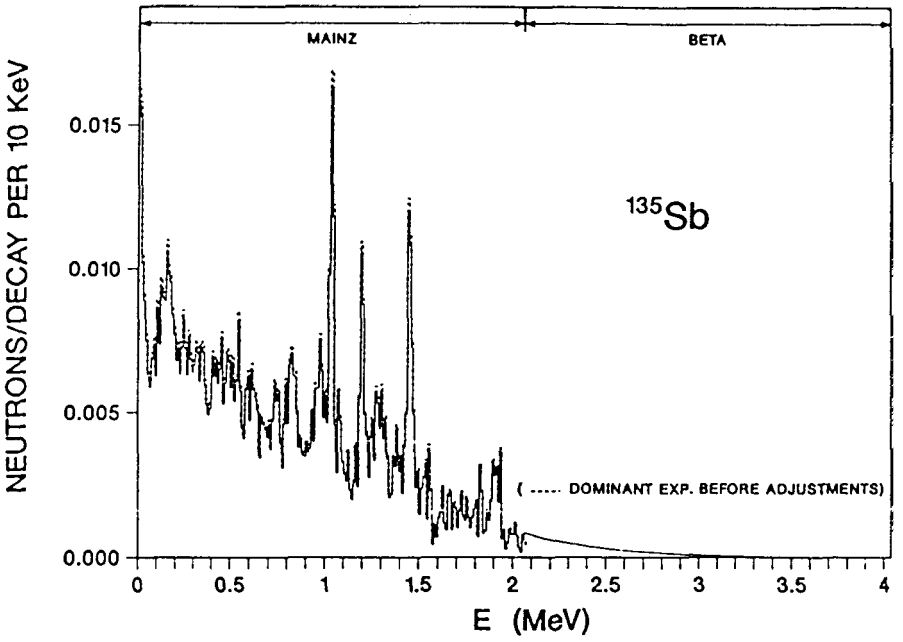

Fig. 32. Normalized delayed neutron spectra for ^{135}Sb.

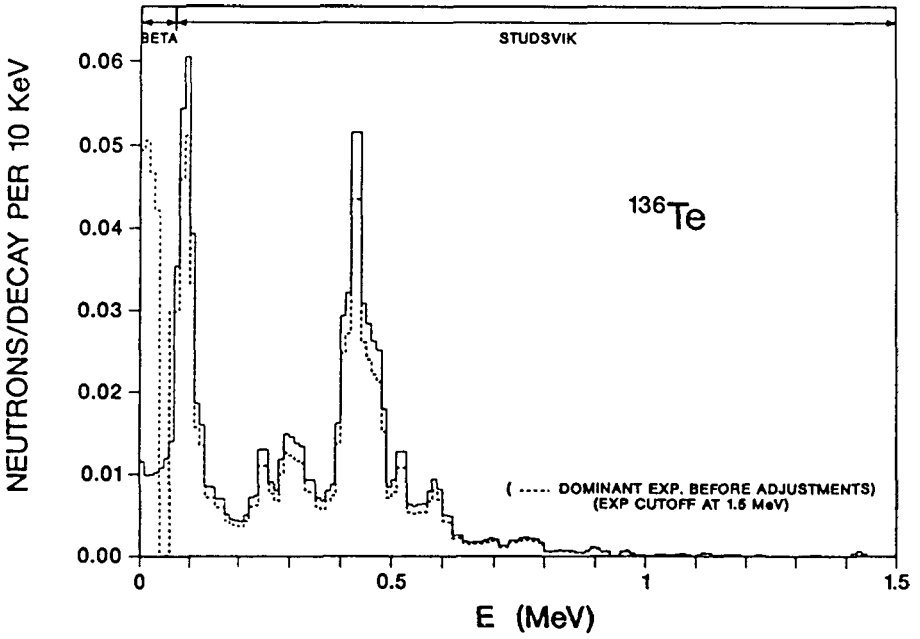

Fig. 33. Normalized delayed neutron spectra for ^{136}Te.

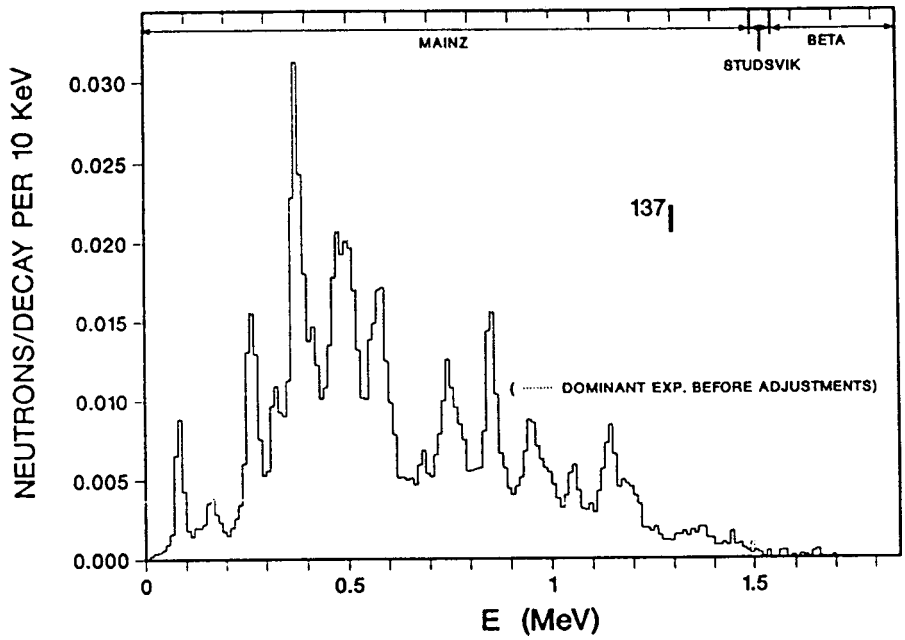

Fig. 34. Normalized delayed neutron spectra for ^{137}I.

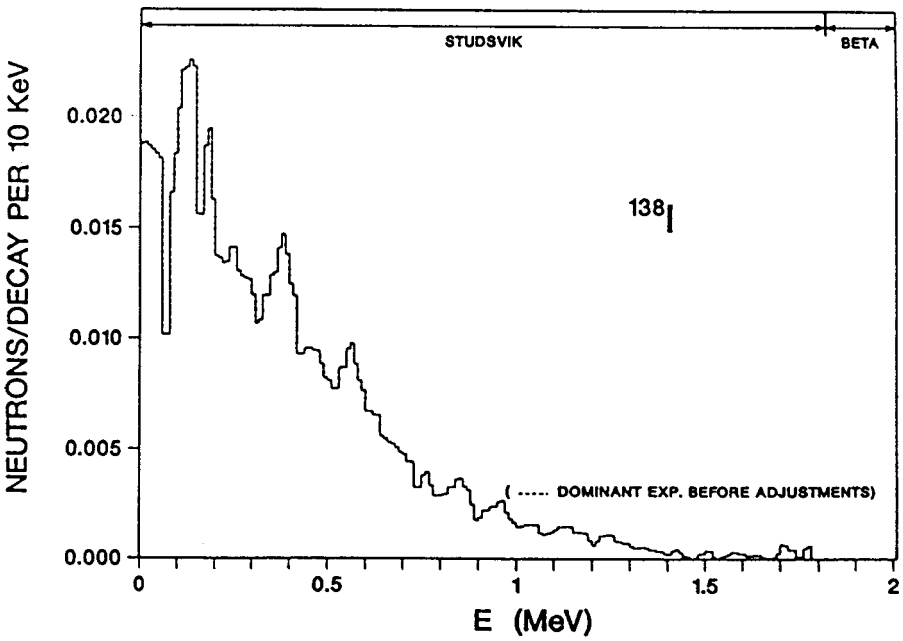

Fig. 35. Normalized delayed neutron spectra for ^{138}I.

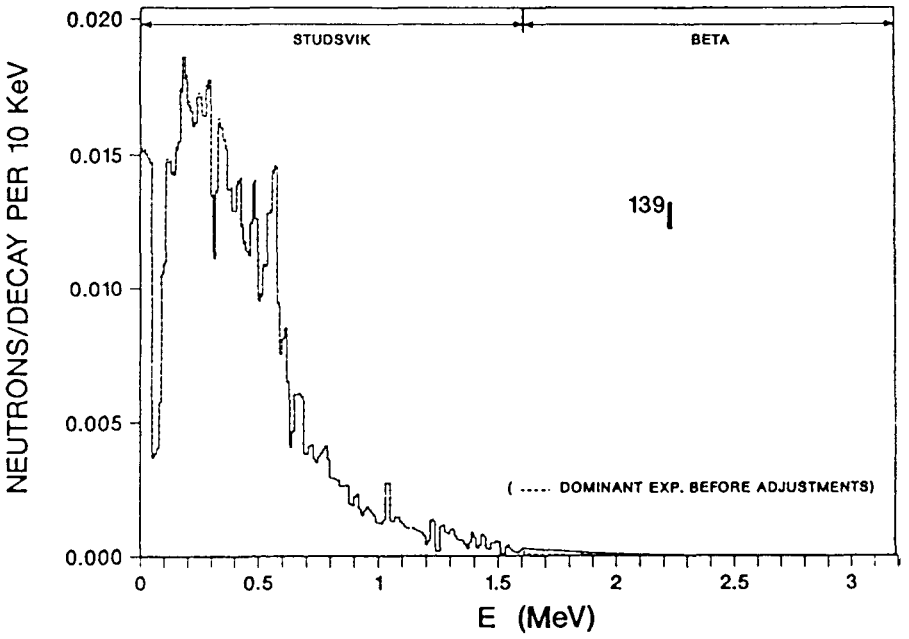

Fig. 36. Normalized delayed neutron spectra for ^{139}I.

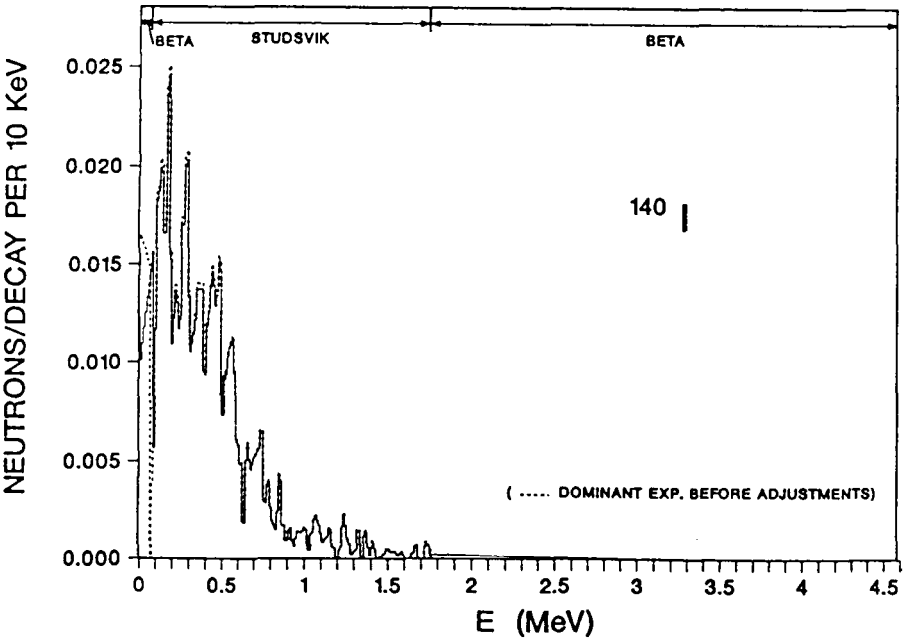

Fig. 37. Normalized delayed neutron spectra for ^{140}I.

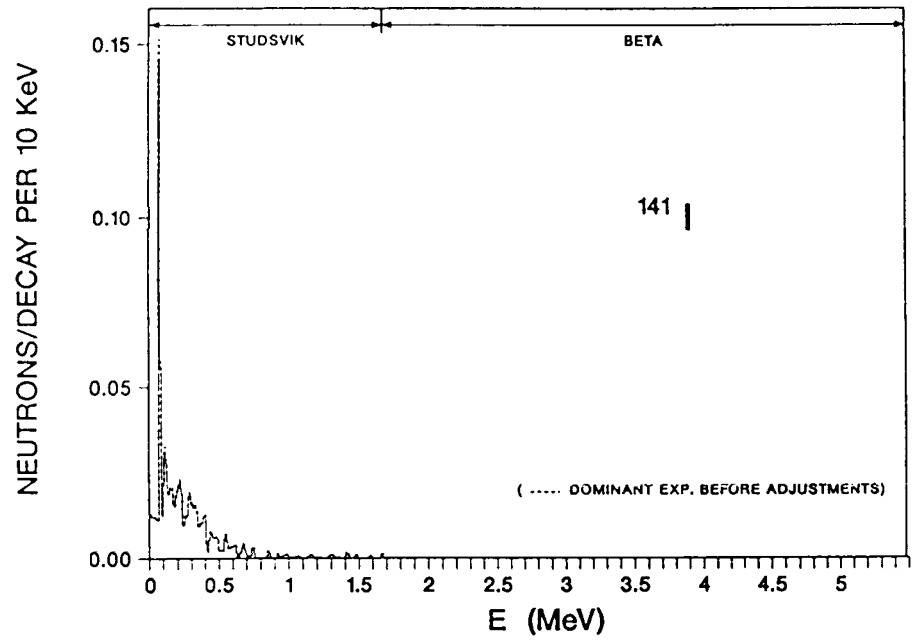

Fig. 38. Normalized delayed neutron spectra for ^{141}I.

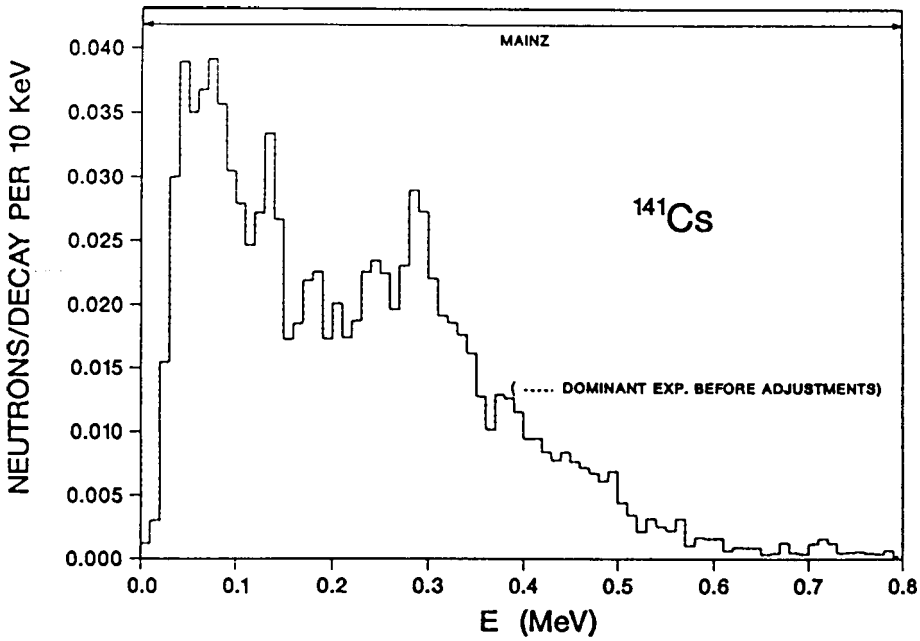

Fig. 39. Normalized delayed neutron spectra for ^{141}Cs.

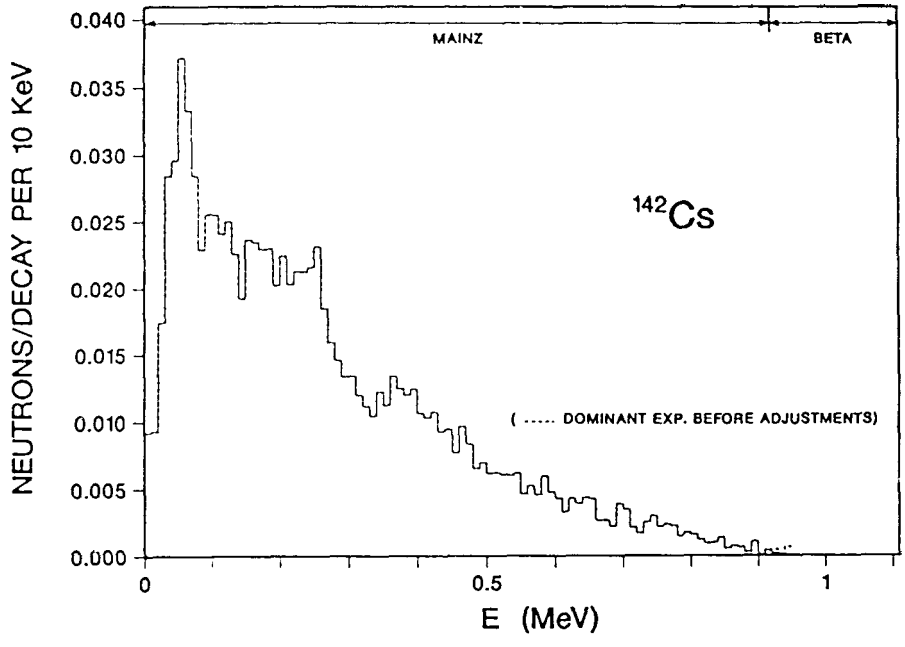

Fig. 40. Normalized delayed neutron spectra for ^{142}Cs.

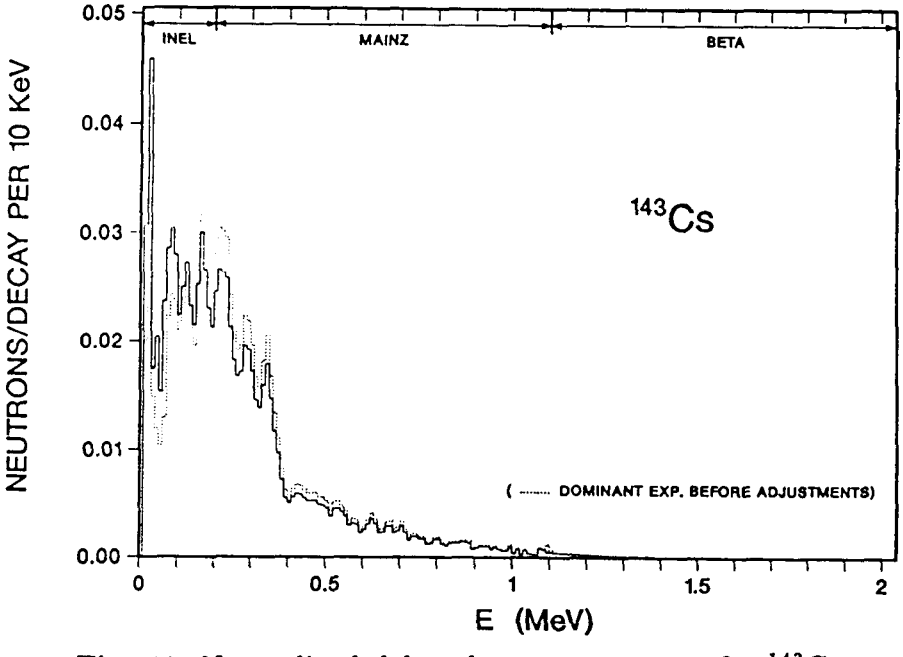

Fig. 41. Normalized delayed neutron spectra for ^{143}Cs.

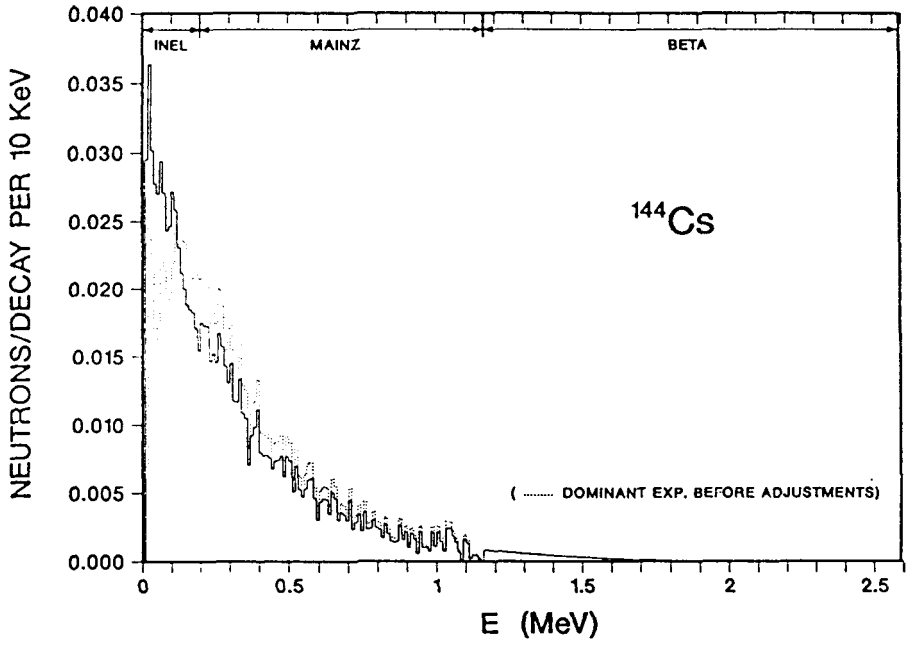

Fig. 42. Normalized delayed neutron spectra for ^{144}Cs.

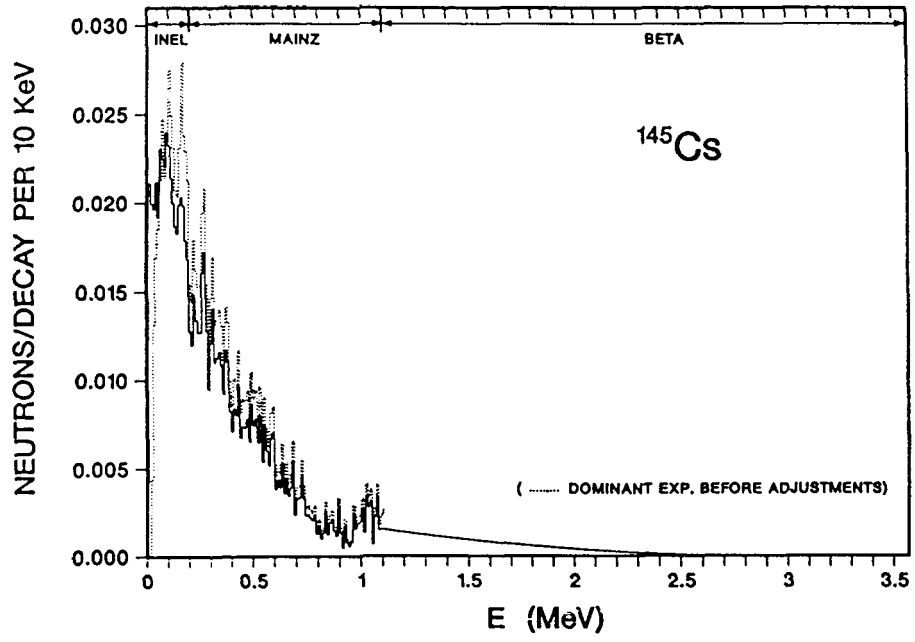

Fig. 43. Normalized delayed neutron spectra for ^{145}Cs.

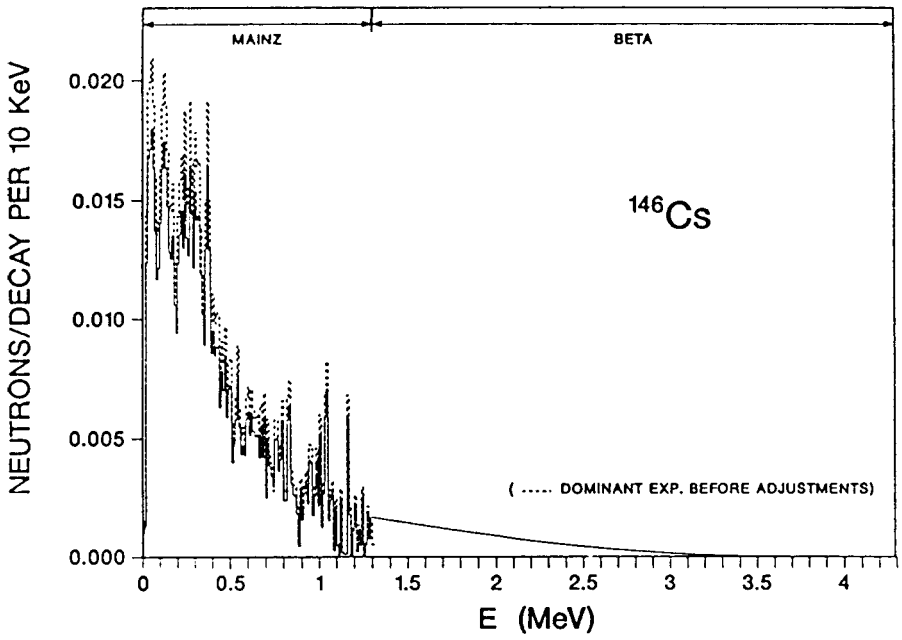

Fig. 44. Normalized delayed neutron spectra for ^{146}Cs.

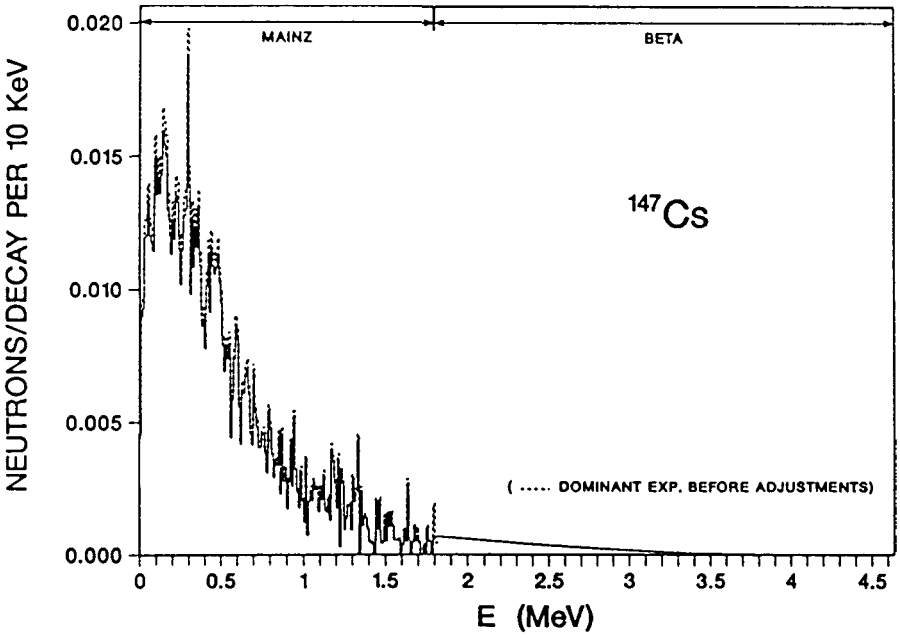

Fig. 45. Normalized delayed neutron spectra for ^{147}Cs.

figures and should be acknowledged here. As discussed earlier, the Studsvik data as received from Prof. Rudstam was not entirely the result of experiments, in some cases augmentations with models had already been made at low energies. These changes were easily recognized from the omission of uncertainties for the augmented data. However, the adjustments made in the data were not always complete, for example in the case of ^{79}Ga (Fig. 12) there is actually a gap in the Rudstam spectrum between the model estimation at very low energies and the beginning of the experimental data at 0.11 MeV. In cases of this type, the earlier augmentations were simply ignored and the BETA calculated spectrum for that nuclide used to augment the experiment. The regions of the evaluated spectrum attributed to the various experimental spectra and/or the BETA model spectra are indicated at the top of Figs. 12-45.

A rather unique situation occurs in the spectra for ^{87}Br (Fig. 16) and ^{92}Rb (Fig. 22) in that the measurement exceeds the theoretical energy window in each of these cases. The measurement for ^{87}Br was assumed to be within the uncertainty associated with the theoretical masses used to calculate the energy window so only a minor adjustment was made and the spectrum was arbitrarily cutoff at 1.5 MeV. This adjustment caused the average energy to decrease by less than 3%. The difference between the measured spectral endpoint energy and the theoretical energy window is much more dramatic in the case of ^{92}Rb. Figure 46 is a plot of the ^{92}Rb spectrum as a fraction above the abscissa energy. It appears from this figure that much of the high energy "measurement" may actually be background caused by perhaps some electronic noise. The spectrum for ^{92}Rb was cut at 1.0 MeV consistent with the data reported by Prof. Kratz in Ref. 6.

MODEL SPECTRA

The majority of the 237 nuclides with no measured spectra are far from the line of beta stability and have little or no measured data, particularly nuclear level information. This eradicated the potential of the BETA code for calculating spectra for these nuclides and prompted the search for a simpler model.

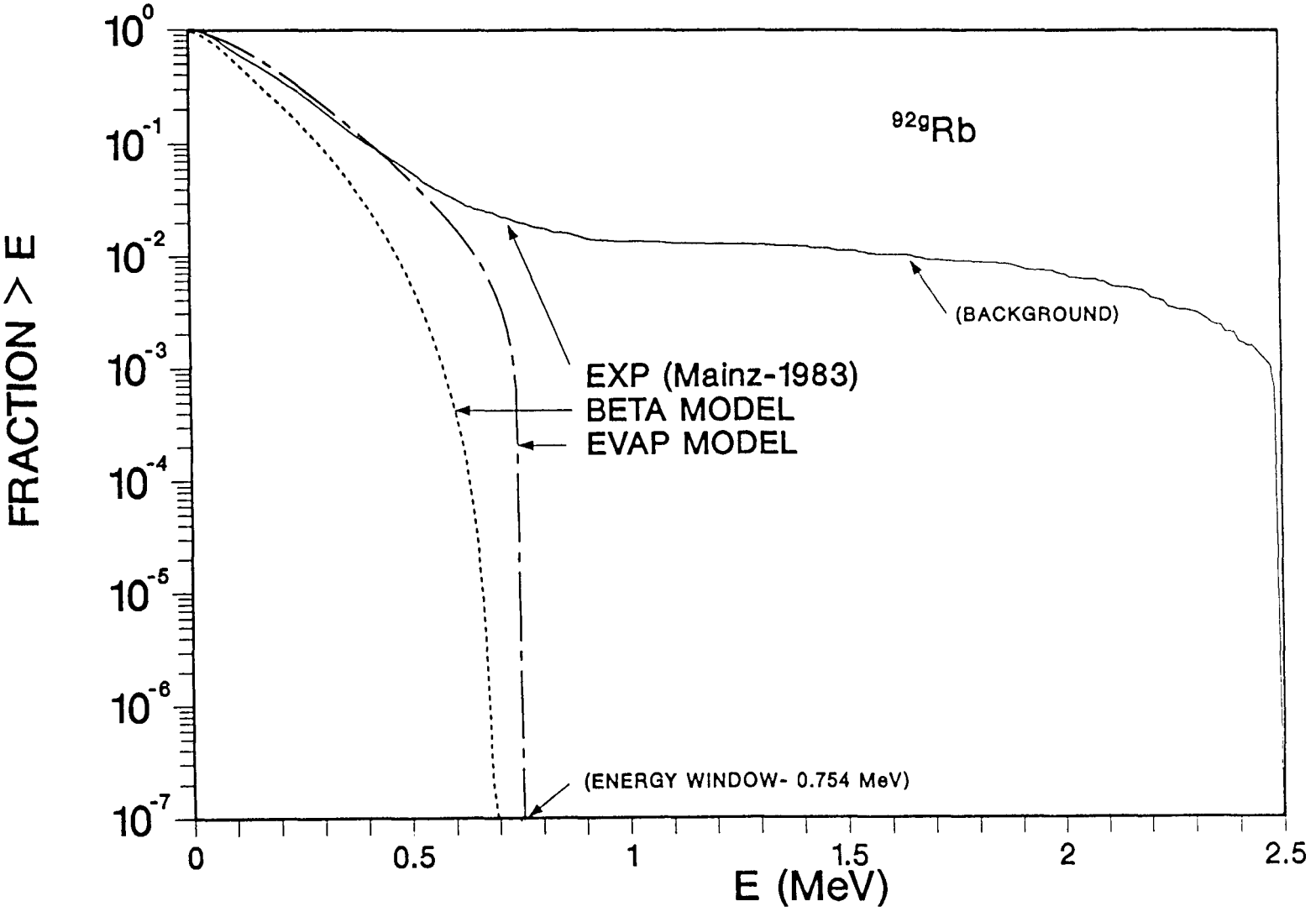

Fig. 46. Spectra as a fraction > E for ^{92}Rb.

Reeder and Warner published comparisons of measured spectra for ^{94}Rb (both Mainz and Studsvik data) and ^{137}I (Mainz data) with a single-parameter (Maxwellian) distribution. The temperature parameter (T) was derived from the experimental average energy for their comparisons. Reasonable agreement was found in their comparisons with the Mainz spectra, but the semi-empirical extrapolations at low energies present in many of the Studsvik spectra were "totally out of phase with a Maxwellian curve".[96] Reeder and Warner made no effort to extend their model to predict spectra for nuclides without measured data.

Comparisons using this type of single-parameter model were made for the thirty-four precursors with experimental spectra in this evaluation. Two separate distributions were used for comparison:

(1) a Maxwellian distribution;

$$N(E) \propto E^{1/2} \exp(-E/T) \ , \tag{18}$$

with an average energy of $\bar{E} = \frac{3}{2}T$,

and (2) an evaporation distribution;

$$N(E) \propto E \exp(-E/T) \ , \tag{19}$$

where the average energy is $\bar{E} = 2T$.

Figures 47 thru 50 are typical examples of the above distributions (calculating the temperature parameter based on the average energy derived from the experimental spectrum in each case) compared with the measured spectra. These models cannot, in view of their simplicity, reproduce the structure that is observed experimentally but they do represent the general shape of the spectra reasonably well. Comparisons of the type shown in Figs. 47-50 were made for all thirty-four nuclides having measured spectral data. Based on those comparisons the evaporation model [Eq. (19)] was chosen as more closely representing the overall shape, considering trends at both low and high energies, as well as the general position of the major peak.

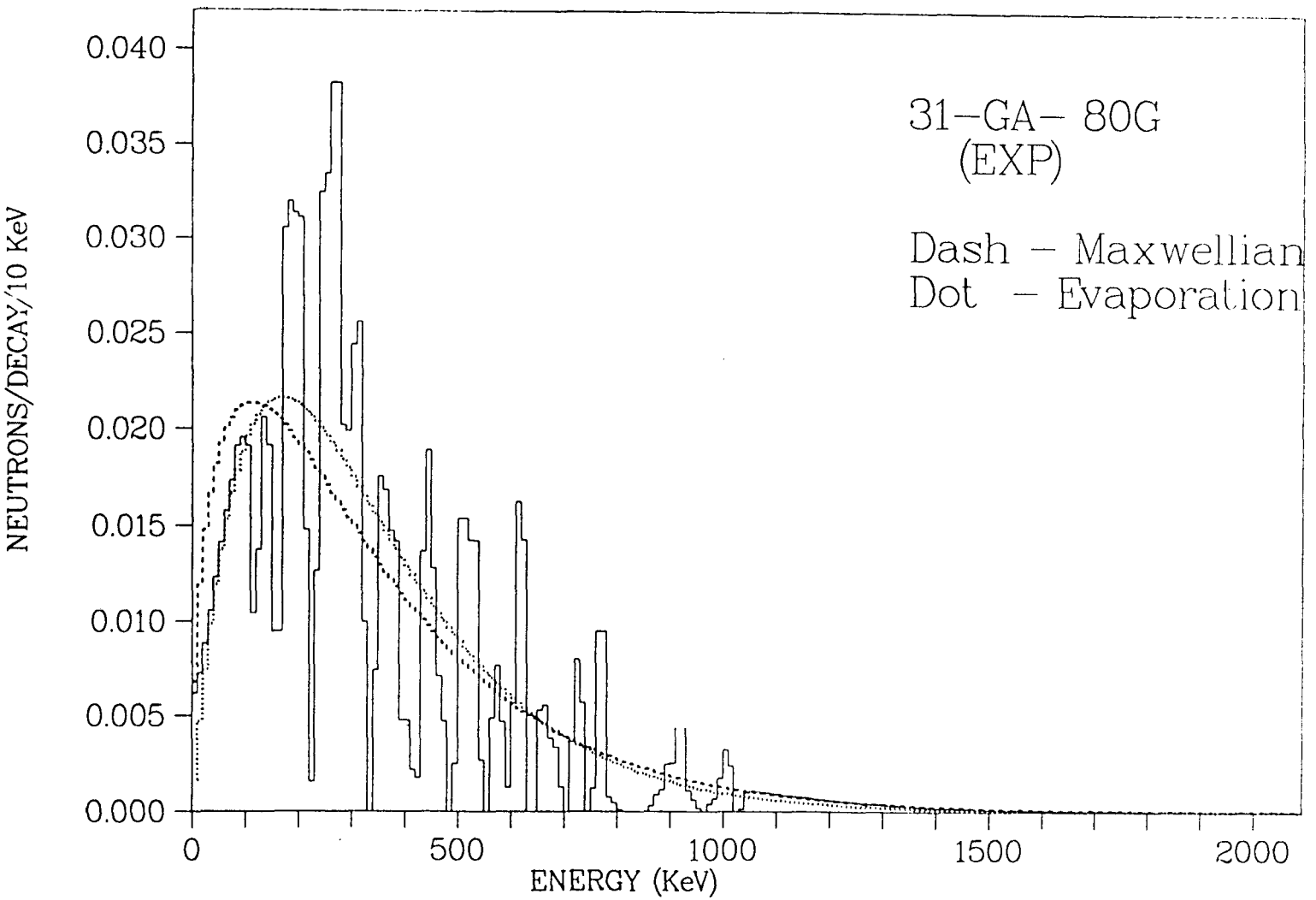

Fig. 47. Comparison of model spectra for ^{80}Ga.

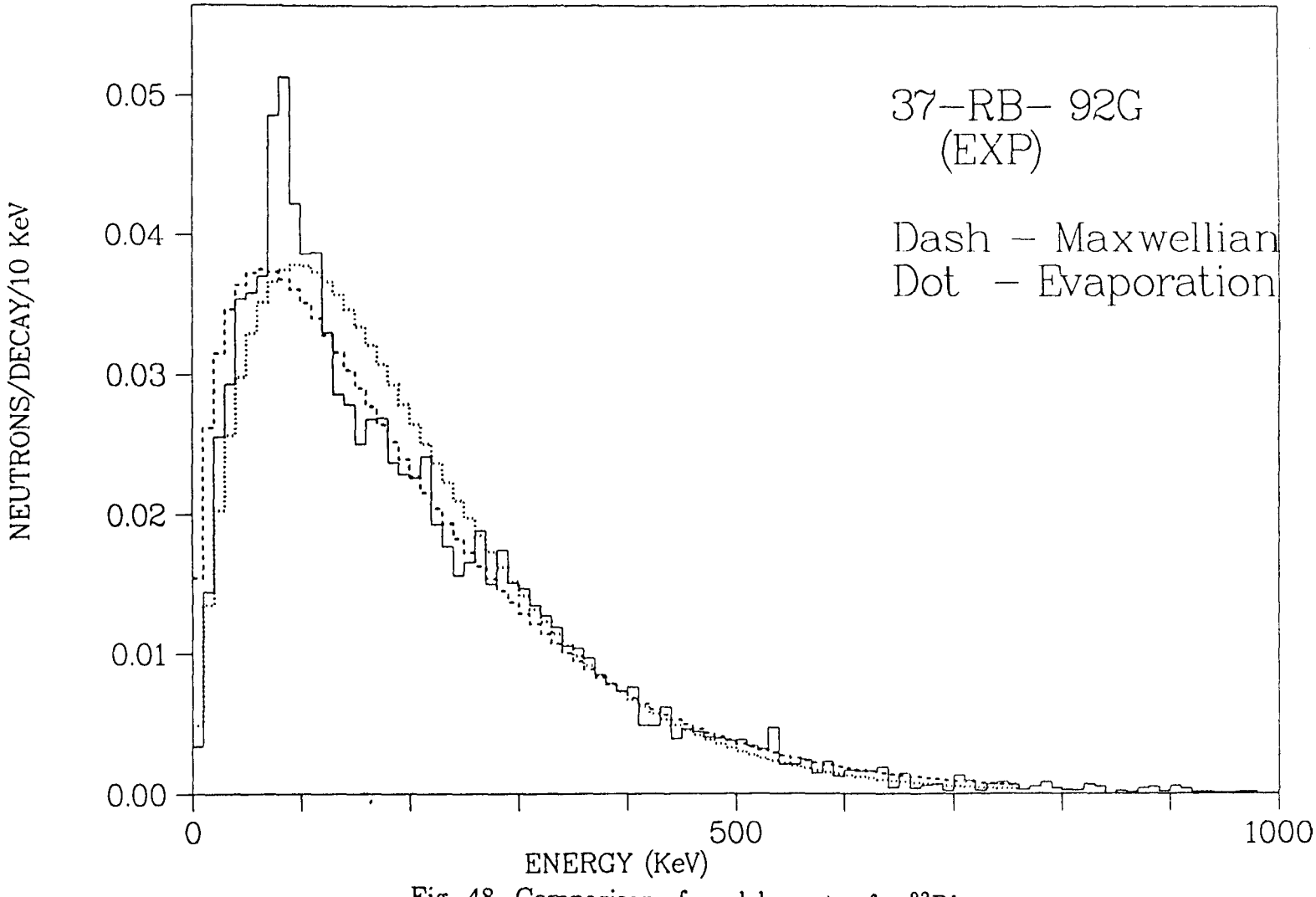

Fig. 48. Comparison of model spectra for ^{92}Rb.

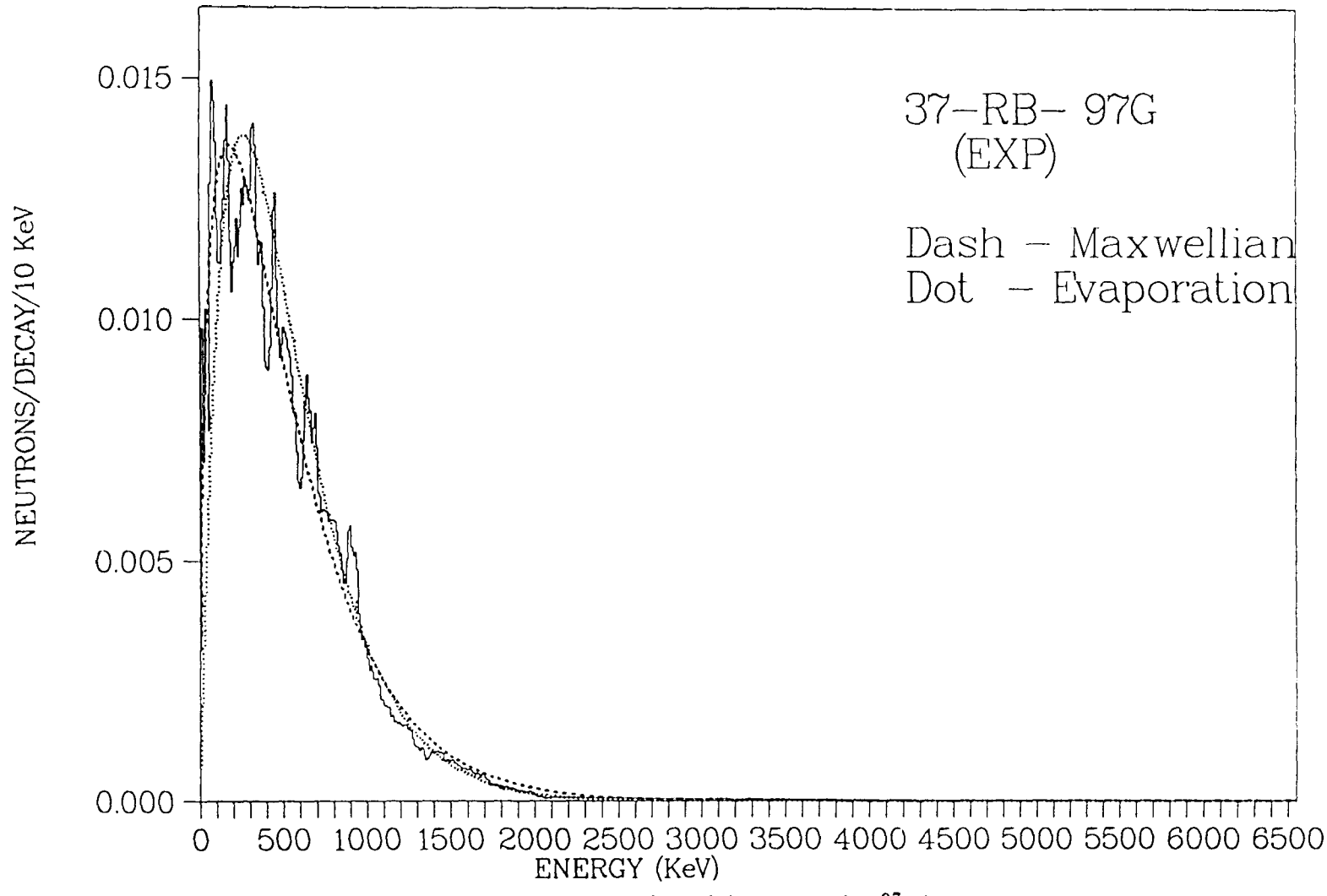

Fig. 49. Comparison of model spectra for ^{97}Rb.

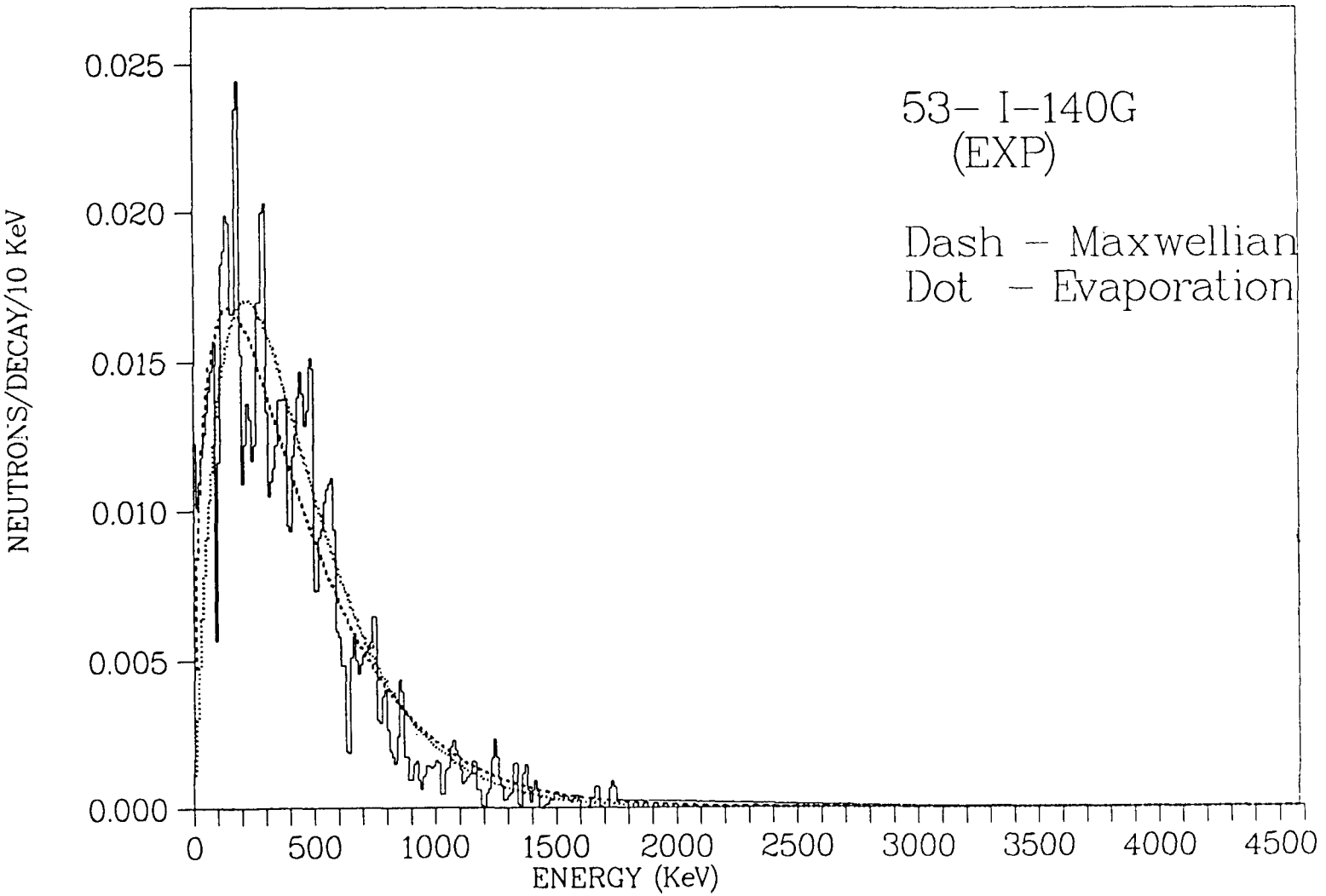

Fig. 50. Comparison of model spectra for ^{140}I.

Nuclides with larger energy windows (generally increasing away from the line of beta stability) that undergo beta decay may leave the daughter nucleus in higher excited states where the level densities are greater. In this case, the emission spectra for delayed neutrons would be expanded to more closely resemble the "boiling off" of neutrons and creating a situation in which the evaporation model would be entirely appropriate.

It must be acknowledged that neither the evaporation model nor the Maxwellian distribution is capable of precisely representing the low energy end of the delayed neutron spectrum. Experiments have shown that several nuclides, such as ^{95}Rb (Fig. 25) and ^{143}Cs (Fig. 41), have high intensity peaks at energies less that 100 keV.[6,32,97,98] Such low energy structure as noted by Reeder and Warner[96] cannot be represented by these simple one-parameter models because, by definition, these distributions are zero at zero energy. However, as will be shown later even the more sophisticated BETA code model fails to predict much of this low energy structure.

The motivation for finding a simple model for the delayed neutron spectra was to permit the calculation of spectra for the 237 precursors with no measured data. In order to accomplish this, a method to determine the temperature parameter T in Eq. (19) independent of the experimental average energy was necessary.

The nucleus can be taken to be a gas of A (atomic mass number) particles concentrated in a volume $\frac{4}{3}\pi R^3$, where R is the radius of the nucleus. In this approximation,[37,61] heavy nuclei may be represented as highly degenerate "gases" and thus the energy E is proportional to T^2. The temperature parameter needed to determine the evaporation spectra is the nuclear temperature of the residual nucleus and may be found by setting E equal to the maximum residual excitation energy (for delayed neutron emission this maximum energy is $Q_\beta - S(n)$) as in Eq. (20).[37]

$$Q_\beta - S(n) = \bar{a}T^2 \tag{20}$$

The proportionality constant, $\bar{a}$, has units of inverse energy and is described by Blatt and Weisskopf[61] as the reciprocal of "the mean energy distance between the lowest proper frequencies, $h\nu_i$. The value of $\bar{a}$ cannot be easily estimated owing to our restricted knowledge of the structure of heavy nuclei."[61] However, it has been observed that there is an overall increase of $\bar{a}$ with increasing values of atomic mass number, A.[99]

Since the average energy of the evaporation spectrum is equal to twice the temperature parameter [Eq. (19)], Eq. (20) can be rewritten in terms of the average energy, $\bar{E}$ as follows:

$$\bar{a}/4 = (Q_\beta - S(n))/\bar{E}^2 \ . \tag{21}$$

The experimental average energies were used to calculate values of $\bar{a}$ (recall that the quantities Q_β and $S(n)$ were given in Table IV) which can be plotted versus A to determine at what rate $\bar{a}$ increases with mass number. Comparisons made by earlier researchers over a much broader range in mass number (not limited strictly to delayed neutron precursors, i.e. fission products, as in this case) suggest that $\bar{a}$ may be linearly correlated with A.[99] Any such correlation derived from the present data will be a crude estimate. However, owing to the desire to keep the model simple, this appears to be the most direct method of predicting $\bar{a}$ that would rely to some extent on existing experimental delayed neutron data. The data, as seen in Fig. 51, fall into two groups. These are generally coincident with the low and high mass peaks of the fission yield curve, and do not represent a wide range in mass number. The line labeled as having a slope of 1/6 appears to be the best linear fit to the data in Fig. 51, where the abscissa is the right hand side of Eq. (21), yielding

$$\bar{a} = 2A/3 \ . \tag{22}$$

Having thus determined $\bar{a}$, the temperature parameter, T, may be found via Eq. (20). Examples of evaporation spectra calculated in this manner (labeled $\bar{a} = 2A/3$) are shown in Figs. 52–56 in comparison with experimental spectra that have been augmented with the BETA code model (solid line). Also in

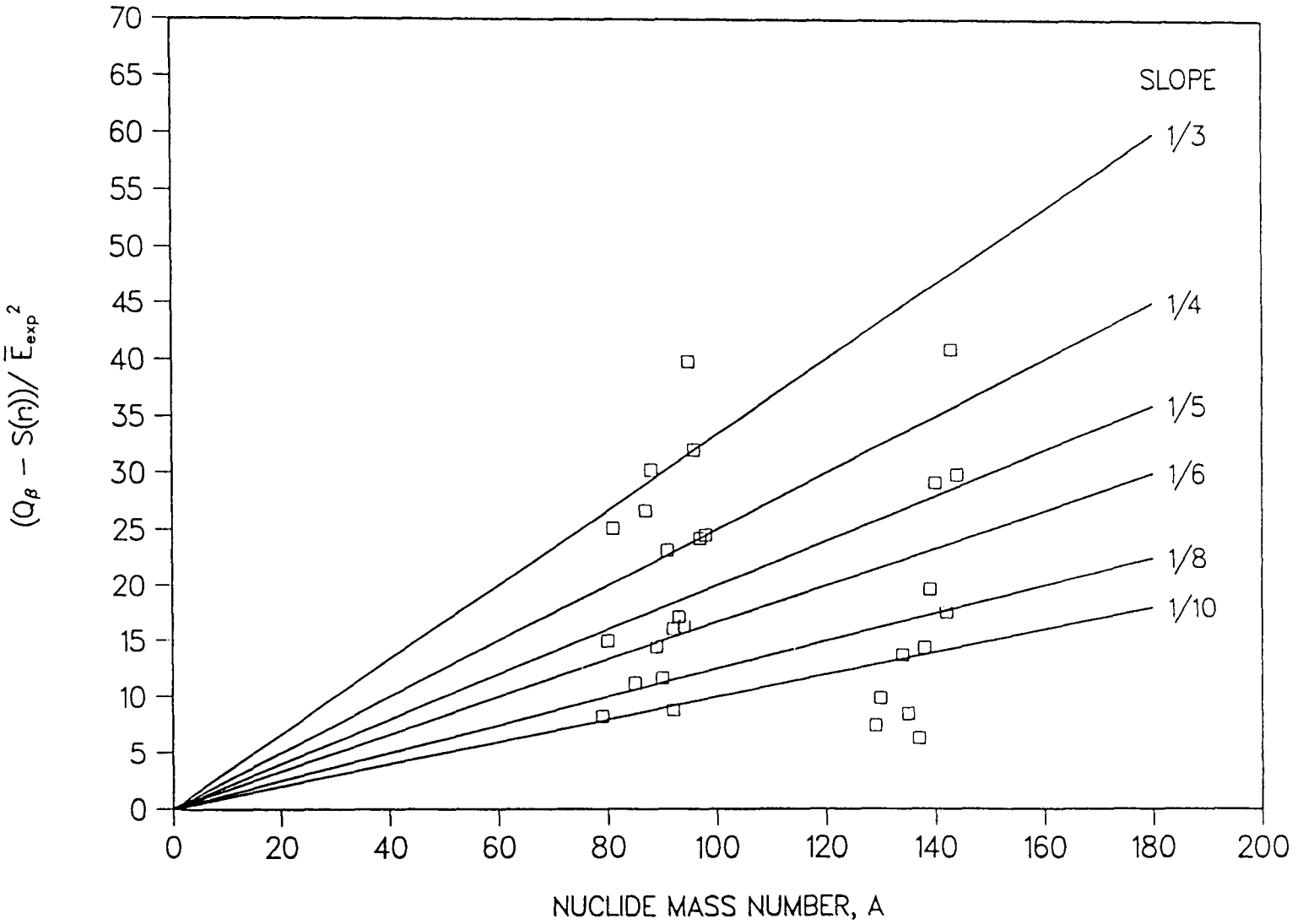

Fig. 51. Correlation of $\bar{a}/4$ [Eq. (21)] with mass number.

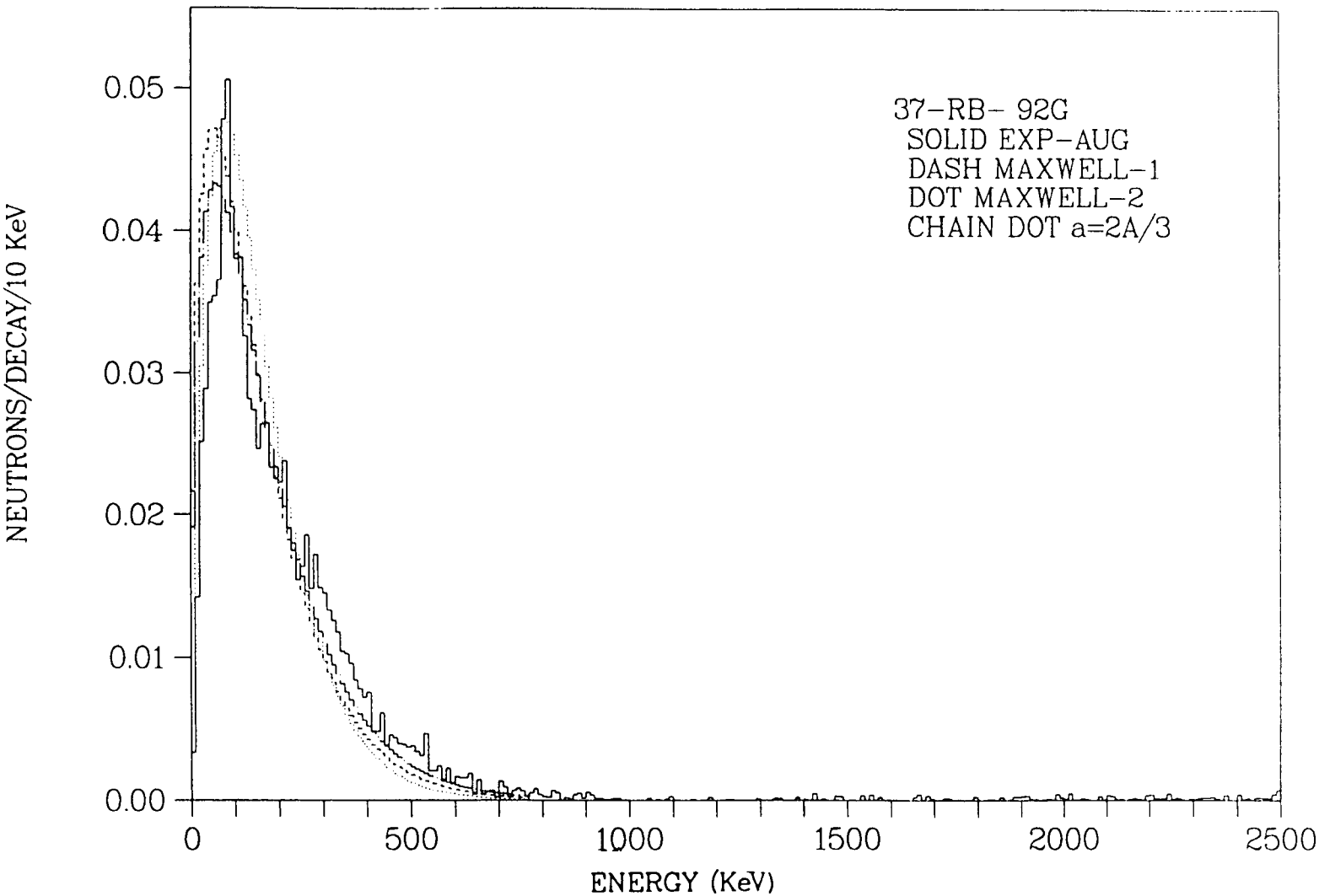

Fig. 52. Comparison of evaporation spectra with $\tilde{a} = 2/3A$ for ^{92}Rb.

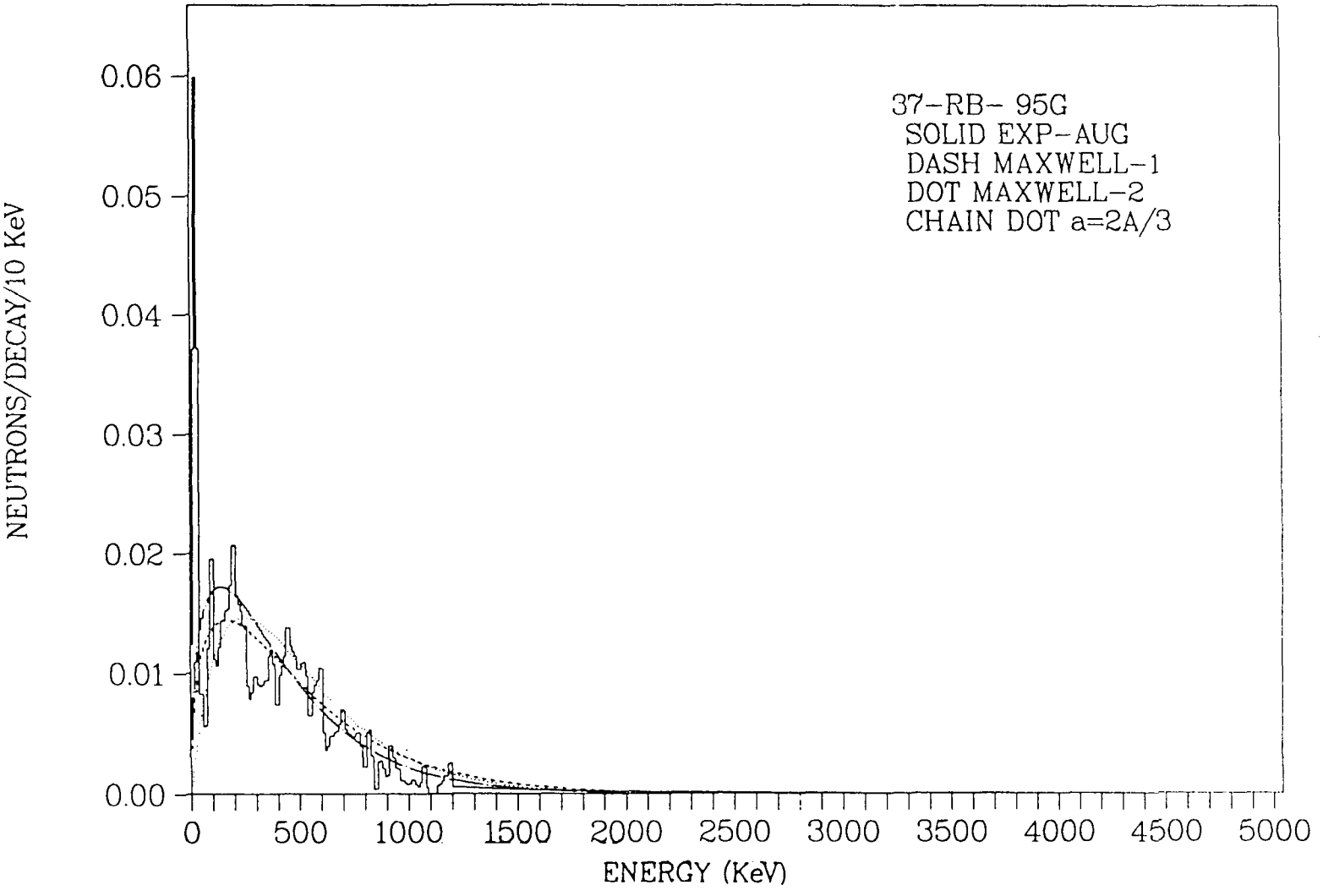

Fig. 53. Comparison of evaporation spectra with $\bar{a} = 2/3A$ for ^{95}Rb.

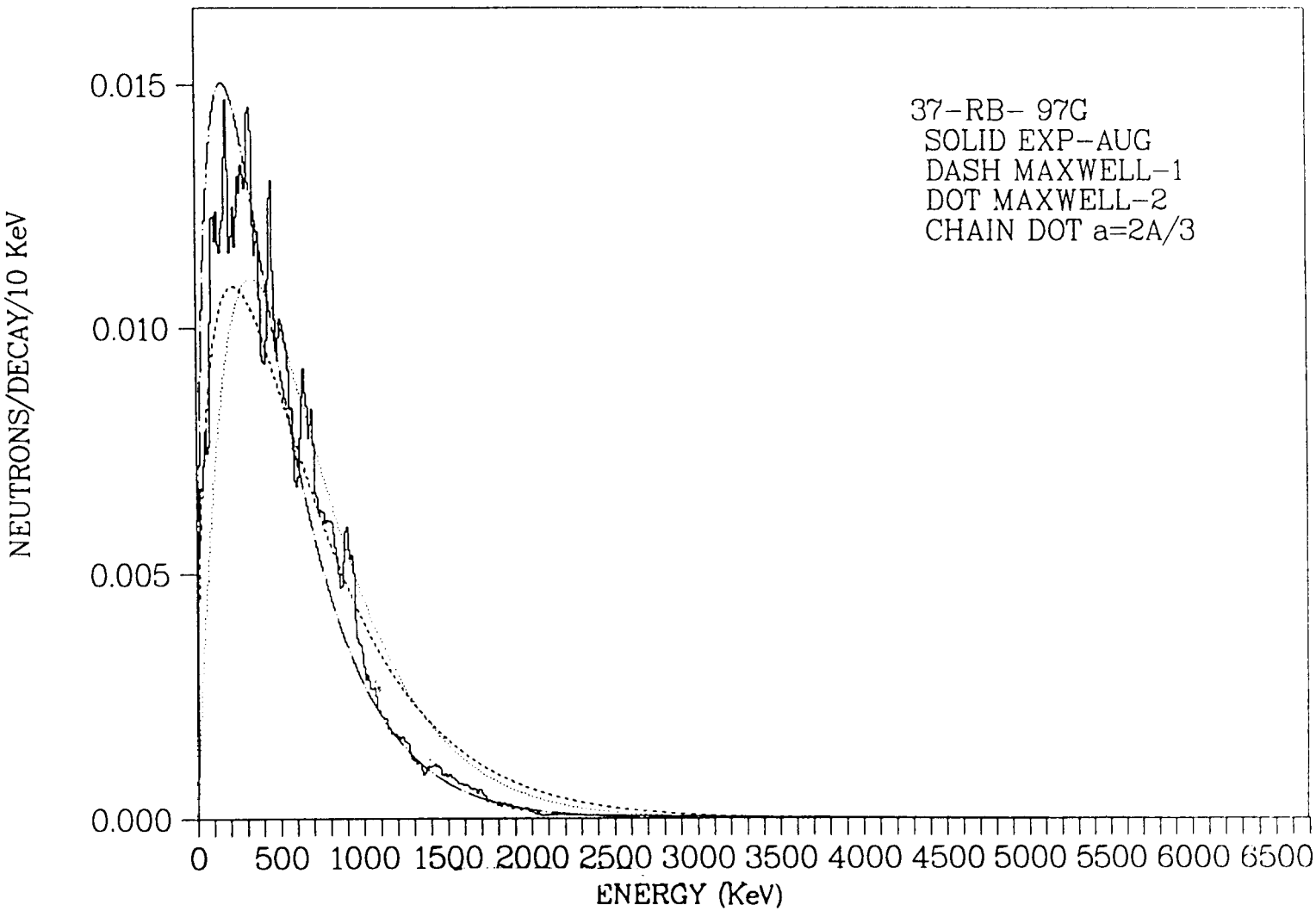

Fig. 54. Comparison of evaporation spectra with $\bar{a} = 2/3A$ for ^{97}Rb.

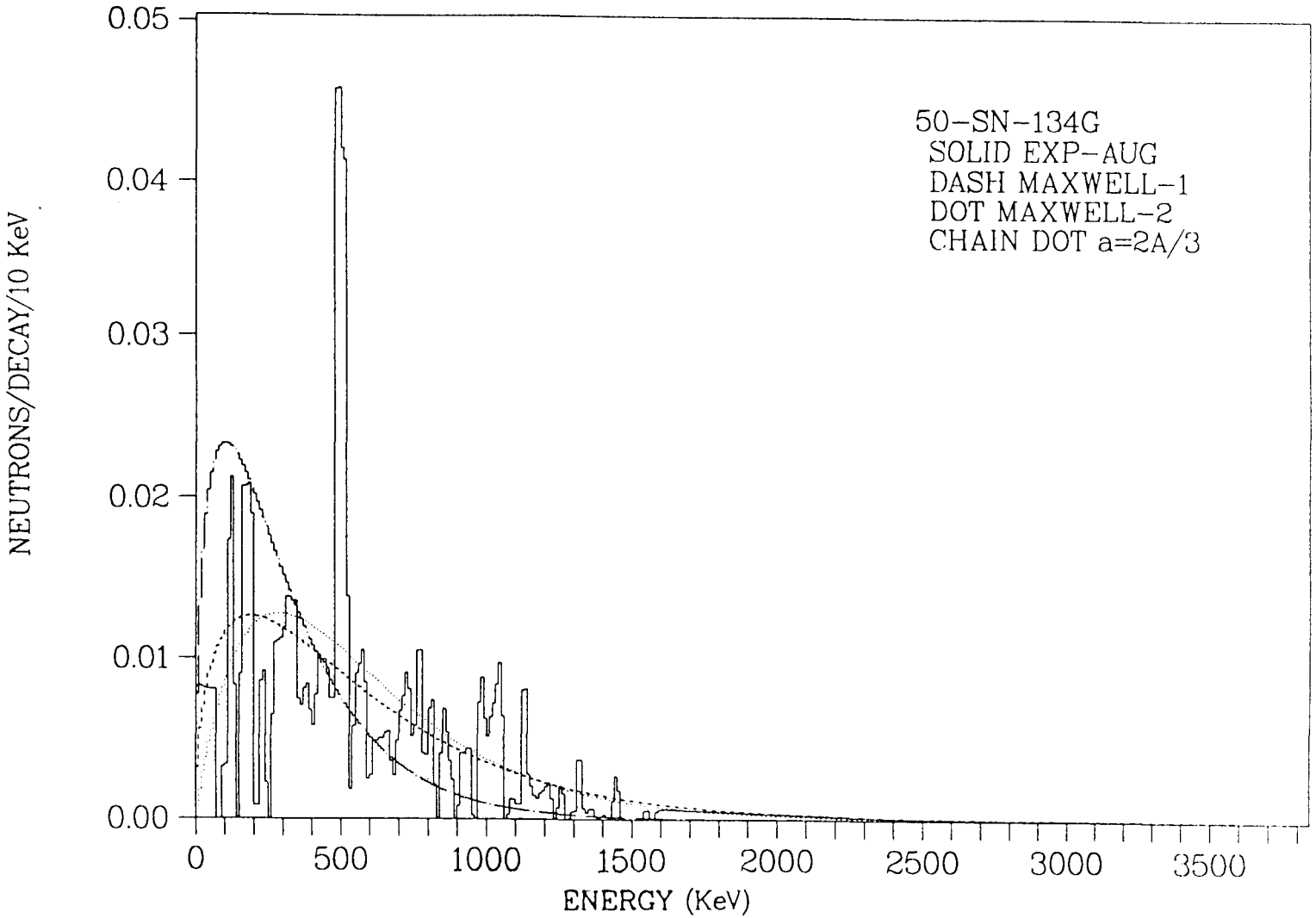

Fig. 55. Comparison of evaporation spectra with $\tilde{a} = 2/3A$ for ^{134}Sn.

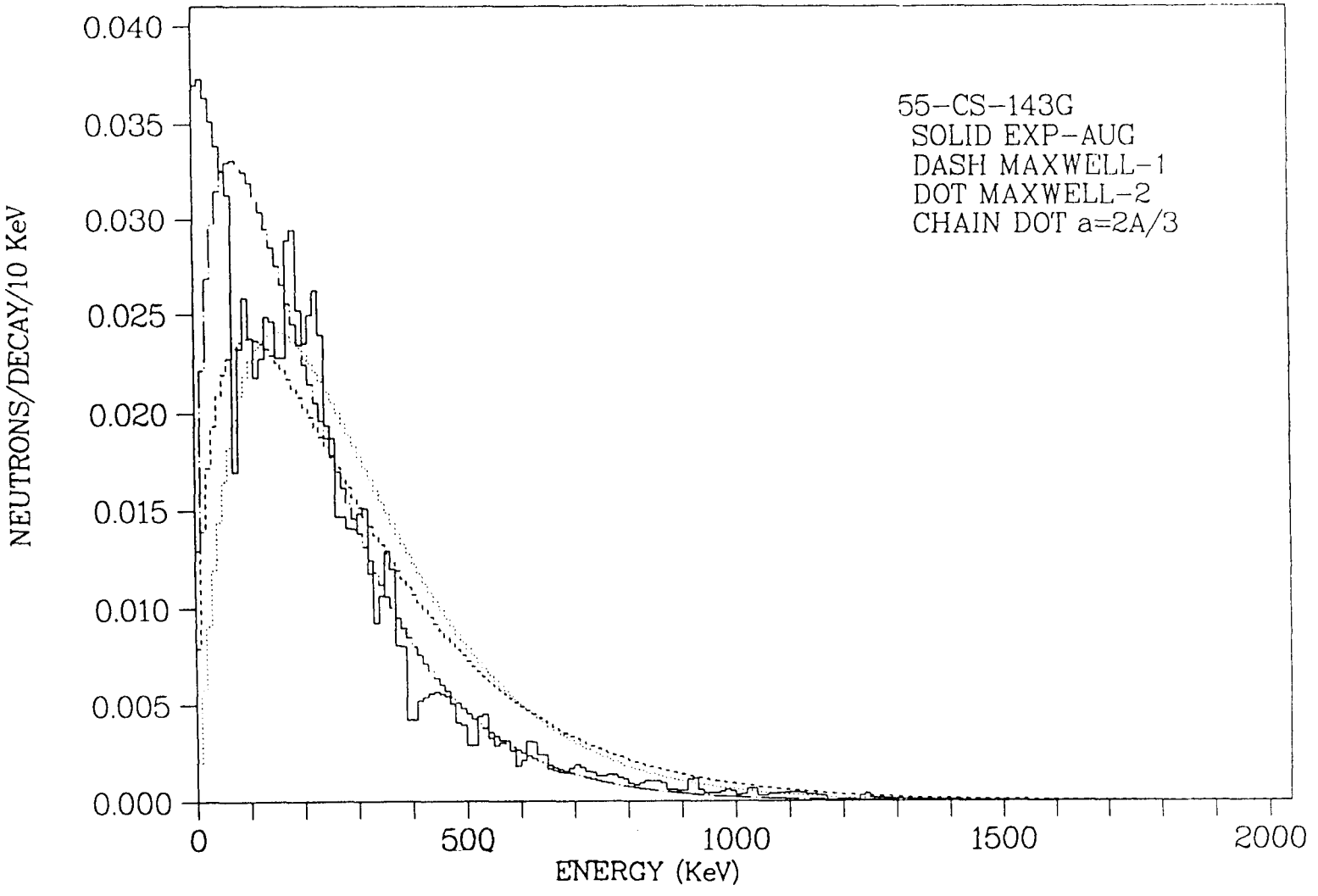

Fig. 56. Comparison of evaporation spectra with $\bar{a} = 2/3A$ for ^{143}Cs.

Figs. 52-56 are the results for both the simple Maxwellian distribution and the evaporation model (calculated from Eqs. (18) and (19), and designated MAXWELL-1 and MAXWELL-2, respectively) where T has been determined from the experimental average energy. These are typical of the results observed for the 34 nuclides with experimental data.

The distribution function for the evaporation model [Eq. (19)] tends to zero in the limit as E goes to infinity, however, the delayed neutron spectra have an endpoint energy of $Q_\beta - S(n)$ at which the intensity should go to zero. In order to satisfy the latter as a boundary condition, the evaporation model was modified as follows:

$$N(E) = C[E\exp(-E/T) - (Q_\beta - S(n))\exp(-aT)] \tag{23}$$

A drawback to this equation is that it allows the intensity of the distribution to be negative when evaluated at zero energy. However, in the present application the spectra are calculated in ten-kilovolt bins by integrating Eq. (23), rather than as a pointwise distribution and therefore it is not required that the distribution be evaluated at precisely zero energy. Precursor nuclides with endpoint energies greater than 1 MeV (as in all but ~30 of the 235 cases) have properties such that the second term in Eq. (23) is generally smaller than the first by more than one order of magnitude for all energy bins, including the first, and for these cases Eq. (23) produces almost exactly the same result as did Eq. (19). Those precursors with energy windows less than one do not show such a marked contrast in magnitude between the two terms in the first energy bin and therefore checks were made to determine if the evaporation spectra for these nuclides were calculated with a negative value in the low energy bin, any such value was reset to zero. Even for these nuclides, the spectra calculated by Eqs. (19) and (23) are very nearly indistinguishable.

Comparisons of these slightly modified evaporation spectra with BETA calculated spectra and experimental spectra are given in Figs. 57 through 61 for ^{92,94,96}Rb. The data is presented in two forms; normalized intensity versus energy, and as the fraction above the abscissa energy. The latter is to emphasize

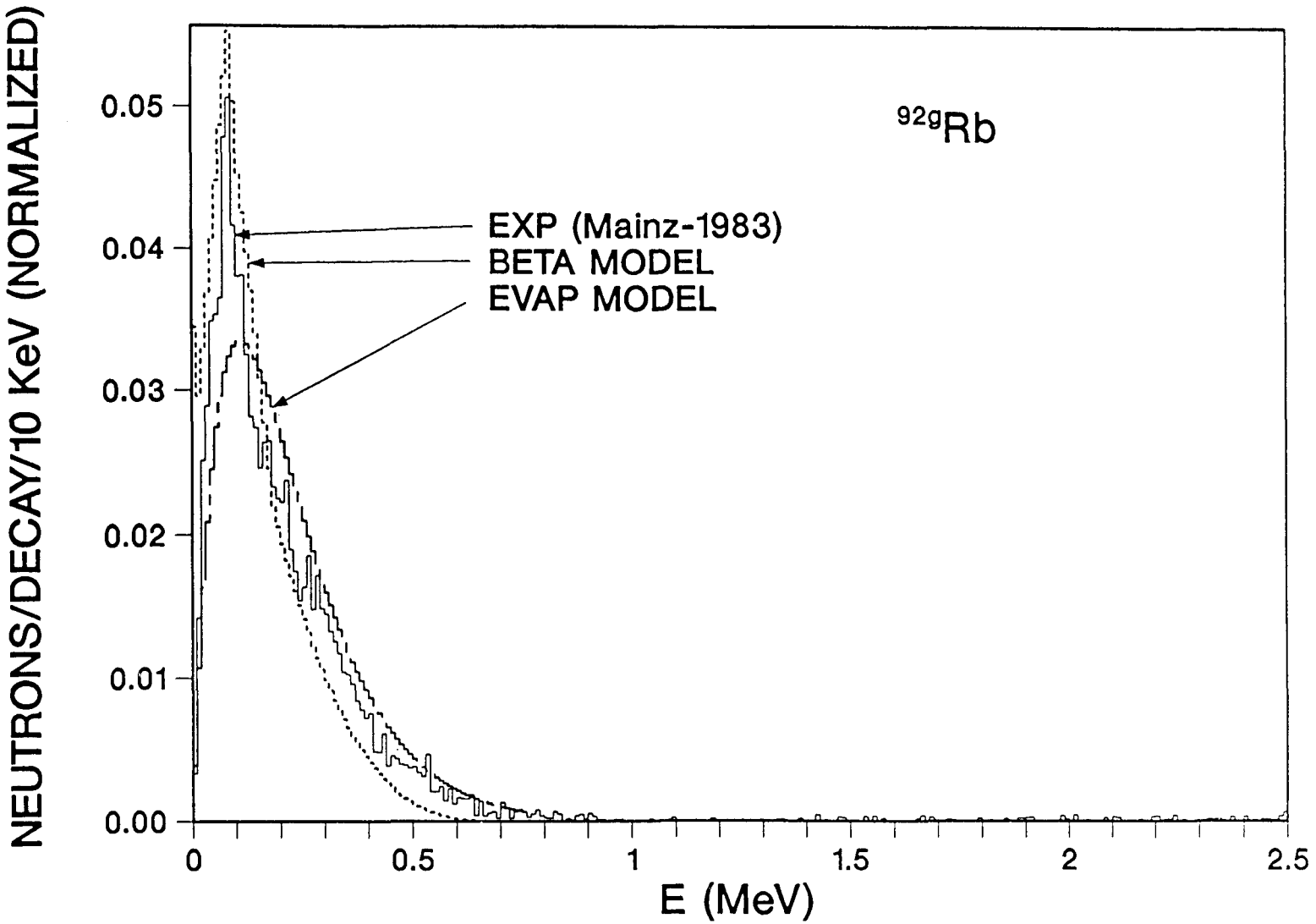

Fig. 57. Comparison of spectra for ^{92}Rb.

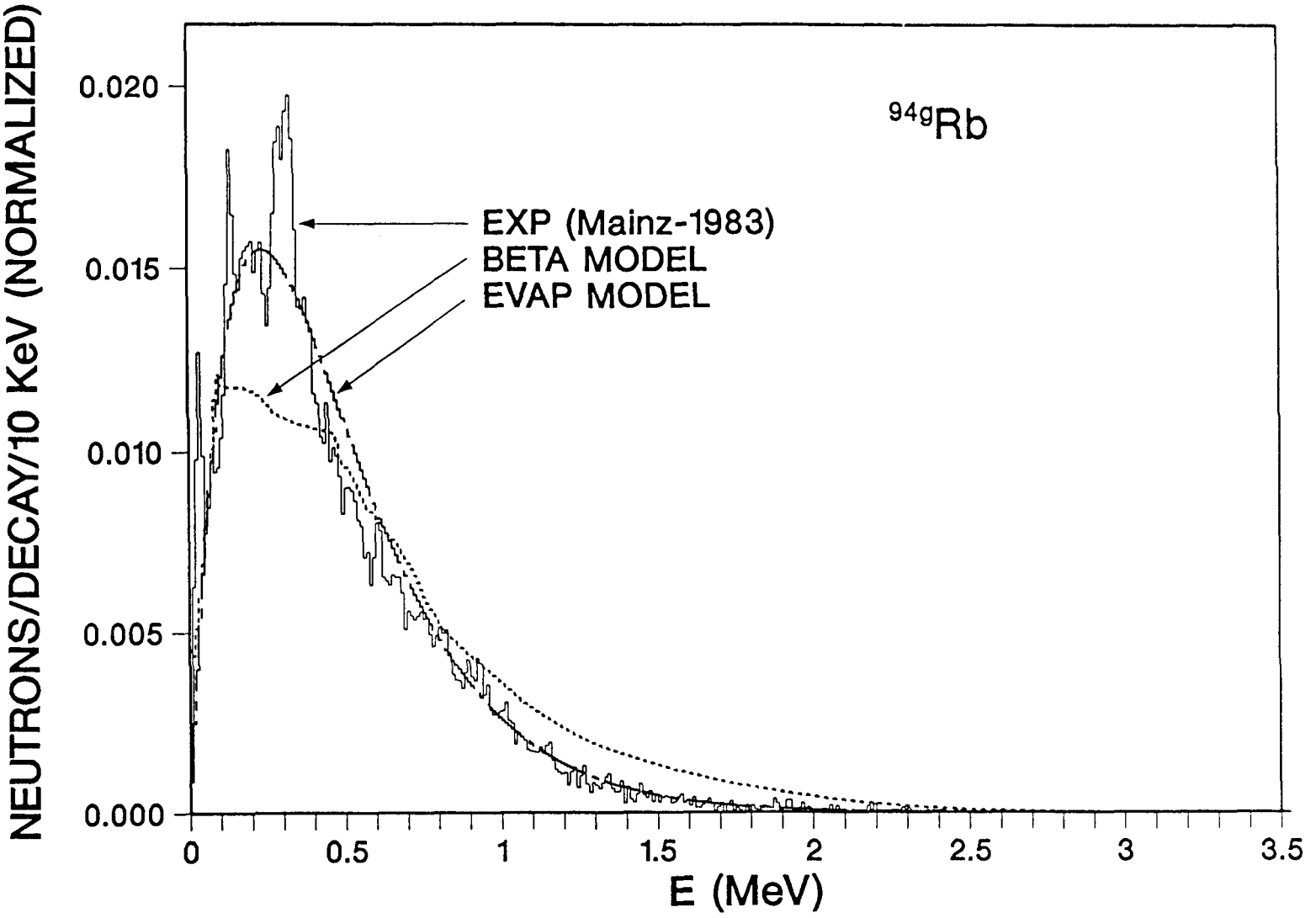

Fig. 58. Comparison of spectra for ^{94}Rb.

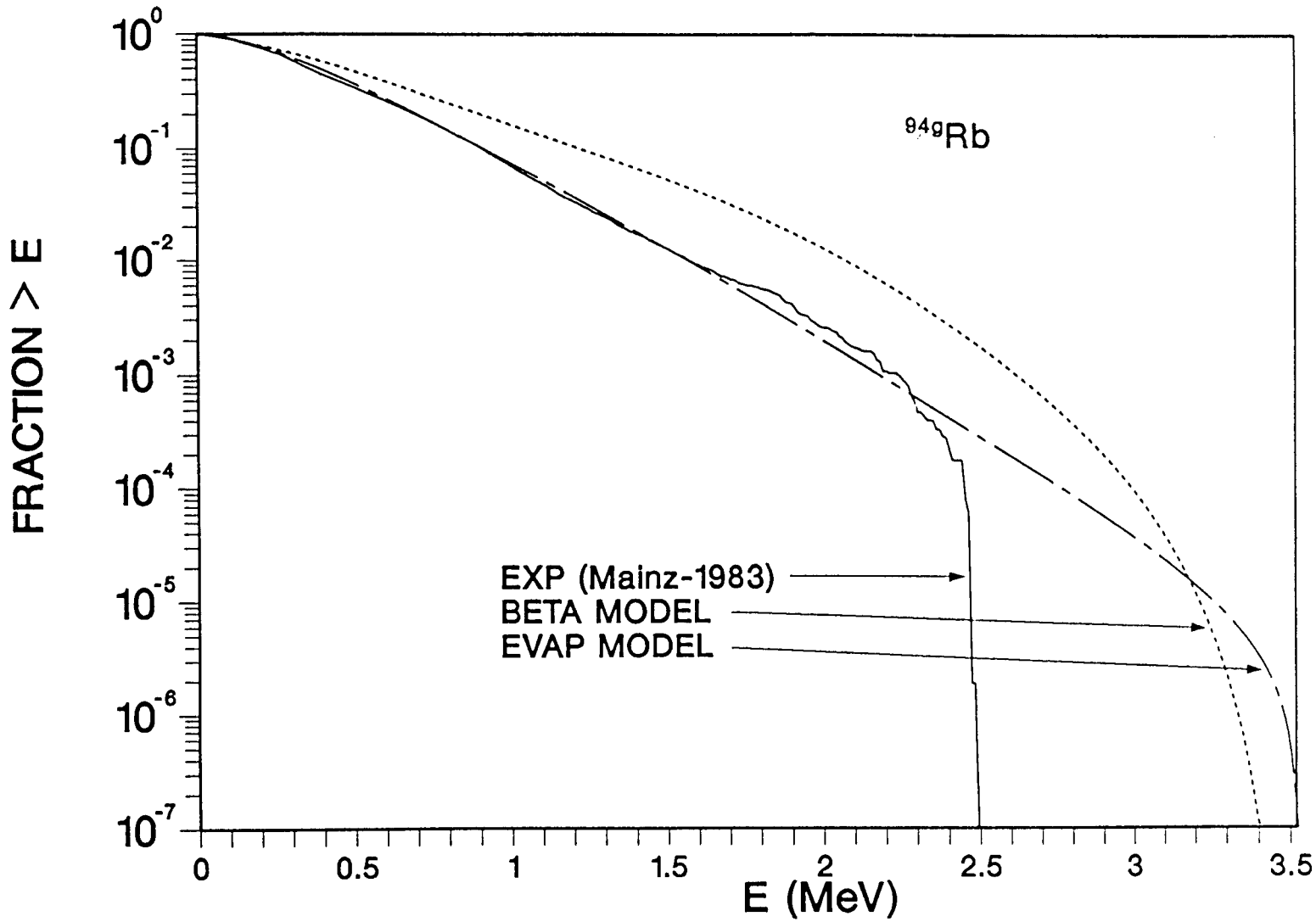

Fig. 59. Spectra as a fraction > E for ^{94}Rb.

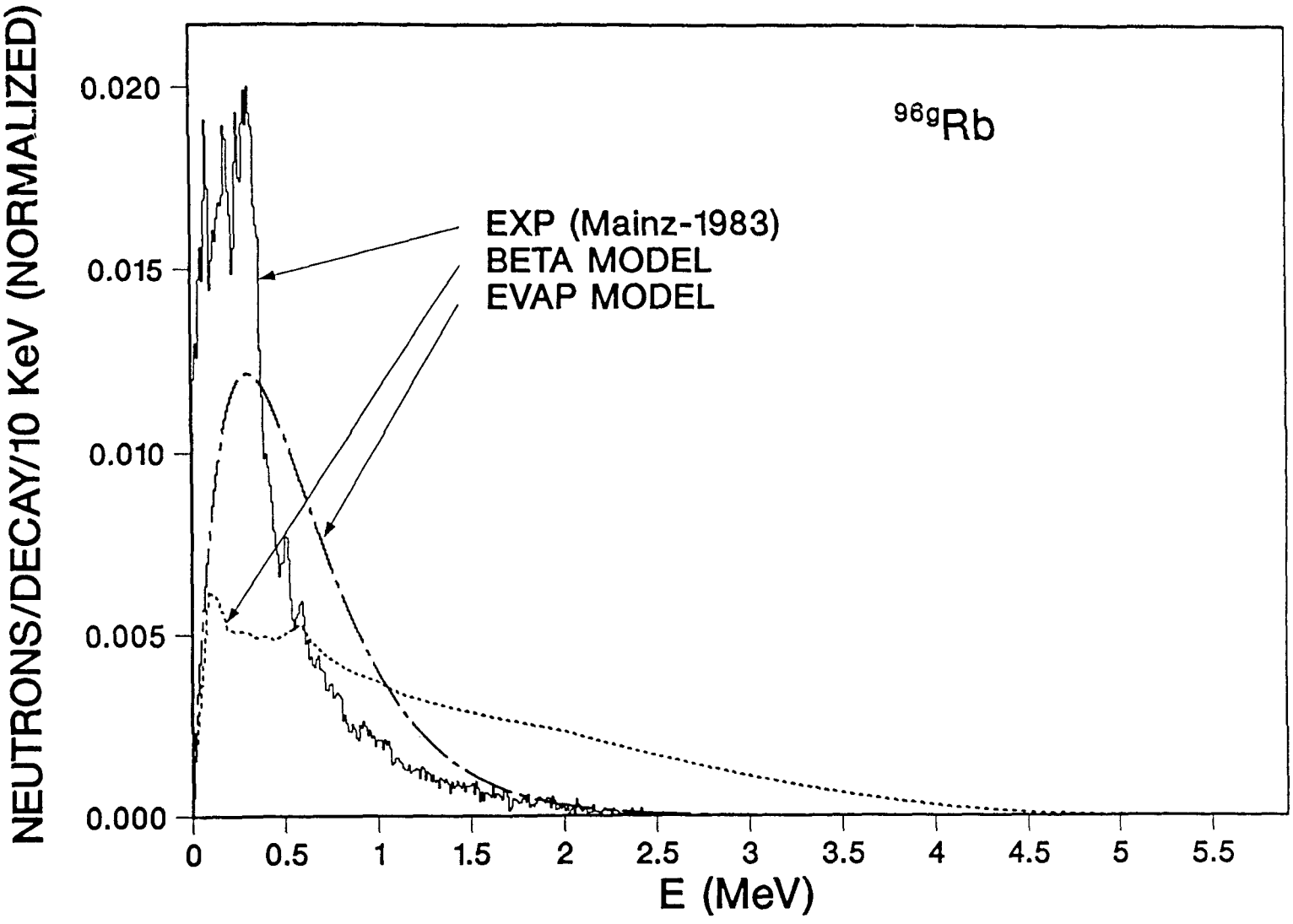

Fig. 60. Comparison of spectra for ^{96}Rb.

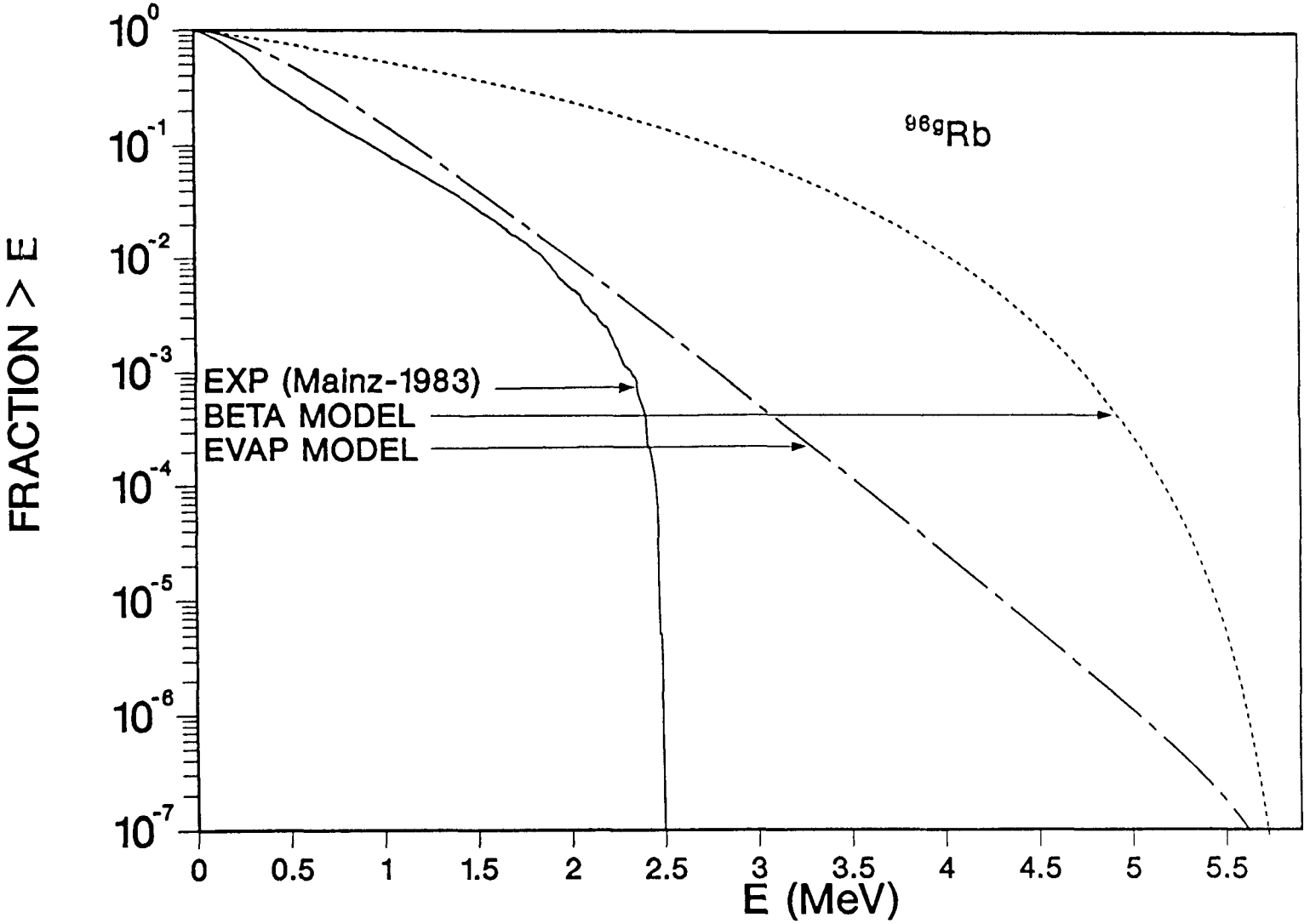

Fig. 61. Spectra as a fraction > E for ^{96}Rb.

the higher energies where the modification of the evaporation model is most evident. The evaporation spectrum, like the BETA code model tapers off smoothly at high energies, if the spectrum were calculated from Eq. (19), it would have been cutoff abruptly at the endpoint energy. Again, these comparisons are typical of the results for the 34 nuclides with experimental spectra.

It is interesting to note that even with the crude approximation for the temperature parameter, in many cases the evaporation model appeared to adequately estimate not only the general shape of the spectrum but more importantly the relative intensities over a large fraction of the energy window. The BETA code is used in the augmentation of the experimental data because of its ability to better predict the shape of the spectra (the rate at which the BETA spectra fall off at high energies appears to be more consistent with the tendencies observed in the experimental data). It does not, however, appear to predict the relative intensities at low and high energies (particularly at high energies) with confidence. When used to augment the experimental spectra the BETA spectra are normalized to the experiment, therefore emphasizing the shape produced from the BETA code but the intensities are basically provided by the experimental data. To predict spectra for the 237 precursors with no experimental data to provide normalization factors, it was considered more conservative to use the modified evaporation model rather than the BETA code. The evaporation model generally results in lower average energies for the individual nuclides.

UNCERTAINTIES FOR THE MODEL SPECTRA

No spectrum can be considered complete without an estimate of its uncertainty. The BETA code does not provide the user with a quantitative measure of the error in its spectral calculations, nor does the evaporation model with its crude temperature parameter lend itself to a simple means of assessing its certitude.

Relying on the thirty-four experimental spectra, systematic studies of the observed uncertainties between each of the models and experiments were made. There were three predetermined requirements for the final uncertainty assignments:

1. the uncertainties should be a function of energy;

2. the largest uncertainty should be at the end of the energy window $(Q_\beta - S(n))$ due to the additional uncertainty in the masses used to predict that point; and

3. the minimum uncertainty was arbitrarily set to 100%.

Plots of the fractional differences between the experimental and model spectra versus energy were made. Consideration of the three points listed above and general trends observed from the plots led to the following functional forms for the uncertainties, δ, in the model spectra.

Evaporation Model:

$$\begin{aligned} 0 < E < T/2;\ \ \delta &= 0.30685 - ln(E/T)\ , \\ E > T/2;\ \ \delta &= ln(E/T + 0.5) + 0.1(E/T)^2 + 0.975\ . \end{aligned} \tag{24}$$

BETA Code Model:

$$\text{all } E;\ \ \delta = ln(E/T + 1.0) + 0.1(E/T)^2 + 1.0\ . \tag{25}$$

Figures 62 and 63 are examples of the plots of the experimental uncertainties versus energy and the estimated uncertainties calculated from either Eq. (24) or Eq. (25). The experimental uncertainties, δ_{exp}, are fractions and are defined as:

$$\delta_{\text{exp}} = abs[(EXP - MODEL)/EXP]\ . \tag{26}$$

The trend indicated in Fig. 62 and reflected in Eq. (24) that the uncertainty decreases between zero energy and $T/2$ was found to be common in all thirty-four cases. The large error at low energies is to be expected since the pointwise evaporation model necessarily predicts that the intensity tends to zero as energy approaches zero as was discussed earlier, whereas there is experimental evidence

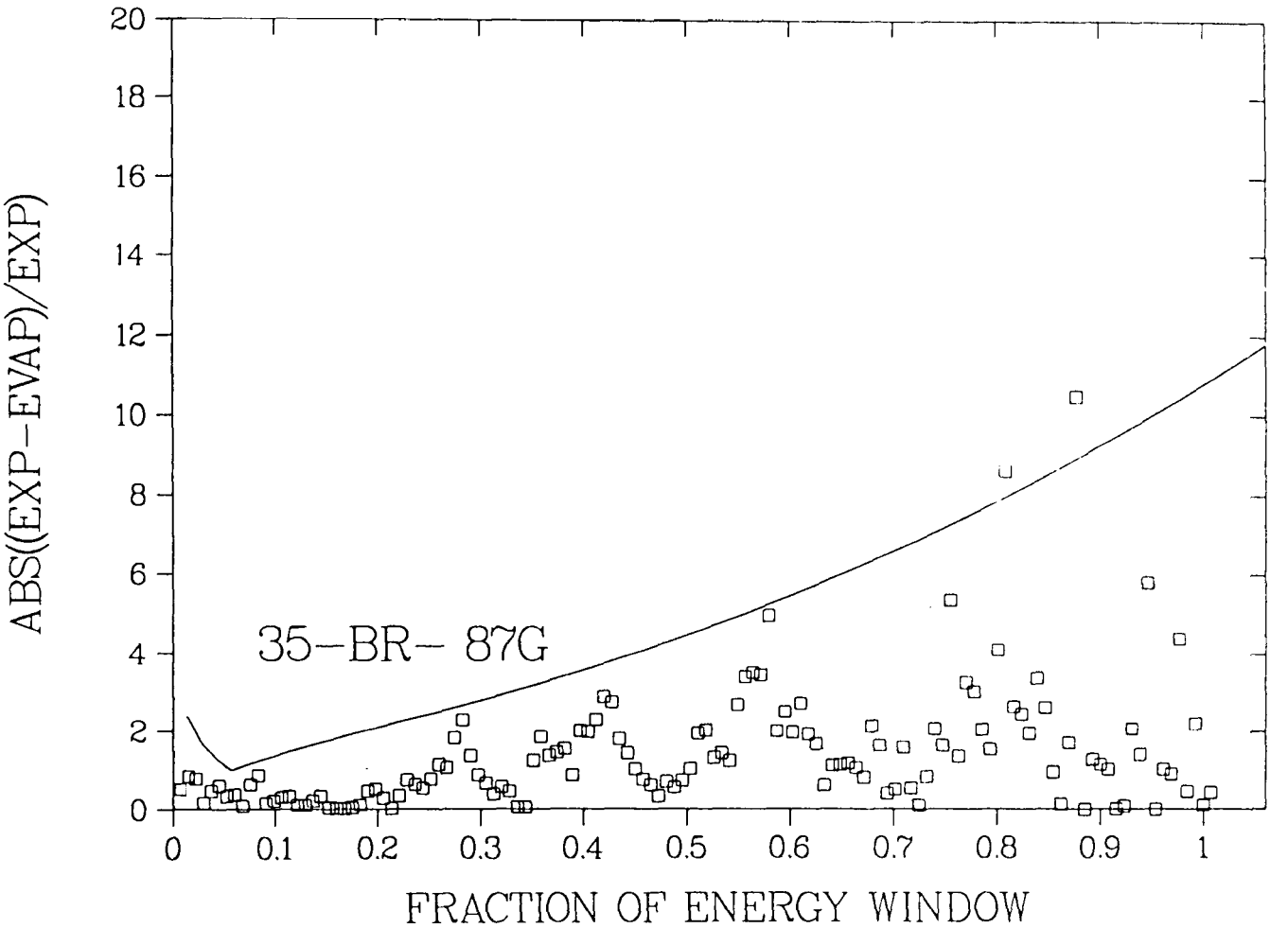

Fig. 62. Example of evaporation model uncertainty.

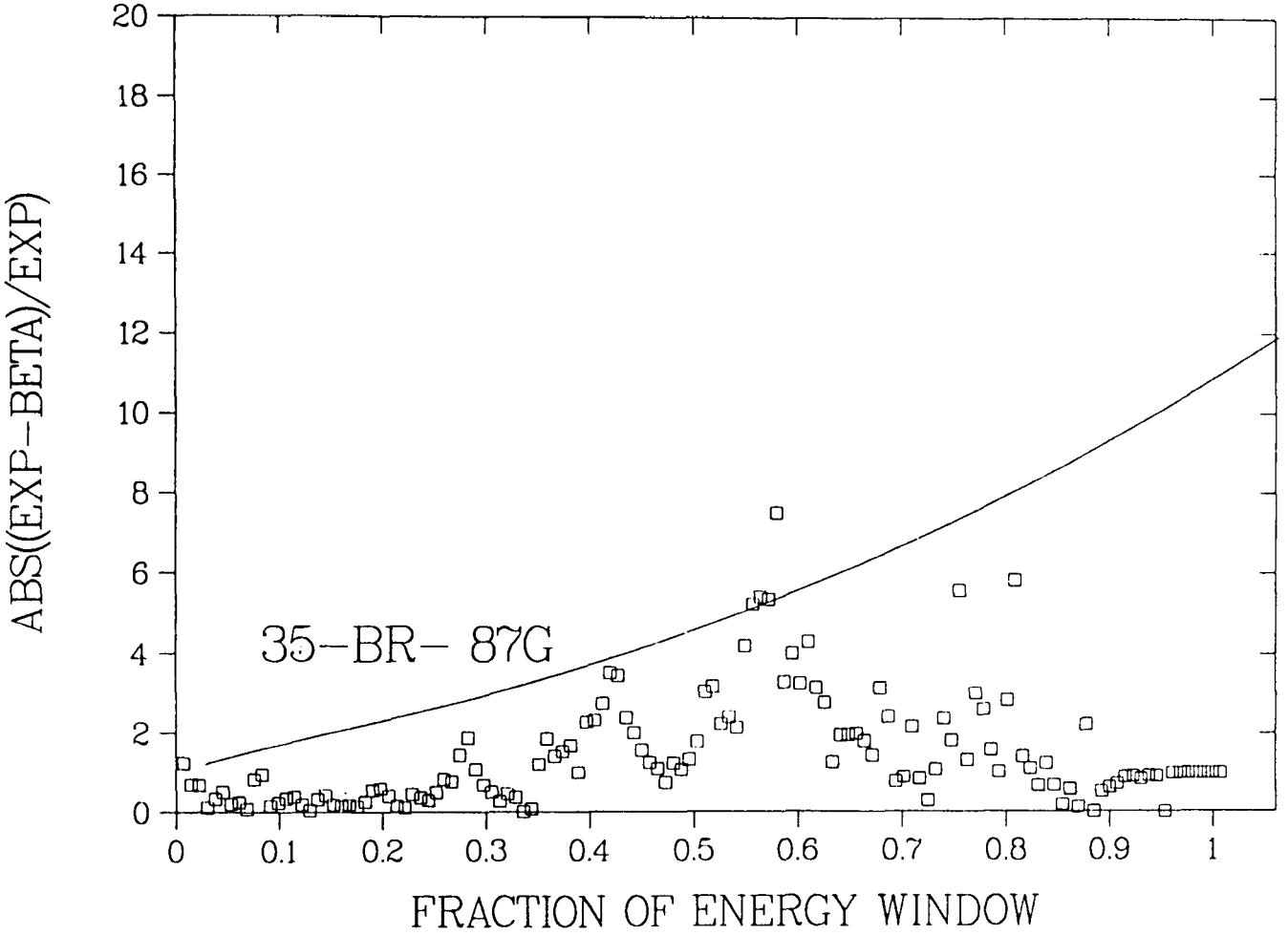

Fig. 63. Example of BETA code model uncertainty.

that the contrary is true for some delayed neutron precursors. Note also that due to background (reactor) thermal neutrons, many of the ^{3}He experiments have difficulty in resolving the very low energy delayed neutrons so that the experimental uncertainties are also larger at low energies.

The BETA code which allows for the input of specific level data to predict delayed neutron emission does not preclude low energy delayed neutrons and thus a similar trend was not observed in that case.

The uncertainty assignments were made as defined in Eqs. (24) and (25) and are somewhat arbitrary, but are considered to be both conservative (as illustrated by the requirement that the minimum uncertainty be 100%) and representative of the trends in the actual data.

SUMMARY OF PRECURSOR DATA

Table V is a succinct review of the contents of the precursor data library as complied and evaluated as described in this chapter. Data in the form of emission probabilities (P_n), energy spectra ($X(E)$), cumulative (y_c) and independent (y_i) fission yields, and half-lives ($t_{1/2}$) for 271 precursor nuclides are contained in the library.

As noted in Table V, there are six isomeric state nuclides which have been identified as delayed neutron precursors. These determinations must have been made on the basis of observed P_n values since the masses used to predict precursors from energetics cannot distinguish between ground and isomeric states. However, the emission probabilities were in some cases (for example, ^{127}In) measured from a mixture of the ground and isomeric states and not the isomeric state itself. Also, there is often confusion in the designation of ground and isomeric states where some experimentalists refer to a particular half-life and/or spin state as the isomeric state and others define the ground state as having those same properties. Published values of emission probabilities are always attributed to either the ground or isomeric state, but it is not always clear which half-life and spin state have been attributed to each. The state designations used in Table III, which is a detailed summary of the precursor library, are taken from

TABLE V

Content of Current Data Base

- 271 Precursors (based on energetics)
- P_n Delayed Neutron Emission Probabilities
  - — 89 evaluated measurements
  - — 182 from systematics (Kratz-Herrmann equation)
- Spectra (10-KeV bins)
  - — 34 measured (30 augmented with the BETA code model)
  - — 237 calculated from simple evaporation model [T correlated with (Q_β - S(n)) and A]
- Fission yields, $\tau_{1/2}$, β^-, and γ Branchings
  - — Yields from a preliminary ENDF/B-VI version
  - — Branchings and half lives from ENDF/B-V

F. M. Mann's 1986 evaluation of emission probabilities.[8] The column P_n Source also relies heavily of the Mann evaluation.

The major emphasis here has been in the compilation and evaluation of the precursor spectra. Details of the primary source and augmentation of the thirty-four experimental spectra are summarized under the column heading "Spectra Source" of Table III, and "Norm Area 1" and "Norm Area 2" in that table as described earlier in this chapter. The evaporation model which estimated the temperature parameter from Eqs. 20 and 22 was used to calculate spectra for 235 nuclides; in Table III these are designated as "EVAP" spectra and the temperature parameter (keV) is given in parentheses under the heading "Spectra Source". Two of the isomeric state precursors, ^{129m}In and ^{130m}In, have ground states whose spectra are measured. The spectrum for each of the isomeric states is taken to be identical to its respective ground state spectrum as indicated by the entry under the "Spectra Source" column.

Both the direct (independent) and cumulative fission yields are taken from a preliminary version of ENDF/B-VI. The half-lives and required branchings, other than P_n values, are taken from ENDF/B-V.[5]

CHAPTER VI.

SUMMATION CALCULATIONS

A principal advantage of the data library for individual precursors is that the total delayed neutron yield, ν_d, and equilibrium spectrum for any fissioning system can be calculated from this single data set given the appropriate fission yields. Calculations of this type involve a simple summation method that has been applied to delayed neutron data by several authors.[28,93,96,100]

TOTAL DELAYED NEUTRON YIELDS

Calculation and Comparison

The initiative for calculating ν_d by summing the individual precursor contributions was originally to provide a test on the quality of fission yields as evaluated for ENDF/B.[48] However, in the work performed here, the calculations are made to validate both the cumulative fission yields and the emission probabilities for the 271 precursors.

As discussed earlier, in the case of an equilibrium (steady-state) irradiation, the production and decay rate of each precursor nuclide are proportional to its cumulative yield. The product of the precursor's delayed neutron branching fraction and its cumulative fission yield represents the number of delayed neutrons per fission produced by the precursor. Summing the contributions from all 271 precursor nuclides as in Eq. (27) gives the total ν_d for the system.

$$\nu_d = \sum_{i=1}^{271} P_n^i y_c^i \tag{27}$$

In Table VI, ν_d values calculated using the data library constructed in Chapter V are compared to the earlier results of England et al.[28] (using 105 precursors), the results of an evaluation of experimental delayed neutron yields by Tuttle,[15,16] as well as the values currently contained in ENDF/B-V. Also noted in Table VI are more recent experimental ν_d values taken from the literature.[17,20] The description of each of the 43 fissioning systems for which delayed neutron yields

TABLE VI

Comparison of Total Delayed Neutron Yield per 100 Fissions

Fissionable Nuclide[a]	Present Calculation	England83[a] (Ref. 28)	ENDF/B-V (Ref. 5)	Tuttle (Ref. 26)	England83[b] (Ref. 48)
^{227}Th(T)	1.41 ± 0.26				1.41 ± 0.41
^{229}Th(T)	1.82 ± 0.29				1.81 ± 0.58
^{232}Th(F)	5.64 ± 0.41	4.76 ± 0.34	5.27	5.31 ± 0.23	5.69 ± 1.05
^{232}Th(H)	4.16 ± 0.36	3.03 ± 0.29	3.00	2.85 ± 0.13	4.16 ± 1.05
^{231}Pa(F)	1.60 ± 0.23			1.11 ± 0.11	1.60 ± 0.35
^{232}U(T)	0.52 ± 0.08		0.44*	0.52 ± 0.09	
^{233}U(T)	0.97 ± 0.16	0.85 ± 0.07	0.74	0.67 ± 0.03	0.96 ± 0.22
^{233}U(F)	0.90 ± 0.12	0.92 ± 0.09	0.74	0.73 ± 0.04	0.91 ± 0.15
^{233}U(H)	0.70 ± 0.10	0.71 ± 0.10	0.47	0.42 ± 0.03	0.70 ± 0.13
^{234}U(F)	1.29 ± 0.15			1.05 ± 0.11	1.30 ± 0.21
^{234}U(H)	0.77 ± 0.11			1.62 ± 0.08	0.76 ± 0.15
^{235}U(T)	1.78 ± 0.10	1.77 ± 0.08	1.67	1.62 ± 0.05	1.77 ± 0.14
^{235}U(F)	2.06 ± 0.20	1.98 ± 0.18	1.67	1.67 ± 0.04	2.06 ± 0.27
^{235}U(H)	1.09 ± 0.13	0.98 ± 0.10	0.90	0.93 ± 0.03	1.08 ± 0.18
^{236}U(F)	2.32 ± 0.23	2.26 ± 0.19		2.21 ± 0.24	2.32 ± 0.31
^{236}U(H)	1.55 ± 0.17			1.30 ± 0.20	1.54 ± 0.23
^{237}U(F)	3.50 ± 0.28				3.50 ± 0.38
^{238}U(F)	4.05 ± 0.29	3.51 ± 0.27	4.40	4.39 ± 0.10	3.54 ± 0.36
^{238}U(H)	2.76 ± 0.25	2.69 ± 0.21	2.60	2.73 ± 0.08	2.71 ± 0.35
^{237}Np(F)	1.14 ± 0.12	1.28 ± 0.13	1.08**		1.14 ± 0.15
^{237}Np(H)	0.97 ± 0.11				0.96 ± 0.13
^{238}Np(F)	2.16 ± 0.19				2.15 ± 0.24
^{238}Pu(F)	0.79 ± 0.09		0.42**	0.47 ± 0.05	0.79 ± 0.11
^{239}Pu(T)	0.76 ± 0.04	0.77 ± 0.06	0.65	0.63 ± 0.04	0.76 ± 0.05
^{239}Pu(F)	0.68 ± 0.08	0.72 ± 0.09	0.65	0.63 ± 0.02	0.68 ± 0.09
^{239}Pu(H)	0.38 ± 0.06	0.39 ± 0.06	0.43	0.42 ± 0.02	0.38 ± 0.07
^{240}Pu(F)	0.81 ± 0.09	0.92 ± 0.11	0.90	0.95 ± 0.08	0.81 ± 0.11
^{240}Pu(H)	0.51 ± 0.07			0.67 ± 0.05	0.50 ± 0.09
^{241}Pu(T)	1.41 ± 0.09	1.58 ± 0.13	1.62	1.52 ± 0.11	1.39 ± 0.12
^{241}Pu(F)	1.42 ± 0.14	1.49 ± 0.16	1.62	1.52 ± 0.11	1.39 ± 0.16
^{242}Pu(F)	1.43 ± 0.14	1.41 ± 0.14	1.97*	2.21 ± 0.26	1.40 ± 0.16
^{241}Am(T)	0.53 ± 0.07				0.53 ± 0.07
^{241}Am(F)	0.51 ± 0.06		0.43**		0.50 ± 0.07
^{241}Am(H)	0.26 ± 0.05				0.25 ± 0.05

TABLE VI (Continued)

Fissionable Nuclide[a]	Present Calculation	England83[a] (Ref. 28)	ENDF/B-V (Ref. 5)	Tuttle (Ref. 16)	England83[b] (Ref. 48)
^{242m}Am(T)	0.78 ± 0.09		0.69*		0.76 ± 0.11
^{243}Am(F)	0.80 ± 0.09				0.79 ± 0.10
^{242}Cm(F)	0.14 ± 0.03				0.13 ± 0.03
^{245}Cm(T)	0.64 ± 0.08		0.59*		0.60 ± 0.09
^{249}Cf(T)	0.16 ± 0.03		0.27*		0.16 ± 0.03
^{251}Cf(T)	0.75 ± 0.08				0.73 ± 0.09
^{252}Cf(S)	0.65 ± 0.07	0.69 ± 0.09	0.86*		0.61 ± 0.07
^{254}Es(T)	0.46 ± 0.06			0.39 ± 0.06	
^{255}Fm(T)	0.28 ± 0.04				0.25 ± 0.04

[a] T, F, H, and S denote thermal, fast, high energy (~ 14 MeV), and spontaneous fission, respectively.

* Values based on measurements but not in ENDF/B-V. (See Ref. 19.)

** Values based on inverse-variance weighted average of data from both Refs. 17 and 19.

were calculated is given in Table VI and includes both the fissionable nuclide's chemical symbol and mass number (e.g. ^{235}U, ^{240}Pu, etc.) and the fission energy (T, F, H, or S, denoting thermal, fast, high energy (14 MeV), and spontaneous fission respectively).

The present calculations are in excellent agreement with the results given in Ref. 48, which were based on the 105 precursor set and emission probabilities of Ref. 28 and a preliminary ENDF/B-VI fission yield set. More than 90% of the delayed neutrons are produced from the decay of odd-Z nuclides,[28,48] therefore the recent change made in the Z-pairing (from 33% to 15%) for the ^{238}U(F) yields resulted in a rather marked improvement in the calculated ν_d for that system from 0.0354 to 0.0405. Another difference in the fission yield sets used in this evaluation is the extensions along mass chains to include $Z_p \pm 4$ nuclides (see Chapter III).

The ν_d values in column three of Ref. 28) of Table VI use data for 105 precursors, based on ENDF/B-V yields and an earlier (1979) Pn evaluation[74] which included measurements for only 67 nuclides. Agreement of the current ν_d calculations with these values is also quite good. The major differences are in the yields for ^{232}Th(T), ^{232}Th(F), and ^{238}U(F) which are attributed to differences in the values of proton-pairing used in the ENDF/B-V fission yield evaluation and those in the current yield evaluation.

Both the ENDF/B-V[5] (1977) and Tuttle[16] (1979) delayed neutron yields are the result of evaluations of experimental data and are thus in excellent agreement with one another. No uncertainties are recorded in Table VI for the ENDF/B-V data because ENDF formats do not permit the inclusion of uncertainties for delayed neutron yields. These uncertainties, which are given in the evaluations of Cox,[14] and Kaiser and Carpenter[27] are quite similar to those cited from Tuttle's evaluated yields. Unique yields taken from the more recent measurements of Benedetti et al.[17] and Waldo et al.[19] are also given without uncertainties. These yields, as noted, were not a part of ENDF/B-V but have been recommended for inclusion in ENDF/B-VI. Delayed neutron yields from Ref. 19 are taken from their table of recommended values and have uncertainties on the order of 7–12%. Measurements of ν_d for ^{237}Np(F), ^{238}Pu(F), and ^{243}Am(T) were reported

in both Refs. 17 and 19. The value given in Table VI for each of these nuclides is take as the inverse-variance weighted average of the two measurements. The uncertainties for these values are slightly higher, 8–18%.

In most cases the calculated and experimental delayed neutron yields are overlapping (within the error bars), and therefore in good agreement. The uncertainties in the calculated ν_d are attributed to the uncertainty in the emission probabilities. This is illustrated by the contrast in the uncertainties of ν_d in the current and "England 83^b" calculations to those from the "England 83^a" calculations where the experimental P_n's appear to have too small uncertainties (in some cases, 5% or less) that are too small.

Discussion of Contribution by Precursor

The relative importance of the various models and approximations used in obtaining the precursor data base may be quantified for the aggregate equilibrium results given in the preceding sections by calculating the fraction of the total delayed neutron yield contributed by precursors with measured spectra and those with measured P_n values. All precursors with measured spectra also have measured emission probabilities as shown in Table III. These thirty-four nuclides contribute an average of 80% of the delayed neutron yield from fission for the 43 systems studied. They account for 96% of the delayed neutrons produced from the thermal fission of ^{227}Th. The eighty-nine precursors with one or more P_n measurements were found to contribute an average of 94% to the total ν_d. The percent contributions for uranium and plutonium systems tend to be somewhat higher than the average with the exception of ^{233}U(T) and ^{242}Pu(F). The results for all 43 fissioning systems are given in Table VII. Improving these fractions would require additional measurements, particularly spectral measurements.

The contribution to the total delayed neutron yield by each precursor is needed in order to recommend specific nuclides for future measurements. Due to the large number of precursor nuclides and the number of fissioning systems addressed in this study it is practical to illustrate the relative importance of the precursors schematically, as in Figs. 64(a) and 64(b), rather than in bulky tables. All nuclides to the right of the broad band in Fig. 64 are recognized as

TABLE VII

Percent of Total DN Yield From Precursors with Measured Data

Fissioning System	Measured Spectra	Measured P_n
^{227}Th(T)	96.238	99.6641
^{229}Th(T)	95.872	99.2874
^{232}Th(F)	85.213	96.6394
^{232}Th(H)	88.050	95.2971
^{231}Pa(F)	94.654	99.6628
^{232}U(T)	92.909	99.7732
^{233}U(T)	73.886	99.2707
^{233}U(F)	91.453	99.5638
^{233}U(H)	90.539	99.0100
^{234}U(F)	90.415	99.3084
^{234}U(H)	89.271	98.8568
^{235}U(T)	84.039	95.7944
^{235}U(F)	88.532	98.8623
^{235}U(H)	88.706	98.6471
^{236}U(F)	86.638	97.9873
^{236}U(H)	87.095	97.8673
^{237}U(F)	84.010	96.8644
^{238}U(F)	80.240	94.9217
^{238}U(H)	83.158	96.0831
^{237}Np(F)	85.721	98.2179
^{237}Np(H)	83.680	97.1610
^{238}Np(F)	84.336	96.8266
^{238}Pu(F)	83.920	97.3978
^{239}Pu(T)	85.838	97.4254
^{239}Pu(F)	82.592	96.9096
^{239}Pu(H)	81.031	97.2945
^{240}Pu(F)	82.674	96.8406
^{240}Pu(H)	80.913	96.3833
^{241}Pu(T)	81.175	94.7845
^{241}Pu(F)	80.782	94.5660
^{242}Pu(F)	78.721	94.0829
^{241}Am(T)	78.341	95.6272
^{241}Am(F)	80.989	96.5504
^{241}Am(H)	77.036	94.7363
^{242m}Am(T)	80.805	94.8138

TABLE VII (Continued)

Fissioning System	Measured Spectra	Measured P_n
^{243}Am(F)	82.216	95.8391
^{242}Cm(F)	77.539	97.0427
^{245}Cm(T)	76.439	91.4171
^{249}Cf(T)	76.382	91.2452
^{251}Cf(T)	82.795	93.1811
^{252}Cf(S)	81.011	90.4431
^{254}Es(T)	67.569	79.6644
^{255}Fm(T)	78.528	85.6547

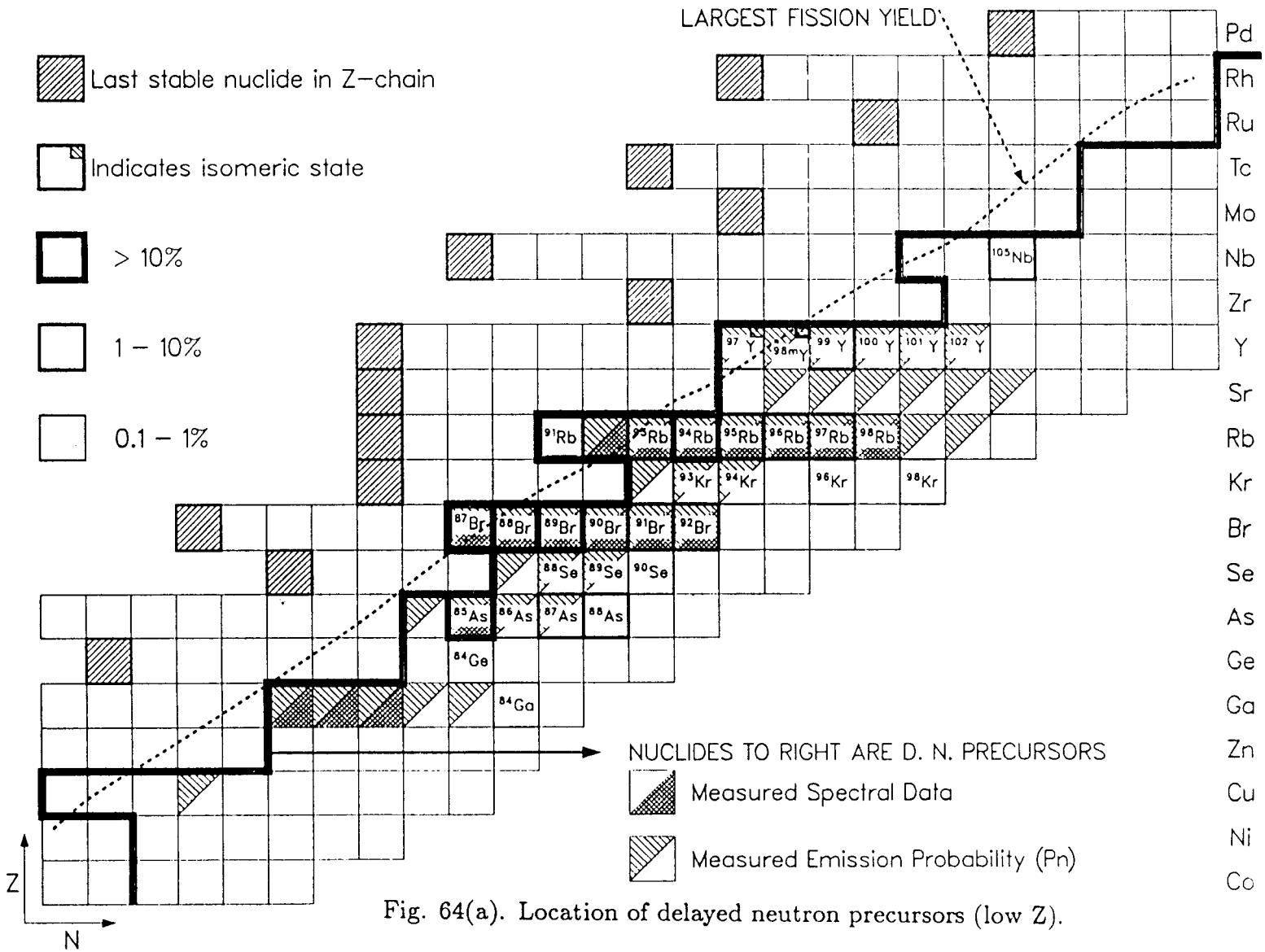

Fig. 64(a). Location of delayed neutron precursors (low Z).

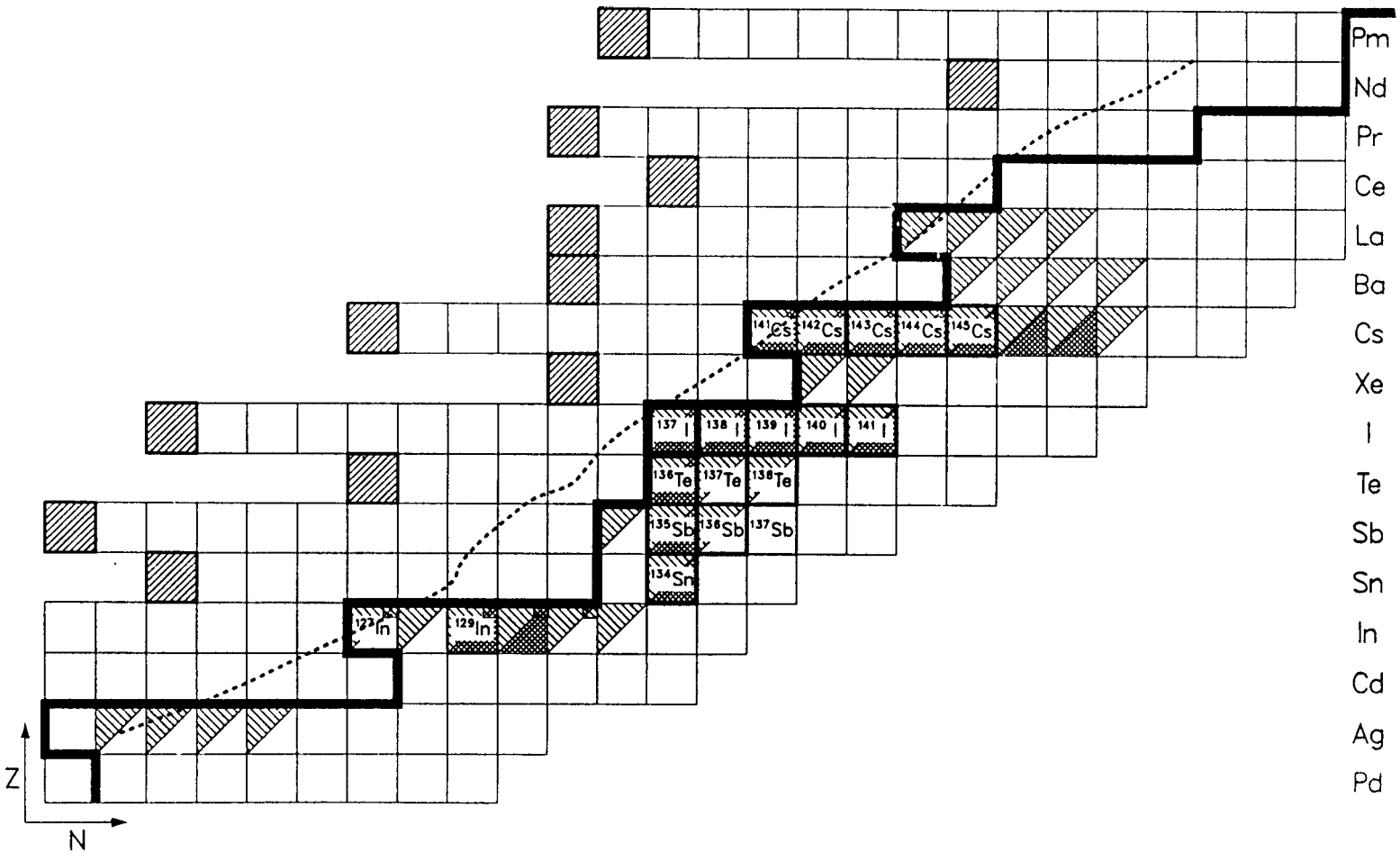

Fig. 64(b). Location of delayed neutron precursors (high Z).

delayed neutron precursors. Each of the fifty-two ground state and two isomeric state (^{97m}Y and ^{98m}Y) precursors whose chemical symbol and mass are explicitly given were found to individually contribute at least 0.1% to the total delayed neutrons from fission in fuels of interest to reactors (all isotopes of uranium and plutonium and ^{232}Th). The relative importance of each of these precursors is classified into one of three groups. Those contributing 10% or more; those contributing between 1 and 10%; and those contributing between 0.1 and 1% make up the three groups. It is interesting to note that for most fuels a single nuclide may contribute in excess of 10% to the total delayed neutron yield and as much as 20–30% in some cases. Figure 64 also illustrates the existing experimental data for both spectra and emission probabilities. Nine of the fifty-four precursors specifically noted in Fig. 64 have neither measured spectra nor emission probabilities, and three of these (^{88}As, ^{91}Rb, and ^{105}Nb) can be responsible for as much as 1 to 10% of the total delayed neutron yield in some cases. It is suggested that an effort be made to experimentally determine the P_n value for these nine precursors and particularly for the three larger contributors.

Only half of the precursors identified in Figs. 64(a) and 64(b) have measured spectra. As discussed above, nine of these also have no measured delayed neutron emission probability and require additional measurements to validate their relative importance. The remaining eighteen nuclides having measured emission probabilities but no measured spectra. Twelve of these contribute only 0.1 to 1% of the total delayed neutrons and the remaining six are responsible for 1–10% of ν_d. The fractions contributed by these final eighteen are calculated using measured emission probabilities and are therefore representative of their importance in predicting delayed neutron emission.

AGGREGATE DELAYED NEUTRON SPECTRA

The results and comparisons of the calculated total delayed neutron yields provide an adequate test of the fission yields and emission probabilities. The validity of the precursor spectra can be tested in much the same manner. Summation techniques may be applied in order to calculate the total (or aggregate)

delayed neutron spectrum for a given fuel which can be compared to the experimental spectrum.

Calculation and Comparison

The aggregate delayed neutron spectrum under equilibrium conditions, X(E), may be calculated by summing the contributions from each precursor as;

$$\mathrm{X}(E) = \sum_j P_n^j y_c^j \mathrm{X}_j(E) \tag{28}$$

where P_n^j, y_c^j, and $\mathrm{X}_j(E)$ are the emission probability, cumulative fission yield and delayed neutron spectrum for the precursor nuclide j.

Calculations of this type were performed for the 43 fissioning systems of interest. The results for ^{235}U(T), ^{238}U(F) and ^{239}Pu(F) are given in Figs. 65-67 as examples. Also given in these figures are the respective delayed neutron spectra from ENDF/B-V and an earlier calculation (Ref. 28) using 105 precursor nuclides. The comparisons are made over the energy range 0–1 MeV in order to emphasize the differences in the spectral shapes rather than the maximum energies (recall that the ENDF spectra are cutoff at ~1.2 MeV and both calculated spectra include experimental data to about 3.0 MeV). In all cases the spectra as shown in Figs. 65–67 are normalized such that the integral from 0–1 MeV is 1.0. The ENDF/B-V total spectra are calculated based on the six-group delayed neutron data given in ENDF/B-V as:

$$\mathrm{X}(E) = \sum_{i=1}^{6} a_i \mathrm{X}_i(E) \tag{29}$$

which, in essence, simply sums the contributions of each of the six groups to the total spectrum. As stated earlier the six group spectra given in ENDF/B-V are normalized to integrate to the group fractional abundance, therefore its contribution to the total is weighted by this fraction,a_i.

The general shapes of the spectra are in agreement for all cases, but especially for ^{235}U(T). The current method provides spectra with detailed information in the region of 0–76 keV. In the ENDF data, this region is approximated

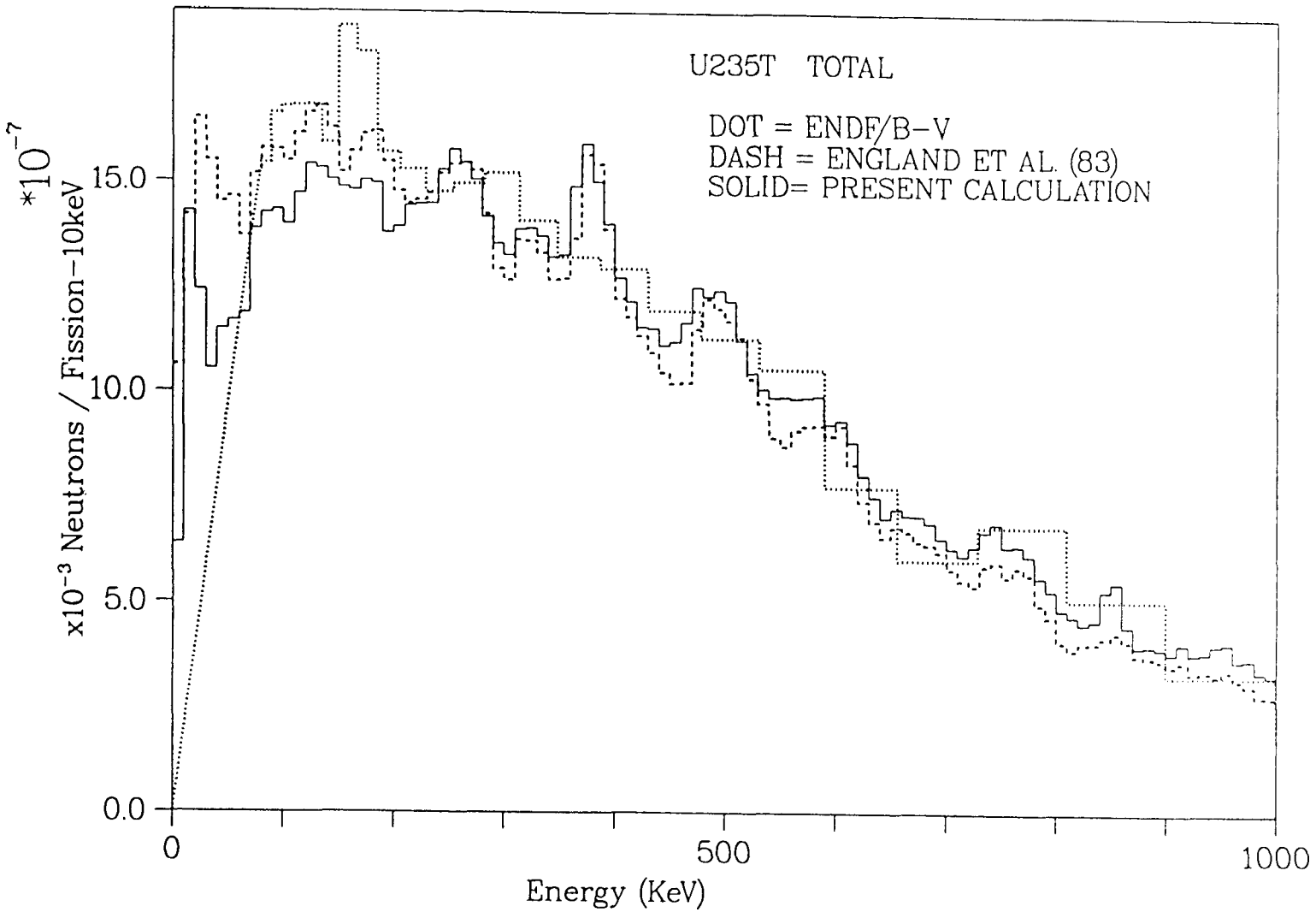

Fig. 65. Aggregate spectra for ^{235}U(T).

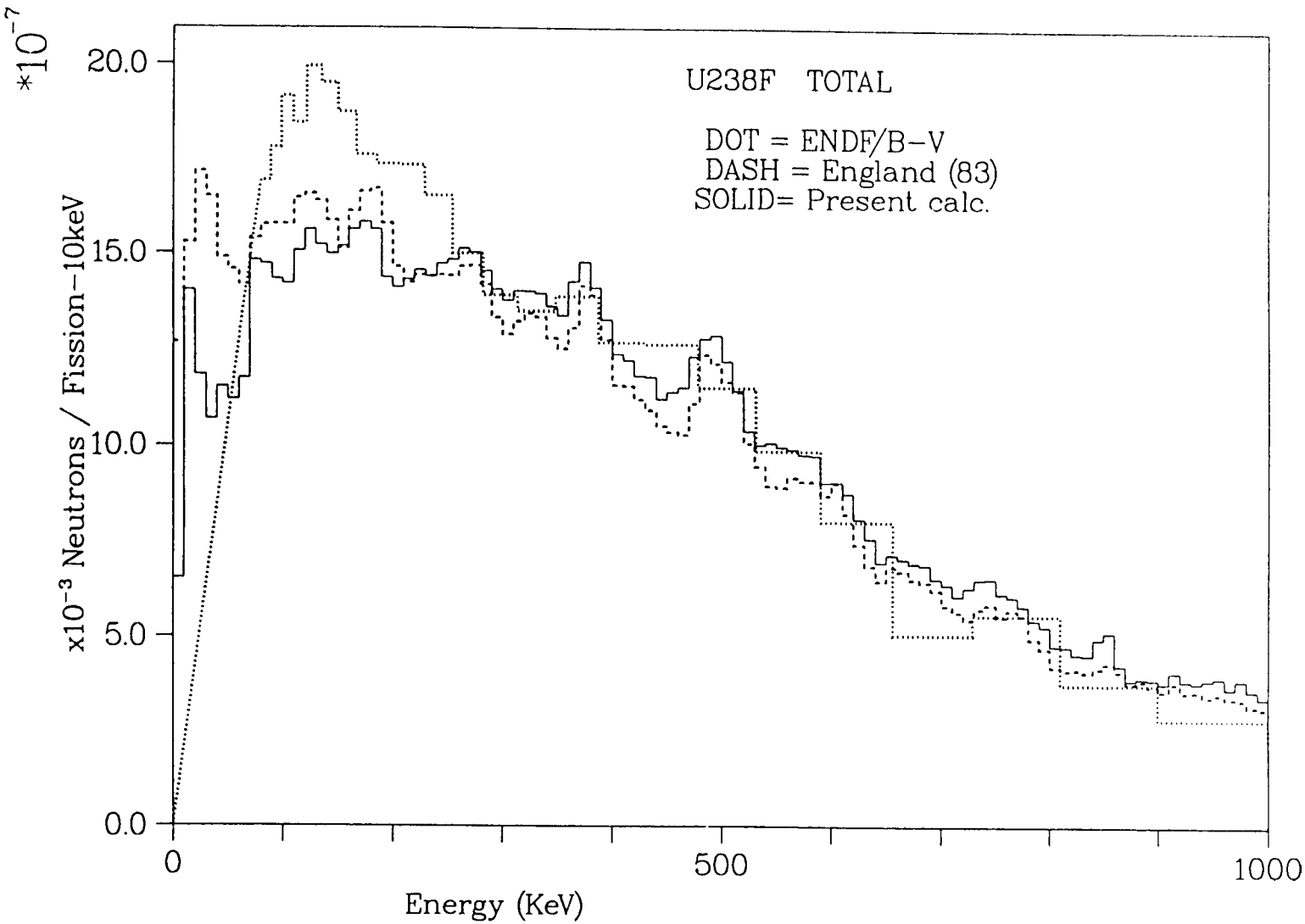

Fig. 66. Aggregate spectra for ^{238}U(F).

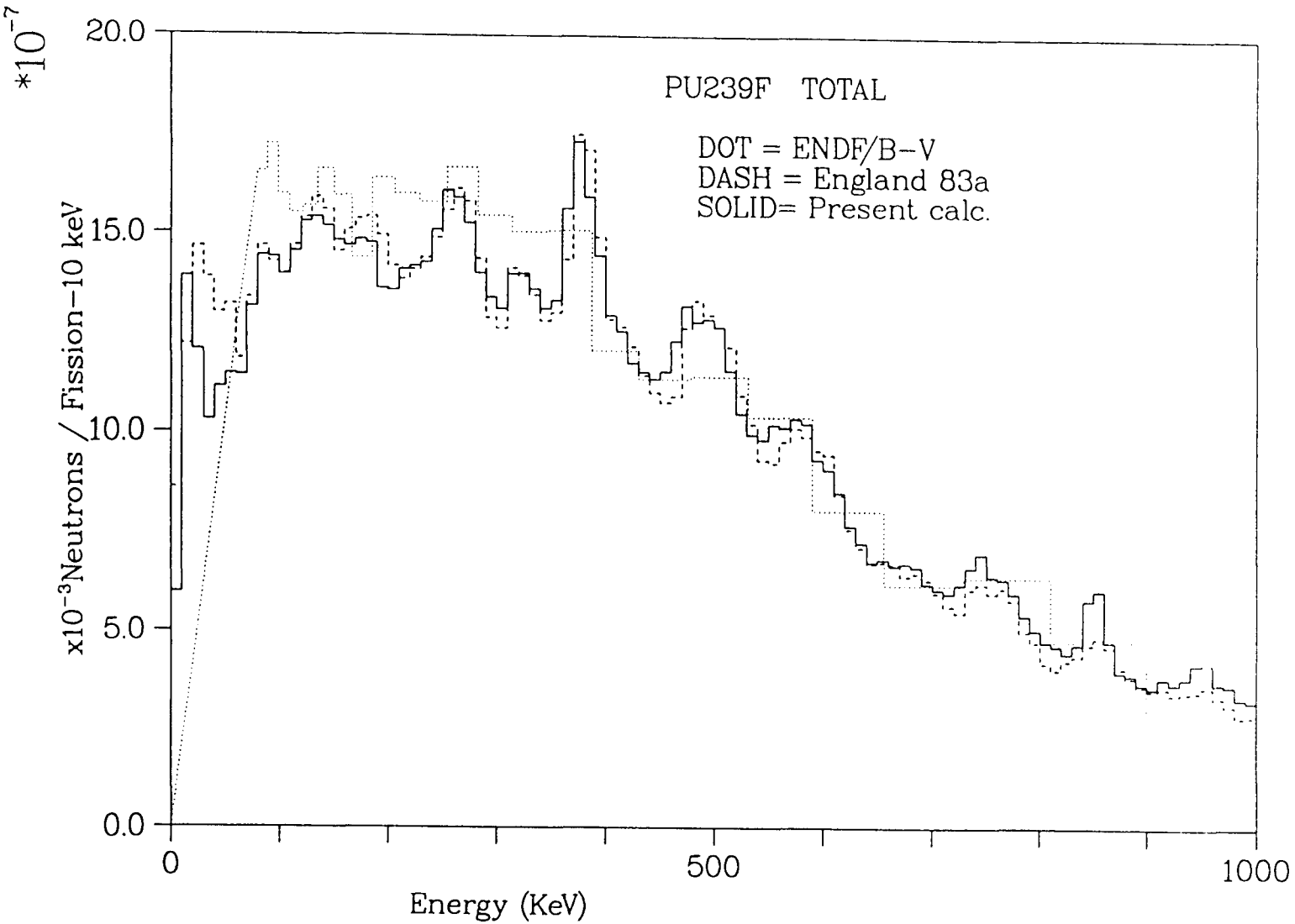

Fig. 67. Aggregate spectra for ^{239}Pu(F).

as a simple linear function in lieu of experimental data for that region, This is significant since many experimentalists (Rudstam, Reeder, Shalev and Kratz) have identified a high intensity peak at about 13 keV in the delayed neutron spectrum for ^{93}Rb, a nuclide that may contribute from 1 to 10% of the total delayed neutron yield in many cases. This result among others, particularly the results of the Greenwood and Caffrey proton-recoil measurements, reveal that there is definite structure in the delayed neutron spectra for energies less than 70 keV. Differences between the two calculations (represented by the dashed and solid curves in Figs. 65-67) at energies less that a few hundred keV are attributed to the inclusion of the proton-recoil measurements.

The England et al.[28] (1983) calculation (dashed curves in Figs. 65–67) was based on a 105 precursor data set; with experimental spectra for 29 precursors as supplied by G. Rudstam which included Mainz spectra for ^{85}As, ^{92}Rb, ^{96}Rb, ^{97}Rb, and ^{98}Rb. Seventy-six BETA code calculated spectra, 67 measured and 38 calculated emission probabilities and ENDF/B-V fission yields. The number of precursors included in the present calculation is more that double that used by England.[28,48] The amount of experimental data (including both spectra and emission probabilities) that was reviewed and considered in this evaluation was also dramatically increased. Model extensions for both the upper and lower region of the spectra and the use of the evaporation model for calculating spectra for nuclides lacking experimental spectra also serve to distinguish the current calculations. A different set of primary fission yield evaluations (ENDF/B-VI) were also used in this evaluation.

Despite the numerous additions and revisions in the basic data used in the two calculations, the results appear to be in very good agreement for the spectral shapes above 200 keV.

Average Energy Comparisons

The first estimate of the mean energy of delayed neutrons from the fission of ^{235}U was made by Roberts and co-workers[11] (1939) based on their observations of recoil nuclei in a cloudchamber, they reported "their [delayed neutrons]

energy is less than one million electron volts and probably near one-half million electron volts."[11] Enrico Fermi later (1943) estimated the average energy from age measurements in graphite to be 640 keV,[3] although his measurement is believed to have preferentially weighted the group two neutrons.[3]

Many measurements and determinations of the average energy of delayed neutrons from ^{235}U as well as other fissioning nuclides have been made since the work of Roberts and Fermi. There is some ambiguity in describing many of the published values as either a measurement or a calculation. Seldom is the average energy the result of a direct measurement, more often it is a value derived from measurements of either integral, group, or precursor spectra.

The most reliable of the early measurements of this type, the work of Batchelor and McK. Hyder[24] (1956), and the most recent work of Tanczyn et al.[9] (1986) are both represented in this table. The other values given represent the onset of the current interest in delayed neutrons (1972-1977). A range of detection systems is also represented by the data in Table VIII. An early version of the current ^{3}He spectrometer was used in the Batchelor and McK. Hyder experiments. Proton-recoil detectors were used in the cases of Fieg,[25] Sloan and Woodruff,[84] and Eccleston and Woodruff.[85] A more modern ^{3}He spectrometer was used by Evans and Krick;[101] and Tanczyn et al.[9] made use of modern time-of-flight techniques. These data are given in Table VIII along with the results of the current evaluation for comparison. Many of these results, particularly those of Batchelor and McK. Hyder,[24] may be misleading in that the experimentalists were limited by the response of their equipment and were able only to make reasonable measurements of delayed neutrons at longer times; i.e. they could only determine spectra for groups one through four, and in effect were basing their results on data representing about 80% of the total delayed neutrons. Evans and Krick as well as Tanczyn et al. attempted to account for the missing fraction of delayed neutrons in their final analyses, thereby resulting in higher values for average energies. Tanczyn points out that the composite spectra are very sensitive to the results at short delay times since approximately 30% of all delayed neutrons are emitted in less than one second after fission.[9] Another observation that can be made from Table VIII is that the results using

TABLE VIII

Table of Measured Average Energy Comparisons

Fission Nuclide	Present Calculation	Ref. 85	Ref. 101	Ref. 25	Ref. 24	Ref. 84	Ref. 9
^{232}Th (H)	568(16)	355					
^{233}U (T)	539(44)	350					
^{235}U (T)	507(16)	385		435	430	339	470
^{235}U (F)	512(13)		457				
^{235}U (H)	498(15)			451			
^{238}U (F)	534(22)	347	542				
^{238}U (H)	526(19)			445			
^{239}Pu (F)	487(18)	369	509				
^{239}Pu (H)	462(22)			425			

^{3}He spectrometry are consistently higher than the proton recoil data (including the early measurements of Batchelor and McK. Hyder) which might be expected from their relative efficiencies and energy resolution (see Chapter V). Overall, agreement with the ^{3}He results is considered good; the proton-recoil measurements of Batchelor and McK. Hyder and those of Fieg are also in fair agreement considering their measurements included only ~80% of the total delayed neutrons. More detailed comparisons with the recent Tanczyn results will be made in the following chapter.

The present evaluation is based on integrating the contribution from each precursor to obtain an integral delayed neutron spectrum for a given fissioning nuclide and the average energy is then calculated from this spectrum. Table IX refers to these values as calculated and compares the current results to those obtained by similar methods, as well as the current ENDF/B-V data.

The earliest data presented in this table are that of Keepin (1965) and are based on only 10 precursor nuclides. In lieu of experimental spectra for each precursor, Keepin estimated the average energy of each precursor as a fixed fraction of its energy window ($Q_\beta - S(n)$) and weighted these values with the corresponding cumulative fission yields and theoretical neutron emission probabilities and obtained the values given in Table IX. Those average energies attributed to ENDF/B-V (1977) were derived from integral spectra calculated by weighting each of the six group spectra by its abundance. The Reeder and Warner[96] (1981) data were obtained using the same methodology as Keepin, however in their situation the average energy of the delayed neutrons from each precursor was based on an evaluation of both experimental spectra as well as their direct measurement of average energies. The results of their evaluation for the 34 precursor nuclides have already been compared in Table IX. Each precursor's average energy was appropriately weighted by its emission probability (taken from an evaluation by Rudstam[74]) and cumulative fission yield. Reeder estimated that the 34 precursors in his study accounted for about 88% of the delayed neutrons from fission.

The 1983 evaluation[28] of England et al. is also given for comparison. Preliminary results from this evaluation were presented at the International Conference

TABLE IX

Table of Calculated Average Energy Comparisons

Fission Nuclide	Present Calculation	Ref. 28	Ref. 102	Ref. 96	Ref. 5	Ref. 3
^{232}Th (F)	548(17)	424.6	495.2		447	490
^{232}Th (H)	568(16)	457.9	547.5			
^{233}U (T)	539(44)	407.7	494.6		447	390
^{233}U (F)	480(14)	394.8	454.4			
^{233}U (H)	469(15)	389.4	449.5			
^{235}U (T)	507(16)	415.8	455.5	440	450	430
^{235}U (F)	512(13)	417.6	475.5	451		
^{235}U (H)	498(15)	400.8	472.7	439		
^{236}U (F)	523(17)	424.0	480.5			
^{238}U (F)	534(22)	421.9	477.6	463	432	490
^{238}U (H)	526(19)	428.5	484.8	458		
^{237}Np (F)	502(15)	418.5	466.7			
^{239}Pu (T)	493(14)	419.8	459.2	450	449	400
^{239}Pu (F)	487(18)	412.9	454.4	448		
^{239}Pu (H)	462(22)	383.2	442.4	417		
^{240}Pu (F)	497(17)	416.6	458.3		447	420
^{241}Pu (T)	502(15)	428.1	483.3		443	
^{241}Pu (F)	506(17)	426.7	465.0			
^{242}Pu (F)	504(17)	420.0	458.3			
^{252}Cf (S)	477(16)	409.8	444.2	460		

on Nuclear Data for Basic and Applied Science (1985) held in Santa Fe, New Mexico.[102] These results are given in Table IX to illustrate how the use of the somewhat harder Mainz spectra influence the average energy of delayed neutrons for the different systems. At that time the evaluation included only 110 precursors; 74 with measured P_n values,[46] 30 having experimental spectra. Of the 30 experimental spectra, 20 were those recommended by Rudstam as used in England's 1983 work, but 10 were the spectra provided by Prof. Kratz. The spectra had not been augmented at that time.

Average energies calculated in the present evaluation are somewhat harder than those previously reported but still appear to be in good agreement. The evolution of the current evaluation can be traced to some degree by contrasting the original England results with the intermediate results of the Santa Fe meeting and the final results given in the first column of Table IX. It is not apparent from the average energy which of the changes in the basic data used in each of these evaluations has had the greatest influence. Each step in the progression is complicated by changes in more than one parameter and in each case different sets of spectra, emission probabilities and even fission yields were used. The comparisons of Tables VIII and IX are made for completeness and should be viewed as an indication of trends in the data as a single gross value such as average energy may not adequately represent the detailed data.

CHAPTER VII.

FEW-GROUP APPROXIMATIONS

The time-dependent behavior of beta-delayed neutrons has traditionally been represented by six precursor groups. As discussed earlier, these groups have no physical basis but rather were originated as six-term, twelve-parameter fits to experimentally measured delayed neutron activities following fission pulse and saturation irradiation experiments in critical assemblies. The explicit precursor data compiled in this evaluation have been used to generate these more common "group" parameters.

GROUP HALF-LIVES AND FRACTIONS

The fission product depletion code, CINDER-10,[103] was used to calculate the inventories of all precursor nuclides for various cooling times (to 300 seconds) following a prompt irradiation in each of the 43 fissioning systems (except ^{252}Cf(S)). These nuclide inventories were weighted with the recently evaluated delayed neutron emission probabilities to determine the delayed neutron activities at the various cooling times. The calculated results for ^{238}U(F), ^{235}U(F), ^{235}U(T), and ^{239}Pu(F) are shown in Fig. 68. The analysis of the calculated data is performed much in the manner that Keepin et al.[4] analyzed their experimental data in 1956, with the exception that current computational capabilities allow the derivation of all constants from the pulse irradiation data, dismissing the need for concomitant infinite irradiation data.

The delayed neutron activity curves can be approximated mathematically by a sum of N exponentials representing N time-groups, as in Eq. (30):

$$n_d(t) = \sum_{i=1}^{N} A_i e^{-\lambda_i t} \tag{30}$$

A non-linear least-squares fitting routine, STEPIT,[104] was used to determine the parameters A_i and λ_i. The constant λ_i represents an effective decay constant for the i^{th} group of delayed neutron precursors. Equation (30) is being used to represent delayed neutron activity following a fission pulse, therefore the

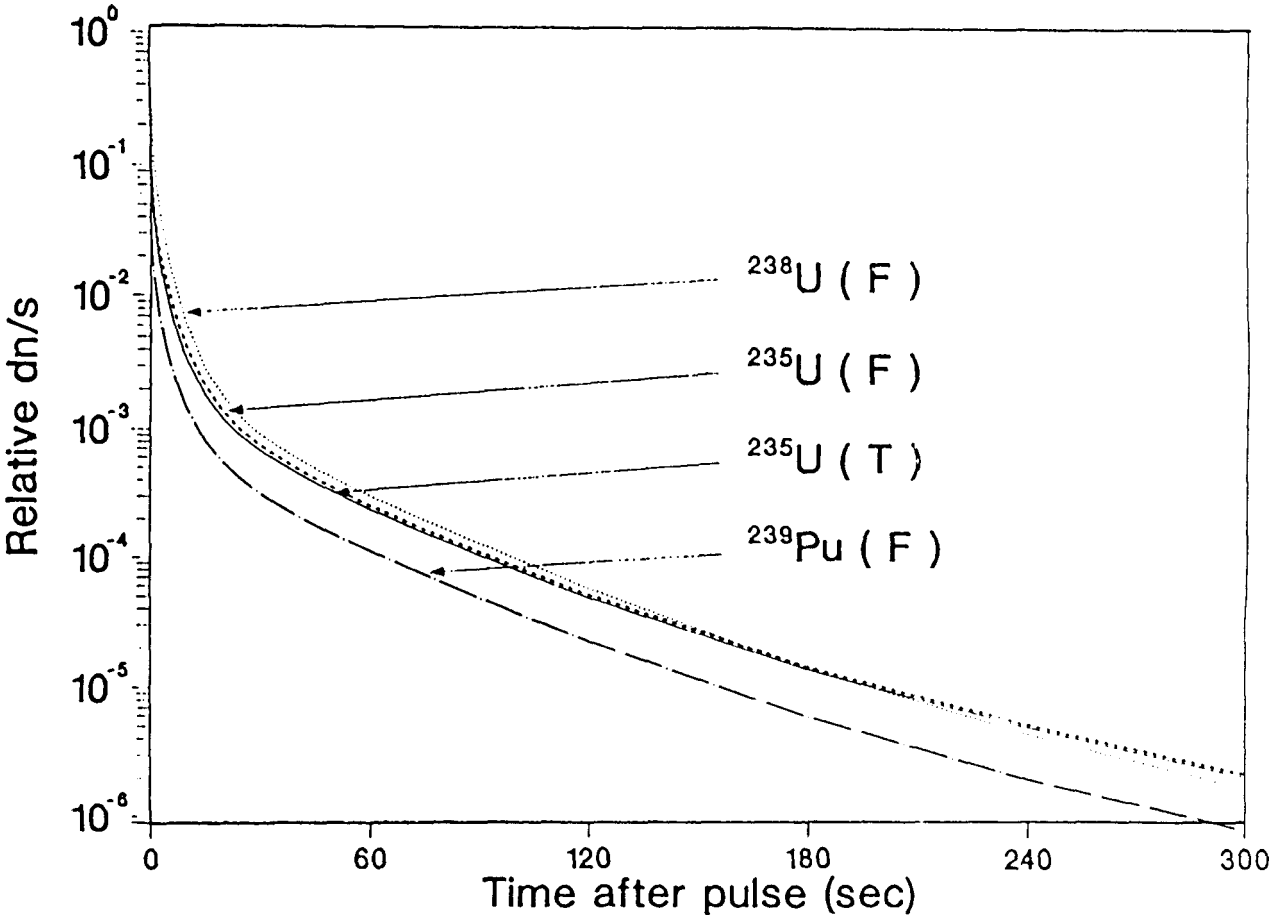

Fig. 68. Delayed neutron activity following a fission pulse.

coefficient, A_i, represents the initial activity of delayed neutrons and is found as the product of the group decay constant, λ_i, and the group yield per fission, α_i.

The fitting procedure was used to produce decay constants and abundances for three-, six-, nine-, and twelve-delayed neutron groups for each of three fissioning nuclides, ^{235}U(F), ^{238}U(F), and ^{239}Pu(F).[105] A parameter representing the goodness of fit was defined as:

$$X^2 = \sum((\text{ fitted value - CINDER})/\text{CINDER}) * *2 \ . \qquad (31)$$

where "CINDER" represents the CINDER calculated result.

The resulting values of X^2 for each fit, the group decay constants, and normalized abundances are given in Table X. The six-group representations fit the data well in all three cases with a X^2 on the order of 1.0E-04 which is a significant improvement over the values on the order of 1.0E-01 for the three-group fits. A significant improvement is seen when the number of groups is further increased to nine. This reduces X^2 by approximately two orders of magnitude for ^{235}U and ^{238}U, and one order of magnitude for ^{239}Pu. As the number of groups is increased further, from nine to twelve, the change in X^2 is less dramatic for ^{235}U(F) and ^{239}Pu(F), being less than a factor of 2, and a factor of four change is seen for ^{238}U(F).

The six- and nine-group parameters have been used via Eq. (29) to calculate the delayed neutron activity curves shown in Fig. 69 to compare to the CINDER-10 results for ^{235}U(F). Also, plotted there is the activity obtained from the ENDF/B-V six-group parameters for ^{235}U. The ENDF/B-V abundances have been normalized to produce the same number of delayed neutrons per fission in order to facilitate the comparison. Figure 70 compares the differences between the current six- and nine-group data, the ENDF/B-V six-group data as a ratio of the CINDER-10 calculation for ^{235}U(F).

Consistent with previously reported results,[106,107] for short times (< 3 s) after a pulse irradiation, the ENDF/B-V data underestimates delayed neutron activity and, for longer times, overestimates delayed neutron activity. As can

TABLE X

Comparison of X^2 Values and Group Parameters for Few-Group Fits

	groups	X^2	group constants $\lambda_i(sec^{-1}), a_i(\beta_i/\beta)$
^{235}U (F)	3	5.4E-01	λ_i 0.0203 0.0983 0.5595 a_i 0.1356 0.3372 0.5272
	6	1.4E-04	λ_i 0.0133 0.0328 0.1219 0.3054 0.8649 2.8776 a_i 0.0350 0.1803 0.1782 0.3859 0.1557 0.0649
	9	3.4E-06	λ_i 0.0128 0.0309 0.0663 0.1581 0.3315 0.3670 0.8685 2.1209 4.0980 a_i 0.0306 0.1645 0.0561 0.2141 0.2025 0.1327 0.1196 0.0603 0.0195
	12	1.3E-06	λ_i 0.0116 0.0127 0.0216 0.0331 0.0495 0.1314 0.2540 0.3722 0.7603 1.6255 3.2145 3.7643 a_i 0.0184 0.0025 0.0396 0.1302 0.0375 0.1665 0.1850 0.2104 0.1073 0.0665 0.0167 0.0192
^{238}U (F)	3	6.1E-01	λ_i 0.0234 0.1514 0.7961 a_i 0.0997 0.3418 0.5585
	6	2.2E-04	λ_i 0.0136 0.0314 0.1242 0.3254 0.9131 3.0632 a_i 0.0139 0.1125 0.1366 0.3831 0.2520 0.1018
	9	7.5E-06	λ_i 0.0130 0.0303 0.0852 0.1761 0.3685 0.3859 0.9237 2.4084 4.9353 a_i 0.0118 0.1083 0.0507 0.1651 0.2882 0.0474 0.2099 0.0967 0.0218
	12	2.3E-07	λ_i 0.0119 0.0236 0.0329 0.0872 0.1191 0.1494 0.2814 0.4237 0.9095 1.7077 2.5588 4.9688 a_i 0.0082 0.0293 0.0868 0.0342 0.0072 0.1086 0.1987 0.2054 0.1917 0.0320 0.0772 0.0206
^{239}Pu (F)	3	4.1E-01	λ_i 0.0213 0.1014 0.6232 a_i 0.1888 0.3725 0.4387
	6	8.4E-05	λ_i 0.0133 0.0309 0.1145 0.2934 0.8638 2.7460 a_i 0.0361 0.2345 0.1866 0.3244 0.1680 0.0504
	9	8.7E-06	λ_i 0.0130 0.0302 0.0885 0.1784 0.3221 0.3556 0.6010 1.2047 3.2091 a_i 0.0332 0.2292 0.1001 0.1981 0.0917 0.1193 0.0917 0.1037 0.0330
	12	5.1E-06	λ_i 0.0128 0.0298 0.0680 0.0993 0.1714 0.3248 0.3422 0.3594 0.5622 0.7863 1.1743 3.1464 a_i 0.0318 0.2248 0.0416 0.0584 0.1970 0.0480 0.0633 0.1202 0.0478 0.0322 0.0998 0.0349

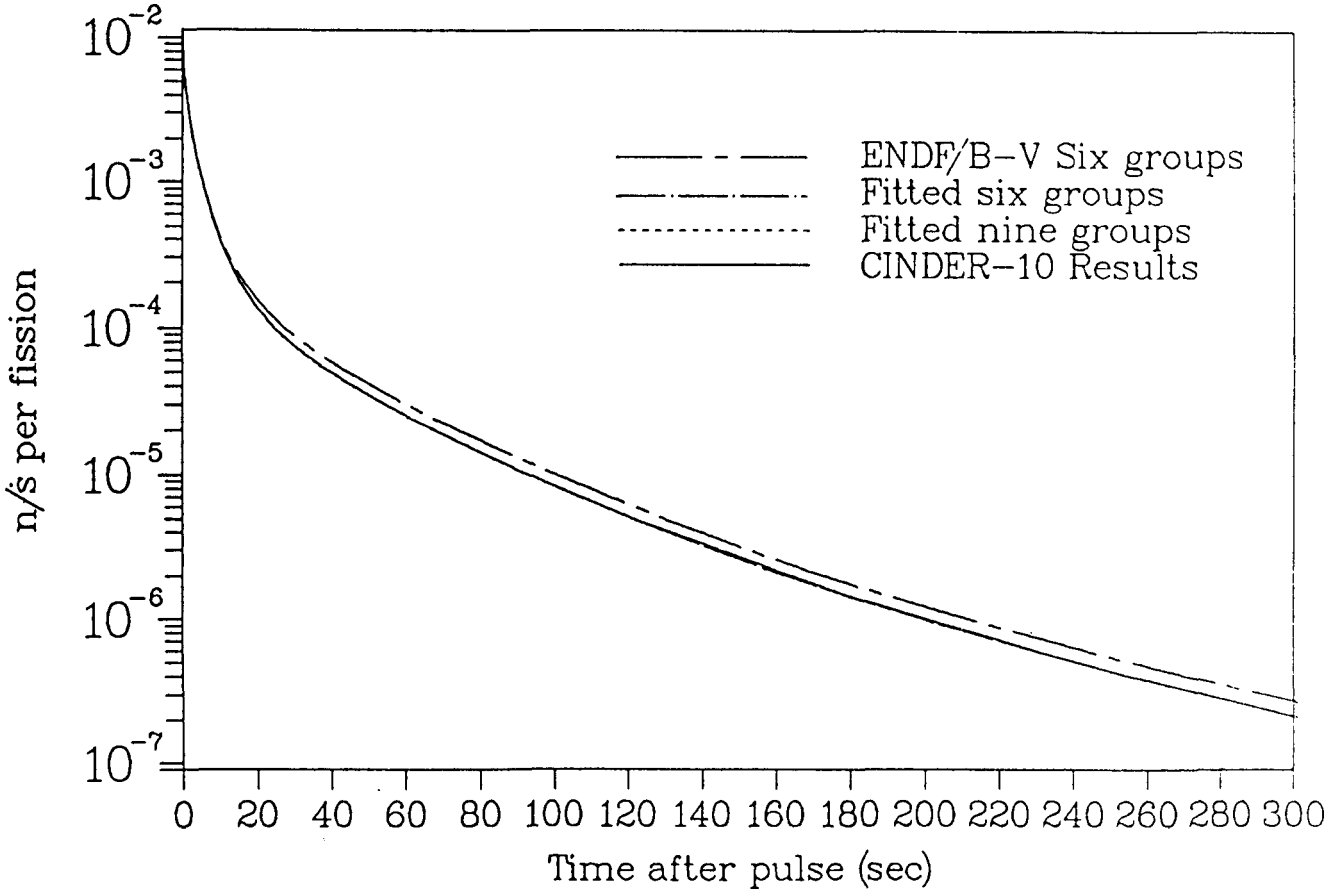

Fig. 69. Comparison of DN activity following a ^{235}U(F) fission pulse.

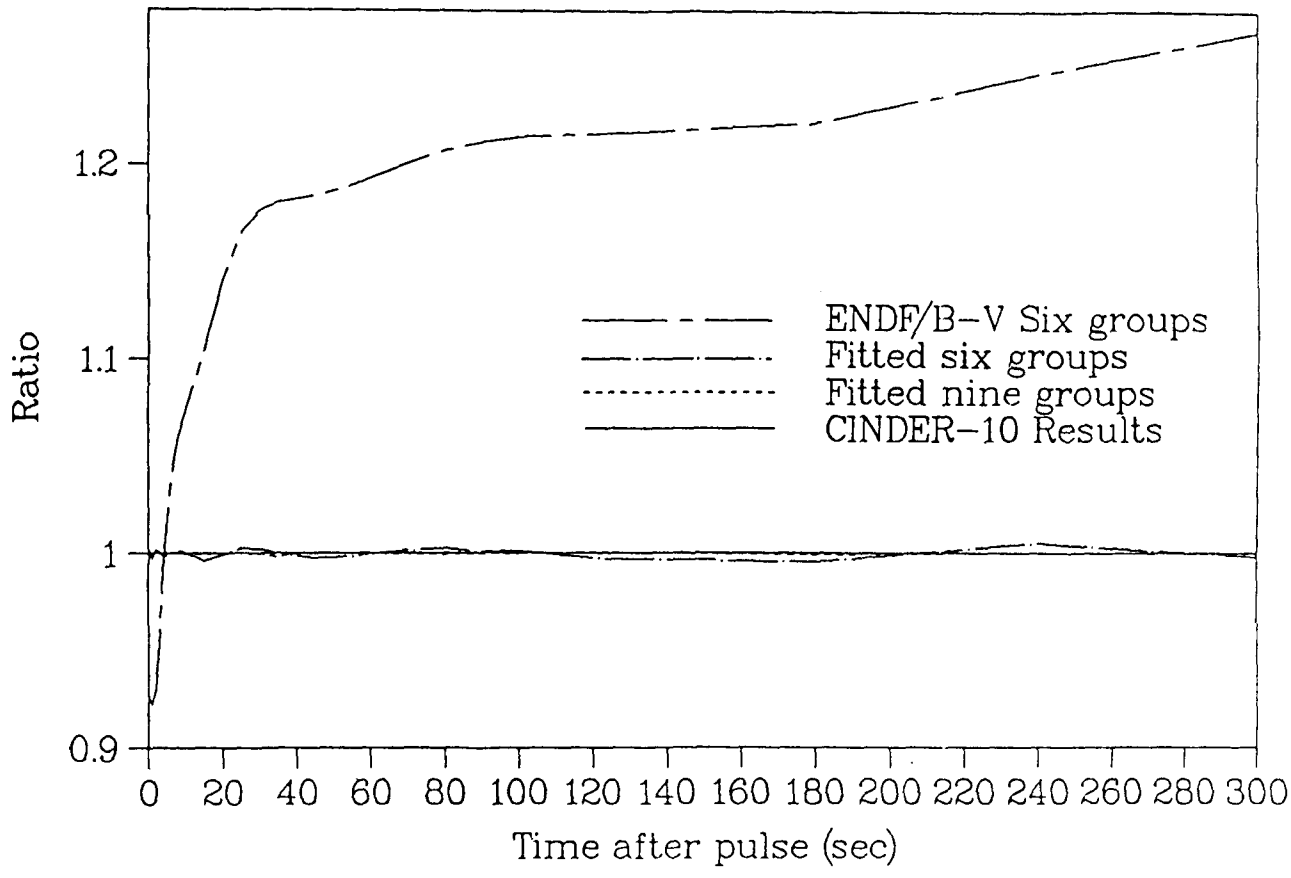

Fig. 70. Ratio of few-group results to CINDER-10 for ^{235}U(F) fission pulse.

be seen from Figs. 69 and 70, both the six- and nine-group representations fit the data well and show significant differences from the ENDF/B-V data. The nine-group representation is nearly indistinguishable from the CINDER-10 calculation in both figures and appears to be the "best" few group fit.

The type of data produced in performing these temporal fits is most commonly used to predict the kinetic response of reactors to changes in reactivity. In order to determine if there is any inherent advantage to using the nine- or twelve-group fits over the six-group fits calculations for a \$0.25 step change in reactivity using the point kinetics equations were performed for a ^{235}U(F) system. The results are presented in Fig. 71. The response of the point kinetics equations appears to be insensitive to the number of terms used.

Based on these results and the general acceptance of the six-group representation the fits for the remaining 40 fissioning systems were performed only for six-groups. Table XI presents the final results for the normalized group abundances and decay constants for all 43 fissioning systems. Appendix E contains tables of six group abundances and decay constants from ENDF/B-V,[5] Keepin,[3] Waldo,[18] Tuttle,[16] Rudstam[93], and England[28] for comparison. The Rudstam and England results are calculated using individual precursor data for 29 and 105 precursor nuclides respectively. The Keepin results are recommended values based on experiments, and the ENDF/B-V and Tuttle six-group parameters are recommended values from evaluations of published data. Thus, having determined the six-group parameters for each fissioning nuclide, the next step was to calculate a consistent set of six-group spectra.

GROUP SPECTRA CALCULATIONS

The previous analyses[28,93] of individual precursor data simply defined arbitrary half-life bounds and, based on these bounds, assigned each precursor nuclide to a particular group. Group abundances were calculated by simply summing the yield from each precursor assigned to each group. Similarly, the group spectra were obtained by summing the individual precursor spectra weighted by their emission probabilities and fission yields with respect to their group designations. The group decay constants (Rudstam only) were taken as the

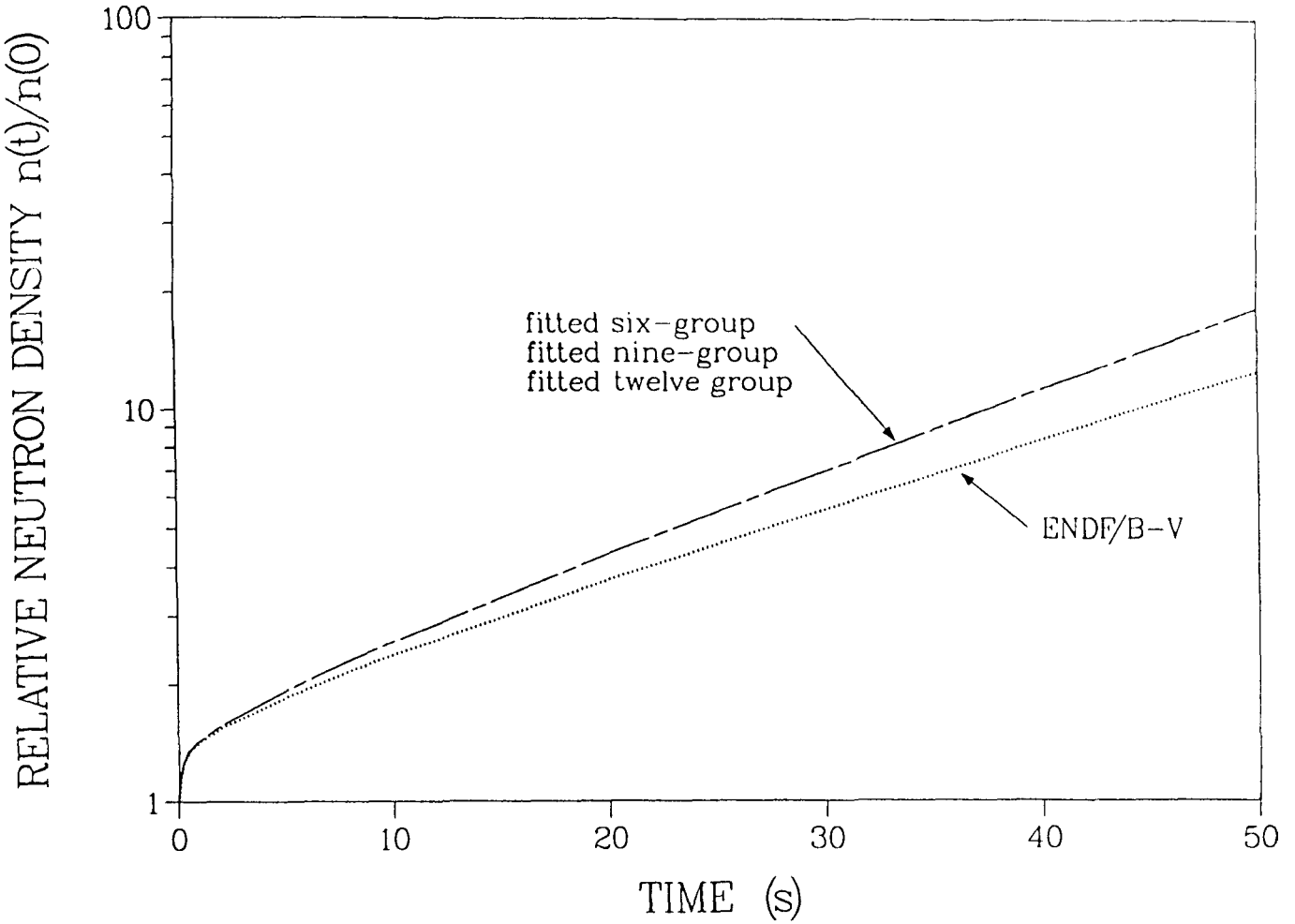

Fig. 71. Kinetic response to \$0.25 reactivity for few-group fits.

TABLE XI

Delayed Neutron Six-group Parameters

Fission Nuclide		Group 1	2	3	4	5	6
^{227}Th(T)	a	0.1027	0.2182	0.1304	0.3555	0.1647	0.0284
	λ	0.0128	0.0354	0.1098	0.2677	0.5022	2.0956
^{229}Th(T)	a	0.0867	0.1907	0.1297	0.3887	0.1729	0.0312
	λ	0.0128	0.0350	0.1123	0.2760	0.4950	2.0456
^{232}Th(F)	a	0.0364	0.1259	0.1501	0.4406	0.1663	0.0808
	λ	0.0131	0.0350	0.1272	0.3287	0.9100	2.8203
^{232}Th(H)	a	0.0326	0.0997	0.1431	0.5062	0.1336	0.0848
	λ	0.0130	0.0350	0.1307	0.3274	0.9638	3.1667
^{231}Pa(F)	a	0.0826	0.2230	0.1608	0.3885	0.1050	0.0401
	λ	0.0129	0.0347	0.1150	0.2856	0.6706	2.3111
^{232}U(T)	a	0.1360	0.2745	0.1509	0.3052	0.1007	0.0326
	λ	0.0128	0.0350	0.1073	0.2577	0.6626	2.0254
^{233}U(T)	a	0.0674	0.1927	0.1383	0.2798	0.1128	0.2091
	λ	0.0129	0.0333	0.1163	0.2933	0.7943	2.3751
^{233}U(F)	a	0.0859	0.2292	0.1781	0.3516	0.1142	0.0409
	λ	0.0129	0.0347	0.1193	0.2862	0.7877	2.4417
^{233}U(H)	a	0.0900	0.2007	0.1912	0.3684	0.1090	0.0405
	λ	0.0128	0.0378	0.1271	0.2981	0.8543	2.5314
^{234}U(F)	a	0.0550	0.1964	0.1803	0.3877	0.1324	0.0482
	λ	0.0131	0.0337	0.1210	0.2952	0.8136	2.5721
^{234}UH	a	0.0808	0.1880	0.1791	0.3888	0.1212	0.0420
	λ	0.0128	0.0364	0.1256	0.2981	0.8475	2.5696
^{235}U(T)	a	0.0380	0.1918	0.1638	0.3431	0.1744	0.0890
	λ	0.0133	0.0325	0.1219	0.3169	0.9886	2.9544
^{235}U(F)	a	0.0350	0.1807	0.1725	0.3868	0.1586	0.0664
	λ	0.0133	0.0327	0.1208	0.3028	0.8495	2.8530
^{235}U(H)	a	0.0458	0.1688	0.1769	0.4079	0.1411	0.0595
	λ	0.0131	0.0356	0.1246	0.2962	0.8260	2.6575
^{236}U(F)	a	0.0302	0.1722	0.1619	0.3841	0.1775	0.0741
	λ	0.0134	0.0322	0.1202	0.3113	0.8794	2.8405
^{236}U(H)	a	0.0438	0.1540	0.1719	0.4018	0.1578	0.0707
	λ	0.0131	0.0333	0.1252	0.3030	0.8802	2.8167
^{237}U(F)	a	0.0178	0.1477	0.1445	0.3864	0.2095	0.0941
	λ	0.0138	0.0316	0.1211	0.3162	0.9073	3.0368

TABLE XI Continued

Fission Nuclide		Group 1	2	3	4	5	6
^{238}U(F)	a	0.0139	0.1128	0.1310	0.3851	0.2540	0.1031
	λ	0.0136	0.0313	0.1233	0.3237	0.9060	3.0487
^{238}U(H)	a	0.0195	0.1184	0.1490	0.3978	0.2081	0.1072
	λ	0.0135	0.0320	0.1214	0.3142	0.9109	3.0196
^{237}Np(F)	a	0.0400	0.2162	0.1558	0.3633	0.1659	0.0589
	λ	0.0133	0.0316	0.1168	0.3006	0.8667	2.7600
^{237}Np(H)	a	0.0326	0.1571	0.1589	0.3929	0.1789	0.0796
	λ	0.0133	0.0322	0.1211	0.2933	0.8841	2.7922
^{238}Np(F)	a	0.0216	0.1845	0.1519	0.3760	0.1861	0.0798
	λ	0.0136	0.0308	0.1189	0.3077	0.8988	2.9676
^{238}Pu(F)	a	0.0377	0.2390	0.1577	0.3562	0.1590	0.0504
	λ	0.0133	0.0312	0.1162	0.2888	0.8561	2.7138
^{239}Pu(T)	a	0.0306	0.2623	0.1828	0.3283	0.1482	0.0479
	λ	0.0133	0.0301	0.1135	0.2953	0.8537	2.6224
^{239}Pu(F)	a	0.0363	0.2364	0.1789	0.3267	0.1702	0.0515
	λ	0.0133	0.0309	0.1134	0.2925	0.8575	2.7297
^{239}Pu(H)	a	0.0678	0.1847	0.1553	0.3685	0.1750	0.0487
	λ	0.0129	0.0353	0.1215	0.2885	0.8486	2.5587
^{240}Pu(F)	a	0.0320	0.2529	0.1508	0.3301	0.1795	0.0547
	λ	0.0133	0.0305	0.1152	0.2974	0.8477	2.796
^{240}Pu(H)	a	0.0534	0.1812	0.1533	0.3715	0.1849	0.0558
	λ	0.0130	0.0329	0.1191	0.2918	0.8462	2.7080
^{241}Pu(T)	a	0.0167	0.2404	0.1474	0.3430	0.1898	0.0627
	λ	0.0137	0.0299	0.1136	0.3078	0.8569	3.0800
^{241}Pu(F)	a	0.0180	0.2243	0.1426	0.3493	0.1976	0.0682
	λ	0.0136	0.0300	0.1167	0.3069	0.8701	3.0028
^{242}Pu(F)	a	0.0196	0.2314	0.1256	0.3262	0.2255	0.0716
	λ	0.0136	0.0302	0.1154	0.3042	0.8272	3.1372
^{241}Am(T)	a	0.0305	0.2760	0.1531	0.3122	0.1825	0.0457
	λ	0.0133	0.0300	0.1145	0.2949	0.8818	2.6879
^{241}Am(F)	a	0.0355	0.2540	0.1563	0.3364	0.1724	0.0454
	λ	0.0133	0.0308	0.1130	0.2868	0.8654	2.6430
^{24}Am(H)	a	0.0740	0.1757	0.1754	0.3589	0.1783	0.0377
	λ	0.0129	0.0346	0.1267	0.3051	0.9536	3.3205
^{242m}Am(T)	a	0.0247	0.2659	0.1512	0.3337	0.1756	0.0489
	λ	0.0135	0.0301	0.1152	0.2994	0.8646	2.8107
^{243}Am(F)	a	0.0234	0.2945	0.1537	0.3148	0.1656	0.0480
	λ	0.0135	0.0298	0.1138	0.2986	0.8820	2.8111
^{242}Cm(F)	a	0.0763	0.2847	0.1419	0.2833	0.1763	0.0375
	λ	0.0130	0.0312	0.1129	0.2783	0.8710	2.1969

TABLE XI Continued

Fission Nuclide		Group 1	2	3	4	5	6
^{245}Cm(T)	a	0.0222	0.1788	0.1672	0.3706	0.2054	0.0559
	λ	0.0134	0.0307	0.1130	0.3001	0.8340	2.7686
^{249}Cf(T)	a	0.0246	0.3919	0.1349	0.2598	0.1614	0.0273
	λ	0.0135	0.0294	0.1053	0.2930	0.8475	2.4698
^{251}Cf(T)	a	0.0055	0.3587	0.1736	0.2693	0.1688	0.0242
	λ	0.0157	0.0288	0.1077	0.3246	0.8837	2.6314
^{252}Cf(S)	a	0.0124	0.3052	0.1813	0.2992	0.1729	0.0290
	λ	0.0136	0.0291	0.1068	0.3024	0.8173	2.6159
^{254}Es(T)	a	0.0073	0.3148	0.1547	0.2788	0.2010	0.0435
	λ	0.0194	0.0289	0.1048	0.3185	0.8332	2.7238
^{255}Fm(T)	a	0.0060	0.4856	0.1766	0.1940	0.1160	0.0218
	λ	0.0149	0.0287	0.1027	0.3130	0.8072	2.5768

mathematical average for the group using the precursor yields as a weighting function. The method used here to determine the group yields and abundances was independent of any arbitrary half-life bounds and requires that the energy spectra for each group will be determined in a consistent manner.

Recall that in the six-group representation, delayed neutron activity following a fission pulse is represented as a sum of exponentials,

$$n_d(t) = \sum_{i=1}^{6} A_i \, e^{-\lambda_i t} \ , \tag{32}$$

and in the individual precursor notation the same situation is expressed as

$$n_d(t) = \sum_{j=1}^{271} \lambda_j \, P_n^j \, YI_j \, e^{-\lambda_j t} \ . \tag{33}$$

In the previous section it was shown that the six group parameters were determined from a least squares fit to delayed neutron activity following a pulse irradiation as calculated by the fission product depletion code, CINDER-10,[103] using the individual precursor data. Although Eq. (33) ignores coupling between mass chains which is included in the CINDER calculations, this is assumed to be negligible. Therefore, in the present evaluation it is required that

$$A_i e^{-\lambda_i t} = \sum_k f_{k,i} \, \lambda_k \, P_n^k \, YI_k e^{-\lambda_k t} \ , \tag{34}$$

where the subscript i represents mathematical group i, the summation is over all precursors, and $f_{k,i}$ is the fraction of delayed neutrons produced by precursor k that contribute to group i. It is assumed that a delayed neutron precursor may contribute to either or both of the adjacent mathematical groups as determined by the decay constants as in

$$\lambda_i < \lambda_k < \lambda_{i+1} \ , \tag{35}$$

It is also required that

$$f_{k,i} + f_{k,i+1} = 1 \ . \tag{36}$$

The fractions $f_{k,i}$ were determined by requiring that the least-squares error

$$\int_0^\infty \left\{ \lambda_k \, e^{-\lambda_k t} - \left[f_{k,i} \, \lambda_i \, e^{-\lambda_i t} + (1 - f_{k,i}) \, \lambda_{i+1} \, e^{-\lambda_{i+1} t} \right] \right\}^2 dt \qquad (37)$$

be a minimum.[100] The equilibrium group spectra were then computed as:

$$\phi_i(E) = \sum_k f_{k,i} \, Y C_k \, P_n^k \, \phi_k(E) \qquad (38)$$

where $\phi_k(E)$ is the delayed neutron spectrum of precursor k.

The normalized six-group spectra for ^{235}U fast and thermal fission are given Figs. 72(a) thru 72(f) over a 1-MeV energy range in comparison with the six-group spectra taken from ENDF/B-V for ^{235}U. The spectra calculated from the evaluated precursor data provide much more detailed structure than the earlier ENDF/B-V spectra. Note that in the energy region from 1–76 keV, where the ENDF spectra have been simply extrapolated to zero, the current spectra reveal several low-energy peaks of varying intensity from group to group. These low-energy delayed neutrons could be very important in fast reactor safety studies and rod oscillation experiments.

The practice in ENDF/B-V of approximating missing group 5 and 6 spectra with group 4 data is apparent in Figs. 72(d)–72(f). Recall that in ENDF/B-V only the spectra for ^{235}U, ^{238}U, and ^{239}Pu are evaluated, and these are used to represent the spectra from all other fissioning nuclides. The ENDF/B-V spectra are also independent of the incident neutron energy. However, differences between the calculated ^{235}U thermal and fast spectra shown in Figs. 72(a)–72(f) are small. This suggests that there is little dependence on incident neutron energy and agrees with earlier results.

Using the method described above, the group one spectrum shown in Fig. 72(a) has three contributing nuclides. The precursor ^{87}Br contributes 100% of its delayed neutrons to group 1, as would be expected; however, two additional precursors, ^{137}I and ^{141}Cs each contribute about 20% of their delayed neutrons to group one in a ^{235}U fueled system. This result allows the group one spectrum

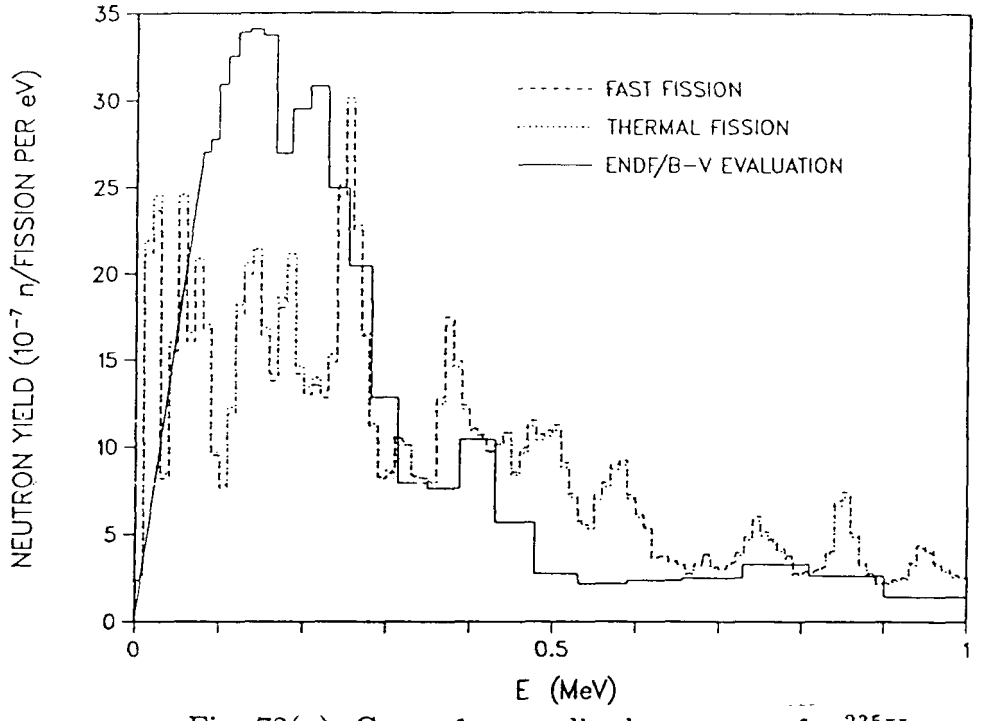

Fig. 72(a). Group 1 normalized ν_d spectra for ^{235}U.

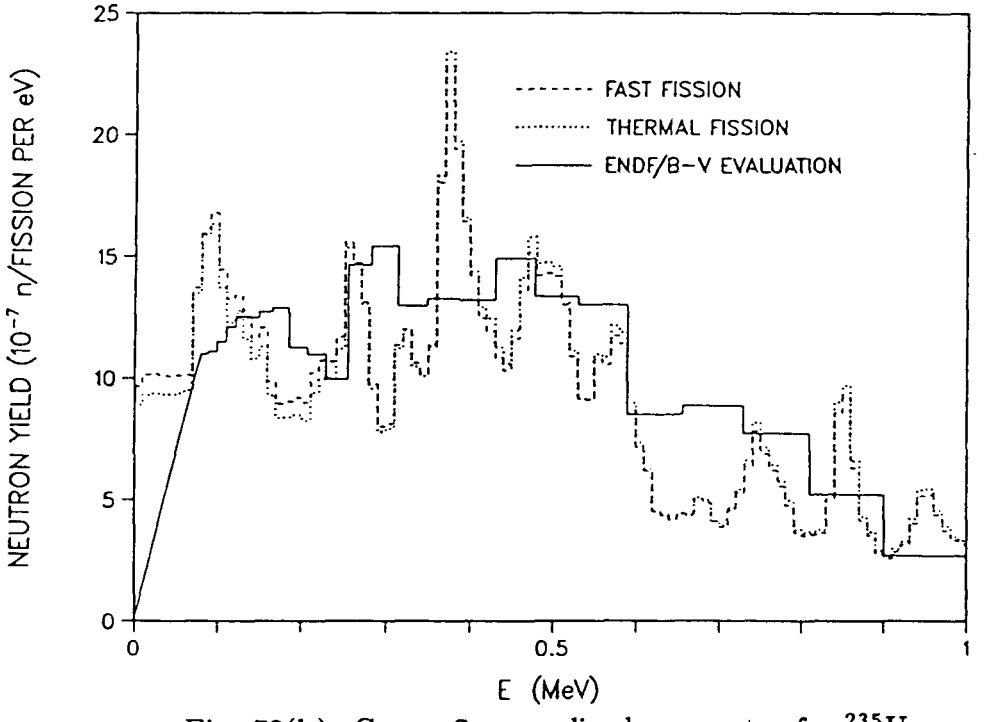

Fig. 72(b). Group 2 normalized ν_d spectra for ^{235}U.

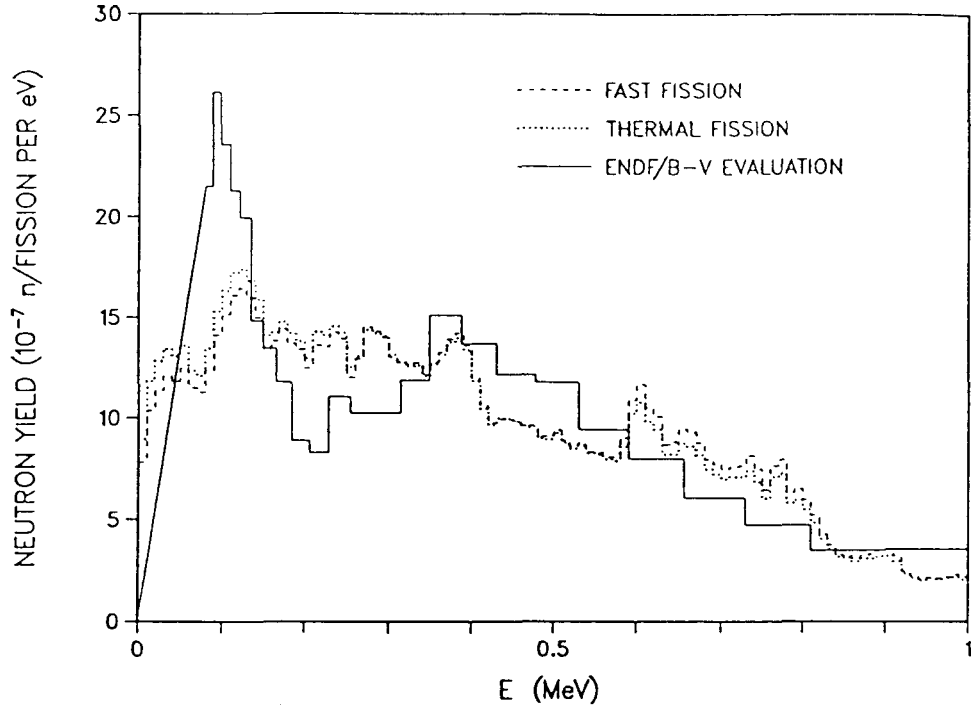

Fig. 72(c). Group 3 normalized ν_d spectra for ^{235}U.

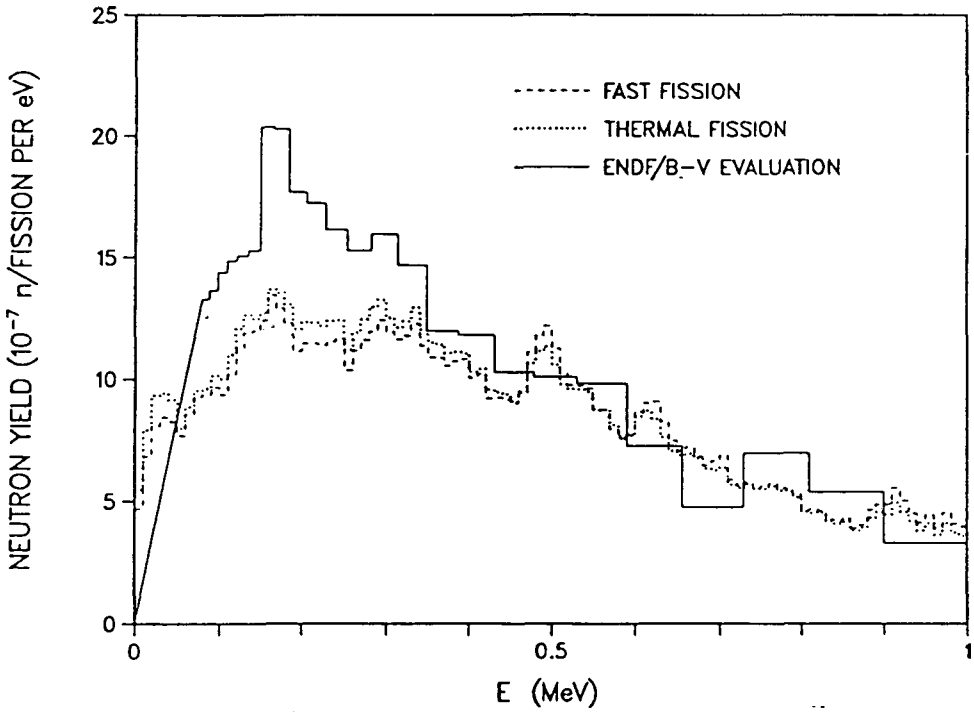

Fig. 72(d). Group 4 normalized ν_d spectra for ^{235}U.

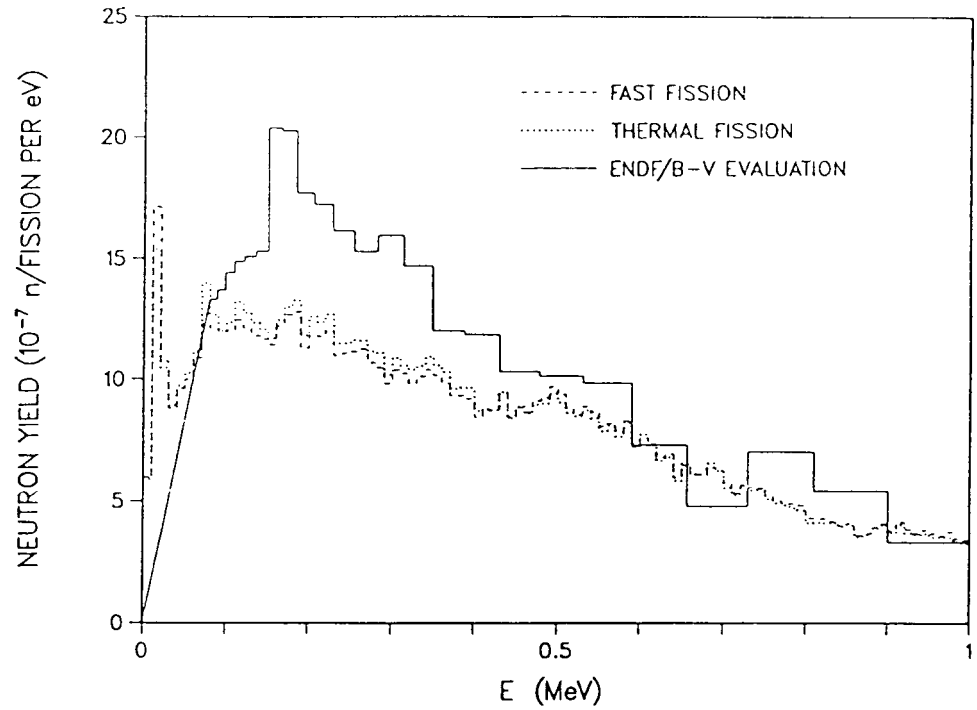

Fig. 72(e). Group 5 normalized ν_d spectra for ^{235}U.

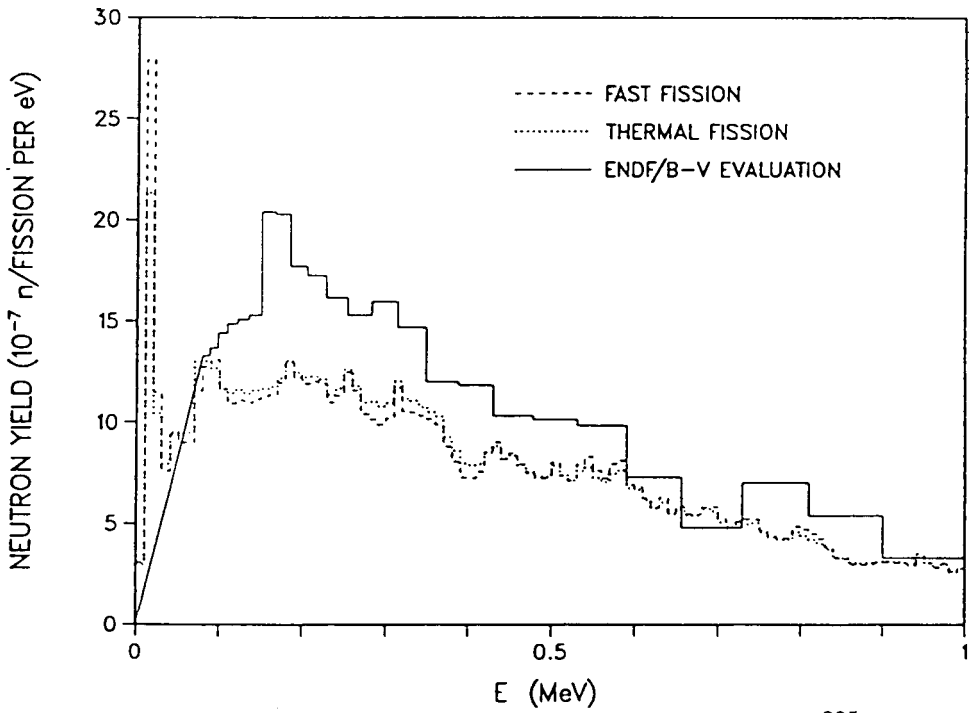

Fig. 72(f). Group 6 normalized ν_d spectra for ^{235}U.

to change for different fissioning systems (since the relative yields of ^{87}Br, ^{137}I, and ^{141}Cs change), as suggested by the ENDF/B-V data (see Fig. 4).

Beta-Effective Calculations

Spectra are of interest in calculating their "effectiveness" or "importance" of delayed neutrons. Delayed neutrons are born at considerably lower average energies than prompt neutrons (whose average energy is about 2 MeV). This affects various properties of the delayed neutrons relative to the prompt neutron properties, such as their leakage probability, cross-section for absorption in the system, and therefore, their mean free path.

In light water reactors (LWRs) delayed neutrons have a greater effectiveness than do prompt neutrons primarily because of their lower fast leakage probability.[13] The situation is somewhat more complicated in the case of fast breeder reactors which typically contain a fissile fuel core (^{235}U, ^{239}Pu, and/or ^{233}U) and a fertile (^{238}U, ^{232}Th, or ^{240}Pu) blanket. The threshold-fissioning nuclides in the blanket have a much higher delayed neutron yield suggesting that they could dominate the kinetic response of the reactor, however this is generally not the case. To understand why this is so one must evaluate the effectiveness of delayed neutrons in the fertile material relative to that of delayed neutrons born in the "fuel," as well as, the relative effectiveness of prompt neutrons born in the blanket and those born in the fuel.

Although fission will occur in the fertile blanket both the prompt and delayed neutrons born there will have a lower importance than those born in the core primarily due to increased leakage probabilities for the blanket neutrons. The importance of the delayed neutrons born in the blanket is also affected by the fact that the threshold-fissioning nuclides which makeup the blanket require higher energy neutrons to induce fission, therefore the lower energy delayed neutrons will not cause fission in the blanket and are not energetic enough to diffuse back into the core where they might induce a thermal fission. Another factor that influences the kinetic response of a fast reactor is that generally the prompt neutron yield increases and the delayed neutron yield decreases with incident neutron energy. The result of this is that the fraction of delayed neutrons, β,

decreases with increasing incident neutron energy. Therefore, the margin of control in a fast breeder reactor is already small before considering the delayed neutron effectiveness. A large fraction of delayed neutrons are produced in the blanket where their effectiveness is smaller and the situation becomes crucial. This largely accounts for the resurgence of interest in delayed neutron spectra. Improvements in isotope separation techniques using radiochemical methods or mass separation that were being made at this time also made it possible to study the delayed neutron spectra of individual precursor nuclides.

The effectiveness of delayed neutrons is commonly represented by the effective delayed neutron fraction, β_{eff}. As a means of validating the method used to calculate the group spectra, β_{eff} calculations were performed to insure that the group spectra produce results which are consistent with those from the aggregate spectra obtained using the individual precursor data. the method used to calculate β_{eff} involved perturbation calculations which require neutron fluxes and adjoint fluxes for the system of interest. The one-dimensional transport theory code, ONEDANT,[108] was used to model the Godiva reactor (a bare sphere of enriched ^{235}U metal) and to calculate the fluxes and adjoint fluxes. The perturbation calculation was performed with the code PERT-V[109] which uses first-order perturbation theory based on the multigroup diffusion model and calculates β_{eff}. The PERT-V code allows the user to input either a single delayed neutron spectrum or individual group spectra, the results for β_{eff} calculated by each of these options are given in Table XII.

The perturbation calculations were performed using the six-group decay constants and fractional abundances from Table XI, and a total delayed neutron yield of 0.0167 neutrons per fission, which is the same as the value recommended by Tuttle and that used in ENDF/B-V.

The ratio of the six-group effective delayed neutron fraction to that using a single delayed neutron group is 0.9943. These results are in excellent agreement and verify the methods used to derive the six-group spectra. Another vehicle used to check the validity of the six-group spectra is a comparison with recently published delay interval spectra measured by researchers at the University of Lowell.

TABLE XII

Comparison of β_{eff} for Godiva [^{235}U(F)]

	β_{eff}	Ratio to Experiment
Experiment (Ref.110)	0.00645	1.000
Aggregate spectrum	0.00653	1.012
Six-group spectra	0.00649	1.006

Delay Interval Spectra

It has been readily acknowledged that delayed neutron spectra are the least adequately known of all parameters required for the calculation of fast reactor kinetics behavior. Recently, a group from the University of Lowell[9] reported results from the measurement of time delay interval spectra following a fast fission pulse in ^{235}U. The Lowell group, using a beta-neutron time-of-flight (TOF) spectrometer, measured spectra for eight successive time intervals between 0.17 and 85.5 seconds. They also reported average neutron energies for each delay interval spectrum.

G. P. Couchell from the University of Lowell provided the time delay interval spectra in a 10-keV bin structure. The comparison plots seen in Figs. 73–80 were made from the data provided by Dr. Couchell and that obtained using the data presented here. In this comparison, both the individual precursor data and the six group data were used to calculate spectra corresponding to the eight delay time intervals measured by the Lowell group. The time-dependent spectrum of delayed neutrons emitted following a fast fission pulse was calculated from the precursor data as:

$$\mathrm{X}(E,t) = \sum_i P_{n_i} Y I_i e^{-\lambda_i t} \mathrm{X}_i(E) \qquad (39)$$

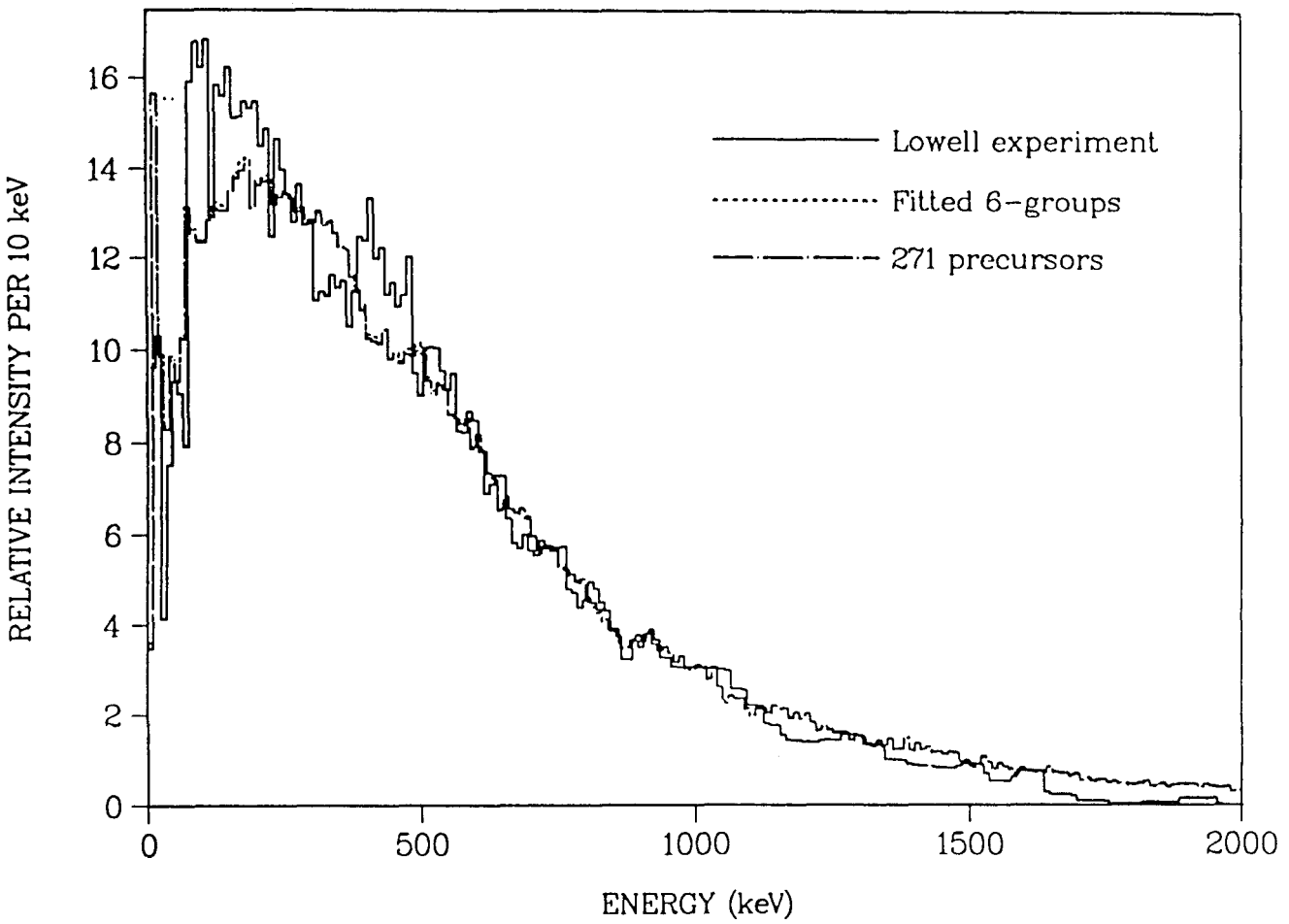

Fig. 73. Comparisons with Lowell spectra for delay interval 1 (0.17–0.37 s).

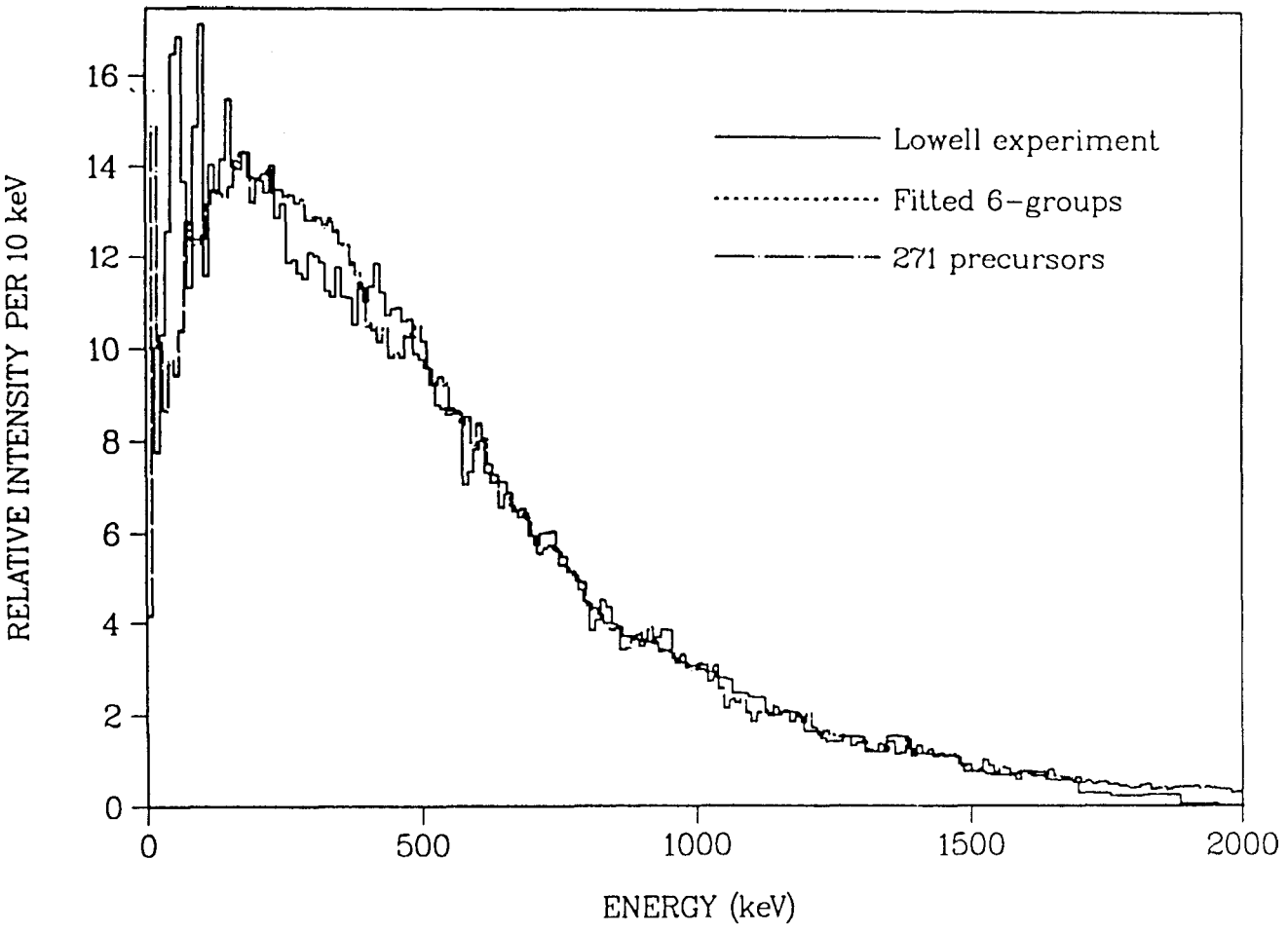

Fig. 74. Comparisons with Lowell spectra for delay interval 2 (0.41–0.85 s).

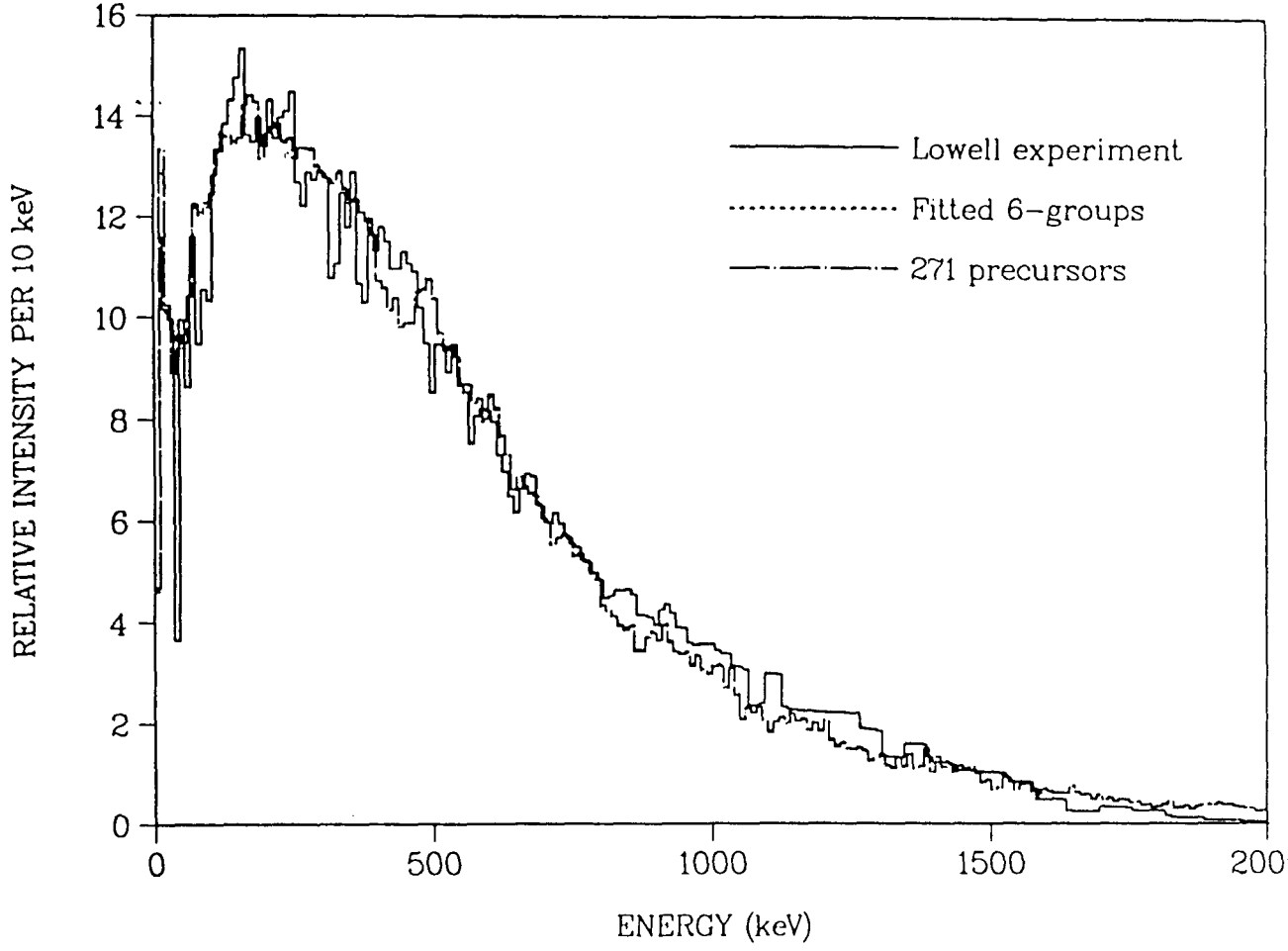

Fig. 75. Comparisons with Lowell spectra for delay interval 3 (0.79–1.25 s).

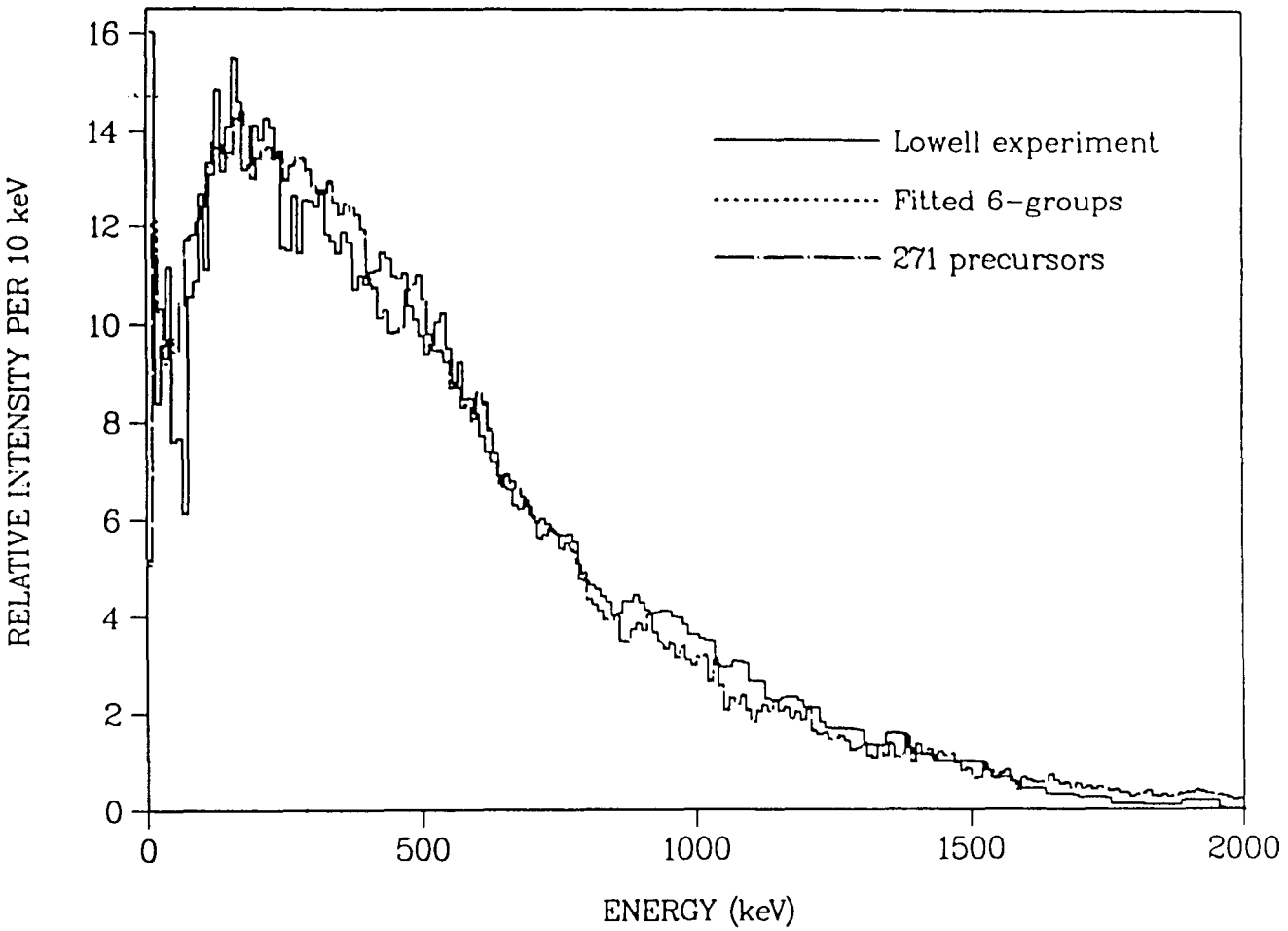

Fig. 76. Comparisons with Lowell spectra for delay interval 4 (1.2–1.9 s).

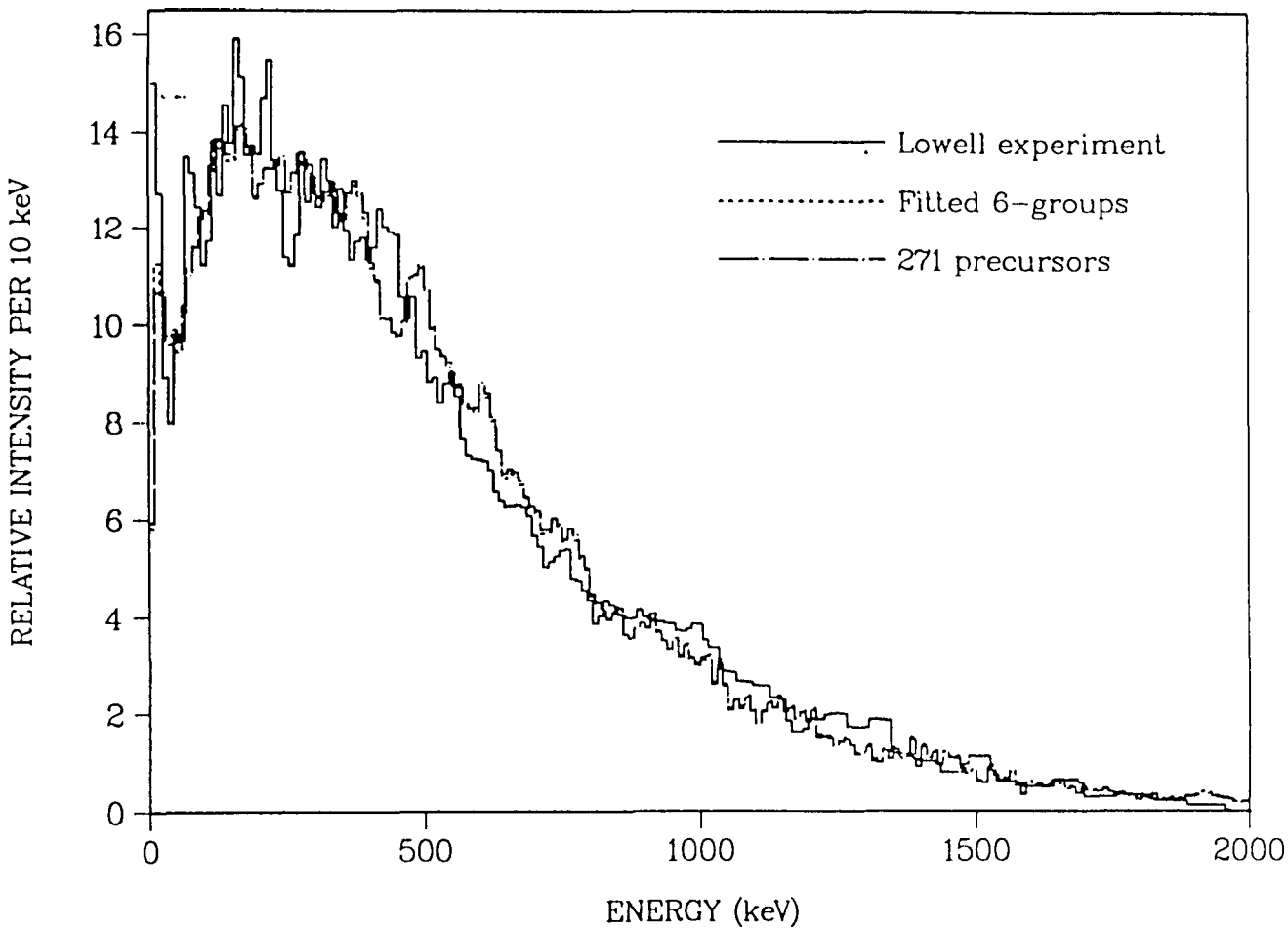

Fig. 77. Comparisons with Lowell spectra for delay interval 5 (2.1–3.9 s).

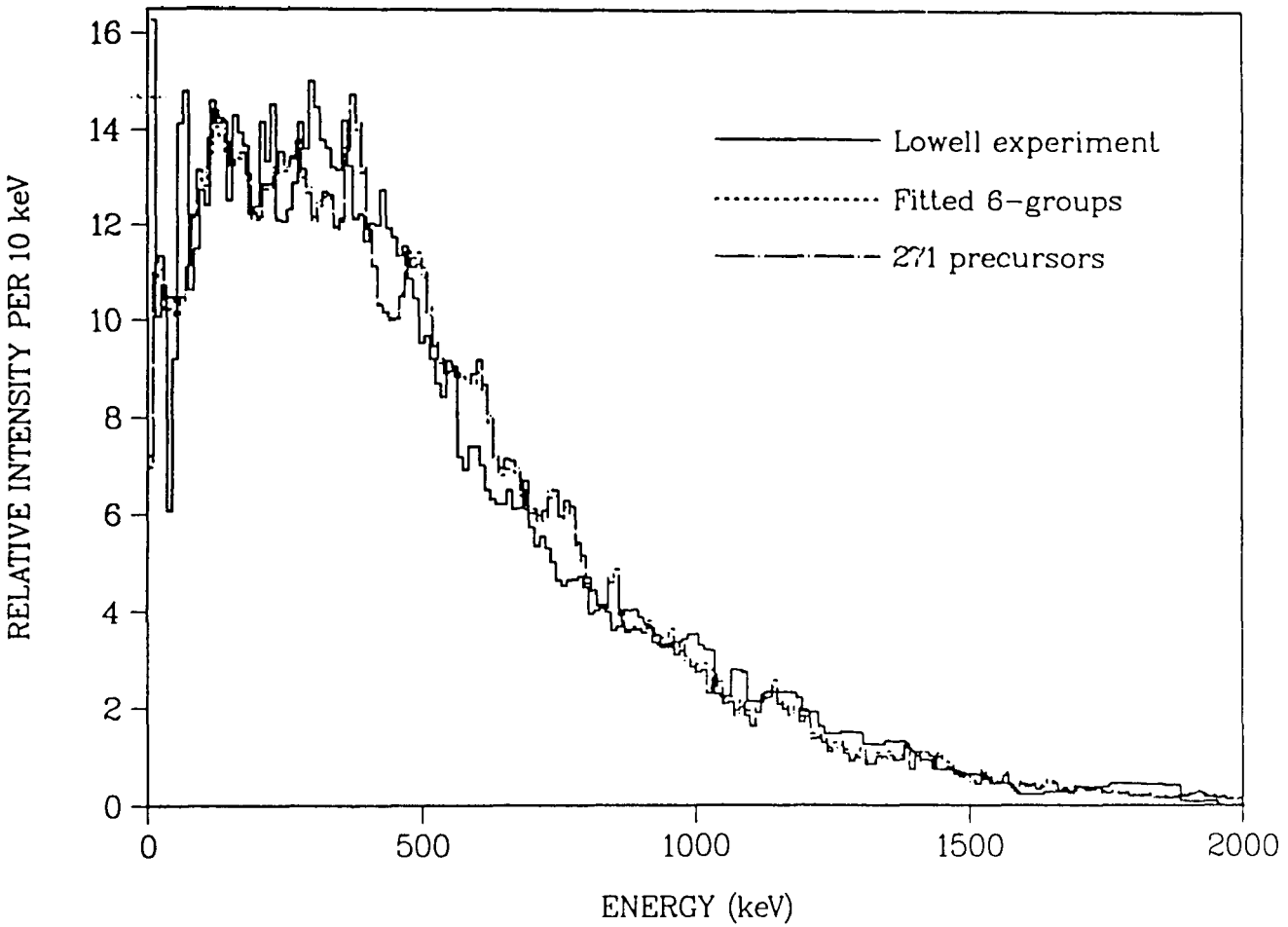

Fig. 78. Comparisons with Lowell spectra for delay interval 6 (4.7–10.2 s).

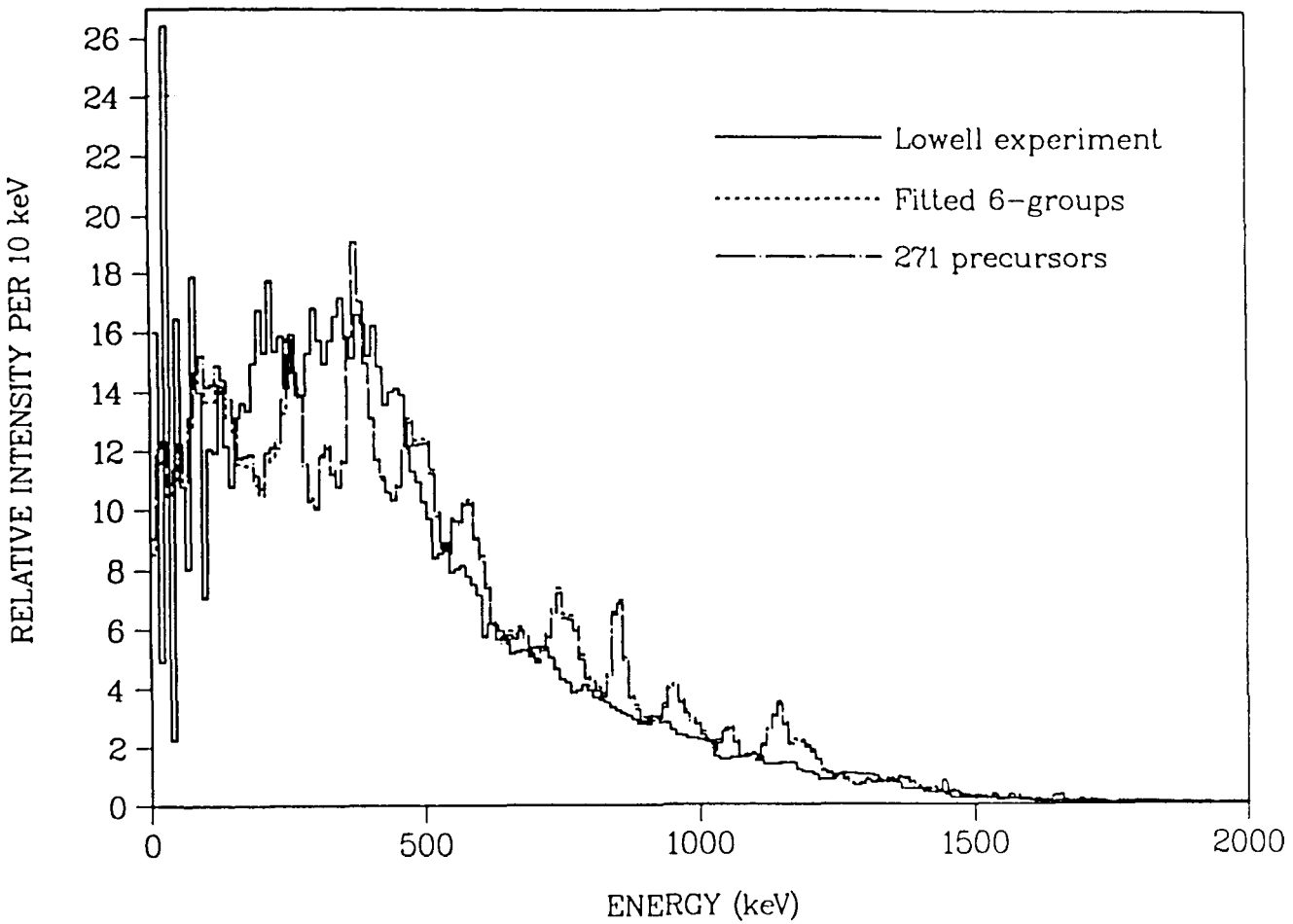

Fig. 79. Comparisons with Lowell spectra for delay interval 7 (12.5–29.0 s).

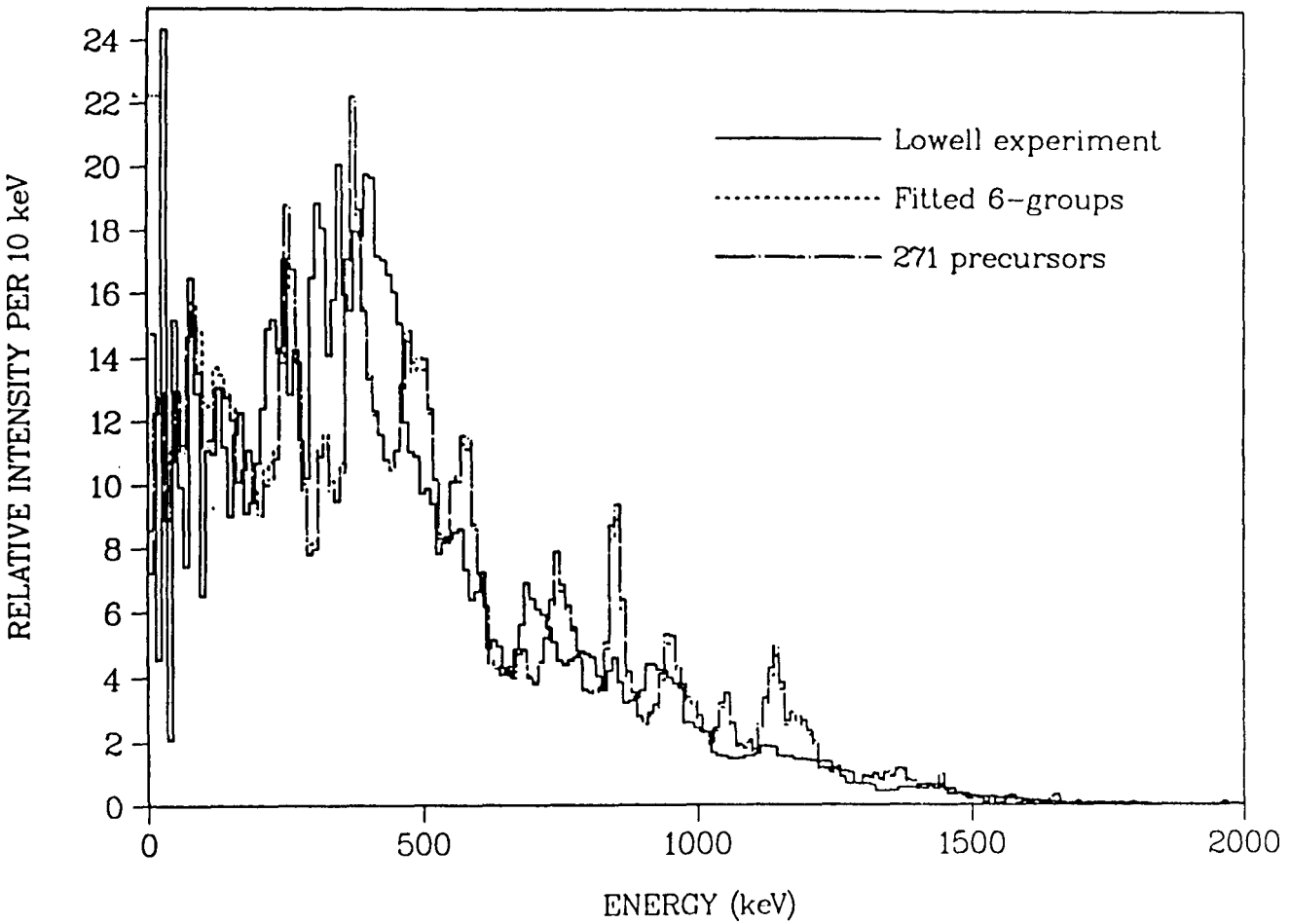

Fig. 80. Comparisons with Lowell spectra for delay interval 8 (35.8–85.5 s).

where λ_i is the decay constant for the i^{th} precursor nuclide; P_{n_i}, and Y_i^r are the delayed neutron emission probability and independent fission yield of the i^{th} precursor, respectively; $X_i(E)$ is the delayed neutron spectrum for the individual precursor and t is time. A similar equation for producing a time-dependent spectrum from the six group data was written as follows:

$$X(E,t) = \sum_j \lambda_j \nu_d a_j e^{-\lambda_j t} X_j(E) \ , \tag{40}$$

where λ_j is the decay constant for the j^{th} group; ν_d is the delayed neutron yield per fission; a_j is the fraction of delayed neutrons attributed to the j^{th} group; $X_j(E)$ is the j^{th} group spectrum and t is again denotes time.

The spectra labeled "271 precursors" in Figs. 73–80 were calculated by integrating Eq. (39) over each delay interval. Similarly, the spectra designated as "fitted 6-groups" in Figs. 73–80 were calculated from the integral of Eq. (40) using the appropriate time intervals.

The results from each of the two calculations as well as the measured spectra are in very good agreement for all eight delay intervals. There is also excellent agreement between the two calculations further supporting the consistency of the group spectra with the aggregated spectrum calculated from the evaluated precursor spectra.

The most notable differences between the calculated spectra and those measured by the University of Lowell are seen in the spectra for delay intervals four thru eight. The measured spectra for these delay intervals show a dominant low energy peak. The calculations predict similar low energy peaks but with slightly lower intensities for delay intervals four thru seven. Delay interval eight (35.8–85.5 sec.) shows the greatest differences between the calculated and measured spectra. In this case the measurement depicts a dominant low energy peak that is not observed at any significant intensity in the calculations. This could be due to the fact the the dominant precursors contributing to this delay interval are those which make up the "group one" delayed neutrons, ^{87}Br, ^{137}I, and ^{141}Cs. None of these nuclides had delayed neutron spectra measured by proton-recoil techniques which could provide higher resolution at low energies. In addition,

the Lowell group reported that "In the 35.8- to 85.5-s interval, however, the TOF spectrum measured with ^{6}Li-glass scintillators had too severe a gamma-ray background and for purposes of normalization in this interval the spectrum of the neighboring time interval was used as an estimate of the spectrum below 130 keV." It is precisely in this energy region below 130 keV that the largest differences occur.

Table XIII represents a more quantitative comparison in which the average energy for each delay interval as reported by the Lowell group is compared with that calculated from the spectra derived from both the individual precursor data and the six-group data. The agreement in the values of average energy is considered very good for all delay intervals. The excellent agreement between the average energies for the two methods of calculating the delay interval spectra further supports the methods used to derive the few-group spectra.

TABLE XIII

Average Energy Comparisons with Lowell Data

Delay	Interval (sec)	Average Energy (keV)		
		Lowell[a]	271 prec.	6-group
1	0.17 - 0.37	473(14)	508.6	506.5
2	0.41 - 0.85	482(12)	501.0	502.2
3	0.79 - 1.25	506(12)	498.0	499.6
4	1.2 - 1.9	502(12)	496.6	498.6
5	2.1 - 3.9	491(13)	494.0	497.3
6	4.7 - 10.2	478(14)	477.7	485.2
7	12.5 - 29.0	420(12)	457.7	466.7
8	35.8 - 85.5	441(17)	476.2	468.5

[a]The values given in parenthesis following the Lowell data represent the uncertainty in the last two digits, i.e. 473(14) may be interpreted as 473 $\pm$ 14 keV.

CHAPTER VIII.

POINT REACTOR KINETICS CALCULATIONS

This chapter will describe how the point reactor kinetics equations were modified to make use of the detailed precursor data. It will also be shown that these modified kinetics equations reduce to the conventional point kinetics equations when considering the more traditional few-group data. In the earlier discussion of the group fits, the results from point reactor kinetics calculations using the six- and nine-group fits were presented and revealed that the number of terms did not produce any large discrepancies in the kinetic response to a step change in reactivity. The intent here is to determine if the production and decay of each precursor nuclide are considered explicitly will result in a different "response" in the point reactor kinetics model.

REFORMULATION OF THE POINT REACTOR KINETICS EQUATIONS

The point reactor kinetics equations are conventionally described as a set of seven coupled ordinary differential equations that characterize the time-dependence of the neutron population in a reactor In the notation of Duderstadt and Hamilton,[111] these equations may be written:

$$\frac{dn(t)}{dt} = \frac{\rho(t) - \beta}{\Lambda} n(t) + \sum_{i+1}^{6} \lambda_i C_i(t) \tag{41}$$

$$\frac{dC_i(t)}{dt} = \frac{\beta_i}{\Lambda} n(t) - \lambda_i C_i(t), \quad i = 1,6 \tag{42}$$

where

- $n(t)$ is the neutron density as a function of time;
- $C_i(t)$ is the 'precursor concentration' as a function of time;
- $\rho(t)$ is the reactivity, this essentially measures the deviation of core multiplication, k, from its critical value $k = 1$,

$$\rho(t) = \frac{k(t) - 1}{k(t)}$$

- β is the total fraction of delayed neutrons;
- β_i is the fraction of delayed neutrons in group i;

Λ is the mean generation time between the birth of a neutron and subsequent absorption inducing fission; and

λ_i is the decay constant of the ith delayed neutron group.

There are two major assumptions about the precursor groups that are implicit in these equations. The first is that each decay in the precursor group leads to the emission of one neutron. Second, the only means of producing a precursor in any group is directly from the fission process. A delayed neutron group may be considered to consist of a fictitious precursor whose delayed neutron emission probability is one and whose yield is equal to the group yield per fission, $\beta_i * \nu$ (where ν is the total neutron yield per fission).

The point reactor kinetics equations as modified to employ the individual precursor data are written as:

$$\frac{dn(t)}{dt} = \frac{\rho(t) - \beta}{\Lambda} n(t) + \sum_j \lambda_j P_n^j C_j(t) \tag{43}$$

$$\frac{dC_j(t)}{dt} = \frac{YI_j}{\nu\Lambda} n(t) + \sum_k \lambda_k \, BF_{k\rightarrow j} \, C_k(t) - \lambda_j C_j(t) \tag{44}$$

and were derived from basic balance equations that are given in Appendix F. Equation (44) includes $BF_{k\rightarrow j}$, the branching fraction describing the probability that a decay in nuclide k will produce nuclide j.

It has been shown that although the delayed neutron emission probability for an individual nuclide may theoretically be as great as one, the values determined for the 271 precursors in this evaluation are usually considerably less than one. Therefore, the second term of Eq. (43) has been modified by the delayed neutron emission probability, P_n. In this form, $C_j(t)$ is the concentration of nuclide j and all other parameters are as previously defined. In the modified precursor equation, the first term represents the production of the precursor j from fission as the product of the independent or direct yield per fission, YI_j, for precursor j and the fission rate which is proportional to the neutron density by a factor of $\frac{1}{\nu\Lambda}$. Many of the precursors considered in this evaluation are produced not only from fission but also from the decay of parent nuclides which

may or may not be precursors themselves. (Fission product parents which are not themselves precursors have zero P_n values and do not contribute to Eq.(43).) Considering each of the 271 precursor nuclides and their fission product parents results in a total of 386 nuclides being required in an explicit calculation. A second production term was added to Eq. (44) to represent the production of precursor nuclides from the decay of other fission product nuclides.

The modified point kinetics equations may be reduced to the conventional form in three steps.

Step 1. The probability of delayed neutron emission for a precursor group is one, i.e. a decay in a group will always yield a delayed neutron. Setting P_n^j equal to 1.0 in Eq. (43) and reducing the number of terms in the summation to six (one for each of the six groups) yields the familiar expression for neutron density as given in Eq. (41).

Step 2. Given that the delayed neutron emission probability for each group is one, all other branching fractions must be zero; $BF_{k-j} = 0$ for all k. This reflects that the groups are not coupled to one another, production and decay within each group are independent of all other groups. Thus the second term in Eq. (44) is zero.

Step 3. The yield per fission for a group is equal to the fraction of delayed neutrons produced in that group times the neutron yield per fission; $YI_j = \beta_j * \nu$. Substituting this expression into Eq. (44) and simplifying yields the conventional expression for the time rate of change in precursor concentration where j ranges from 1 to 6.

SOLVING THE MODIFIED POINT REACTOR KINETICS EQUATIONS

In the simple case of a step change in reactivity the modified kinetics equations become a set of ordinary, linear, first-order differential equations with constant coefficients. By assuming a solutions of the form

$$\begin{aligned} n(t) &= \sum A * \exp(wt) \\ C_j(t) &= \sum C_j * \exp(wt) \end{aligned} \tag{45}$$

the equations reduce to an algebraic eigenvalue problem where w denotes the appropriate eigenvalues. Common Los Alamos Mathematical Software (CLAMS) routines SGEEV and CGEIR were used to find the eigenvalues and eigenvectors, and to solve the system of equations using equilibrium initial conditions to find the coefficients (C_j's and A's), respectively. SGEEV employs Householder matrices to reduce the coefficient matrix, A, to upper Hessenberg form and a shifted QR algorithm to further reduce A to triangular form. The eigenvalues were then calculated and the eigenvectors found by back substitution. The routine CGEIR uses Gaussian elimination to reduce A to the product of an upper triangular matrix and a lower triangular matrix and then evaluates the system of equations. This quasi-analytic solution method was applied using England's dataset for 105 precursors. The description of the activity and delayed neutron production rate of each of these 105 precursors required an additional 121 parent radionuclides also be described. The system of equations solved included the neutron production rate equation and production rate equations for 226 nuclides resulting in a coefficient matrix, A, of size 227x227.

The results of these semianalytic calculations were used to validate Perry et al.'s[106] modifications to the AIREK-3 point kinetics code.[109] The modified code, AIREK-10,[106] uses the individual precursor data to calculate precursor inventories and neutron densities at specified times following a reactivity insertion.

There are several advantages to using the AIREK-10 code for the explicit kinetics calculations over the quasi-analytic method. The first is that the restriction to step changes in reactivity is removed. AIREK-10 employs numerical techniques that do not require that the reactivity be constant in time. Secondly, AIREK-10 allows for the various mechanisms of reactivity feedback to be included, resulting in a more realistic model of the reactor's time dependent behavior. The third and final advantage of the AIREK-10 code for this type of calculation is that it is more efficient in terms of computing time and cost.

Results of the Modified Kinetics Calculations

Calculations using the AIREK-10 code were performed for the fast fission of ^{235}U for both positive and negative step changes in reactivity. These calculations

were performed using three sets of input data. First, the explicit 386 nuclide library including the 271 precursor nuclides of the present evaluation was used in conjunction with the appropriate fission yields taken from a preliminary ENDF/B-VI evaluation. Second, data for the current six-group fits were also used as input to the AIREK-10 code. The third and final dataset used in the comparison was the ENDF/B-V six-group data for ^{235}U.

Figure 81 shows the results of the AIREK-10 calculations. The units for the step changes in reactivity are dollars, where one dollar is the amount of reactivity that equals the delayed neutron fraction, β. In these calculations all three datasets were normalized to the same delayed neutron yield.

The explicit library and the current six-group data appear to be in good agreement for all cases. The largest differences between the explicit result and the current six-groups is seen in the case of a large ($0.50) positive reactivity insertion at long times. The agreement is good for all cases for very short times (less than about two seconds), and the prompt drop or jump predicted using each of the three sets of input data are in excellent agreement. Agreement for the ENDF/B-V six-group data is best for small positive changes in reactivity (less than about $0.10) and for negative changes in reactivity.

A set of control rod calibration curves (roddrop curves) were also generated using the explicit data library, the fitted six group data and the ENDF/B-V six-group data. These curves are given in Fig. 82. The reactivity required to produce a relative neutron density (or power density) of 0.10 at 20 seconds was estimated from these curves for each the three data sets. A value of $-$1.48 was estimated from the explicit 386 nuclide library. Values of $-$1.45 and $-$1.68 were assessed for the fitted and ENDF/B-V six-group data, respectively.

The agreement observed for the 386 nuclide library and the fitted six-group data (within 2%) suggests that the simple uncoupled data set involving six "average" precursor nuclides not only adequately reproduces the delayed neutron activity following a pulse irradiation but is also sufficient to predict the temporal response of a reactor to abrupt changes in reactivity. Differences between the

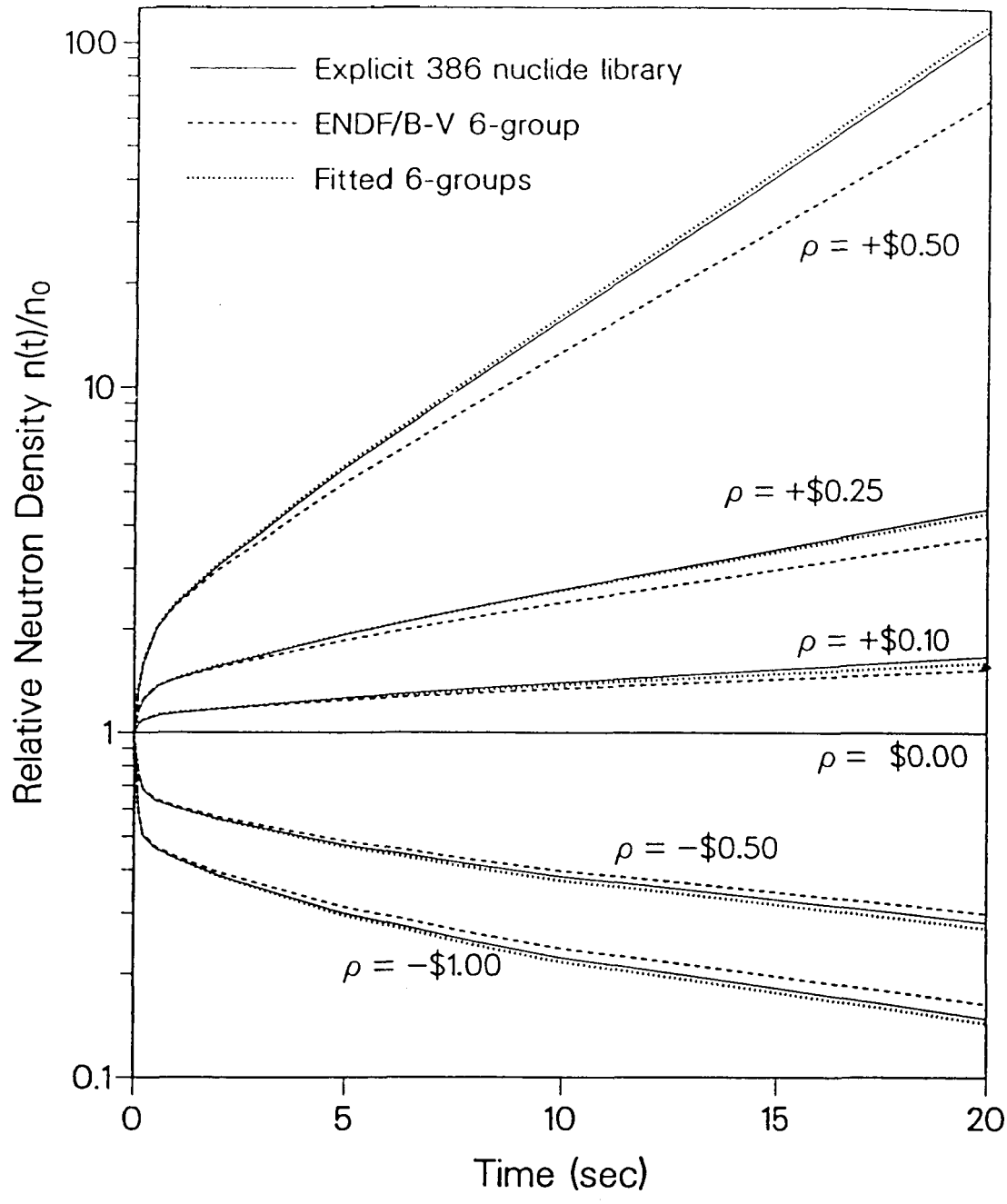

Fig. 81. Comparison of predicted responses to step changes in reactivity for ^{235}U(F).

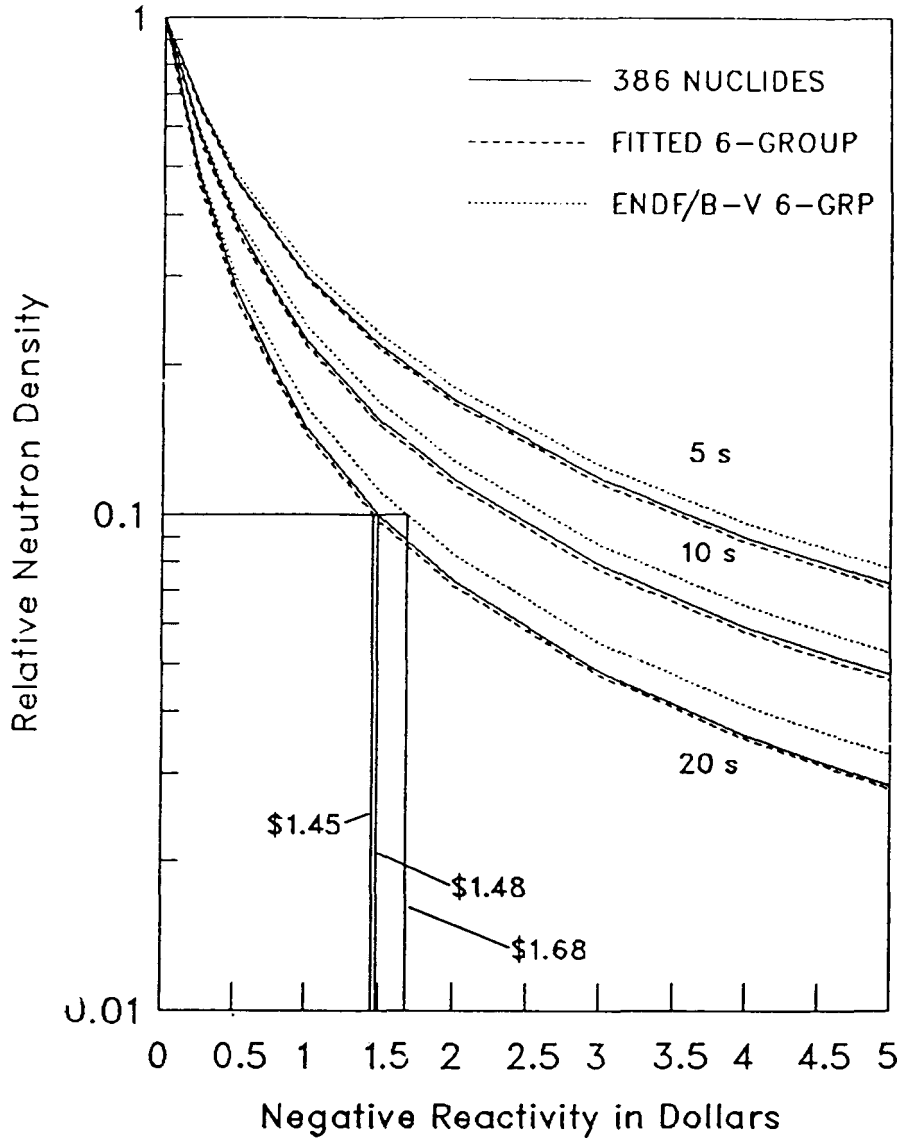

Fig. 82. Comparison of rod calibration curves for ^{235}U(F).

results produced by these two sets of data and the ENDF/B-V six-group data ($\sim$16%) appear to reflect basic differences in the data.

CHAPTER IX.

SUMMARY AND CONCLUSIONS

The work presented here represents a compilation of the current generation of delayed neutron data for individual precursor nuclides, the evaluation and extension of that data, and the application of that data to practical problems. [This is the largest single set of evaluated precursor data to date.] This chapter will review and summarize the contents of the database, use of the precursor database in generating the familiar six-temporal group delayed neutron constants and spectra, and the use of both the explicit precursor data and six-group data in reactor kinetics calculations.

PRECURSOR DATA LIBRARY

Based on energetics, 271 fission product nuclides have been identified as delayed neutron precursors. Three basic quantities are needed to describe the yield and spectrum of delayed neutrons in the precursor approach. These are fission product decay data (i.e., fission yields, half-lives, and branchings), emission probabilities, and delayed neutron spectra. These quantities are required for each of the 271 precursor nuclides. The content of the current data library is summarized in Table XIV. The question mark in Table XIV reflects the reluctance of some experimenters and evaluators to either identify or accept a measurement as being for an isomeric rather than ground state.

The fission yields used here were taken from a preliminary version of ENDF/B-VI[48] with some additions and extensions. Half-lives and branchings (other than P_n values) were taken directly from ENDF/B-V.[5]

Emission probabilities for 89 nuclides were taken from a 1986 evaluation by F. M. Mann.[8] The P_n values for the additional 182 precursors were calculated from the systematic Kratz-Herrmann equation using the fitted parameters from the Mann evaluation.

The primary emphasis in this dissertation was in the compilation and evaluation of precursor spectral data. Data from United States, German, and Swedish measurements are included in the final evaluation for a total of 34 precursor

TABLE XIV

Delayed Neutron (DN) Precursor Library

- 271 PRECURSORS (Based on energetics)
- P_n - DN EMISSION PROBABILITIES
  - — 83 ground state nuclides with measured P_n values
  - — 6(?) isomeric states with measured P_n values
  - — 182 from systematics (Kratz-Hermann equation)

  Nuclides with measured P_n values account for 79.66–99.77% of equilibrium DN (95.79% for ^{235}U(T)).
- SPECTRA
  - — 34 measured spectra (30 augmented with the BETA code)
  - — 235 calculated based on an evaporation model
  - — isomeric state substitutions

  Nuclides with measured spectra account for 67.57–96.24% of equilibrium DN (84.04% for ^{235}U(T)).
- FISSION PRODUCT YIELDS
  - — Preliminary ENDF/B-VI (1983)
- HALF-LIVES AND BRANCHING FRACTIONS
  - — ENDF/B-V

nuclides. The spectra for 30 of these nuclides were augmented with model calculations to provide information for the entire energy window ($Q_\beta - S(n)$). The BETA code model was used for these augmentations. This statistical code relies heavily on nuclear level data and has been shown to reliably predict spectral shapes, particularly at low energies.[46] However, due to its specific requirements for level information for the daughter and granddaughter states, it was not particularly useful for predicting the spectra for the additional 237 precursors. Many of these nuclides are far from the line of beta stability and have little or no measured nuclear data. A simple, single-parameter model based on an evaporation spectrum was developed and used to predict spectra for those nuclides with no measured data. The temperature parameter of this evaporation model was correlated to the mass of the precursor nuclide and its energy window for delayed neutron emission. In comparisons with the 34 experimental spectra, this simple model appears to reliably predict the spectral shapes. Uncertainty assignments were made for both sets of model spectra.

The precursor data library constructed here represents the most current and comprehensive compilation of its kind. The improvements and expansions of the spectral data are unique and represent a significant contribution to evaluated delayed neutron data. The delayed neutron spectra for the 271 individual precursor nuclides have been submitted for inclusion in ENDF/B-VI as a part of the fission product decay files.

SUMMATION CALCULATIONS

Calculations were performed using a summation technique to predict the delayed neutron yield per fission, ν_d, for 43 fissioning systems. The same calculational technique was used to predict total (aggregate) delayed neutron spectra. These calculations were performed as a means of validating the precursor data base. The results of the ν_d calculations compared well with previous calculations of the same type, as well as evaluated and experimental values. Aggregate spectra calculated using the summation technique compared well with spectra derived from ENDF/B-V delayed neutron data (Figs. 65–67).

TEMPORAL GROUP REPRESENTATIONS

The precursor data library was used in conjunction with the burnup and depletion code CINDER-10 to predict delayed neutron activity as a function of cooling time following a pulse irradiation. These delayed neutron activity curves were produced for each of 43 fissioning systems. A non-linear least-squares procedure was then used to fit these curves, thereby producing equivalent few-group constants. Initial comparisons for three-, six-, nine-, and twelve-groups were made and are given in Table X. The six-group representation is the most common method of presenting delayed neutron data; therefore, the final fits for 43 fissioning systems were made using six-groups. These six-group decay constants and normalized abundances were presented in Table XI for all 43 cases.

A method of deriving a consistent set of six-group spectra has been presented that does not rely on the arbitrary half-life bounds usually found in calculations of this kind.[112] Six-group spectra were also calculated for each of the 43 fissioning systems. The reduction of the detailed precursor data into six groups has resulted in the largest set of evaluated six-group data to date. This data, including the group spectra, have been formatted and submitted for inclusion in ENDF/B-VI.

APPLICATIONS OF DATA

The six-group data for the fast fission of ^{235}U were used to calculate spectra for the same delay intervals for which the University of Lowell has reported measured spectra.[9] The Lowell data are the most recently published delayed neutron spectral data. Comparisons of the Lowell spectra and average energies with those calculated based on the fitted six-group data showed very good agreement.

Beta-effective calculations were made using the PERT code.[109] Both the six-group data and the individual precursor data were used to calculate β-effective for a ^{235}U bare sphere reactor (GODIVA). The results were in excellent agreement, not only with one another, but also with the measured value.

POINT KINETICS CALCULATIONS

The point reactor kinetics equations were modified to include the explicit representation of individual delayed neutron precursors. The results using the explicit data in these modified equations were in excellent agreement with results using the fitted six-group data in the conventional point kinetics equations. In addition to the 271 precursor nuclides, 115 parent nuclides were required to calculate the kinetic response from the explicit data. The agreement observed between these cases suggests that the kinetic response is not highly dependent on representing the physical coupling between precursor nuclides. Comparisons using the ENDF/B-V six-group data were also made.

All three sets of data (the explicit precursor data, the fitted six-group, and the ENDF/B-V six-group data) were found to predict nearly identical responses in power for times on the order of 1 s after a step change in reactivity. This period of time accounts for the most dramatic change in power, the "prompt jump" or "prompt drop." After this, there are additional changes in reactivity by various feedback and/or control mechanisms.

The agreement observed between the calculations using the explicit precursor data and that using the fitted six-group data is significant. The method used to derive the six-group parameters insures that the delayed neutron activity is the same in both representations. Until this work, it had not been shown that the six-groups would also predict a kinetic response consistent with the explicit data.

SIGNIFICANCE OF COMPLETED WORK

As a result of the evaluation presented in this dissertation, the delayed neutron data in ENDF/B-VI will be substantially improved over that of ENDF/B-V. The number of fissioning nuclides with delayed neutron data has been increased from 7 to 28. Another major improvement is that the energy range of the spectra has been increased from 1.2 MeV to 3.0 MeV. The actual spectra extended the full range of theoretical delayed neutron emission (in excess of 10 MeV) but were truncated at 3 MeV for ENDF/B-VI. Only a small fraction of delayed neutrons

have energies greater than 3 MeV and for reactor applications (the primary use of ENDF/B data) the lower energies are of greatest importance. The spectra to be included in ENDF/B-VI will be given in histogram form with equal bin widths of 10 keV, making a total of 300 energy groups. This is in contrast to the 27 energy groups in ENDF/B-V.

Due to ENDF/B format constraints, it was possible to submit only one set of six-group data for each fissioning nuclide; i.e., there is no dependence on incident neutron energy. However, it has been shown in this work that the spectra do not exhibit a strong dependence on incident neutron energy.

The delayed neutron yields, ν_d, recommended for ENDF/B-VI for the 7 fissioning nuclides in ENDF/B-V are unchanged. Of the remaining 21 nuclides, only 9 have measurements of ν_d that were found in the literature as given in Table VI. The calculated values from this work were recommended for the nuclides with no measured data.

Unlike for ENDF/B-V, the delayed neutron spectra for the individual precursors are to be included in the fission product decay files in ENDF/B-VI. These spectra will also be in 10-keV bins and will be cut off at 3 MeV.

CONCLUSIONS

In conclusion, the evaluation of individual precursor spectra and the reduction of the explicit data to the six-group formalism represent unique and significant contributions to the current status of delayed neutron data. As further measurements are performed and theoretical models developed, the data should be updated and improved. The data contained in the precursor library and the six-group data have been derived using experimental data to mid-1986 as well as current calculational models.

REFERENCES

1. R. B. ROBERTS, L. R. HOFSTAD, R. C. MEYER, and P. WANG, "The Delayed Neutron Emission which Accompanies Fission of Uranium and Thorium," *Phys. Rev.*, **55**, 664 (1939).

2. G. R. KEEPIN, "Delayed Neutrons," *Progress in Nucl. Energy*, **1**, 191-225 (1965).

3. G. R. KEEPIN, *Physics of Nuclear Kinetics*, Addison-Wesley Publishing Co., Reading, Massachusetts (1956), Chapter 4.

4. G. R. KEEPIN, T. F. WIMETT, and R. K. ZEIGLER, "Delayed Neutrons from Fissionable Isotopes of Uranium, Plutonium, and Thorium," *J. Nucl. Energy*, **6**, 1-21 (1957).

5. ENDF/B: Evaluate Nuclear Data Files, available from and maintained by the National Nuclear Data Center, Brookhaven National Laboratory, Upton, New York. Version V (ENDF/B-V) is currently available. Some preliminary files for Version VI are essentially complete but are still subject to change.

6. K. -L. KRATZ, "Review of Delayed Neutron Energy Spectra," *Proc. Consultants Mtg. on Delayed Neutron Properties*, Vienna, Austria, March 26–30, 1979 [International Atomic Energy Agency Report INDC NDS-107/G+Special (1979)].

7. F. M. MANN, C. DUNN, and R. E. SCHENTER, "Beta Decay Properties Using a Statistical Model," *Phys. Rev. C*, **25**(1), 524-526 (1982).

8. F. M. MANN, "1986 Evaluation of Delayed-Neutron Emission Probabilities," *Proc. of the Specialists' Mtg. on Delayed Neutrons*, Univ. of Birmingham, Birmingham, England, Sept. 15-19, 1986 (1987).

9. R. S. TANCZYN, Q. SHARFUDDIN, W. A. SCHIER, D. J. PULLEN, M. H. HAGHIGHI, L. FISTEAG, and G. P. COUCHELL, "Composite Delayed Neutron Energy Spectra for Thermal Fission of ^{235}U," *Nucl. Sci. and Eng.*, **94**, 353-364 (1986).

10. N. BOHR and J. A. WHEELER, "The Mechanism of Nuclear Fission," *Phys. Rev.*, **56**, 426-450 (1939).

11. R. B. ROBERTS, R. C. MEYER, and P. WANG, "Further Observations on the Splitting of Uranium and Thorium," *Phys. Rev.*, **55**, 510-511 (1939).

12. G. R. KEEPIN, T. F. WIMETT, and R. K. ZEIGLER, "Delayed Neutrons from Fissionable Isotopes of Uranium, Plutonium, and Thorium," *Phys. Rev.*, **107**, 1044, 1049 (1957).

13. J. R. LAMARSH, *Introduction to Nuclear Reactor Theory*, Addison-Wesley Publishing Co., Reading, Massachusetts (1966), Chapter 3.

14. SAMSON A. COX, "Delayed Neutron Data – Review and Evaluation," ANL/NDM-5, April 1974.

15. R. J. TUTTLE, "Delayed-Neutron Data for Reactor-Physics Analysis," *Nucl. Sci. and Eng.*, **56**, 37-71 (1975).

16. R. J. TUTTLE, "Review of Delayed Neutron Yields in Nuclear Fission," *Proc. Consultants' Mtg. on Delayed Neutron Properties*, Vienna, Austria, March 26–30, 1979, p. 29 [International Atomic Energy Agency Report INDC NDS-107/G+Special (1979)].

17. G. BENEDETTI, A. CESANA, V. SANGIUST, M. TERRANI and G. SANDRELLI, "Delayed Neutron Yields from Fission of ^{233}U, ^{237}Np, ^{238,240,241}Pu, and ^{241}Am," *Nucl. Sci. and Eng.*, **80**, 379-387 (1982).

18. R. W. WALDO, R. A. KARAM, and R. A. MEYER, "Delayed Neutron Yields: Time Dependent Measurements and a Predictive Model," *Phys. Rev. C*, **23**(3), 1113-1127 (1981).

19. R. W. WALDO, R. A. KARAM, "Measured Delayed Neutron Yields," *Trans. Am. Nucl. Soc.*, **39**, 879-880 (1982).

20. S. SYNETOS, J. G. WILLIAMS, "Delayed Neutron Yield and Decay Constants for Thermal Neutron-Induced Fission of ^{235}U," *Nucl. Energy*, **22**, 267-274 (1983).

21. D. J. HUGHES, J. DABBHS, A. CAHN, and D. HALL, "Delayed Neutrons from Fission of ^{235}U," *Phys. Rev.*, **73**, 111-124 (1948).

22. M. BURGY, L. A. PARDUE, H. B. WILLARD and E. O. WOLLAN, "Energy of Delayed Neutrons from ^{235}U Fissions," *Phys. Rev.*, **70**, 104 (1946).

23. T. W. BONNER, S. J. BAME, JR., and J. E. EVANS, "Energy of the Delayed Neutrons from the Fissions of ^{235}U," *Phys. Rev.*, **101**, 1514-1515 (1956).

24. R. BATCHELOR and H. R. McK. HYDER, "The Energy of Delayed Neutrons from Fission," *J. Nucl. Energy*, **3**, 7-17 (1956).

25. G. FIEG, "Measurements of Delayed Fission Neutron Spectra of ^{235}U, ^{238}U, and ^{239}Pu with Proton Recoil Proportional Counters," *J. Nucl. Energy*, **26**, 585-592 (1972).

26. S. SHALEV and J. M. CUTTLER, "The Energy Distribution of Delayed Fission Neutrons," *Nucl. Sci. and Eng.*, **51**, 52-66 (1973).

27. R. E. KAISER and S. G. CARPENTER, "Suggested Delayed Neutron Data for ENDF/B Version V," memorandum to E. M. Bohn, February 8, 1977, (private collection M. C. Brady).

28. T. R. ENGLAND, W. B. WILSON, R. E. SCHENTER, and F. M. MANN, "Aggregate Delayed Neutron Intensities and Spectra Using Augmented ENDF/B-V Precursor Data," *Nucl. Sci. and Eng.*, **85**, 139-155 (1983).

29. H. F. ATWATER, C. A. GOULDING, C. E. MOSS, R. A. PEDERSON, A. A. ROBBA, T. F. WIMETT, P. L. REEDER, and R. A. WARNER, "Delayed Neutron Spectra for Short Pulse Fast Fission of Uranium-235," *Proc. of the Specialists' Mtg. on Delayed Neutrons*, Univ. of Birmingham, Birmingham, England, Sept. 15–19, 1986 (1987).

30. G. RUDSTAM, Swedish Research Council's Laboratory at Studsvik, personal communication (1981).

31. H. OHM, "Statistiche und Nichtstatistische Effekte bei der Emission β-verzogerter Neutronen; Untersuchung des Zerfalls der Nuklide ^{137,138}J und $^{93-97}$Rb," doctoral dissertation der Johannes-Gutenberg-Universitat in Mainz (1981).

32. R. C. GREENWOOD and A. J. CAFFREY, "Delayed-Neutron Energy Spectra of $^{93-97}$Rb and $^{143-145}$Cs," *Nucl. Sci. and Eng.*, **91**, 305-323 (1985).

33. P. L. REEDER, L. J. ALQUIST, R. L. KIEFER, F. H. RUDDY, and R. A. WARNER, "Energy Spectra of Delayed Neutrons from the Separated Precursors ^{93,94,95}Rubidium and ^{143}Cesium," *Nucl. Sci. and Eng.*, **75**, 140-150 (1980).

34. Y. S. LYUTOSTANSKII, I. V. PANOV, and V. K. SIROTKIN, "The Possibility of Emission of Two Neutrons in β Decay of Nuclei with $A \geq 50$," *Sov. J. Nucl. Phys.*, **37**(2), 163-164 (1983).

35. P. REEDER, R. WARNER, T. YEH, R. CHRIEN, R. GILL, M. SHMID, H. LIOU, and M. STELTS, "Beta-Delayed Two-Neutron Emission from ^{96}Pb," *Phys. Rev. Lett.*, **47**(7), 483 (1981).

36. I. KAPLAN, *Nuclear Physics*, Addison-Wesley Publishing Co., Inc., Reading, Massachusetts (1962).

37. ROBLEY D. EVANS, *The Atomic Nucleus*, McGraw Hill Book Co., Inc., New York, New York (1955), Chapter 11.

38. A. C. PAPPAS and G. RUDSTAM, "An Approach to the Systematics of Delayed Neutron Precursors," *Nucl. Phys.*, **21**, 353-366 (1960).

39. A. C. PAPPAS and T. SVERDRUP, "Gross Properties of Delayed Neutron Emission and Beta-Strength Functions," *Nucl. Phys. A*, **188**, 48-64 (1972).

40. W. RUDOLPH and K. -L. KRATZ, "Attempt to Calculation of Delayed Neutrons Emission Probabilities Using Simple Statistical Model Considerations," *Z. Physik A*, **281**, 269-275 (1977).

41. C. L. DUKE, P. G. HANSEN, D. B. NIELSEN, and G. RUDSTAM, "Strength-Function Phenomena in Electron-Capture Beta Decay," *Nucl. Phys.*, **A151** 609-633 (1970).

42. K. ALEKLETT, G. NYMAN, and G. RUDSTAM, "Beta-Decay Properties of Strongly Neutron-Rich Nuclei," *Nucl. Phys.*, **A246**, 425-444 (1975).

43. S. AMIEL and H. FELDSTEIN, "A Semi-Empirical Treatment of Neutron Emission Probabilities from Delayed Neutron Precursors," *Phys. Lett.*, **31B**(2), 59-60 (1970).

44. O. K. GJOTTERUD, P. HUFF, and A. C. PAPPAS, "Detailed Structure of Delayed Neutron Spectra," *Nucl. Phys. A*, **303**, 295-312 (1978).

45. K. -L. KRATZ and G. HERRMANN, "Systematics of Neutron Emission Probabilities from Delayed Neutron Precursors," *Z. Physik*, **363**, 435-442 (1973).

46. F. M. MANN, M. SCHREIBER, R. E. SCHENTER, and T. R. ENGLAND, "Evaluation of Delayed-Neutron Emission Probabilities," *Nucl. Sci. and Eng.*, **87**, 418-431 (1984).

47. General Electric (San Jose, California) report series, "Compilation of Fission Product Yields:" M. E. MEEK and B. F. RIDER, NEDO-2154 (1972); B. F. RIDER and M. E. MEEK, NEDO-2154-1 (1972); B. F. RIDER, NEDO-2154-2(E) (1978); B. F. RIDER, NEDO-2154-3(B), [ENDF-292] (1980); and B. F. RIDER, NEDO-2154-3(C), [ENDF-322] (1981).

48. T. R. ENGLAND and B. F. RIDER, "Status of Fission Yield Evaluations," *NEANDC Specialists' Mtg on Yields and Decay Data of Fission Product Nuclides*, Brookhaven National Laboratory, Upton, New York, October 24-29, 1983 (BNL-51778).

49. D. G. MADLAND and T. R. ENGLAND, "The Influence of Pairing on the Distribution of Independent Yield Strengths in Neutron-Induced Fission," Los Alamos National Laboratory report LA-6430-MS (ENDF-240) (July 1976).

50. D. G. MADLAND and T. R. ENGLAND, "The Influence of Isomeric States on Independent Fission Product Yields," *Nucl. Sci. Eng.*, **64**, 859 (1976); see also Los Alamos National Laboratory report LA-6595-MS (ENDF-241) (November 1976).

51. A. C. WAHL, R. L. FERGUSON, D. R. NETHAWAY, D. E. TROUTNER, and K. WOLFSBERG, "Nuclear-Charge Distribution in Low-Energy Fission," *Phys. Rev.*, **126**, 1112-1127 (1962).

52. A. C. WAHL, "Systematics of Nuclear Charge Distribution in Fission, the Z_p Model," *J. Radioanal. Chem.*, **55**, 111-123 (1980).

53. K. TAKAHASHI, "Application of the Gross Theory of Beta-Decay to Delayed Neutron Emissions," *Prog. of Theor. Phys.*, **47**, No. 5 (1972).

54. T. JAHNSEN, A. C. PAPPAS, and T. TUNAL, *Proc. Panel on Delayed Fission Neutrons*, Vienna, 1967, p. 35 (IAEA, Vienna, 1968).

55. H. GAUVIN and R. de TOURREIL, *Proc. of the Second IAEA Symposium on Physics and Chemistry of Fission*, Vienna, 1969, p. 621 (IAEA, Vienna, 1969).

56. S. SHALEV and G. RUDSTAM, "Energy Spectra of Delayed Neutrons from Separated Fission Products (I). The Precursors ^{85}As, ^{87}Br, ^{134}Sn, ^{135}Sb, ^{136}Te, and ^{137}I," *Nucl. Phys. A*, **230**, 153-172 (1974).

57. K. TAKAHASHI and M. YAMADA, "Gross Theory of Nuclear Beta-Decay," *Prog. of Theor. Phys.*, **41**, 1470-1503 (1969).

58. K. TAKAHASHI, "Gross Theory of First Forbidden Beta-Decay," *Prog. of Theor. Phys.*, **45**, 1466-1492 (1969).

59. P. G. HANSEN and B. JONSON, "Beta-Delayed Particle Emission from Neutron-Rich Nuclei," CERN-EP/87-44, 26 February 1987 (Contribution prepared for the book *Particle Emission from Nuclei*, Eds. M. Ivasen and D. Poenaru (to be published by the CRC Press, Cleveland, Ohio).

60. P. MARMIER and E. SHELDON, *Physics of Nuclei and Particles*, Academic Press, New York, New York (1969).

61. J. M. BLATT and V. F. WEISSKOPF, *Theoretical Nuclear Physics*, John Wiley and Sons, New York, New York (1952).

62. C. WU and S. A. MOSZKOWSKI, *Beta Decay*, Interscience Publishers, New York, New York (1966).

63. S. SHALEV and G. RUDSTAM, *Trans. Am. Nucl. Soc.*, **14**, 373 (1971).

64. G. RUDSTAM, "Characterization of Delayed-Neutron Spectra," *Journal of Radioanalytical Chem*, **36**, 591-618 (1977).

65. O. K. GJOTTERUD, P. HOFF, and A. C. PAPPAS, "Gross Properties of Delayed Neutron Spectra," *Nucl. Phys. A*, **303**, 281-294 (1978).

66. S. SHALEV and G. RUDSTAM, "Energy Spectra of Delayed Neutrons from Separated Fission Products," *Nucl. Phys. A*, **275**, 76-92 (1977).

67. H. V. KLAPDOR, "Beta Decay Far From Stability and Its Role in Nuclear Physics and Astrophysics," presented at the International School-Seminar on Heavy Ion Physics, Alushta, Crimea, USSR, 14-21 April 1983.

68. H. V. KLAPDOR, "Beta Decay Calculations and Their Applications in Nuclear Technology and Astrophysics," KTG/END-International State of the Art Seminar on Nuclear Data, Cross Section Libraries and their Application in Nuclear Technology, October 1-2, 1985, Wissenschaftszentrum, Bonn.

69. F. M. MANN, C. DUNN, and R. E. SCHENTER, "Beta Decay Properties from a Statistical Model," *Trans. Am. Nucl. Soc.*, **39**, 880-883 (1981).

70. F. M. MANN, "Calculating Beta Decay Properties in the Fission Product Region," *NEANDC Specialists' Mtg. on Yields and Decay Data of Fission Product Nuclides*, Brookhaven National Laboratory, Upton, New York, October 24-29, 1983 (BNL-51778), 449-453.

71. L. TOMLINSON, "Delayed Neutron Precursors," *Atomic Data and Nuclear Data Tables*, **12**, 179-194 (1973).

72. A. H. WAPSTRA and G. AUDI, "The 1983 Atomic Mass Evaluation," *Nucl. Phys. A*, **432**, 1 (1985).

73. P. MÖLLER and J. R. NIX, "Atomic Masses and Nuclear Ground-State Deformations Calculated with a New Macroscopic-Microscopic Model," *Atomic and Nuclear Data Tables*, **26**(2), 165-196 (March 1981).

74. G. RUDSTAM, "Review of Delayed Neutron Branching Ratios, *Proc. Consultants Mtg. on Delayed Neutron Properties*, Vienna, Austria, March 26-30, 1979, p. 69 [International Atomic Energy Agency Report INDC NDS-107/G+Special (1979)].

75. E. LUND, P. HOFF, K. ALCKLETT, O. GLOMSET, and G. RUDSTAM, "Delayed Neutron Emission Probabilities of Gallium, Bromine, Rubidium, Indium, Antimony, Iodine, and Cesium Precursors," *Z. Phys. A*, **294**, 233-240 (1980).

76. E. LUND, G. RUDSTAM, K. ALEKLETT, B. EKSTRON, B. FOGELBERG, and L. JACOBSEN, "A Status Report on Delayed Neutron Branching Ratios of Fission Products and the Delayed Neutron Program at OSIRIS Using the New Ion-Source ANU-BIS," *Proc. of the Specialists' Mtg on Delayed Neutrons*, Univ. of Birmingham, Birmingham, England, Sept. 15-19, 1986 (1987).

77. G. F. KNOLL, *Radiation Detection and Measurement*, John Wiley & Sons, Inc., New York, New York (1979), Chapters 14 and 15.

78. G. RUDSTAM, "The Uncertainty of Neutron Energy Spectra Deduced from Measured Pulse Spectra in a ^{3}He Spectrometer," *Nucl. Inst. and Methods*, **177**, 529-536 (1980).

79. H. FRANZ, W. RUDOLPH, H. OHM, K. -L. KRATZ, G. HERRMANN, F. M. NUH, D. R. SLAUGHTER, and S. G. PRUSSIN, "Delayed-Neutron Spectroscopy with He-3 Spectrometers," *Nucl. Instr. and Meth.*, **144**, 253-261 (1977).

80. R. C. GREENWOOD and A. J. CAFFREY, "Measuring Delayed Neutron Spectra – A Comparison of Techniques," *NEANDC Specialists' Mtg on Yields and Decay Data of Fission Product Nuclides*, Brookhaven National Laboratory, Upton, New York, October 24-29, 1983 (BNL-51778), 365-393.

81. G. RUDSTAM, S. SHALEV, and O. C. JOHNSON, "Delayed Neutron Emission from Separated Fission Products," *Nucl. Instr. Method*, **120**, 333-344 (1974).

82. P. L. REEDER, "Status of and Outstanding Problems in Delayed Neutron Data, Pn Values and Energy Spectra," *Proc. of the Conf. on Nuclear Data Evaluation Methods and Procedures*, Brookhaven National Laboratory, Upton, New York, September 22-25, 1980 (BNL-NCS-51363).

83. J. M. CUTTLER, S. GREENBERGER, and S. SHALEV, "Pulse Risetime Discrimination for ^{3}He Counters," *Nucl. Instr. and Meth.*, **75**, 309-311 (1969).

84. W. R. SLOAN and G. L. WOODRUFF, "Spectrum of Delayed Neutrons from the Thermal Neutron Fission of ^{235}Uranium," *Nucl. Sci. and Eng.*, **55**, 28-40 (1974).

85. G. W. ECCLESTON and G. L. WOODRUFF, "Measured Near-Equilibrium Delayed Neutron Spectra Produced by Fast-Neutron-Induced Fission of ^{232}Th, ^{233}U, ^{235}U, ^{238}U, and ^{239}Pu," *Nucl. Sci. and Eng.*, **62**, 636-651 (1977).

86. P. K. RAY and E. S. KENNEY, *Nucl. Instr. and Methods*, **134**, 559 (1976).

87. D. D. CLARK, R. D. McELROY, T. -R. YEH, R. E. CHRIEN, and R. L. GILL, "Neutron Resonances in Nuclides Far From Stability Via Energy Spectra of Beta-Delayed Neutrons," *NEANDC Specialists' Mtg on Yields and Decay Data of Fission Product Nuclides*, Brookhaven National Laboratory, Upton, New York, October 24-29, 1983 (BNL-51778), 449-453.

88. D. D. CLARK, T.-R. YEH, C.-H. LEE, L.-J. YUAN, M. SHMID, R. L. GILL, and R. E. CHRIEN, "Beta-Delayed Neutron Spectra From $^{93-97}$Rb and $^{143-146}$Cs," *NEANDC Specialists' Mtg on Yields and Decay Data of Fission Product Nuclides*, Brookhaven National Laboratory, Upton, New York, October 24-29, 1983 (BNL-51778), 455-457.

89. N. G. CHRYSOCHOIDES, J. N. ANOUSSIS, C. A. MITSONIAS, and D. C. PERRICOS, "Measurement of the Low Energy Spectrum of Delayed Neutrons from ^{87}Br and ^{88}Br Precursors," *J. Nucl. Energy*, **25**, 551-556 (1971).

90. G. RUDSTAM and S. SHALEV, "Energy Spectra of Delayed Neutrons from Separated Fission Products," *Nucl. Phys. A*, **235**, 397-409 (1974).

91. G. T. EWAN, P. HOFF, B. JONSON, K.-L. KRATZ, P. O. LARSON, G. NYMAN, H. L. RAVIN, and W. ZIEGERT, "Intense Mass-Separated Beams of Halogens and Beta-Delayed Neutron Emission from Heavy Bromine Isotopes," *Z. Phys. A*, **318**, 309-314 (1984).

92. G. RUDSTAM and E. LUND, "Energy Spectra of Delayed Neutrons from the Precursors ^{79}(Zn, Ga), ^{80}Ga, ^{81}Ga, ^{94}Rb, ^{95}Rb, ^{129}In, and ^{130}In," *Nucl. Sci. and Eng.*, **64**, 749-760 (1977).

93. G. RUDSTAM, "Six-Group Representation of the Energy Spectra of Delayed Neutrons from Fission," *Nucl. Sci. and Eng.*, **80**, 238-255 (1982).

94. H. GABELMANN, University of Mainz, private communication (May 1985).

95. G. RUDSTAM, "Status of Delayed Neutron Data," *Proc. 2nd IAEA Advisory Group Mtg on Fission Product Nuclear Data*, Petten, Netherlands, September 5-9, 1977, Vol. 2, 567.

96. P. L. REEDER and R. A. WARNER, "Average Energy of Delayed Neutrons from Individual Precursors and Estimation of Equilibrium Spectra," *Nucl. Sci. and Eng.*, **79**, 56-64 (1981).

97. K.-L. KRATZ, "The Beta-Decay of ^{95}Rb and ^{97}Rb," *Z. Phys. A*, **312**, 43-57 (1983).

98. K.-L. KRATZ, A. SCHRODER, H. OHM, M. ZENDEL, H. GABELMANN, W. ZEIGERT, P. PEUSER, G. JUNG, B. PFEIFFER, K. D. WUNSCH, H. WOLLNIK, C. RISTORI, and J. CRANCON, "Beta-Delayed Neutron Emission from $^{93-100}$Rb to Excited States in the Residual Sr Isotopes," *Z. Phys. A*, **306**, 239-257 (1982).

99. J. R. HUIZENGA and L. G. MORETTO, *Ann. Rev. Nucl. Sci.*, **22**, 427 (1972).

100. D. SAPHIER, D. ILBERG, S. SHALEV, and S. YIFTAH, "Evaluated Delayed Neutron Spectra and Their Importance in Reactor Calculations," *Nucl. Sci. and Eng.*, **62**, 660-694 (1977).

101. A. E. EVANS and M. S. KRICK, "Equilibrium Delayed Neutron Spectra from Fast Fission of ^{235}U, ^{238}U, and ^{239}Pu," *Nucl. Sci. and Eng.*, **62**, 562-659 (1977).

102. T. R. ENGLAND, M. C. BRADY, W. B. WILSON, R. E. SCHENTER, and F. M. MANN, "Delayed Neutron Spectra and Intensities from Evaluated Precursor Data," *Proc. Int. Conf. Nucl. Data for Basic and Applied Sci.*, Santa Fe, New Mexico, May 13-17, 1985 (Gordon and Breach Science Pubs., New York), Vol. 1, p. 739 (1986).

103. T. R. ENGLAND, R. WILCZYNSKI, and N. L. WHITTEMORE, "CINDER-7: An Interim Report for Users," Los Alamos Scientific Laboratory Report LA-5885-MS (April 1975). [CINDER-10 is a modification of CINDER-7.]

104. J. H. BURRILL, JR., *360 STEPIT: A User's Manual*, Ohio State University, TNP-1966-2, 10 May 1966.

105. M. C. BRADY, T. R. ENGLAND, and W. B. WILSON, "Few Group Analysis of Current Delayed Neutron Data," *Trans. Am. Nucl. Soc.*, **53**, 469 (1986).

106. R. T. PERRY, W. B. WILSON, T. R. ENGLAND, and M. C. BRADY, "Application of Evaluated Fission-Product Delayed Neutron Precursor Data in Reactor Kinetics Calculations," *Proc. Int. Conf. Nucl. Data for Basic and Applied Sci.*, Santa Fe, New Mexico, May 13-17, 1985 (Gordon and Breach Science Pubs., New York), Vol. 1, 717 (1986).

107. M. C. BRADY, R. T. PERRY, W. B. WILSON, and T. R. ENGLAND, "Quasi-Analytic Point Reactor Kinetics Calculations Using Individual Precursor Data," *Trans. Am. Nucl. Soc.*, **50**, 549 (1985).

108. R. DOUGLAS O'DELL, F. W. BRINKLEY, JR., D. R. MARR, "User's Manual for ONEDANT: A Code Package for One-Dimensional, Diffusion-Accelerated, Neutral-Particle Transport," Los Alamos National Laboratory manual LA-9184-M (February 1982).

109. D. C. GEORGE and R. J. LaBAUVE, "PERTV-A Standard File Version of the PERT-V Code," Los Alamos National Laboratory Report LA-11206-MS (February 1988). [Original report prepared by R. W. Hardie and W. W. Little, Jr., BNWL-1162 (September 1969).]

110. Fast Reactor Benchmark No. 5, Cross Section Evaluation Working Group Benchmark Specifications (BNL-19302).

111. J. J. DUDERSTADT and L. J. HAMILTON, *Nuclear Reactor Analysis*, John Wiley & Sons, Inc., New York, New York (1976).

112. M. C. BRADY and T. R. ENGLAND, "Few-Group Representation of the Energy Spectra of Delayed Neutrons," *Trans. Am. Nucl. Soc.*, **54**, 342-344 (1987). (See also Los Alamos informal document LA-UR 87-48.)

113. A. H. WAPSTRA, "Determination and Use of Nuclear Masses," *Neutron-Capture Gamma-Ray Spectroscopy and Related Topics 1981, Proceedings of the Fourth International Symposium*, Grenoble, France, 7-11 Sept. 1981 (Bristol England: IOP 1982), pp. 535-547.

APPENDIX A

GENERAL BIBLIOGRAPHY

GENERAL BIBLIOGRAPHY

(References are listed alphabetically by leading author)

M. Akiyama, Y. Oka, S. Kondo, and S. An, "Fission-Product Decay Heat for Fast-Neutron Fissions of ^{238}U and ^{232}Th," Proc. Int. Conf. Nucl. Data for Basic and Applied Sci., Santa Fe, New Mexico, May 13-17, 1985 (Gordon and Breach Science Pubs., New York), Vol. 1, 743-746.

K. Aleklett, P. Hoff, E. Lund, and G. Rudstam, "Delayed Neutron Emission Probabilities of the Precursors ^{89,90,91}Br and ^{139,140,141}I," Z. Phys. A **295**, 331-332 (1980).

D. R. Alexander and M. S. Krick, "Delayed Neutron Yield Calculations for the Neutron-Induced Fission of ^{235}U as a Function of the Incident Neutron Energy," Nucl. Sci. Eng. **62**, 627-635 (1977).

I. Amarel, H. Gauvin and A. Johnson, "Delayed Neutron Emission Probabilities of Rb and Cs Precursors. The Half-Life of ^{97}Pb," J. Inorg. Nucl. Chem. **31**, 577-584 (1969).

S. Amiel and H. Feldstein, "A Semi-Empirical Treatment of Neutron Emission Probabilities from Delayed Neutron Precursors," Phys. Lett. **31B**, No. 2, 59-60 (1970).

M. Asghar, J. Crancon, J. P. Gautheron, and C. Ristori, "Delayed Neutron Emission Probabilities of ^{92,93}Rb, ^{141,142}Xe, and ^{141,142}Cs Precursors," J. Inorg. Nucl. Chem. **37**, 1563-1567 (1975).

M. Asghar, J. P. Gautheron, G. Bailleul, J. P. Bocquet, J. Greif, H. Schrader, G. Siegert, C. Ristori, J. Crancon, and G. I. Crawford, "The Pn Values of the ^{235}U(n_{th},f) Produced Precursors in the Mass Chains 90, 91, 93-95, 99, 134, and 137-139," Nucl. Phys. A **247**, 359-376 (1975).

H. F. Atwater, C. A. Goulding, C. E. Moss, R. A. Pederson, A. A. Robba, T. F. Wimett, P. L. Reeder, and R. A. Warner, "Delayed Neutron Spectra from Short Pulse Fast Fission of Uranium-235," Proc. of the Specialists' Mtg. on Delayed Neutrons, U. of Birmingham, Birmingham, England, Sept. 15-19, 1986.

R. Batchelor and H. R. McK. Hyder, "The Energy of Delayed Neutrons from Fission," J. Nucl. Energy **3**, 7-17 (1956).

G. Benedetti, A. Cesana, V. Sangiust, M. Terrani and G. Sandrelli, "Delayed Neutron Yields from Fission of ^{233}U, ^{237}Np, ^{238,240,241}Pu, and ^{241}Am," Nucl. Sci. and Eng. **80**, 379-387 (1982).

T. Bjornstad, H. A. Gustafsson, P. G. Hanson, B. Jonson, V. Lindfors, S. Mattsson, A. M. Poskanzer and H. L. Ravin, "Delayed Neutron Emission Probabilities of ^{9}Li and ^{11}Li," Nucl. Phys. A **359**, 1-8 (1981).

J. M. Blatt and V. F. Weisskopf, *Theoretical Nuclear Physics*, John Wiley and Sons, New York, New York (1952).

T. W. Bonner, S. J. Bame, Jr., and J. E. Evans, "Energy of the Delayed Neutrons from the Fissions of ^{235}U," Phys. Rev. **101**, 1514-1515 (1956).

M. C. Brady, R. T. Perry, W. B. Wilson, and T. R. England, "Quasi-Analytic Point Reactor Kinetics Calculations Using Individual Precursor Data," Trans. Am. Nucl. Soc. **50**, 549 (1985).

M. C. Brady, T. R. England, and W. B. Wilson, "Few Group Analysis of Current Delayed Neutron Data," Trans. Am. Nucl. Soc. **53**, 469 (1986).

M. C. Brady and T. R. England, "Few-Group Representation of the Energy Spectra of Delayed Neutrons," Trans. Am. Nucl. Soc. **54**, 342-344 (1987). (See also Los Alamos informal document LA-UR 87-48.)

M. Burgy, L. A. Pardue, H. B. Willard and E. O. Wollan, "Energy of Delayed Neutrons from ^{235}U Fissions," Phys. Rev. **70**, 104 (1946).

N. G. Chrysochoides, J. N. Anoussis, C. A. Mitsonias, and D. C. Perricos, "Measurement of the Low Energy Spectrum of Delayed Neutrons from ^{87}Br and ^{88}Br Precursors," J. Nucl. Energy **25**, 551-556 (1971).

C. Ciarcia, G. Couchell, L. Fisteag, W. Schier, and R. Tanczyn, "Data Reduction and Analysis in Composite Delayed-Neutron Time-of-Flight Studies," Proc. Int. Conf. Nucl. Data for Basic and Applied Sci., Santa Fe, New Mexico, May 13-17, 1985 (Gordon and Breach Science Pubs., New York), Vol. 1, 747-749.

D. D. Clark, R. D. McElroy, T.-R. Yeh, R. E. Chrien, and R. L. Gill, "Neutron Resonances in Nuclides Far From Stability Via Energy Spectra of Beta-Delayed Neutrons," NEANDC Specialists' Mtg. on Yields and Decay Data of Fission Product Nuclides, Brookhaven National Laboratory, Upton, New York, October 24-29, 1983 (BNL-51778), 449-453.

D. D. Clark, T.-R. Yeh, C.-H. Lee, L.-J. Yuan, M. Shmid, R. L. Gill, and R. E. Chrien, "Beta-Delayed Neutron Spectra From $^{93-97}$Rb and $^{143-146}$Cs," NEANDC Specialists' Mtg. on Yields and Decay Data of Fission Product Nuclides, Brookhaven National Laboratory, Upton, New York, October 24-29, 1983 (BNL-51778), 455-457.

G. P. Couchell, W. A. Schier, D. J. Pullen, L. Fisteag, M. H. Haghighi, Q. Sharfuddin, and R. S. Tanczyn, "Composite Delayed Neutron Spectra for Fast Reactor Kinetics," Proc. of the Specialists' Mtg. on Delayed Neutrons, Univ. of Birmingham, Birmingham, England, Sept. 15-19, 1986 (to be published).

G. Couchell, R. Tanczyn, L. Fisteag, M. Haghighi, D. Pullen, W. Schier, and Q. Sharfuddin, "Composite Delayed-Neutron Spectra from ^{235}U," Proc. Int. Conf. Nucl. Data for Basic and Applied Sci., Santa Fe, New Mexico, May 13-17, 1985 (Gordon and Breach Science Pubs., New York), Vol. 1, 707-710.

Samson A. Cox, "Delayed Neutron Data – Review and Evaluation," ANL/NDM-5, April 1974.

J. Crancon, C. Ristori, H. Ohm, W. Rudolph, K.-L. Kratz, and M. Asghar, "Half-Lives and Pn Values of Delayed-Neutron Precursors in the Mass Chains 85-87, 92, 135, 136, and 145," Z. Physik A **287**, 45-50 (1978).

P. del Marmol, M. Neve de Mevergnies, "Investigation of Delayed Neutron Precursors of As, Sb and Ge," J. Inorg. Nucl. Chem. **29**, 273-279 (1967).

P. del Marmol, P. Fettweis, and D. C. Perricos, "On the Delayed Neutron Yields of the Longer-Lived Halogen Precursors in the Thermal Fission of ^{235}U," Radiocheimica Acta **16**, 4-7 (1971).

P. del Marmol and D. C. Perricos, "Identification of ^{88}Se and Search for Delayed Neutron Emission from ^{87}Se and ^{88}Se," J. Inorg. Nucl. Chem. **32**, 705-712 (1970).

P. del Marmol, "Delayed Neutron Precursors," Nuclear Data Tables A **6**, 141-151 (1969).

George W. Eccleston, "Analytical Applications for Delayed Neutrons," NEANDC Specialists' Mtg. on Yields and Decay Data of Fission Product Nuclides, Brookhaven National Laboratory, Upton, New York, October 24-29, 1983 (BNL-51778), 411-422.

G. W. Eccleston and G. L. Woodruff, "Measured Near-Equilibrium Delayed Neutron Spectra Produced by Fast-Neutron-Induced Fission of ^{232}Th, ^{233}U, ^{235}U, ^{238}U and ^{239}Pu," Nucl. Sci. and Eng. **62**, 636-651 (1977).

T. R. England and B. F. Rider, "Status of Fission Yield Evaluations," NEANDC Specialists' Mtg. on Yields and Decay Data of Fission Product Nuclides, Brookhaven National Laboratory, Upton, New York, October 24-29, 1983 (BNL-51778).

T. R. England, W. B. Wilson, R. E. Schenter, and F. M. Mann, "Aggregate Delayed Neutron Intensities and Spectra Using Augmented ENDF/B-V Precursor Data," Nucl. Sci. and Eng. **85**, 139-155 (1983).

T. R. England, M. C. Brady, W. B. Wilson, R. E. Schenter, and F. M. Mann, "Delayed Neutron Spectra and Intensities from Evaluated Precursor Data," Proc. Int. Conf. Nucl. Data for Basic and Applied Sci., Santa Fe, New Mexico, May 13-17, 1985 (Gordon and Breach Science Pubs., New York), Vol. 1, p. 739 (1986).

T. R. England, M. C. Brady, E. D. Arthur, R. J. LaBauve, "Status of Evaluated Precursor and Aggregate Spectra," Presentation at Specialist' Mtg. on Delayed Neutrons, Birmingham, England, September 15-19, 1986 (to be published). (See also Los Alamos informal document LA-UR 86-2983.)

T. R. England, M. C. Brady, E. D. Arthur, R. J. LaBauve, and F. M. Mann, "Evaluated Delayed Neutron Precursor Data," Trans. Am. Nucl. Soc. **54**, 350-352 (1987). (See also Los Alamos informal document LA-UR 87-49.)

T. R. England, R. E. Schenter and F. Schmittroth, "Delayed Neutron Calculations using ENDF/B-V Data," Proc. of the ANS/APS International Conference on Nuclear Cross Sections for Technology, Knoxville, Tenn. (Oct. 22-26, 1979).

T. R. England, W. B. Wilson, R. E. Schenter, and F. Mann, "Delayed Neutron Spectral Calculations Using Augmented ENDF/B-V Data," Trans. Am. Nucl. Soc. **41**, 567 (June 1982).

T. R. England, W. B. Wilson, R. E. Schenter, F. M. Mann, "Aggregate Delayed Neutrons and Spectral Calculations Using Preliminary Precursor Data Evaluated for Inclusion in ENDF/B-VI," invited paper, American Chemical Society Symposium on Beta-Delayed Neutron Emission, Las Vegas, Nevada, (March 31), 1982). [See also Los Alamos informal document LA-UR-82-84(Rev.).]

G. Engler and E. Ne'eman, "Delayed Neutron Emission Probabilities and Half-Lives of Rb, Sr, Y, In, Cs, Ba, and La Precursors with A=93-98, A=127-131 and A=142-148," Nucl. Phys. A **367**, 29-40 (1981).

A. E. Evans, M. M. Thorpe, and M. S. Krick, "Revised Delayed-Neutron Yield Data," Nucl. Sci. and Eng. **50**, 80-82 (1973).

A. E. Evans and M. S. Krick, "Equilibrium Delayed Neutron Spectra from Fast Fission of ^{235}U, ^{238}U, and ^{239}Pu," Nucl. Sci. and Eng., **62**, 562-659 (1977).

Robley D. Evans, *The Atomic Nucleus*, McGraw Hill Book Co., Inc. (1955), Chapter 11.

G. T. Ewan, P. Hoff, B. Jonson, K.-L. Kratz, P. O. Larson, G. Nyman, H. L. Ravin, and W. Ziegert, "Intense Mass-Separated Beams of Halogens and Beta-Delayed Neutron Emission from Heavy Bromine Isotopes," Z. Phys. A **318**, 309-314 (1984).

E. Feenberg and G. Trigg, "The Interpretation of Comparative Half-Lives in the Fermi Theory of Beta Decay," Rev. Mod. Phys. **22**, 399-406 (1950).

G. Fieg, "Measurements of Delayed Fission Neutron Spectra of ^{235}U, ^{238}U, and ^{239}Pu with Proton Recoil Proportional Counters," J. Nucl. Energy **26**, 585-592 (1972).

H. Franz, W. Rudolph, H. Ohm, K.-L. Kratz, G. Herrmann, F. M. Nuh, D. R. Slaughter, and S. G. Prussin, "Delayed-Neutron Spectroscopy with He-3 Spectrometers," Nucl. Instr. and Meth. **144**, 253-261 (1977).

H. Franz, J. -V. Kratz, K. -L. Kratz, W. Rudolph, and G. Herrmann, "Delayed-Neutron Spectra Following Decay of ^{85}As and ^{135}Sb," Phys. Rev. Lett. **33**, 14, 859 (1974).

H. Gabelmann, J. Munzel, B. Pfeiffer, G. I. Crawford, H. Wollnik, and K. -L. Kratz, "Pn-values of Short-Lived Sr, Y, Ba, and La Precursors," Z. Phys. A. **308**, 359-360 (1982).

O. K. Gjotterud, P. Hoff, and A. C. Pappas, "Detailed Structure of Delayed Neutron Spectra," Nucl. Phys. A **303**, 295-312 (1978).

O. K. Gjotterud, P. Hoff, and A. C. Pappas, "Gross Properties of Delayed Neutron Spectra," Nucl. Phys. A **303**, 281-294 (1978).

Patrick J. Grant and Gene L. Woodruff, "Near-Equilibrium Measurements of Delayed Neutron Spectra from Fast Fission of ^{240}Pu," Nucl. Sci. and Eng. **76**, 56-62 (1980).

R. C. Greenwood and A. J. Caffrey, "Delayed-Neutron Energy Spectra of $^{93-97}$Rb and $^{143-145}$Cs," Nucl. Sci. and Eng. **91**, 305-323 (1985).

R. C. Greenwood and A. J. Caffrey, "Measuring Delayed Neutron Spectra-A Comparison of Techniques," NEANDC Specialists' Mtg. on Yields and Decay Data of Fission Product Nuclides, Brookhaven National Laboratory, Upton, New York, October 24-29, 1983 (BNL-51778), 365-393.

Ph. Hammer, "Review of the Requirements of Delayed Neutron Data for the Design, Operation, Dynamics and Safety of Fast Breeder and Thermal Power Reactors," Proc. Consultants' Mtg. on Delayed Neutron Properties, Vienna, Austria, March 26-30, 1979 [International Atomic Energy Agency report INDC NDS-107/G+Special (1979)], p. 1.

P. G. Hansen and B. Jonson, "Beta-Delayed Particle Emission from Neutron-Rich Nuclei," CERN-EP/87-44, 26 February 1987 (Contribution prepared for the book 'Particle Emission from Nuclei," Eds., M. Ivasen and D. Poenaru (to be published by the CRC Press).

D. J. Hughes, J. Dabbs, A. Cahn, and D. Hall, "Delayed Neutrons from Fission of ^{235}U," Phys. Rev. **73**, 111-124 (1948).

T. Izak-Biran and S. Amiel, "Reevaluation of the Emission Probabilities of Delayed Neutrons from Fission Products," Nucl. Sci. and Eng. **57**, 117-121 (1975).

K. (Aleklett) Johansson, G. Nyman, and G. Rudstam, "Beta-Decay Properties of Strongly Neutron-Rich Nuclei," Nucl. Phys. A **246**, 425-444 (1975).

G. R. Keepin, T. F. Wimett, and R. K. Zeigler, "Delayed Neutrons from Fissionable Isotopes of Uranium, Plutonium, and Thorium," Phys. Rev. **107**, 1044, 1049 (1957).

G. R. Keepin, T. F. Wimett, and R. K. Zeigler, "Delayed Neutrons from Fissionable Isotopes of Uranium, Plutonium, and Thorium," J. Nucl. Energy **6**, 1-21 (1957).

G. R. Keepin, "Delayed Neutrons," Progress in Nucl. Energy **1**, 191-225 (1956).

G. R. Keepin, *Physics of Nuclear Kinetics*, Addison-Wesley Publishing Co., Reading, Massachusetts (1965), Chapter 4.

G. R. Keepin, "Interpretation of Delayed Neutron Phenomena," J. Nucl. Energy **7**, 13-34 (1958).

G. R. Keepin, "Prediction of Delayed Neutron Precursors," Phys. Rev. **106**, 1359-1360 (1957).

H. V. Klapdor, "Beta Decay Far From Stability and Its Role in Nuclear Physics and Astrophysics," presented at the International School-Seminar on Heavy Ion Physics, Alushta, Crimea, USSR, 14-21 April 1983.

H. V. Klapdor, "Beta Decay Calculations and their Applications in Nuclear Technology and Astrophysics," KTG/ENS-International State of the Art Seminar on Nuclear Data, Cross Section Libraries and their Application in Nuclear Technology, October 1-2, 1985, Wissenschaftszentrum, Boon.

E. J. Konopinski, "Beta-Decay," Rev. Mod. Phys. **15**, 209-245 (1943).

J. -V. Kratz, H. Franz, and G. Herrmann, "Delayed-Neutrons from Arsenic Isotopes ^{84}As, ^{85}As, and ^{86}As," J. Inorg. Nucl. Chem. **35**, 1407-1417 (1973).

J. -V. Kratz and G. Herrmann, "Half-lives, Fission Yields, and Neutron Emission Probabilities of ^{87}Se and ^{88}Se, and Evidence for ^{87}As," J. Inorg. Nucl. Chem. **32**, 3713-3723 (1970).

K. -L. Kratz, W. Rudolph, H. Ohm, H. Franz, M. Zendel, G. Herrmann, S. G. Prussin, F. M. Nuh, A. A. Shihab-Eldin, D. R. Slaughter, W. Halverson, and H. V. Klapdor, "Investigation of Beta Strength Functions by Neutron and Gamma-Ray Spectroscopy (I). The Decay of ^{87}Br, ^{137}I, ^{85}As, and ^{135}Sb," Nucl. Phys. A. **317**, 335-362 (1979).

K. -L. Kratz, A. Schroder, H. Ohm, M. Zendel, H. Gabelmann, W. Zeigert, P. Peuser, G. Jung, B. Pfeiffer, K. D. Wunsch, H. Wollnik, C. Ristori, and J.

Crancon, "Beta-Delayed Neutron Emission from $^{93-100}$Rb to Excited States in the Residual Sr Istopes," Z. Phys. A **306**, 239-257 (1982).

K. -L. Kratz and G. Herrmann, "Systematics of Neutron Emission Probabilities from Delayed Neutron Precursors," Z. Physik **363**, 435-442 (1973).

K. -L. Kratz and H. Gabelmann, "Beta-Delayed Neutron Spectra for Application in Reactor Technology, Nuclear Physics and Astrophysics," Proc. Int. Conf. Nucl. Data for Basic and Applied Sci., Santa Fe, New Mexico, May 13-17, 1985 (Gordon and Breach Science Pubs., New York), Vol. 1, 661-672.

K. -L. Kratz, "Review of Delayed Neutron Energy Spectra," Proc. Consultants Mtg. on Delayed Neutron Properties, Vienna, Austria, March 26-30, 1979 [International Atomic Energy Agency report INDC NDS-107/G+Special (1979)].

K. -L. Kratz, "The Beta-Decay of ^{95}Rb and ^{97}Rb," Z. Phys. A **312**, 43-57 (1983).

K. -L. Kratz, W. Rudolph, H. Ohm, H. Franz, G. Herrmann, C. Ristori, J. Crancon, M. Asghar, G. I. Crawford, F. M. Nuh, and S. G. Prussin, "Decay of Individual levels in Delayed Neutron Emitters to Excited States in the Final Nuclei," Phys. Lett. **65B**, 3, 231 (1976).

K. -L. Kratz and G. Herrmann, "Delayed-Neutron Emission from Short-Lived Br and I Isotopes," Nucl. Phys. A **229**, 179-188 (1974).

M. S. Krick and A. E. Evans, "The Measurement of Total Delayed-Neutron Yields as a Function of the Energy of the Neutron Inducing Fission," Nucl. Sci. Eng. **47**, 311-318 (1972).

J. R. Liaw and T. R. England, "Some Integral Tests on ENDF/B-IV Based On Conservation Principles," Proceedings of the "Topical Conference on Advances in Reactor Physics," Gatlinburg, Tenn. April 10-12, 1978.

J. R. Liaw and T. R. England, "Calculations of Delayed-Neutron Yields from ENDF/B-VC," Trans. Am. Nucl. Soc. **28**, 750 (June 1978).

E. Lund, G. Rudstam, K. Aleklett, B. Ekstron, B. Fogelberg, and L. Jacobsen, "A Status Report on Delayed Neutron Branching Ratios of Fission Products and the Delayed Neutron Program at OSIRIS Using the New Ion-Source ANUBIS," Proc. of the Specialists' Mtg on Delayed Neutrons, Univ. of Birmingham, Birmingham, England, Sept. 15-19, 1986 (to be published).

E. Lund, P. Hoff, K. Aleklett, O. Glomset, and G. Rudstam, "Delayed Neutron Emission Probabilities of Gallium, Bromine, Rubidium, Indium, Antimony, Iodine and Cesium Precursors," Z. Phys. A **294**, 233-240 (1980).

B. P. Maksyutenko, "Relative Yields of Delayed Neutrons in Fission of ^{238}U, ^{235}U, and ^{232}Th by Fast Neutrons," J. Exptl. Theoret. Phys., (USSR), 35, 815-816 (1958).

B. P. Maksyutenko, "Absolute Yields of Delayed Neutrons in the Fission of ^{238}U, ^{235}U, and ^{232}Th by Fast Neutrons," Atomnaya Energiya **7**, No. 5, 474-475 (1959).

F. M. Mann, M. Schreiber, R. E. Schenter, and T. R. England, "Evaluation of Delayed-Neutron Emission Probabilities," Nucl. Sci. and Eng. **87**, 418-431 (1984).

F. M. Mann, C. Dunn, and R. E. Schenter, "Beta Decay Properties from a Statistical Model," Trans. Am. Nucl. Soc. **39**, 880-883 (1981).

F. M. Mann, C. Dunn, and R. E. Schenter, "Beta Decay Properties Using a Statistical Model," Phys. Rev. C **25**, 1, 524-526 (1982).

F. M. Mann, "Calculating Beta Decay Properties in the Fission Product Region," NEANDC Specialists' Mgt. on Yields and Decay Data of Fission Product Nuclides, Brookhaven National Laboratory, Upton, New York, October 24-29, 1983 (BNL-51778), 449-453.

F. M. Mann, "1986 Evaluation of Delayed-Neutron Emission Probabilities," Proc. of the Specialists' Mtg. on Delayed Neutrons, Univ. of Birmingham, Birmingham, England, Sept. 15-19, 1986 (to be published).

F. M. Mann, M. Schreiber, R. E. Schenter, and T. R. England, "Compilation of Neutron Precursor Data," Trans. Am. Nucl. Soc. **45**, 704 (Oct.-Nov. 1983).

C. F. Masters, M. M. Thorpe, and D. B. Smith, "The Measurement of Absolute Delayed-Neutron Yields from 3.1- to 14.9-Mev Fission," Nucl. Sci. Eng. **36**, 202-208 (1969).

G. Moscati and J. Goldenberg, "Delayed Neutron Yields in the Photo-fission of ^{238}U and ^{232}Th," Phys. Rev. **126** 3, 1098 (1962).

S. A. Moszkowski, "A Rapid Method for Calculating log(ft) Values of Beta-Transitions," Phys. Rev. **82**, 35-37 (1951).

F. M. Nuh, D. R. Slaughter, S. G. Prussin, H. Ohm, W. Rudolph, and K. -L. Kratz, "Delayed Neutrons and High-Energy Gamma-Rays from Decay of ^{87}Br," Nucl. Phys. A **293**, 410-424 (1977).

H. L. Pai and D. G. Andrews, "The Systematics of the (n,2n) Cross Section (the Csikai-Peto Effect)," Can. J. Phys. **55**, 2145 (1977).

H. L. Pai and D. G. Andrews, "A Simple Formula for Calculation of Prompt Neutron Yield from Spontaneous Fission of Transuranics," Nucl. Sci. and Eng. **76**, 323-330 (1980).

A. C. Pappas and G. Rudstam, "An Approach to the Systematics of Delayed Neutron Precursors," Nucl. Phys. **21**, 353-366 (1960).

A. C. Pappas and T. Sverdrup, "Gross Properties of Delayed Neutron Emission and Beta-Strength Functions," Nucl. Phys. A **188**, 48-64 (1972).

R. T. Perry, W. B. Wilson, T. R. England, and M. C. Brady, "Application of Evaluated Fission-Product Delayed Neutron Precursor Data in Reactor Kinetics Calculations," Proc. Int. Conf. Nucl. Data for Basic and Applied Sci., Santa Fe, New Mexico, May 13-17, 1985 (Gordon and Breach Science Pubs., New York), Vol. 1, 717 (1986).

P. Peuser, H. Otto, M. Weis, G. Nyman, E. Roeckl, J. Bonn, L. von Reisky, and C. Spath, "Half-lives, Neutron Emission Probabilities and Fission Yields of Neutron-Rich Rubidium Isotopes in the Mass Region A=96 to A=100," Z. Phys. A **289**, 219-224 (1979).

P. Reeder, R. Warner, T. Yeh, R. Chrien, R. Gill, M. Shmid, H. Liou, and M. Stelts, "Beta-Delayed Two-Neutron Emission from ^{98}Rb," Phys. Rev. Lett. **47**, 7, 483 (1981).

P. L. Reeder, L. J. Alquist, R. L. Kiefer, F. H. Ruddy, and R. A. Warner, "Energy Spectra of Delayed Neutrons from the Separated Precursors ^{93,94,95}Rubidium and ^{143}Cesium," Nucl. Sci. and Eng. **75**, 140-150 (1980).

P. L. Reeder and R. A. Warner, "Average Energy of Delayed Neutrons from Individual Precursors and Estimation of Equilibrium Spectra," Nucl. Sci. and Eng. **79**, 56-64 (1981).

P. L. Reeder, R. A. Warner, R. Gill, and A. Piotrowski, "Pn Measurements at TRISTAN by a Beta-N Coincidence Technique," Proc. of Specialists' Mtg. on Delayed Neutrons, Univ. of Birmingham, Birmingham, England, Sept. 15-19, 1986 (to be published).

P. L. Reeder and R. A. Warner, "Delayed Neutron Data from TRISTAN," Proc. Int. Conf. Nucl. Data for Basic and Applied Sci., Santa Fe, New Mexico, May 13-17, 1985 (Gordon and Breach Science Pubs., New York), Vol. 1, 701-705.

P. L. Reeder, "Status of and Outstanding Problems in Delayed Neutron Data, Pn Values and Energy Spectra," Proc. of the Conf. on Nuclear Data Evaluation Methods and Procedures, Brookhaven National Laboratory, Upton, New York, September 22-25, 1980 (BNL-NCS-51363).

P. L. Reeder, "Survey of Delayed Neutron Emission Probabilities," NEANDC Specialists' Mtg. on Yields and Decay Data of Fission Product Nuclides,

Brookhaven National Laboratory, Upton, New York, October 24-29, 1983 (BNL-51778), 337-364.

P. L. Reeder and R. A. Warner, "Distribution of Delayed Neutron Yields Versus Proton, Neutron, and Mass Numbers: Application to Proton Pairing in Fission Yields," Nucl. Sci. and Eng. **87**, 181-194 (1984).

P. L. Reeder and R. A. Warner, "Delayed Neutron Precursors at Masses 97-99 and 146-148," Phys. Rev. C **28**, 1740-1751 (1983).

P. L. Reeder, J. F. Wright, and L. J. Alquist, "Delayed-Neutron Emission Probabilities of Separated Isotopes of Br, Rb, I and Cs," Phys. Rev. C **15**, 2108-2118 (1977).

P. L. Reeder, R. A. Warner, R. M. Liebsch, R. L. Gill, and A. Piotrowski, "Delayed Neutron Precursor ^{75}Cu," Phys. Rev. C **31**, 1029-1031 (1985).

C. Ristori, J. Crancon, K. D. Wunsch, G. Jung, R. Decker, and K. -L. Kratz, "Half-lives and Delayed Neutron Emission Probabilities of Short-Lived Rb and Cs Precursors," Z. Phys. A **290**, 311-318 (1979).

R. B. Roberts, L. R. Hofstad, R. C. Meyer, and P. Wang, "The Delayed Neutron Emission which Accompanies Fission of Uranium and Thorium," Phys. Rev. **55**, 664 (1939).

R. B. Roberts, R. C. Meyer, and P. Wang, "Further Observations on the Splitting of Uranium and Thorium," Phys. Rev. **55**, 510-511 (1939).

E. Roeckl, P. F. Dittner, R. Kalpisch, C. Thibault, C. Rigaud, and R. Prieels, "Delayed Neutron Emission from the Decay of Neutron-Rich Rb and Cs Isotopes," Nucl. Phys. A **222**, 621-628 (1974).

W. Rudolph, K. -L. Kratz, and G. Herrmann, "Half-lives, Fission Yields and Neutron Emission Probabilities of Neutron-Rich Antimony Isotopes," J. Inorg. Nucl. Chem. **39**, 753-758 (1977).

W. Rudolph and K. -L. Kratz, "Attempt to Calculation of Delayed Neutrons Emission Probabilities Using Simple Statistical Model Considerations," Z. Physik A **281**, 269-275 (1977).

G. Rudstam and E. Lund, "Energy Spectra of Delayed Neutrons from the Precursors ^{79}(Zn, Ga), ^{80}Ga, ^{81}Ga, ^{94}Rb, ^{95}Rb, ^{129}In, and ^{130}In," Nucl. Sci. and Eng. **64**, 749-760 (1977).

G. Rudstam, "Status of Delayed Neutron Data," Proc. 2nd IAEA Advisory Group Mtg. on Fission Product Nuclear Data, Petten, Netherlands, September 5-9, 1977, Vol. 2, 567.

G. Rudstam, "Six-Group Representation of the Energy Spectra of Delayed Neutrons from Fission," Nucl. Sci. and Eng. **80**, 238-255 (1982).

G. Rudstam and S. Shalev, "Energy Spectra of Delayed Neutrons from Separated Fission Products," Nucl. Phys. A **235**, 397-409 (1974).

G. Rudstam, "Characterization of Delayed-Neutron Spectra," Journal of Radioanalytical Chem. **36**, 591-618 (1977).

G. Rudstam, "The Uncertainty of Neutron Energy Spectra Deduced from Measured Pulse Spectra in a ^{3}He Spectrometer," Nucl. Inst. and Methods **177**, 529-536 (1980).

G. Rudstam, "Review of Delayed Neutron Branching Ratios," Proc. Consultants Mgt. on Delayed Neutron Properties, Vienna, Austria, March 26-30, 1979 [International Atomic Energy Agency report INDC NDS-107/G+Special (1979)], 69.

G. Rudstam, S. Shalev, and O. C. Johnson, "Delayed Neutron Emission from Separated Fission Products," Nucl. Instr. Method **120**, 333-344 (1974).

D. Saphier, D. Ilberg, S. Shalev, and S. Yiftah, "Evaluated Delayed Neutron Spectra and Their Importance in Reactor Calculations," Nucl. Sci. and Eng. **62**, 660-694 (1977).

W. Schier, Q. Sharfuddin, G. Couchell, L. Fisteag, M. Haghighi, D. Pullen, and R. Tanczyn, "Search for Energy Dependence Among Composite Delayed Neutron Spectra of ^{235}U," Proc. Int. Conf. Nucl. Data for Basic and Applied Sci., Santa Fe, New Mexico, May 13-17, 1985 (Gordon and Breach Science Pubs., New York), Vol. 1, 751-754.

H. -D. Schussler and G. Herrmann, "Hauptkomponenten unter den Vorlaufern Verzogerter Neutronen bei der Spaltung von Uran-235 durch thermische Neutronen," Radiochimica Acta **18**, 13-144 (1972).

S. Shalev and G. Rudstam, "Energy Spectra of Delayed Neutrons from Separated Fission Products," Nucl. Phys. A **275**, 76-92 (1977).

S. Shalev and J. M. Cuttler, "The Energy Distribution of Delayed Fission Neutrons," Nucl. Sci. and Eng. **51**, 52-66 (1973).

S. Shalev and G. Rudstam, "Energy Spectra of Delayed Neutrons from Separated Fission Products (I). The Precursors ^{85}As, ^{87}Br, ^{134}Sn, ^{135}Sb, ^{136}Te, and ^{137}I.," Nucl. Phys. A **230**, 153-172 (1974).

S. Shalev and G. Rudstam, "Delayed Neutron Emission from ^{137}I," Phys. Rev. Lett. **28**, 687-690 (1972).

W. R. Sloan and G. L. Woodruff, "Spectrum of Delayed Neutrons from the Thermal Neutron Fission of ^{235}Uranium," Nucl. Sci. and Eng. **55**, 28-40 (1974).

M. G. Stamatelatos and T. R. England, "Accurate Approximations to Average Beta-Particle Energies and Spectra," Nucl. Sci. Eng. **63**, 204-208 (1977).

S. Synetos, J. G. Williams, "Delayed Neutron Yield and Decay Constants for Thermal Neutron-Induced Fission of ^{235}U," Nucl. Energy **22**, 267-274 (1983).

K. Takahashi, "Application of the Gross Theory of Beta-Decay to Delayed Neutron Emissions," Prog. of Theor. Phys. **47**, No. 5 (1972).

K. Takahashi and M. Yamada, "Gross Theory of Nuclear Beta-Decay," Prog. of Theor. Phys. **41**, 1470-1503 (1969).

K. Takahashi, "Gross Theory of First Forbidden Beta-Decay," Prog. of Theor. Phys. **45**, 1466-1492 (1969).

W. L. Talbert, Jr., A. B. Tucker, and G. M. Day, "Delayed Neutron Emission in the Decays of Short-Lived Separated Isotopes of Gaseous Fission Products," Phys. Rev. **177**, 1805-1816 (1969).

R. S. Tanczyn, Q. Sharfuddin, W. A. Schier, D. J. Pullen, M. H. Haghighi, L. Fisteag, and G. P. Couchell, "Composite Delayed Neutron Energy Spectra for Thermal Fission of ^{235}U," Nucl. Sci. and Eng. **94**, 353-364 (1986).

L. Tomlinson and M. H. Hurdus, "Delayed Neutron Precursors - I; Antimony and Arsenic Precursors Separated by Electrolysis," J. Inorg. Nucl. Chem. **30**, 1125-1138 (1968).

L. Tomlinson and M. H. Hurdus, "Delayed Neutron Precursors - III Selenium-87," J. Inorg. Nucl. Chem. **30**, 1995-2002 (1968).

L. Tomlinson, "Delayed Neutron Precursors," Atomic Data and Nuclear Data Tables **12**, 179-194 (1973).

L. Tomlinson and M. H. Hurdus, "A New Antimony Delayed Neutron Precursor," Phys. Lett. **25B**, 9, 545 (1967).

L. Tomlinson, "Theory of Delayed Neutron Physics," United Kingdom Atomic Energy Authority Research Group Report, Chemistry Division, Atomic Energy Research Establishment, Harwell, Berkshire, AERE-R 6596 (1970).

L. Tomlinson and M. H. Hurdus, "Antimony and Arsenic Precursors Separated Chemically," J. Inorg. Nucl. Chem. **30**, 1649-1661 (1968).

L. Tomlinson and M. H. Hurdus, "^{87}Se, ^{88}Se, and ^{89}Se; Half-Lives, Neutron Emission Probabilities and Fission Yields," J. Inorg. Nucl. Chem. **33**, 3609-3620 (1971).

R. J. Tuttle, "Delayed-Neutron Data for Reactor-Physics Analysis," Nucl. Sci. and Eng. **56**, 37-71 (1975).

R. J. Tuttle, "Review of Delayed Neutron Yields in Nuclear Fission," Proc. Consultants' Mtg. on Delayed Neutron Properties, Vienna, Austria, March 26-30, 1979 [International Atomic Energy Agency report INDC NDS-107/G+Special (1979)], p. 29.

R. W. Waldo, R. A. Karam, "Measured Delayed Neutron Yields," Trans. Am. Nucl. Soc. **39**, 879-880 (1982).

R. W. Waldo, R. A. Karam, and R. A. Meyer, "Delayed Neutron Yields: Time Dependent Measurements and a Predictive Model," Phys. Rev. C **23**, 3, 1113-1127 (1981).

J. Walker, D. R. Weaver, J. G. Owen, and S. J. Chilton, "Extended Analysis of Delayed Neutron Spectra from Fast Fission in U-235," Proc. Int. Conf. Nucl. Data for Basic and Applied Sci., Santa Fe, New Mexico, May 13-17, 1985 (Gordon and Breach Science Pubs., New York), Vol. 1, 775-778.

A. H. Wapstra and G. Audi, "The 1983 Atomic Mass Evaluation," Nucl. Phys. A **432**, 1, (1985).

D. R. Weaver, J. G. Owen, and J. Walker, "Delayed Neutron Spectrum Measurements and Covariance Analysis, NEANDC Specialists' Mtg. on Yields and Decay Data of Fission Product Nuclides, Brookhaven National Laboratory, Upton, New York, October 24-29, 1983 (BNL-51778), 459-467.

C. S. Wu, "Recent Investigation of the Shapes of Beta-Ray Spectra," Rev. Mod. Phys. **22**, 386-398 (1950).

T. R. Yeh, D. D. Clark, G. Scharff-Goldhaber, M. Shmid, R. L. Gill, L. Yuan, R. E. Chrien, and A. Evans, "Low Energy Delayed-Neutron Spectra by Time-of-Flight," Bull. Am. Phys. Soc. **27**, 498 (1982).

APPENDIX B

BETA CODE

B.1. ROUTINES OF THE BETA CODE

Brief descriptions of the routines used in the BETA code are given below. The relationships of these routines are also given in Fig. B.1.1.

- BETA (main program) is the driver routine. The BETA code calculates beta decay properties using aveage log ft values. These properties include half-lives for the beta transition; beta, gamma, neutrino, and delayed neutron spectra; and delayed neutron emission probabilities.
  Reads from input unit 5.
  Assigns (opens) output units 2, 3, 6, 7, 12, and 26.
  Calls subroutines INITIAL, DREAD, TGREAD, TRANS, CAL and EOUT.
- INITIAL (subroutine) sets up the energy structure for the delayed neutron spectra (presently 10 keV bins with a maximum energy of 10 MeV). It also determines the coefficients of the Fermi function as described in *NSE* **63** (1977) 204.
- DREAD (subroutine) reads the nuclear level information for each of the daughter states and for each of the granddaughter states. This includes the energy, spin, and parity of each state. It also reads gamma branching information of desired.
  Reads from input unit 5.
  Writes on unit 6.
  Calls subroutines DEFAUL, TBR, and LEVDEN.
- TGREAD (subroutine) reads the gamma transmission coefficients or calculates default values.
  Reads from input unit 5.
  Writes on unit 6.
  Calls subroutines DEFAUL and TGAM.
- TRANS (subroutine) reads or calculates total transmission coefficients.
  Reads from input unit 5.
  Writes on unit 6 and 7.
  Calls subroutines DEFAUL, ONCE, and OPTMOD.

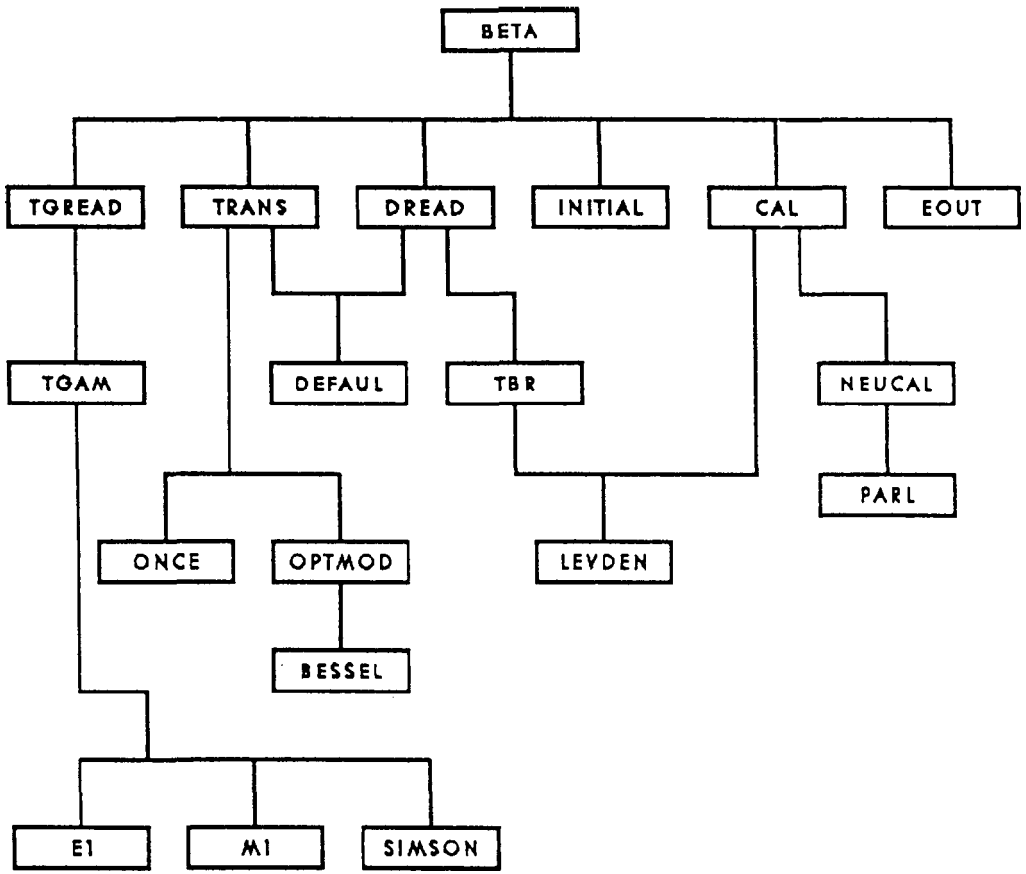

Fig. B.1.1. Subroutine Relationships in the BETA Code.

- CAL (subroutine) provides for the calculation of the beta, gamma, neutrino, and delayed neutron spectra either within itself or via calls to additional subroutines.
  Writes on unit 7.
  Calls subroutines NEUCAL and LEVDEN.
- TGAM (subroutine) calculates gamma transmission coefficients using the Woosley-Holmes model (*Atomic and Nuclear Data Tables* **18**, (1976) 305).
  Writes on units 6 and 7.
  Calls functions E1, M1, and SIMSON.
- E1 (function) returns the E1 form factor for gamma-ray transmission coefficient.
- M1 (function) returns the M1 form factor for gamma-ray transmission coefficient.
- SIMSON (function) is a Romberg integration routine.
- DEFAUL (subroutine) sets potentials and level density parameters to default values and defines various other parameters required to calculate particle transmission coefficients. Reference Gilbert and Cameron [A. Gilbert and A. G. W. Cameron, *Can. J. of Physics*, **43**, 1446 (1965)] for the shell correction and pairing energy parameters; Holmes et al. for the gamma-ray parameters; and Wilmore and Hodgson (*Nucl. Phys.* **55**, (1964) 673) for the neutron potentials and radii.
- ONCE (subroutine) computes potentials once for all energy values.
  Writes on unit 6.
- OPTMOD (subroutine) calculates particle transmission coefficients based on an optical model (uses the integral of the Schrodinger wave equation).
  Calls subroutine BESSEL.
- BESSEL (subroutine) calculates Bessel functions.
- TBR (subroutine) calculates gamma branching using single particle estimates.
  Writes on units 6 and 7.
  Calls subroutine LEVDEN.
- LEVDEN (subroutine) calculates level density using either constant temperature or Fermi formulism. Reference Gilbert and Cameron.

- NEUCAL (subroutine) computes delayed neutron spectra.
  Calls subroutine PARL.
- PARL (subroutine) linearly interpolates in a table.
- EOUT (subroutine) writes final output to units 2, 3, 6, and 26.

B.2. INPUT DESCRIPTION

A description of the input required to execute the BETA code was provided by F. M. Mann. Some corrections were made in the original description. The corrected input requirements are given below.

```
     BETA is a computer code which calculates spectra and other
properties from beta decay.  Although the code can calculate
these properties exactly given the appropiate physics data (energy
levels, log ft values, gamma and neutron transmission propabilities),
the code is normally used to calculate these properties using
statistical considerations.
     The input to the code consists of
1. Title card (20a4)
2. Control card (2i5,5f10.0)
    ns      = number of discrete states in daughter
              (if ns negative, read in gamma branching infomation
              (if ns positive, code will calculate gamma branching)
    nsx     = number of discrete states in delayed neutron granddaughter
    qb      = q value (MeV) from parent to ground state of daughter
    xj      = spin * parity of parent
    esep    = neutron separation energy (MeV) of daughter
    z       = atomic number of parent
    a       = atomic mass of parent
    ft      = average value of log ft
3. Daughter's discrete States (4f10.0) :  repeated ns times
    ed(i)   = energy (MeV) of discrete state
    x       = spin*parity of discrete state
    dft(i)  = log ft value (if 0., default (J,pi dependent) used)
    pgex(i)= 0
4. Daughter's level density (7f10.0,2f5.0)
    xd(1)   = delta of level density formula (MeV)
    xa(1)   = little a parameter of level density formula
    xb(1)   = b parameter in u= a*t**2+b
```

```
    xc(1)  = spincutt off factor
    xex(1) = ex parameter in Gilbert and Cameron formulism
    xe0(1) = e0 parameter in Gilbert and Cameron formulism
    xtt(1) = T parameter in Gilbert and Cameron formulism
    xk(1)  = factor by which formulae are multiplied to get level density
5. Daughter's level density used in for beta transitions (7f10.0,2f5.0)
    xd(3)  = delta of level density formula (MeV)
    xa(3)  = little a parameter of level density formula
    xb(3)  = b parameter in u= a*t**2+b
    xc(3)  = spincutt off factor
    xex(3) = ex parameter in Gilbert and Cameron formulism
    xe0(3) = e0 parameter in Gilbert and Cameron formulism
    xtt(3) = T parameter in Gilbert and Cameron formulism
    xk(1)  = factor by which formulae are multiplied to get level density
6. Granddaughter's discrete states (4F10.0)
    EN(I)  = level energy
    x      = spin and parity
7. Grandaughter's level density (7f10.0,2f5.0)
    xd(2)  = delta of level density formula (MeV)
    xa(2)  = little a parameter of level density formula
    xb(2)  = b parameter in u= a*t**2+b
    xc(2)  = spincutt off factor
    xex(2) = ex parameter in Gilbert and Cameron formulism
    xe0(2) = e0 parameter in Gilbert and Cameron formulism
    xtt(2) = T parameter in Gilbert and Cameron formulism
    xk(2)  = factor by which formulae are multiplied to get level density
8. ENDL signifies end of level information, used as a check
9. Gamma branching information (if ns negative) (8f10.3) : repeat ns times
    (gbr(i,j),j=1,21) = gamma branching from state i to state j
10. Gamma branching information (if ns negative) (8f10.0) : repeat for each
          0.1 MeV from last discrete state to qb
    (gbr(i,j),j=1,21) = gamma branching from state i (in continuum)
                        to state j
```

```
11. Gamma transmission control card (2i5,f10.3)
    ne  = number of energies at which transmission coefficients are given
          (if nge negative, read in values  cards 10-13
           if nge positive, calculate values  cards 14-16)
    nl  = number of coefficients given for each energy and parity, one per J
          (must be less than 8)
    corr = multiplicative correction factor
12. Gamma transmission comments (20a4) : used if nge <0 repeated 4 times
    comment(i) = comments on calculation, usually parameters used
13. Gamma energy (f10.0) : cards 11-13 repeated nge times if nge negative
    tge(i) = energy in compound nucleus (MeV)
14. Positive parity gamma transmission coefficients (8f10.3) : repeated
    (tgamp(i,j),j=1,8) = positive parity gamma transmission coefficients
15. Negative parity gamma transmission coefficients (8f10.3) : repeated
    (tgamn(i,j),j=1,8) = negative parity gamma transmission coefficients
16. Gamma energy (f10.0) : repeated nge times, cards 14-16 used if nge
     positive
    tge(i) = energy in compound nucleus (MeV)
17. gamma parameters (3f10.0)
    smre = fraction of sum rule to be used in E1 calculations
          (if zero, defaults used for all paramters on this card)
    gre  = width of giant dipole rsonance (MeV)
    ere  = energy of giant dipole resonance (MeV)
    dom  = fraction of M1 single particle strngth used
18. gamma parameters (2f10.0)
    ecc  = continuum step size (MeV)
          (if zero, defaults used for all parameters on this card)
    ag   = little a of level density formula
    delg = delta in level density fomula
19. Neutron transmission control card (2i5,f10.3)
    nel  = number of energies at which transmission coefficients are given
          (if nne negative, read in values   cards  19-20
           if nge positive, calculate values cards  21-23  )
```

```
    nl    = number of coefficients given for each energy and oribital
            angular momentum (must be less than 8)
    corr = multiplicative correction factor
20. Neutron transmission comments (20a4) : used if nne< 0 repeated 4 times
    comment(i) = comments on calculation, usually parameters used
21. Neutron energy (f10.0) : cards 19-20 repeated nne times if nne negative
    tge(i) = energy in compound nucleus (MeV)
22. Neutron transmission coefficients, one for each orbital angular
    momentum  (8f10.3) : (tgamp(i,j),j=1,8)
23. Neutron energy (f10.0) : repeated nne times, cards 14-16 used if nne
     positive
    te(i) = energy of incoming neutron (MeV)
24. Neutron parameters (8f10.0)
    vo = depth of real Woods-Saxon potential (MeV)
    dvo = change of depth of real  Woods-Saxonpotential per MeV
    ddvo = second derative of real Woods-Saxon potential per MeV per MeV
    wo = depth of imaginary Woods-Saxon potential (MeV)
    dwo = change of depth of imaginary Woods-Saxon potential per MeV
    ws = depth of imaginary derative Woods-Saxon potential (MeV)
    dws = change of depth of imaginary derative Woods-Saxon potential per MeV
    wgau = depth of imaginary Gaussian potential
25. Neutron parameters (8f10.0)
    ro = coulomb radius (fermis*A**(-1/3) )
    rr = real radius (fermis*A**(-1/3) )
    ri = imaginary radius (fermis*A**(-1/3) )
    ar = real difuseness (fermi)
    ai = imaginary difuseness (fermi)
    rc = shift from surface for Gaussian centroid (fermi)
    ndif = number of difuseness lengths passed real radius at which wave
            functions are matched
    delr = intregration step size (fermi)
26. parameters to repeat calculation (7f10.0) : repeat for each recalculation
    xan  = new xa(3) of card 5
```

```
qbn  = new qb of card 2
elcn = new ed(ns) of card 3
```

B.3. SAMPLE INPUT

The input file used to calculate theoretical delayed neutron spectra for the 34 precursors with experimental data is given below.

```
  ga-79
    3    7    6.7700   -1.5000    5.7400       31.       79.
  0.0            -0.5
   .103           3.5
   .468          -1.5

                .6020
  0.0             0.
   .563           2.
  1.108           2.
  1.410           4.
  1.539           3.
  1.911           0.
  2.020           4.

endl
    3
2.0
4.0
9.0


    8
0.001
0.01
0.1
0.6
1.0
2.0
4.0
10.


  ga-80
    7    3   10.0      -3.0       7.9200       31.       80.
  0.0             0.0
   .56            2.0
  1.11            2.0
  1.41            4.0
  1.54            3.0
  1.91            0.0
  2.02            4.0
```

```
                .6020
  0.0            -0.5
   .103           3.5
   .468          -1.5

endl
    3
2.0
4.0
9.0


    8
0.001
0.01
0.1
0.6
1.0
2.0
4.0
10.


  ga-81
    5    7    8.32     -1.5       4.9900       31.       81.
  0.0              4.5
   .23            -0.5
   .96             1.5
  1.33             2.5
  2.08             2.5

                .6020
  0.0              0.0
   .56             2.0
  1.11             2.0
  1.41             4.0
  1.54             3.0
  1.91             0.0
  2.02             4.0

endl
    3
2.0
4.0
9.0
```

```
    8
0.001
0.01
0.1
0.6
1.0
2.0
4.0
10.


  as-85
    6    9    8.91      -1.5        4.5400        33.        85.
  0.0              2.5
  1.205            0.5
  1.466            2.5
  1.882            3.5
  2.042            1.5
  2.131            4.5

                 .6020
  0.0              0.0
  1.455            2.0
  2.122            2.0
  2.247            0.0
  2.655            0.0
  2.700            2.0
  2.984            2.0
  3.541           -3.0
  3.693            4.0

endl
    3
2.0
4.0
9.0


    8
0.001
0.01
0.1
0.6
1.0
2.0
4.0
10.
```

```
  br-87
    6     4     6.826     -1.5        5.5154        35.        87.
  0.0               2.5
   .531             0.5
  1.466             2.5
  1.882             3.5
  2.042             1.5
  2.131             4.5

                   .6020
  0.0               0.0
  1.565             2.0
  2.249             4.0
  2.350             2.0

endl
    3
2.0
4.0
9.0


    8
0.001
0.01
0.1
0.6
1.0
2.0
4.0
10.


  br-88
    6     6     8.967     -1.0        7.0530        35.        88.
  0.0               0.
   .775             2.
  1.578             2.
  1.644            -3.
  2.11              4.
  2.126             2.

                   .6020
  0.0               2.5
   .531             0.5
  1.466             2.5
```

```
  1.882          3.5
  2.042          1.5
  2.131          4.5

endl
    3
2.0
4.0
9.0


    8
0.001
0.01
0.1
0.6
1.0
2.0
4.0
10.



  br-89
    4    6    8.3      -1.5       5.1100       35.       89.
  0.0            2.5
  1.20           0.5
  1.47           2.5
  1.88           3.5

               .6020
  0.0            0.
   .775          2.
  1.578          2.
  1.644         -3.
  2.11           4.
  2.126          2.

endl
    3
2.0
4.0
9.0


    8
0.001
0.01
0.1
```

```
0.6
1.0
2.0
4.0
10.


  br-90
    6    4   10.7       -0.0        6.3100        35.        90.
  0.0              0.0
   .707            2.
  1.363            2.
  1.654            4.
  2.115           -3.
  2.216            2.

                 .6020
  0.0              2.5
  1.20             0.5
  1.47             2.5
  1.88             3.5

endl
    3
2.0
4.0
9.0


    8
0.001
0.01
0.1
0.6
1.0
2.0
4.0
10.


  br-91
   10    6   11.8       -1.5        4.4930        35.        91.
  0.0              2.5
   .481            1.5
   .658            0.5
   .680            0.5
   .719            1.5
```

```
   .721          2.5
   .888          0.5
  1.024          3.5
  1.093          2.5
  1.117          4.5

                .6020
  0.0           0.0
   .707         2.
  1.363         2.
  1.654         4.
  2.115        -3.
  2.216         2.

endl
    3
2.0
4.0
9.0


    8
0.001
0.01
0.1
0.6
1.0
2.0
4.0
10.



  br-92
    6   10   13.96     -1.0       5.3500       35.       92.
  0.0           0.0
   .956         2.0
  1.363         2.0
  1.654         4.0
  2.115        -3.0
  2.216         2.0

                .6020
  0.0           2.5
   .481         1.5
   .658         0.5
   .680         0.5
   .719         1.5
   .721         2.5
```

```
   .888          0.5
  1.024          3.5
  1.093          2.5
  1.117          4.5

endl
    3
2.0
4.0
9.0


    8
0.001
0.01
0.1
0.6
1.0
2.0
4.0
10.



  rb-92
    4    4    8.12      -1.0        7.3660        37.        92.
  0.0             0.0
   .814           2.
  1.384           2.
  1.778           4.

                .6020
  0.0             2.5
  0.09364         1.5
   .9471          0.5
  1.4254          1.5

endl
    3
2.0
4.0
9.0


    8
0.001
0.01
0.1
0.6
```

```
1.0
2.0
4.0
10.


  rb-93
    5     4    7.442     -1.5        5.2370        37.        93.
  0.0              2.5
   .48             1.5
   .66             0.5
   .68             0.5
   .72             1.5

                .6020
  0.0              0.0
   .814            2.
  1.384            2.
  1.778            4.

endl
    3
2.0
4.0
9.0


    8
0.001
0.01
0.1
0.6
1.0
2.0
4.0
10.


  rb-94
    4     5   10.307     -1.0        6.7860        37.        94.
  0.0              0.0
   .81             2.0
  1.38             2.0
  1.78             4.0

                .6020
  0.0              2.5
```

```
   .48            1.5
   .66            0.5
   .68            0.5
   .72            1.5

endl
    3
2.0
4.0
9.0


    8
0.001
0.01
0.1
0.6
1.0
2.0
4.0
10.


   rb-95
     7     4     9.282     -1.5        4.3300        37.        95.
   0.0              0.5
    .10             2.5
    .24             3.5
    .35             1.5
    .53             0.5
    .55             1.5
    .62             2.5

                   .6020
    0.0             0.0
     .81            2.0
    1.38            2.0
    1.78            4.0

   endl
       3
   2.0
   4.0
   9.0


       8
   0.001
```

```
0.01
0.1
0.6
1.0
2.0
4.0
10.


  rb-96
    4    7   11.75      -1.0        5.8600        37.        96.
  0.0              0.0
   .81             2.0
  1.38             2.0
  1.78             4.0

                 .6020
  0.0              0.5
   .10             2.5
   .24             3.5
   .35             1.5
   .53             0.5
   .55             1.5
   .62             2.5

endl
    3
2.0
4.0
9.0


    8
0.001
0.01
0.1
0.6
1.0
2.0
4.0
10.


  rb-97
    8    4   10.52      -1.5        3.9800        37.        97.
  0.0              0.5
   .06             1.5
```

```
   .24          1.5
   .26          3.5
   .28         -5.5
   .29          1.5
   .31          2.5
   .35          0.5

               .6020
  0.0           0.0
   .81          2.0
  1.38          2.0
  1.78          4.0

endl
    3
2.0
4.0
9.0


    8
0.001
0.01
0.1
0.6
1.0
2.0
4.0
10.


  rb-98
    4    8    12.43    -1.0       5.7600       37.       98.
  0.0           0.0
   .81          2.0
  1.38          2.0
  1.78          4.0

               .6020
  0.0           0.5
   .06          1.5
   .24          1.5
   .26          3.5
   .28         -5.5
   .29          1.5
   .31          2.5
   .35          0.5
```

```
endl
    3
2.0
4.0
9.0


    8
0.001
0.01
0.1
0.6
1.0
2.0
4.0
10.



  in-129
    8     6     7.6000    -0.5000     5.390         49.       129.
  0.0              0.
  1.15             2.
  2.05            -5.
  2.17             6.
  2.22            -7.
  2.38             2.
  2.72            -3.
  2.89            -5.

               0.6020
  0.0              1.5
   .035           -5.5
   .315            0.5
   .53             2.5
   .68             1.5
   .74            -3.5

endl
    3
2.0
4.0
9.0


    8
0.001
0.010
0.1
```

```
0.6
1.0
2.0
4.0
10.


  in-130
    8     6   10.2       -1.0        7.6300        49.       130.
  0.0              0.
  1.15             2.
  2.05            -5.
  2.17             6.
  2.22            -7.
  2.38             2.
  2.72            -3.
  2.89            -5.

                 .6020
  0.0              1.5
    .035          -5.5
    .315           0.5
    .53            2.5
    .68            1.5
    .74           -3.5

endl
    3
2.0
4.0
9.0


    8
0.001
0.01
0.1
0.6
1.0
2.0
4.0
10.


  sn-134
    2     8     6.925      0.0        3.0910        50.       134.
  0.0              0.0
```

```
  0.01            0.0

                .6020
  0.0             3.5
   .33            2.5
   .64            1.5
   .92            0.5
  1.07            4.5
  1.09            5.5
  1.35            3.5
  1.42            4.5

endl
    3
2.0
4.0
9.0


    8
0.001
0.01
0.1
0.6
1.0
2.0
4.0
10.


  sb-135
    5    7    7.54      3.5       3.5100       51.      135.
  0.0             -3.5
   .60            -2.5
   .91            -0.5
  1.12            -4.5
  1.20            -2.5

                .6020
  0.0             0.
  1.279           2.
  1.576           4.
  1.691           6.
  2.4             6.
  1.92           -7.
  2.05           -5.

endl
```

```
    3
2.0
4.0
9.0


    8
0.001
0.01
0.1
0.6
1.0
2.0
4.0
10.


  te-136
    9    7    5.1       0.0       3.7600       52.       136.
  0.0            -2.0
  0.087          -2.0
   .150          -6.0
   .223          -3.0
   .333          -1.0
   .578          -2.0
   .630          -1.0
   .738          -2.0
  2.656           1.0

                .6020
  0.0            3.5
   .15           2.5
   .49           1.5
   .60           2.5
   .77           5.5
   .85           4.5
   .88           0.5

endl
    3
2.0
4.0
9.0


    8
0.001
0.01
```

```
0.1
0.6
1.0
2.0
4.0
10.



   i-137
     5     8     5.885      3.5        4.0255        53.       137.
  0.0              -3.5
   .601            -1.5
   .91             -0.5
  1.12             -4.5
  1.20             -2.5

                  .6020
  0.0               0.0
  1.313             2.0
  1.694             4.0
  1.892             6.0
  2.126             4.0
  2.262             6.0
  2.289             2.0
  2.414             2.0

endl
    3
2.0
4.0
9.0


    8
0.001
0.01
0.1
0.6
1.0
2.0
4.0
10.



   i-138
     4     5     7.82      -0.0        5.8200        53.       138.
  0.0               0.
```

```
   .589          2.
  1.073          4.
  1.464          2.

               .6020
  0.0          -3.5
   .601        -1.5
   .91         -0.5
  1.12         -4.5
  1.20         -2.5

endl
    3
2.0
4.0
9.0


    8
0.001
0.01
0.1
0.6
1.0
2.0
4.0
10.


   i-139
    4    4    6.82      3.5       3.6400       53.      139.
  0.0           -3.5
  0.03          -1.5
   .07          -2.5
   .50          -1.5

               .6020
  0.0           0.
   .589         2.
  1.073         4.
  1.464         2.

endl
    3
2.0
4.0
9.0
```

```
    8
0.001
0.01
0.1
0.6
1.0
2.0
4.0
10.



   i-140
    3    4    9.967    -0.0       5.3920       53.      140.
  0.0            0.0
   .377          2.0
   .835          4.0

                .6020
  0.0           -3.5
  0.0           -1.5
   .07          -2.5
   .50          -1.5

endl
    3
2.0
4.0
9.0


    8
0.001
0.01
0.1
0.6
1.0
2.0
4.0
10.



   i-141
   10    3    8.892     3.5       3.4170       53.      141.
  0.0            -2.5
   .050          -3.5
   .128          -2.5
```

```
   .190          -4.5
   .215          -0.5
   .315          -1.5
   .463          -1.5
   .516          -2.5
   .575          -3.5
   .605          -0.5

                .6020
  0.0             0.0
   .377           2.0
   .835           4.0

endl
    3
2.0
4.0
9.0


    8
0.001
0.01
0.1
0.6
1.0
2.0
4.0
10.



  cs-141
    2    8    5.2560    3.5000    4.5480       55.       141.
  0.0            -1.5
  0.049          -2.5

                0.6020
  0.0              0.
  0.602            2.
  1.130            4.
  1.510            2.
  1.802           -3.
  1.823            0.
  1.951            3.
  1.994            2.

endl
    3
```

```
2.0
4.0
9.0


    8
0.001
0.010
0.1
0.6
1.0
2.0
4.0
10.


  cs-142
    5     2    7.32        1.0        6.2100        55.        142.
  0.0               0.
   .360             2.
   .835             4.
  1.326             2.
  1.467             6.

                  .6020
 -0.0               -1.5
   .049             -2.5

endl
    3
2.0
4.0
9.0


    8
0.001
0.01
0.1
0.6
1.0
2.0
4.0
10.


  cs-143
```

```
  10     5    6.28       3.5        4.2400        55.       143.
 0.0              -2.5
  .050            -3.5
  .128            -2.5
  .190            -4.5
  .215            -0.5
  .315            -1.5
  .463            -1.5
  .516            -2.5
  .575            -3.5
  .604            -0.5

                .6020
 0.0              0.
  .360            2.
  .835            4.
 1.326            2.
 1.467            6.

endl
    3
2.0
4.0
9.0


    8
0.001
0.01
0.1
0.6
1.0
2.0
4.0
10.


 cs-144
   3   10    8.46      -1.0        5.8700        55.       144.
 0.0              0.0
  .199            2.0
  .530            4.0

                .6020
 0.0              -2.5
  .050            -3.5
  .128            -2.5
  .190            -4.5
```

```
   .215          -0.5
   .315          -1.5
   .463          -1.5
   .516          -2.5
   .575          -3.5
   .604          -0.5

endl
    3
2.0
4.0
9.0


    8
0.001
0.01
0.1
0.6
1.0
2.0
4.0
10.


  cs-145
    7    3    7.8000    3.5000    4.2400       55.       145.
  0.0            -2.5
  0.11           -3.5
  0.14           -2.5
  0.17           -1.5
  0.22           -4.5
  0.26           -1.5
  0.27            4.5

               0.6020
  0.0             0.0
  0.199           2.0
  0.530           4.0

endl
    3
2.0
4.0
9.0


    8
```

```
0.001
0.010
0.1
0.6
1.0
2.0
4.0
10.


  cs-146
    4    7    9.4100   -2.0000    5.1300       55.      146.
  0.0             0.
  0.36            2.
  0.83            4.
  1.32            2.

                0.6020
  0.0             -2.5
  0.11            -3.5
  0.14            -2.5
  0.17            -1.5
  0.22            -4.5
  0.26            -1.5
  0.27             4.5

endl
    3
2.0
4.0
9.0


    8
0.001
0.010
0.1
0.6
1.0
2.0
4.0
10.


  cs-147
    4    8    8.8800    3.5000    4.240        55.      147.
  0.0             0.
```

```
   .36            2.
   .83            4.
  1.32            2.

                0.6020
  0.0             1.5
   .008           2.5
   .036          -1.5
   .054           3.5
   .07            4.5
   .091          -2.5
   .10           -5.5
  1.7            -1.5

endl
    3
2.0
4.0
9.0


    8
0.001
0.010
0.1
0.6
1.0
2.0
4.0
10.
```

APPENDIX C

DELAYED NEUTRON EMISSION PROBABILITIES

TABLE C-I

Measurements of Delayed Neutron Emission Probability
(Some values have been renormalized using current data.)

Precursor	Original P_n	ΔP_n	Reference	Normalization	Notes
29-Cu-75	* 3.500E−02	0.600E−02	SOLAR-85		
31-Ga-79	* 9.800E−04	1.000E−04	OSRIS-80		
	* 5.500E−04	1.200E−04	SOLAR-86		
31-Ga-80	* 8.400E−03	6.000E−04	OSRIS-80		
	* 6.900E−03	1.600E−03	SOLAR-86		
31-Ga-81	* 1.200E−01	9.000E−03	OSRIS-80		
	* 1.170E−01	0.120E−01	SOLAR-86		
31-Ga-82	* 2.140E−01	2.200E−02	OSRIS-80		
	* 2.090E−01	0.220E−01	SOLAR-86		
31-Ga-83	* 4.300E−01	7.000E−02	OSRIS-80		
	* 6.280E−01	0.630E−01	SOLAR-86		
33-As-84	* 2.000E−02	1.000E−02	MAINZ-73	N/F	(0.13±0.06)
33-As-85	* 9.700E+00	0.800E+00	HARWE-68	N/F	
	* 2.640E+00	0.980E+00	LOHEN-78	N/F	(22±8)
	* 7.800E+00	1.200E+00	MAINZ-73	N/F	
33-As-86	* 4.725E−01	1.233E−01	LOHEN-78	N/F	(10.5±2.2)
	* 0.570E+00	0.200E+00	MAINZ-73	N/F	
33-As-87	* 6.952E−01	3.120E−01	LOHEN-78	N/F	(44±14)
34-Se-87	* 1.600E−03	3.000E−04	HARWE-71		(5.41)Br87 (55.65s,2.3±0.4)
	* 2.500E−03	6.000E−04	MAINZ-70		(.85)Br87 (s,2.4±0.1)
	* 2.300E−03	7.000E−04	MOL-70		(5.8s) Br87 (55.65s,2.62±0.05)
34-Se-88	* 7.500E−03	6.000E−04	HARWE-71		(1.53)Br88 (15.85s,4.7±0.4)
	* 1.540E−03	9.000E−04	MAINZ-70		(1.4s)Br88 (s,4.0±0.5)
34-Se-89	* 5.000E−02	1.500E−02	HARWE-71		(0.41)Br89 (4.45s,8.8±0.9)

TABLE C-I (Continued)

Precursor	Original P_n	Original ΔP_n	Reference	Normalization	Notes
35-Br-87	* 5.100E+00	8.000E−01	MAINZ-72	N/F	
	* 5.500E+00	1.100E+00	MAINZ-74	N/F	(2.3±0.5)
	* 2.100E−02	3.000E−03	MOL-71		(gamma)
	* 5.800E+00	4.000E−01	MOL-71	N/F	
	* 2.570E−02	1.500E−03	OSRIS-80		
	* 2.500E−02	3.000E−03	SOLAR-77		
	a 3.100E−02	6.000E−03	RUSSI-64		
35-Br-88	* 1.210E+01	1.200E+00	MAINZ-72	N/F	
	* 9.900E+00	1.400E+00	MOL-71	N/F	
	* 6.600E−02	4.000E−03	OSRIS-80		
	a 6.000E−02	1.300E−02	RUSSI-64		
	* 7.400E−02	5.000E−03	SOLAR-77		
35-Br-89	* 1.700E+01	3.000E+00	MAINZ-72	N/F	
	* 1.640E+01	2.400E+00	MAINZ-74	N/F	(6.2±1.4)
	* 1.420E−01	8.000E−03	OSRI-80A		
	* 1.390E−01	9.000E−03	OSRIS-80		
	a 7.000E−02	2.000E−02	RUSSI-64		
	* 1.690E−01	1.700E−02	SOLAR-77		
35-Br-90	* 2.260E−01	3.100E−02	LOHEN-75		
	* 1.600E+01	3.000E+00	MAINZ-72	N/F	
	* 1.060E+01	2.200E+00	MAINZ-74	N/F	(7.8±1.8)
	* 2.460E−01	1.700E−02	OSRI-80A		
35-Br-91	* 9.860E−02	1.970E−02	LOHEN-75		
	* 2.900E+00	1.400E+00	MAINZ-72	N/F	
	* 3.000E+00	6.000E−01	MAINZ-74	N/F	(8.3±2.5)
	* 1.920E−01	1.300E−02	OSRI-80A		
35-Br-92	* 9.450E−02	4.784E−02	LOHEN-78	N/F	(21±8)
	* 1.000E+00	0.400E+00	MAINZ-74	N/F	(16±7)
36-Kr-92	* 3.230E−04	2.600E−05	ARIEL-75		
	* 4.000E−04	7.000E−05	TRIST-69		
36-Kr-93	* 1.920E−02	1.400E−03	ARIEL-75		
	* 1.900E−02	2.000E−03	LOHEN-75		
	* 2.600E−02	5.000E−03	TRIST-69		
36-Kr-94	* 5.700E−02	2.200E−02	LOHEN-75		

TABLE C-I (Continued)

Precursor	Original P_n	ΔP_n	Reference	Normalization	Notes
37-Rb-92	* 1.250E−04	1.500E−05	ARIEL-75		
	* 1.090E−04	1.200E−05	OSRIS-80		
	* 1.200E−04	2.000E−05	SOLAR-77		
	a 9.800E−05	3.000E−06	SOLAR-80		
	* 1.200E−04	4.000E−05	TRIST-69		
37-Rb-93	* 1.164E−02	8.100E−04	ARIEL-75		
	* 1.200E−02	1.000E−03	LOHEN-75		
	* 6.300E+00	1.800E+00	MAINZ-72	N/F	
	* 1.430E−02	1.800E−03	ORSAY-69		
	* 1.240E−02	1.400E−03	ORSAY-74		
	* 1.400E−02	8.000E−04	OSRIS-80		
	* 1.860E−02	1.300E−03	SOLAR-77		
	a 1.360E−02	4.000E−04	SOLAR-80		
	* 1.970E−02	2.200E−03	SOLIS-81		
	* 1.650E−02	3.000E−03	TRIST-69		
37-Rb-94	* 1.670E+01	2.600E+00	MAINZ-72	N/F	
	* 1.125E−01	1.460E−02	ORSAY-69		
	* 8.460E−02	9.200E−03	ORSAY-74		
	* 1.010E−01	6.000E−03	OSRIS-80		
	* 9.700E−02	5.000E−03	OSTIS-79		
	a 1.010E−01	2.000E−03	SOLAR-80		
	* 1.110E−01	9.000E−03	SOLIS-81		
	* 1.370E−01	1.000E−02	SOLAR-77		
37-Rb-95	* 8.400E−02	5.000E−03	LOHEN-75		
	* 7.100E−02	9.300E−03	ORSAY-69		
	* 8.540E−02	9.100E−03	ORSAY-74		
	* 8.900E−02	6.000E−03	OSRIS-80		
	* 8.600E−02	5.000E−03	OSTIS-79		
	* 1.100E−01	8.000E−03	SOLAR-77		
	a 8.710E−02	9.000E−04	SOLAR-80		
	* 9.000E−02	1.100E−02	SOLAR-86		
	* 8.200E−02	8.000E−03	SOLIS-81		
37-Rb-96	* 1.270E−01	1.500E−02	ORSAY-69		
	* 1.300E−01	1.400E−02	ORSAY-74		
	* 1.350E−01	9.000E−03	OSRIS-80		
	* 1.250E−01	9.000E−03	OSTIS-79		
	* 1.760E−01	1.200E−02	SOLAR-77		

TABLE C-I (Continued)

Precursor	Original P_n	ΔP_n	Reference	Normalization	Notes
	a 1.450E−01	3.000E−03	SOLAR-80		
	* 1.420E−01	1.200E−02	SOLIS-81		
37-Rb-97	* 2.720E−01	3.000E−02	ORSAY-74		
	* 2.520E−01	1.800E−02	OSTIS-79		
	* 3.590E−01	2.600E−02	SOLAR-77		
	a 2.790E−01	1.100E−02	SOLAR-80		
	* 2.610E−01	0.540E−01	SOLAR-86		
	* 2.150E−01	2.500E−02	SOLIS-81		
37-Rb-98	* 1.330E−01	2.100E−02	ORSAY-74		
	* 1.840E−01	2.900E−02	OSTIS-79		
	a 1.280E−01	5.000E−03	SOLAR-80		
	* 1.670E−01	1.600E−02	SOLIS-81		
37-Rb-99	* 1.500E−01	3.000E−02	MAINZ-79		norm to Rb98 (13.3±2.1)
	* 2.070E−01	0.230E−01	SOLAR-86		
37-Rb-100	* 5.000E−02	1.000E−02	SOLAR-86		
38-Sr-97	* 5.000E−05	2.000E−05	OSTIS-82		
	* <2.000E−04		SOLAR-83		
	*<45.000E−04		SOLAR-86		LIMIT
	* 2.700E−03	9.000E−04	SOLIS-81		DE×100
38-Sr-98	* 8.000E−03	2.000E−03	OSTIS-82		
	* 1.800E−03	2.000E−04	SOLAR-83		DE×10
	* 2.300E−03	0.500E−03	SOLAR-86		
	* 3.600E−03	1.100E−04	SOLIS-81		
38-Sr-99	* 3.400E−02	2.400E−02	LOHEN-75		
	* 3.500E−03	1.500E−03	OSTIS-82		
	* 3.100E−03	1.100E−03	SOLAR-83		
	* 9.300E−04	1.200E−04	SOLAR-86		
38-Sr-100	* 7.500E−03	0.800E−03	SOLAR-86		
38-Sr-101	* 2.490E−02	0.250E−02	SOLAR-86		
38-Sr-102	* 4.800E−02	2.300E−02	SOLAR-86		

TABLE C-I (Continued)

Precursor	Original P_n	ΔP_n	Reference	Normalization	Notes
39-Y-97	* 6.000E−05	1.000E−05	OSTIS-82		(3600ms) DE×10
	* 6.100E−04	7.000E−05	SOLAR-83		(3.72s)
	* 5.400E−04	0.120E−04	SOLAR-86		(3.76s)
	* 6.000E−04	1.000E−04	SOLIS-81		
39-Y-97	** 1.100E−03	3.000E−04	SOLAR-83		(1.19s)
	*<8.000E−04		SOLAR-86		(1.18s) LIMIT
39-Y-98	* 3.000E−03	1.000E−03	OSTIS-82		(655ms)
	* 2.100E−03	4.000E−04	SOLAR-83		(0.51s)
	* 2.300E−03	0.500E−03	SOLAR-86		(0.548s)
39-Y-98	** 3.440E−02	9.500E−03	SOLIS-81		(2.1s)
39-Y-99	* 1.200E−02	8.000E−03	LOHEN-75		
	* 3.000E−02	2.000E−03	OSTIS-82		
	* 9.600E−03	1.500E−03	SOLAR-83		
	* 1.090E−02	0.110E−02	SOLAR-86		
39-Y-100	* 8.500E−03	0.900E−03	SOLAR-86		
39-Y-101	* 2.070E−02	0.210E−02	SOLAR-86		
39-Y-102	* 6.000E−02	1.700E−02	SOLAR-86		
47-Ag-120	a <3.000E−05		SOLA-83A		LIMIT
47-Ag-121	a 7.600E−04	3.000E−05	SOLA-83A		
47-Ag-122	a 1.860E−03	6.000E−05	SOLA-83A		
47-Ag-123	a 5.500E−03	2.000E−04	SOLA-83A		
49-In-127	* 6.800E−03	6.000E−04	OSRIS-80		(3.8s)
	* 5.400E−03	1.100E−03	SOLAR-86		(3.7s)
49-In-127	** <0.0004		OSRIS-80		(1.12s,9/2+)
	* <0.0015		SOLIS-81		(?s,9/2+)
49-In-128	* 3.000E−04	0.700E−04	SOLAR-86		(0.8s)
49-In-128	** 5.900E−04	8.000E−05	OSRIS-80		(0.8s)

TABLE C-I (Continued)

Precursor	Original P_n	ΔP_n	Reference	Normalization	Notes
49-In-129	* 2.500E−02	5.000E−03	OSRIS-80		(1.26s)
	* 2.520E−02	0.520E−02	SOLAR-86		(1.18s)
	* 3.500E−02	5.000E−03	SOLIS-81		(0.84s- poss. 2 isomers)
49-In-129	** 2.500E−03	5.000E−04	OSRIS-80		(0.59s)
	* 1.300E−03	0.300E−03	SOLAR-86		(0.61s)
49-In-130	* 1.400E−02	9.000E−04	OSRIS-80		(0.53s -2 isomers similar t1/2)
	* 1.720E−02	0.180E−02	SOLAR-86		(0.532s)
49-In-130	** 1.400E−02	9.000E−04	OSRIS-80		(0.53s -2 isomers similar t1/2)
	* 0.910E−02	0.100E−02	SOLAR-86		(0.278s)
49-In-131	* 1.700E−02	0.180E−02	SOLAR-86		(0.276s)
	* 5.500E−02	1.900E−02	SOLIS-81		
49-In-131	** 1.720E−02	2.300E−03	OSRIS-80		(0.29s -2 isomers maybe)
49-In-132	* 4.200E−02	9.000E−03	OSRIS-80		(0.22s)
	* 6.800E−02	1.400E−02	SOLAR-86		
51-Sb-134	* 2.800E−02	4.000E−03	HARWE-68	N/F	
	* 1.700E−01	1.300E−01	LOHEN-75		
	* 4.300E−02	6.000E−03	MAINZ-77	N/F	(0.09±0.015)
	* 1.200E−03	8.000E−05	OSRIS-80		
51-Sb-135	* 3.500E+00	3.000E−01	HARWE-68	N/F	
	* 3.600E+00	5.000E−01	HARW-68A	N/F	
	* 3.220E−01	2.693E−02	LOHEN-78	N/F	(14±1)
	* 3.100E+00	3.000E−01	MAINZ-77	N/F	(19.9±2.1)
	* 1.750E−01	2.000E−02	OSRIS-80		
51-Sb-136	* 5.320E−02	3.529E−02	LOHEN-78	N/F	(19±9)
	* 0.700E+00	0.300E+00	MAINZ-77	N/F	(32.±14.)
52-Te-136	* 2.000E−02	1.000E−02	LOHEN-78	136Sb	
	* 7.000E−03	4.000E−03	MAINZ-77		
52-Te-137	* 2.500E−02	5.000E−03	LOHEN-75		
52-Te-138	* 6.300E−02	2.100E−02	LOHEN-75		

TABLE C-I (Continued)

Precursor	Original P_n	Original ΔP_n	Reference	Normalization	Notes
53-I-137	* 6.100E−02	8.000E−03	LOHEN-75		
	b 4.700E−02	1.000E−02	MAINZ-69		(? K.L. Kratz diss.)
	* 2.170E+01	1.900E+00	MAINZ-72	N/F	
	* 8.600E−02	1.200E−02	MOL-71		(gamma)
	* 2.810E+01	2.300E+00	MOL-71	N/F	
	* 6.700E−02	4.000E−03	OSRIS-80		
	a 3.000E−02	5.000E−03	RUSSI-64		DE×10
	* 8.500E−02	9.000E-03	SOLAR-77		
53-I-138	* 2.580E−02	2.200E−03	LOHEN-75		
	* 7.200E+00	1.500E+00	MAINZ-72	N/F	
	* 7.200E+00	1.300E+00	MAINZ-74	N/F	(3.0±0.7)
	* 5.500E−02	4.000E−03	OSRIS-80		
	a 1.900E−02	5.000E−03	RUSSI-64		DE×10
	* 6.000E−02	3.500E−02	SOLAR-77		
53-I-139	* 1.020E−01	9.000E−03	LOHEN-75		
	* 9.300E+00	1.600E+00	MAINZ-72	N/F	
	* 6.300E+00	1.800E+00	MAINZ-74	N/F	(6.5±2.6)
	* 9.500E−02	6.000E−03	OSRI-80A		
	* 9.100E−02	7.000E−03	OSRIS-80		
53-I-140	* 6.500E+00	2.500E+00	MAINZ-72	N/F	
	* 2.800E+00	7.000E−01	MAINZ-74	N/F	(14±5)
	* 9.200E−02	6.000E−03	OSRI-80A		
53-I-141	* 1.200E+00	4.000E−01	MAINZ-74	N/F	(30±17)
	* 2.120E−01	3.000E−02	OSRI-80A		
54-Xe-141	* 4.260E−04	23300E−05	ARIEL-75		
	* 5.400E−04	9.000E−05	TRIST-69		
54-Xe-142	* 4.060E−03	3.400E−04	ARIEL-75		
	* 4.500E−03	8.000E−04	TRIST-69		
55-Cs-141	* 5.290E−04	2.900E−05	ARIEL-75		
	* 2.900E−04	2.000E−05	OSRIS-80		DE×10
	* 4.300E−04	7.000E−05	SOLAR-77		
	a 3.400E−04	3.000E−05	SOLAR-80		
	* 7.300E−04	1.100E−04	TRIST-69		

TABLE C-I (Continued)

Precursor	Original P_n	ΔP_n	Reference	Normalization	Notes
55-Cs-142	* 2.850E−03	2.600E−04	ARIEL-75		DE×10
	* 9.700E−04	7.000E−05	OSRIS-80		
	* 9.600E−04	8.000E−05	SOLAR-77		
	a 1.050E−03	6.000E−05	SOLAR-80		
	* 8.200E−04	8.000E−05	SOLIS-81		
	* 2.700E−03	7.000E−04	TRIST-69		
55-Cs-143	* 1.130E−02	2.500E−03	ORSAY-69		
	* 1.540E−02	9.000E−04	OSRIS-80		
	* 1.740E−02	1.200E−03	OSTIS-79		
	* 1.950E−02	1.400E−03	SOLAR-77		
	a 1.610E−02	3.000E−04	SOLAR-80		
	* 1.900E−02	2.000E−03	SOLIS-81		
55-Cs-144	* 1.100E−02	2.500E−03	ORSAY-69		DE×10
	* 2.790E−02	1.800E−03	OSRIS-80		
	* 2.950E−02	2.500E−03	OSTIS-79		
	* 4.300E−02	3.000E−03	SOLAR-77		
	a 3.120E−02	1.200E−03	SOLAR-80		
	* 4.070E−02	3.200E−03	SOLIS-81		
55-Cs-145	* 2.825E−01	7.748E−02	LOHEN-78	N/F	(12.5±3)
	* 1.210E−01	1.400E−02	ORSAY-74		
	* 1.360E−01	9.000E−03	OSRIS-80		
	* 1.220E−01	9.000E−03	OSTIS-79		
	* 2.180E−01	1.500E−02	SOLAR-77		
	a 1.330E−01	2.700E−02	SOLAR-80		
	* 1.950E−01	1.500E−02	SOLIS-81		
55-Cs-146	* 1.420E−01	1.700E−02	ORSAY-74		
	* 1.320E−01	8.000E−03	OSTIS-79		
	* 1.310E−01	1.300E−02	SOLIS-81		
55-Cs-147	*22.540E−01	3.200E−02	OSTIS-79		
	* 2.640E−01	0.290E−01	SOLAR-86		
55-Cs-148	* 2.510E−01	0.250E−01	SOLAR-86		
56-Ba-146	*<2.000E−04		SOLAR-83		LIMIT

TABLE C-I (Continued)

Precursor	Original P_n	ΔP_n	Reference	Normalization	Notes
56-Ba-147	*<1.000E−05		OSTIS-82		
	* 3.000E−04	1.600E−04	SOLAR-83		
	* 2.100E−04	1.800E−04	SOLAR-86		
	* 5.210E−02	5.200E−03	SOLIS-81		DE×1000
56-Ba-148	*<1.000E−03		OSTIS-82		
	*<3.000E−04		SOLAR-83		LIMIT
	* 5.700E−04	2.000E−04	SOLAR-86		
	* 2.390E−01	2.100E−02	SOLIS-81		DE×1000
56-Ba-149	*5.800E−03	8.000E−04	SOLAR-86		
57-La-146	*<7.000E−5		SOLAR-83		LIMIT
57-La-147	*<1.000E−4		OSTIS-82		
	* 3.300E−04	0.600E−04	SOLAR-83		
	* 4.100E−04	1.700E−04	SOLAR-86		
	* 5.000E−03	1.700E−03	SOLIS-81		DE×10
57-La-148	*<1.000E−03		OSTIS-82		
	* 1.300E−03	1.000E−04	SOLAR-83		
	* 1.430E−03	1.500E−04	SOLAR-86		
57-La-149	* 1.070E−02	1.300E−03	SOLAR-86		

a - indicates F. Man's reference could not be found, but values were checked against those in NSE87 (1984), 418-431.

b - indicates value for this nuclide not found in Mann's reference, but was checked against NSE 1984.

* - indicates value was checked against Mann's reference and corrected if needed.

REFERENCES FOR TABLE C-I

ARIEL-75 Asghar, Crancon, Gautheron, and Ristori; *J. Inorg. and Nucl. Chem.*, **37** (1975) 1563.

HARWE-68 Tomlinson and Hurdus; *J. Inorg. and Nucl. Chem.*, **30** (1968) 1649.

HARW-68A Tomlinson and Hurdus; *J. Inorg. and Nucl. Chem.*, **30** (1968) 1125.

HARWE-71 Tomlinson and Hurdus; *J. Inorg. and Nucl. Chem.*, **33** (1971) 3609.

LOHEN-75 Asghar, Gautheron, Bailleul, Bocquet, Greif, Schrader, Siegert, Ristori, Crancon, and Crawford; *Nucl. Phys.*, **A247** (1975) 359.

LOHEN-78 Crancon, Ristori, Ohm, Rudolph, Kratz, and Asghar; *Z. Phys. A*, **287** (1978) 45.

MAINZ-70 Kratz and Herrmann; *J. Inorg. and Nucl. Chem.*, **32** (1970) 3713.

MAINZ-72 Schussler and Herrmann; *Radiochim Acta*, **18** (1972) 123.

MAINZ-73 Kratz, Franz, and Herrmann; *J. Inorg. and Nucl. Chem.*, **35** (1973) 1407.

MAINZ-74 Kratz and Herrmann; *Nucl. Phys.*, **A229** (1974) 179.

MAINZ-77 Rudolph, Kratz, and Herrmann; *J. Inorg. and Nucl. Chem.*, **39** (1977) 753.

MAINZ-79 Peuser, Otto, Weis, Nyman, Roeckl, Bonn, von Reisky, and Spath; *Z. Physik A*, **289** (1979) 219.

MOL-70 del Marmol and Perricos; *J. Inorg. and Nucl. Chem.*, **32** (1970) 705.

MOL-71 del Marmol, Fettweis, and Perricos; *Radiochimica Acta*, **16** (1971) 4.

ORSAY-69 Amarel, Gauvin, and Johnson; *J. Inorg. and Nucl. Chem.*, **31** (1969) 577.

ORSAY-74 Roeckl, Dittner, Klapisch, Thibault, Rigaud, and Prieels; *Nucl. Phys.*, **A222** (1974) 621.

OSRIS-80 Lund, Hoff, Aleklett, Glomset, and Rudstam; *Z. Phys.*, **A294** (1980) 233.

OSRI-80A Aleklett, Hoff, Lund, and Rudstam; *Z. Phys.*, **A295** (1980) 331.

OSTIS-79 Ristori, Crancon, Wunsch, Jung, Decker, and Kratz; *Z. Phys. A*, **290** (1979) 311.

OSTIS-82 Gabelmann, Munzel, Pfieffer, Crawford, Wollnik, and Kratz *Z. Phys.*, **A308** (1982) 359.

RUSSI-64 Aron, Kostochkin, Petrzhak, and Shpakov; *Soviet J. of Nucl.Phys.*, **16** (1964) 447. ++couldn't find this ref.

SOLIS-81 Engler and Ne'eman; *Nuclear Physics*, **A367** (1981) 29.

SOLAR-77 Reeder, Wright, and Alquist; *Physical Review*, **C15** (1977) 2108.

SOLAR-80 Reeder and Warner; PNL report SA-8766 (1980).

SOLAR-83 Reeder and Warner; *Physical Review*, **C28** (1983) 1740.

SOLA-83A Reeder, Warner, and Gill; PNL report PNL-SA-11, 100 (1983).

SOLAR-85 Reeder, Warner, Liebsch, Gill, and Piotrowski; *Physical Review*, **C31** (1985) 1029.

SOLAR-86 Reeder, Warner, Gill, and Piotrowski, *Proceedings Specialists Mtg. on Delayed Neutrons*, Birmingham, England (1986).

TRIST-69 Talbert, Tucker, and Day; *Physical Review*, **177**, (1969) 1805.

TABLE C-II

Recommended P_n Values

Z	A	$P_n(\%)$	Measurements	Comments
29	75	3.47 ± 0.63 (18)	1	
31	79	0.089 ± 0.020 (22)	2	
31	80	0.83 ± 0.07 (8)	2	
31	81	11.9 ± 0.94 (8)	2	
31	82	21.1 ± 1.83 (9)	2	
31	83	56.2 ± 9.9 (18)	2	
33	84	0.086 ± 0.043 (50)	1	
33	85	[9.30 ± 1.01] (11)	3	(a)
33	86	[0.528 ± 0.100] (19)	2	(a)
33	87	[2.26 ± 1.03] (46)	1	(a)
34	87	0.188 ± 0.021 (11)	3	
34	88	0.966 ± 0.021 (22)	3	
34	89	[7.7 ± 2.4] (31)	1	(a)
35	87	2.54 ± 0.16 (6)	7	
35	88	6.26 ± 0.38 (6)	5	
35	89	14.0 ± 0.84 (6)	6	
35	90	24.6 ± 1.85 (8)	4	
35	91	18.1 ± 1.48 (8)	4	
35	92	[1.14 ± 0.26] (23)	2	(a)
36	92	0.0332 ± 0.0031 (9)	2	
36	93	2.01 ± 0.16 (8)	3	
36	94	6.13 ± 2.41 (39)	1	
37	92	0.0099 ± 0.0005 (5)	5	
37	93	1.35 ± 0.07 (5)	10	
37	94	10.0 ± 0.50 (5)	7	
37	95	8.62 ± 0.42 (5)	8	
37	96	14.0 ± 0.71 (5)	7	
37	97	26.6 ± 1.48 (6)	5	
37	98	13.3 ± 1.20 (9)	4	
37	99	17.1 ± 4.2 (25)	2	
37	100	4.95 ± 1.02 (21)	1	
38	97	0.0054 ± 0.0021 (39)	4	(b)
38	98	0.326 ± 0.034 (10)	4	(b)
38	99	0.129 ± 0.111 (86)	4	(b),(c)
38	100	0.743 ± 0.086 (12)	1	
38	101	2.47 ± 0.28 (11)	1	
38	102	4.76 ± 2.29 (48)	1	
39	97	0.054 ± 0.0028 (5)	4	
39	97*	0.109 ± 0.030 (28)	2	

TABLE C-II (Continued)

	A	P_n(%)	Measurements	Comments
39	98	0.228 ± 0.012 (5)	3	
39	98*	3.41 ± 0.96 (28)	1	
39	99	2.02 ± 1.45 (72)	4	(c)
39	100	0.842 ± 0.099 (12)	1	
39	101	2.05 ± 0.23 (11)	1	
39	102	5.94 ± 1.71 (29)	1	
47	120	less than 0.003	1	
47	121	0.0753 ± 0.0048 (6)	1	
47	122	0.184 ± 0.011 (6)	1	
47	123	0.545 ± 0.034 (6)	1	
49	127	0.66 ± 0.063 (10)	2	
49	128*	0.061 ± 0.037 (62)	3	(c)
49	129	2.92 ± 0.37 (12)	2	
49	129*	0.76 ± 2.50 (328)	2	(c)
49	130	1.04 ± 0.95 (91)	2	(c)
49	130*	1.48 ± 0.105 (7)	2	
49	131	1.84 ± 1.07 (58)	2	(c)
49	131	1.73 ± 0.24 (14)	1	
49	132	5.36 ± 0.83 (15)	2	
50	134	18.3 ± 13.9 (76)	1	
51	134	0.104 ± 0.035 (34)	3	(c)
51	135	17.87 ± 2.16 (12)	5	
51	136	[0.577 ± 0.062] (11)	2	(a)
52	136	1.14 ± 0.43 (38)	2	
52	137	2.69 ± 0.63 (23)	1	
52	138	6.78 ± 2.26 (33)	1	
53	137	6.97 ± 0.42 (6)	8	
53	138	5.38 ± 0.43 (8)	6	
53	139	9.81 ± 0.62 (6)	5	
53	140	9.27 ± 0.79 (9)	3	
53	141	21.3 ± 3.2 (15)	2	
54	141	0.0353 ± 0.0061 (17)	2	
54	142	0.404 ± 0.038 (9)	2	
55	141	0.0474 ± 0.055 (12)	5	(b)
55	142	0.0949 ± 0.094 (10)	6	(b)
55	143	1.60 ± 0.08 (5)	5	
55	144	3.13 ± 0.17 (5)	6	(b)
55	145	13.59 ± 0.90 (7)	7	
55	146	13.3 ± 1.72 (13)	3	

TABLE C-II (Continued)

	A	P_n(%)	Measurements	Comments
55	147	26.1 ± 2.5 (10)	2	
55	148	25.1 ± 2.8 (11)	1	
56	146	less than 0.02	1	
56	147	0.021 ± 0.002 (10)	4	(b)
56	148	0.006 ± 0.002 (34)	4	(b)
56	149	0.575 ± 0.084 (15)	1	
57	146	less than 0.007	1	
57	147	0.033 ± 0.006 (17)	4	(b)
57	148	0.133 ± 0.010 (8)	3	
58	149	1.06 ± 0.14 (13)	1	

(a) Values given as neutron per 10000 fissions.

(b) Dataset contains one or more measurements whose values are more than five standard deviations from the evaluated value. Thus standard deviations were increased by 10 or more.

(c) Reduced X^2 is greater than 3. The standard deviations for the measurements were increased by the reduced X^2..

TABLE C-III

Precursors having significant different values than 1984 evaluation

		P_n (%)	
Z	A	Present Evaluation	1984 Evaluation
29	75	3.47 ± 0.63 (18)	xxxxxxxxxxxxx
37	100	4.95 ± 1.02 (21)	xxxxxxxxxxxxx
38	100	0.743 ± 0.086 (12)	xxxxxxxxxxxxx
38	101	2.47 ± 0.28 (11)	xxxxxxxxxxxxx
38	102	4.76 ± 2.29 (48)	xxxxxxxxxxxxx
39	100	0.842 ± 0.099 (12)	xxxxxxxxxxxxx
39	101	2.05 ± 0.23 (11)	xxxxxxxxxxxxx
39	102	5.94 ± 1.71 (29)	xxxxxxxxxxxxx
49	130	1.04 ± 0.95 (91)	4.4 ± 1.6 (36)
49	131	1.84 ± 1.07 (58)	5.0 ± 1.8 (36)
56	147	0.021 ± 0.002 (10)	0.031 ± 2.17 (700)
56	148	0.006 ± 0.002 (34)	0.055 ± 0.013 (24)
56	149	0.575 ± 0.084 (15)	xxxxxxxxxxxxxx
58	149	1.06 ± 0.14 (13)	xxxxxxxxxxxxxx

Table C-IV

Laboratory Bias Factors

Laboratory	Number of Measurements	(Bias-1.) (%)
ARIEL	8	-2 ± 6
Harwell	6	0 ± 10
LOHENGRIN	17	-7 ± 5
Mainz	30	-4 ± 6
Mol	6	11 ± 7
Orsay-69	6	-3 ± 6
Orsay-74	8	32 ± 9
ORSIS	36	-1 ± 5
OSTIS	20	-2 ± 5
Russia	5	-4 ± 10
SOLAR	63	1 ± 5
SOLIS	19	11 ± 6
TRISTAN	8	18 ± 10

Table C-V

Parameters from the Kratz-Herrmann Equation

Study	a	b
1984	123.4	4.34
present	54.0 (+31, -20)	3.44 ($\pm$0.51)
England	44.08	4.119

APPENDIX D

DELAYED NEUTRON SPECTRA REFERENCES BY NUCLIDE

APPENDIX D

REFERENCES FOR EXPERIMENTAL SPECTRAL DATA

Precursor ID	Half-life (sec)	Energy Window* $(Q_\beta - S(n))$ MeV	Spectra References
^{79}Ga	3.00	1.03(W83)	**Ru81**(^{3}He;0.05-1.1 MeV) Ru77(^{3}He;0.1-1.0 MeV)
^{80}Ga	1.66	2.08(W83)	**Ru81**(^{3}He;0.03-1.06 MeV) Ru77(^{3}He;0.1-0.85 MeV)
^{81}Ga	1.23	3.33(W83)	**Ru81**(^{3}He;0.05-1.69 MeV) Ru77(^{3}He;0.1-1.35 MeV)
^{85}As	2.03	4.37(W83)	**Ru81**(^{3}He;0.07-2.8 MeV)[a] Kr79(^{3}H3;0.07-2.8 MeV) **Fr74a**(^{3}He;0.07-1.6 MeV) see also Sh74, Kr79a
^{87}Br	55.70	1.311(W83)	**Kr83**(^{3}He;0.0-1.3 MeV) **Ru81**(^{3}He;0.0-0.96 MeV) Kr79(^{3}He;0.0-0.81 MeV) Kr79a(^{3}He;0.0-1.3 MeV) Ru74a(^{3}He;0.05-1.3 MeV) Sh74(^{3}He;0.1-1.0 MeV) Fi72(p-recoil;0.1-1.2 MeV)[b] Ch71(TOF;0.05-0.25 MeV)[c] Ba56(^{3}He;0.1-1.2 MeV)[b]
^{88}Br	16.0	1.914(W83)	**Ru81**(^{3}He;0.0-1.8 MeV) Sh77(^{3}He;0.1-1.5 MeV) Ru74a(^{3}He;0.05-1.3 MeV) Ch71(TOF;0.05-0.25 MeV)[c]
^{89}Br	4.38	3.19(W83)	**Kr83**(^{3}He;0.05-2.59 MeV) Ru81(^{3}He;0.08-1.83 MeV) Ru74(^{3}He;0.1-1.6 MeV)
^{90}Br	1.8	4.39(W83)	**Kr83**(^{3}He;0.05-2.83 MeV) Ew84(^{3}He;0.0-2.6 MeV) **Ru81**(^{3}He;0.05-1.88 MeV) Sh77(^{3}He;0.1-1.6 MeV)
^{91}Br	0.6	7.305(MN/W81)	Ew84(^{3}He;0.0-2.9 MeV) **Kr83**(^{3}He;0.05-2.94 MeV) **Ru81**(^{3}He;0.1-1.88 MeV) Ru74(^{3}He;0.1-1.6 MeV)

APPENDIX D (Continued)

Precursor ID	Half-life (sec)	Energy Window* ($Q_\beta - S(n)$) MeV	Spectra References
^{92}Br	0.36	8.613(MN/W81)	Ew84(^{3}He;0.0-3.25 MeV) **Kr83**(^{3}He;0.05-3.0 MeV)
^{92}Rb	4.53	0.754(W83)	**Kr83**(^{3}He;0.0-0.75 MeV) **Ru81**(^{3}He;0.0-1.0 MeV)[a] Kr79(^{3}He;0.0-1.0 MeV)
^{93}Rb	5.86	2.205(W83)	**Gr85**(p-recoil;0.0138-1.262 MeV) **Oh81**(^{3}He;0.0-1.86 MeV)[d] **Ru81**(^{3}He;0.0-1.25 MeV) Re80(^{3}He;0.0-1.4 MeV) Kr79(^{3}He;0.0-1.6 MeV) Ru74(^{3}He;0.1-1.2 MeV)
^{94}Rb	2.76	3.521(W83)	**Gr85**(p-recoil;0.008-1.262 MeV) **Kr83**(^{3}He;0.0-2.46 MeV) Oh81(^{3}He;0.0-1.86 MeV) **Ru81**(^{3}He;0.0-1.5 MeV) Re80(^{3}He;0.0-1.4 MeV) Kr79(^{3}He;0.0-1.6 MeV) Ru77(^{3}He;0.05-1.50 MeV)
^{95}Rb	0.38	4.952(W83)	**Gr85**(p-recoil;0.007-1.262 MeV) Kr83a(^{3}He;0.0-1.15 MeV) Kr83a(TOF;0.0-0.03 MeV) Y82(TOF;0.0-0.1 MeV) **Ru81**(^{3}He;0.0-1.2 MeV) **Oh81**(^{3}He;0.0-1.8 MeV) Re80(^{3}He;0.0-1.4 MeV) Kr79(^{3}He;0.0-1.2 MeV) Ru77a(^{3}He;0.05-1.6 MeV)
^{96}Rb	0.204	5.89(W83)	**Gr85**(p-recoil;0.008-1.262 MeV) Y82(TOF;0.0-0.1 MeV) **Kr83**(^{3}He;0.0-2.22 MeV) **Ru81**(^{3}He;0.0-1.55 MeV)[a] Oh81(^{3}He;0.0-1.5 MeV) Kr79(^{3}He;0.0-1.5 MeV)

APPENDIX D (Continued)

Precursor ID	Half-life (sec)	Energy Window* ($Q_\beta - S(n)$) MeV	Spectra References
^{97}Rb	0.17	6.54(W83)	**Gr85**(p-recoil;0.007-1.262 MeV) Kr83a(^{3}He;0.0-1.6 MeV) Kr83(^{3}He;0.0-2.11 MeV) Y82(TOF;0.0-0.1) **Ru81**(^{3}He;0.0-2.0 MeV)[a] **Oh81**(^{3}He;0.0-1.5 MeV)[d] Kr79(^{3}He;0.0-2.0 MeV)
^{98}Rb	0.11	6.67(W83)	**Kr83**(^{3}He;0.0-2.45 MeV) **Ru81**(^{3}He;0.0-2.0 MeV)[a] Kr79(^{3}He;0.0-2.0 MeV)
^{129}In	0.99	2.21(W83)	**Ru81**(^{3}He;0.06-1.62 MeV) Ru77a(^{3}He;0.1-1.48 MeV)
^{130}In	0.58	2.57(W83)	**Ru81**(^{3}He;0.08-1.62 MeV) Ru77a(^{3}He;0.1-1.3 MeV)
^{134}Sn	1.04	3.834(MN/W81)	**Ru81**(^{3}He;0.08-1.62 MeV) Sh74(^{3}He;0.1-1.4 MeV)
^{135}Sb	1.82	4.03(W83)	**Ru81**(^{3}He;0.08-2.0 MeV) Kr79a(^{3}He;0.05-2.0 MeV) Sh74(^{3}He;0.1-1.6 MeV) **Fr74**(^{3}He;0.09-2.1 MeV)[d]
^{136}Te	19.0	1.34(W83)	**Ru81**(^{3}He;0.06-1.8 MeV) Ru74a(^{3}He;0.05-1.1 MeV) Sh74(^{3}He;0.1-1.1 MeV)
^{137}I	24.5	1.86(W83)	**Ru81**(^{3}He;0.0-1.75 MeV) **Oh81**(^{3}He;0.05-1.7 MeV)[d] Kr79(^{3}He;0.0-1.7 MeV) Kr79a(^{3}He;0.0-1.7 MeV) Fr77(^{3}He;0.0-1.4 MeV) Ru74a(^{3}He;0.05-1.3 MeV) Sh74(^{3}He;0.1-1.6 MeV) Sh72(^{3}He;0.1-1.5 MeV)
^{138}I	6.5	2.0(W83)	**Ru81**(^{3}He;0.07-1.67 MeV) **Oh81**(^{3}He;0.0-1.6 MeV)[d] Sh77(^{3}He;0.1-1.6 MeV)
^{139}I	2.38	3.18(W83)	**Ru81**(^{3}He;0.06-1.61 MeV) Ru74(^{3}He;0.1-1.6 MeV)

APPENDIX D (Continued)

Precursor ID	Half-life (sec)	Energy Window* ($Q_\beta - S(n)$) MeV	Spectra References
^{140}I	0.86	4.575(MN/W81)	**Ru81**(^{3}He;0.08-1.75 MeV) Sh77(^{3}He;0.1-1.3 MeV)
^{141}I	0.46	5.475(MN/W81)	**Ru81**(^{3}He;0.08-1.7 MeV) Ru74(^{3}He;0.1-1.25 MeV)[e]
^{141}Cs	24.9	0.708(W83)	**MnAR77**(^{3}He;0.0-0.7 MeV)[d]
^{142}Cs	1.69	1.11(W83)	**Ru81**(^{3}He;0.08-1.04 MeV) Sh77(^{3}He;0.1-1.0 MeV)[f] **MnAR77**(^{3}He;0.0-0.93 MeV)[d]
^{143}Cs	1.78	2.04(W83)	**Gr85**(p-recoil;0.01-1.262 MeV) **Ru81**(^{3}He;0.08-1.3 MeV) Re80(^{3}He;0.0-1.4 MeV) **MnAR77**(^{3}He;0.0-1.1 MeV)[d] Ru74(^{3}He;0.1-1.3 MeV)
^{144}Cs	1.001	2.59(W83)	**Gr85**(p-recoil;0.01-1.262 MeV) **Ru81**(^{3}He;0.05-1.45 MeV) **MnAR77**(^{3}He;0.0-1.2 MeV)[d] Sh77(^{3}He;0.1-1.3 MeV)
^{145}Cs	0.59	3.56(W83)	**Gr85**(p-recoil;0.008-1.262 MeV) **MnAR77**(^{3}He;0.0-1.1 MeV)[d]
^{146}Cs	0.34	4.28(W83)	**MnAR77**(^{3}He;0.0-1.3 MeV)[d]
^{147}Cs	0.546	4.64(W83)	**MnAR78**(^{3}He;0.0-1.8 MeV)[d]

NOTES:

*The notation in parenthesis indicates the source of the nuclide masses used to calculate the energy window.

W83 Wapstra 1983, Ref. 72
MN Moller-Nix, Ref. 73
W81 Wapstra 1981, Ref. 113

[a]Not measured by Studsvik, data taken from Mainz group.

[b]Actual measurement of group one spectrum.

[c]Data reported for a mixture ^{87}Br and ^{88}Br.

[d]An additional Mainz spectrum taken directly from quoted reference (data obtained by Mainz group).

[e]Data reported for a mixture 141 (I + Cs).

[f]Data reported for a mixture 142(Xe + Cs).

References for Appendix D

Ru81 Rudstam, G., personal communication (1981), see also: Rudstam, G., *Nucl. Sci. Eng.*, **80**, 238-255 (1982); Rudstam, G., *J. Radioanal. Chem.*, **36**, 591-618 (1977).

Ru77 Rudstam, G. and Lund, E. *Nucl. Sci. Eng.*, **64**, 749-760 (1977).

Kr79a Kratz, K. -L., Rudolph, W., Ohm, H., Franz, H., Zendel, M. Herrmann, G., Prussin, S. G., Nuh, F. M., Shihab-Eldin, A. A., Slaughter, D. R., Halverson, W., and Klapdor, H. V., *Nucl. Phys.*, **A317**, 335-362 (1979).

Fr74 Franz, H., Kratz, J.-V., Kratz, K.-L., Rudolph, W., Herrmann, G., Nuh, F. M., Prussin, S. G., and Shihab-Eldin, A. A., *Phys. Rev. Lett.*, **33**, 859-862 (1974).

Kr83 Kratz, K.-L., personal communication (1983).

Sh74 Shalev, S., and Rudstam, G., *Nucl. Phys.*, **A230**, 153-172 (1974).

Ew84 Ewan, G. T., Hoff, P., Jonson, B., Kratz, K.-L., Larson, P. O., Nyman, G., Ravin, H. L., and Ziegert, W., *Z. Phys.*, **A318**, 309-314 (1984).

Kr79 Kratz, K.-L., "Review of Delayed Neutron Energy Spectra", *Proceedings of the Consultant's Meeting on Delayed Neutron Properties*, Vienna, 26-30 March 1979, pp.103-182, INDC(NDS)-107/G+Special, August 1979.

Ch71 Chrysochides, N. G., Anoussis, J. N., Mitsonias, C. A., and Perricos, D. C., *J. of Nucl. Energy*, **25**, 551-556 (1971).

Ba56 Batchelor, R., and McK. Hyder, H. R., *J. Nucl. Energy*, **3**, 7-17 (1956).

Fi72 Fieg, G., *J. Nucl. Energy*, **26**, 585-592 (1972).

Ru74a Rudstam, G., Shalev, S., and Jonson, O. C., *Nucl. Instr. Meth.*, **120**, 333-344 (1974).

Ru74 Rudstam, G., and Shalev, S., *Nucl. Phys.*, **A235**, 397-409 (1974).

Sh77 Shalev, S., and Rudstam, G., *Nucl. Phys.*, **A275**, 76-92 (1977).

Gr85 Greenwood, R. C., and Caffrey, A. J., *Nucl. Sci. and Engr.*, **91**, 305-323 (1985).

Kr83a Kratz, K.-L., Ohm, H., Schroder, A., Gablemann, H., Ziegert, W., Pfiefer, B., Jung, G., Monnand, E., Pinston, J. A., Schussler, F., Crawford, G. I., Prussin, S. G., and de Oliveira, Z. M., *Z. Phys.*, **A312**, 33-57 (1983).

Re80 Reeder, P. L., Alquist, L. J., Kiefer, R. L., Ruddy, F. H., andWarner, R. A., *Nucl. Sci. and Engr.*, **75**, 140-150 (1980).

Oh81 Ohm, Henner, "Statistiche und Nichtstatistische Effekte bei der Emission β-verzogerter Neutronen; Untersuchung des Zerfalls der Nuklide ^{137,138}J und $^{93-97}$Rb", doctoral dissertation der Johannes-Gutenberg-Universitat in Mainz (1981).

Fr77 Franz, H., Rudolph, W., Ohm, H., Kratz, K.-L., Herrmann, G., Nuh, F. M., Slaughter, D. R. and Prussin, S. G., *Nucl. Instr. and Methods*, **144**, 253-261 (1977).

Sh72 Shalev, S., and Rudstam, G., *Phys. Rev. Lett.*, **28**, 687-690 (1972).

Y82 Yeh, T. R. et al., *International Conference on Nuclear Data for Science and Technology*, 6-10 Sept. 1982, Antwerp, (1983), p. 261; see also Yeh, T. R. et al. *Bull. Am. Phys. Soc.*, **27**, 498 (1982).

MnAR77 University of Mainz Institute Für Kernphysik 1977 Annual Report (1977).

MnAR78 University of Mainz Institute Für Kernphysik 1978 Annual Report (1978).

APPENDIX E

SIX-GROUP PARAMETERS

TABLE E-I

Keepin Recommended Six-Group Parameters (Ref. 3)

Fission Nuclide		Group 1	2	3	4	5	6
^{235}U(F)	a_i	.038 ±.003	.213 ±.005	.188±.016	.407±.007	.128±.008	.026±.003
	λ_i	.0127±.0002	.0317±.0008	.115±.003	.311±.008	1.40 ±.081	3.87 ±.369
^{238}U(F)	a_i	.013 ±.001	.137 ±.002	.162±.020	.388±.012	.225±.013	.075±.005
	λ_i	.0132±.0003	.0321±.006	.139±.005	.358±.014	1.41 ±.067	4.02 ±.214
^{233}U(F)	a_i	.086 ±.003	.274 ±.005	.227±.035	.317±.011	.073±.014	.023±.007
	λ_i	.0126±.0004	.0334±.0014	.131±.005	.302±.024	1.27 ±.266	3.13 ±.675
^{239}Pu(F)	a_i	.038 ±.003	.28 ±.004	.216±.018	.328±.01	.103±.009	.035±.005
	λ_i	.0129±.0002	.0311±.0005	.134±.003	.331±.012	1.26 ±.115	3.21 ±.255
^{240}Pu(F)	a_i	.028 ±.003	.273 ±.004	.192±.053	.350±.02	.128±.018	.029±.006
	λ_i	.0129±.0004	.0313±.0005	.135±.011	.333±.031	1.36 ±.205	4.04 ±.782
^{232}Th(F)	a_i	.034 ±.002	.150 ±.005	.155±.021	.446±.015	.172±.013	.043±.006
	λ_i	.0124±.0002	.0334±.0011	.121±.005	.321±.011	1.21 ±.090	3.29 ±.297
^{235}U(T)	a_i	.033 ±.003	.219 ±.009	.196±.022	.395±.011	.115±.009	.042±.008
	λ_i	.0124±.0003	.0305±.0010	.111±.004	.301±.011	1.14 ±.15	3.01 ±.29
^{239}Pu(T)	a_i	.035 ±.009	.298 ±.035	.211±.048	.326±.033	.086±.029	.044±.016
	λ_i	.0128±.0005	.0301±.0022	.124±.009	.325±.036	1.12 ±.39	2.69 ±.48
^{233}U(T)	a_i	.086 ±.003	.299 ±.004	.252±.040	.278±.020	.051±.024	0.034±.014
	λ_i	.0126±.0003	.0337±.0006	.139±.006	.325±.030	1.13 ±.40	2.50 ±.42

TABLE E-II

ENDF/B-V Six-Group Parameters (Ref. 5)

Fission Nuclide		Group 1	2	3	4	5	6
^{232}Th	a_i	0.0340	0.150	0.155	0.446	0.172	0.043
	λ_i	0.01237	0.03340	0.121	0.321	1.21	3.29
^{233}U	a_i	0.086	0.274	0.227	0.317	0.073	0.023
	λ_i	0.01258	0.03342	0.131	0.303	1.27	3.14
^{235}I	a_i	0.038	0.213	0.213	0.188	0.128	0.026
	λ_i	0.01272	0.03174	0.116	0.311	1.40	3.87
^{238}U	a_i	0.013	0.127	0.162	0.388	0.225	0.075
	λ_i	0.01323	0.03212	0.139	0.359	1.41	4.03
^{239}Pu	a_i	0.038	0.280	0.216	0.328	0.103	0.035
	λ_i	0.0129	0.0311	0.134	0.332	1.26	3.21
^{240}Pu	a_i	0.028	0.273	0.192	0.35	0.128	0.029
	λ_i	0.01294	0.03131	0.135	0.333	1.36	4.03
^{241}Pu	a_i	0.010	0.229	0.173	0.390	0.182	0.016
	λ_i	0.01280	0.0299	0.124	0.352	1.61	3.47

TABLE E-V

England Six-Group Abundances (Ref. 28)

Fission Nuclide	Group					
	1	2	3	4	5	6
^{232}Th(F)	0.0354	0.1748	0.1880	0.4125	0.1281	0.0611
^{232}Th(H)	0.0351	0.1451	0.1726	0.4637	0.1007	0.0828
^{233}U(T)	0.0645	0.2714	0.2222	0.3467	0.0762	0.0190
^{233}U(F)	0.0742	0.2776	0.2292	0.3061	0.0971	0.0157
^{233}U(H)	0.0650	0.2314	0.2408	0.3358	0.1098	0.0172
^{235}U(T)	0.0288	0.2198	0.1786	0.3838	0.1335	0.0555
^{235}U(F)	0.0272	0.2113	0.1973	0.3804	0.1432	0.0405
^{235}U(H)	0.0414	0.2189	0.2246	0.3664	0.1237	0.0250
^{236}U(F)	0.0227	0.2013	0.1770	0.3997	0.1559	0.0433
^{238}U(F)	0.0106	0.1547	0.1524	0.4327	0.1897	0.0599
^{238}U(H)	0.0144	0.1343	0.1413	0.4390	0.1960	0.0750
^{237}Np(F)	0.0283	0.2344	0.1711	0.3806	0.1563	0.0293
^{239}Pu(T)	0.0229	0.2850	0.1750	0.3583	0.1405	0.0183
^{239}Pu(F)	0.0264	0.2556	0.1870	0.3515	0.1566	0.0228
^{239}Pu(H)	0.0569	0.2134	0.2088	0.3416	0.1627	0.0166
^{240}Pu(F)	0.0218	0.2615	0.1615	0.3727	0.1517	0.0309
^{241}Pu(T)	0.0105	0.2282	0.1346	0.4328	0.1493	0.0446
^{241}Pu(F)	0.0112	0.2295	0.1444	0.4132	0.1618	0.0399
^{242}Pu(F)	0.0135	0.2424	0.1464	0.3963	0.1565	0.0449

TABLE E-VI

Normalized Waldo Recommended Six-Group Parameters (Ref. 18)

Fission Nuclide		Group 1	2	3	4	5	6
^{232}Th	a_i	.0035 ±.0024	.1546 ±.0078	.1598± .0224	.4606±.0222	.1772± .0152	.0442± .0065
	λ_i	.0124 ±.002	.0334 ±.0011	.121 ± .005	.321 ±.011	1.21 ± .090	3.29 ± .30
^{232}U	a_i	.1198 ±.0091	.2995 ±.0229	.3064± .032	.2583±.0274	.0160± .0892*	
	λ_i	.01276±.00004	.03502±.00029	.1439± .0059	.396 ±.045	1.35*	
^{233}U	a_i	.0865 ±.0041	.2986 ±.0135	.2514± .0405	.2784±.0243	.0514± .0243	.0338± .0135
	λ_i	.0126 ±.0003	.0337 ±.0006	.139 ± .006	.325 ±.030	1.13 ± .40	2.50 ± .42
^{235}U	a_i	.0329 ±.003	.2190 ±.0227	.1963± .0227	.395 ±.016	.1149± .0096	.0419± .0048
	λ_i	.0127 ±.0003	.0317 ±.0012	.115 ± .004	.311 ±.012	1.40 ± .12	3.87 ± .55
^{238}U	a_i	.0130 ±.0009	.1371 ±.0020	.1621± .0201	.3879±.0113	.2255± .0135	.0744± .0045
	λ_i	.0132 ±.0003	.0321 ±.006	.139 ± .005	.358 ±.014	1.41 ± .07	4.02 ± .21
^{237}Np	a_i	.0348 ±.0032	.2302 ±.0226	.0660± .0311	.1444±.0613	.4001± .0500	.1245± .0292
	λ_i	.01258±.00004	.0306 ±.00034	.0653± .016	.139 ±.019	.328 ± .030	1.62 ± .69
^{238}Pu	a_i	.0426 ±.0067	.3074 ±.0476	.1143± .0671	.1764±.0281	.3268± .0519	.0325± .1885*
	λ_i	.01262±.00013	.03026±.00035	.0851± .012	.197 ±.023	.345 ± .051	1.35*
^{239}Pu	a_i	.0342 ±.0093	.2981 ±.0373	.2112± .0497	.3261±.0357	.0854± .0295	.0450± .0171
	λ_i	.0128 ±.0005	.0301 ±.0022	.124 ± .009	.325 ±.036	1.12 ± .39	2.69 ± .48
^{240}Pu	a_i	.0249 ±.0034	.2689 ±.0181	.1830± .0497	.3559±.0305	.1345± .0203	.0328± .0068
	λ_i	.0129 ±.0003	.0313 ±.0005	.135 ± .11	.333 ±.030	1.36 ± .20	4.03 ± .77
^{241}Pu	a_i	.0099 ±.003	.2276 ±.0057	.1779± .0249	.3876±.0497	.1811± .0191	.0159± .0057
	λ_i	.0128 ±.0002	.0299 ±.0006	.124 ± .013	.352 ±.018	1.61 ± .15	3.47 ±1.70
^{242}Pu	a_i	.0112 ±.0014	.1608 ±.0529	.0313± .0493	.1638±.0153	.3668± .0361	.2661± .086
	λ_i	.0134 ±.00027	.0295 ±.0015	.0409± .014	.127 ±.0056	.397 ± .033	2.22 ± .87
^{241}Am	a_i	.0364 ±.0043	.2891 ±.0354	.3029± .0374	.3029±.0374	.0708± .0944	
	λ_i	.01271±.00003	.02985±.00004	.152 ± .003	.446 ±.022	2.63 ±2.11	
^{241m}Am	a_i	.0256 ±.00174	.2835 ±.01890	.1195± .0134	.3548±.0378	.173 ± .0189	.0436± .0654*
	λ_i	.01273±.0005	.030 ±.00011	.093 ± .0054	.2462±.0067	.656 ± .083	1.35*
^{245}Cm	a_i	.02359±.0152	.3027 ±.0203	.0912± .0287	.2938±.0523	.2296± .027*	.0591 .09455
	λ_i	.01335±.00009	.03031±.00014	.104 ± .014	.211 ±.011	.537 ± .073	1.35*
^{249}Cf	a_i	.02867±.00210	.3536 ±.0259	.3823± .0322	.2354±.0259		
	λ_i	.01285±.00002	.03037±.00004	.1678± .0037	.541 ±.063		
^{252}Cf(S)	a_i	.2558 ±.0116	.3372 ±.081	.407 ± .116			
	λ_i	.0347 ±.0009	.35 ±.07	1.4 ±1.1			

*Value is assumed.

APPENDIX F

EXPLICIT REACTOR KINETICS EQUATIONS

DERIVATION OF MODIFIED POINT REACTOR KINETICS EQUATIONS

In this appendix, a system of equations describing the neutron flux in a reactor including delayed neutron precursors and their parents is derived. The rate of change in neutron concentration may be written as

$$\frac{1}{\mathrm{v}}\frac{d\phi}{dt} = \text{PRODUCTION} - \text{LOSSES} \qquad (\mathrm{F}-1)$$

PRODUCTION = prompt n from fission + delayed neutrons from decay of a precursor

$$= (1-\beta)\nu\Sigma_f\phi(\vec{r},t) + \sum_{\text{all } i} P_n^i\lambda_i C_i(\vec{r},t) \qquad (\mathrm{F}-2)$$

$C_i(\vec{r},t)$ = precursor isotope concentration, number of precursors of type i per cm^3 at time t

P_n^i = probability of delayed neutron emission by precursor i

λ_i = decay constant for precursor i

$\lambda_i C_i(\vec{r},t)$ = rate of decay of i^{th} precursors

$P_n^i\lambda_i C_i(\vec{r},t)$ = rate of production of delayed neutrons from precursor i

LOSSES = leakage + absorption

$$= -D\nabla^2\phi + \Sigma_a\phi(\vec{r},t)) \qquad (\mathrm{F}-3)$$

Substituting Eqs. (F-2) and (F-3) into Eq. (F-1) gives

$$\frac{1}{\mathrm{v}}\frac{d\phi}{dt} = (1-\beta)\nu\Sigma_f\phi(\vec{r},t) + \sum_{\text{all } i} P_n^i\lambda_i C_i(\vec{r},t) + D\nabla^2\phi - \Sigma_a\phi(\vec{r},t)\ . \qquad (\mathrm{F}-4)$$

Recall $(1-\beta)\nu = \bar{\nu}_p$, therefore

$$\frac{1}{\mathrm{v}}\frac{d\phi}{dt} = \bar{\nu}_p\Sigma_f\phi(\vec{r},t) + \sum_{\text{all } i} P_n^i\lambda_i C_i(\vec{r},t) + D\nabla^2\phi - \Sigma_a\phi(\vec{r},t) \qquad (\mathrm{F}-5)$$

The rate of change in precursor (or parent) concentration is defined as

$$\text{time rate of change in concentration of precursor i (or parent)} \Rightarrow \frac{dC_i}{dt} = \text{PRODUCTION} + \text{LOSSES} \ .$$

Assuming the precursor does not diffuse (leak) from the system before decay,

$$\text{LOSSES} = \lambda_i C_i(\vec{r},t) \ . \qquad (\text{F}-6)$$

There are two mechanisms for production: (1) fission, and (2) decay of parent (may or may not be a delayed neutron precursor). The latter necessitates the inclusion of a production equation for not only precursor nuclides but also any parent nuclide. Production from fission for either a precursor or its parent may be represented as $y_i \Sigma_f \phi(\vec{r},t)$ which is the rate nuclide i is produced from fission/cm^3, where y_i fission yield of nuclide i.

Given that BF_{j-i} defines the branching fraction for the production of nuclide i from nuclide j, the production of precursor i from the decay of any nuclide j may be written as

$$BF_{j-i}\lambda_j C_j(\vec{r},t) \ . \qquad (\text{F}-7)$$

Therefore, the production of precursor i may be represented as

$$\text{PRODUCTION} \ = y_i \Sigma_f \phi(\vec{r},t) + \sum_j BF_{j-i}\lambda_j C_j(\vec{r},t) - \lambda_i C_i(\vec{r},t) \ . \qquad (\text{F}-8)$$

This gives

$$\frac{dC_i(\vec{r},t)}{dt} = y_i \Sigma_f \phi(\vec{r},t) + \sum_j BF_{j-i}\lambda_j C_j(\vec{r},t) - \lambda_i C_i(\vec{r},t) \ . \qquad (\text{F}-9)$$

Writing the flux and precursor concentrations as separable functions of space and time;

$$\phi(\vec{r},t) = \text{v}n(t)\psi_1(\vec{r}) \ , \qquad (\text{F}-10)$$

$$\text{and} \quad C_i(\vec{r},t) = C_i(t)\psi_1(\vec{r}) \ . \qquad (\text{F}-11)$$

The shape function, $\psi_i(\vec{r})$, is the fundamental mode of the Helmholtz equation:

$$\nabla^2\psi_n + B_n^2\psi_n(\vec{r}) = 0 \qquad (F-12)$$

$$\lambda_n = \mathrm{v}DB_n^2 + \mathrm{v}\Sigma_a - \mathrm{v}\nu\Sigma_f \ . \qquad (F-13)$$

Substituting Eqns. (F-10) and (F-11) into (F-5) and (F-6) and noting that

$$\frac{d\phi(\vec{r},t)}{dt} = \mathrm{v}\frac{dn}{dt}\psi_1(\vec{r}) \ ,$$
$$\frac{dC_i(\vec{r},t)}{dt} = \frac{dC_i}{dt}\psi_1(\vec{r}) \ ,$$

and

$$\nabla^2\phi(r,t) = \mathrm{v}n(t)\nabla^2\psi_1(\vec{r}) = \mathrm{v}n(t)B_1^2\phi_1(r) \text{ (from Helmholtz equation)}, \qquad (F-14)$$

yields

$$\frac{dn}{dt} = \nu_p\Sigma_f\,\mathrm{v}n(t) + \sum_{\text{all } i} P_n^i\lambda_i C_i(t) - DB_1^2 vn(t) - \Sigma_a \mathrm{v}n(t) \ . \qquad (F-15)$$

The details of the substitution and reduction of Eq. (F-5) to Eq. (F-14) may be seen in rewriting (F-6) as

$$a = b + \mathrm{c} + d - e \qquad (F-16)$$

and solving each term separately.

$$a = \frac{1}{\mathrm{v}}\frac{d\phi}{dt} = \frac{1}{v}\mathrm{v}\psi_1(\vec{r})\frac{d(t)}{dt} = \psi_1\frac{dn}{dt}$$
$$\bar{\nu}_p = (1-\beta)\nu$$
$$b = (1-\beta)\nu\Sigma_f\phi(\vec{r},t) = (1-\beta)\nu\Sigma_f\mathrm{v}\psi_1(\vec{r})n(t)$$
$$c = \sum P_n^i\lambda_i C_i(\vec{r},t) = \sum P_n^i\lambda_i C_i(t)\psi_1(\vec{r})$$
$$D\nabla^2\phi$$

$$\nabla^2\phi(\vec{r},t) = \mathrm{v}n(t)\nabla^2\psi_1(\vec{r})$$

$$\nabla^2\psi_1(\vec{r}) + B_1^2\psi_1(\vec{r}) = 0$$

$$\nabla^2\psi_1(\vec{r}) = -B_1^2\psi_1(\vec{r})$$

$$d = D\nabla^2\phi = -\mathrm{v}n(t)DB_1^2\psi_1(\vec{r})$$

$$e = \Sigma_a\phi(\vec{r},t) = \Sigma_a\mathrm{v}n(t)\psi(\vec{r})$$

Recombining terms yields

$$\frac{dn}{dt} = (1-\beta)\nu\Sigma_f\mathrm{v}n(t) + \sum P_n^i\lambda_i C_1(t) - DB_1^2\mathrm{v}n(t) - \mathrm{v}\Sigma_a n(t) \qquad (\mathrm{F}-17)$$

Simplifying

$$\begin{aligned}\frac{dn}{dt} &= \bar{\nu}_p\Sigma_f\mathrm{v}n(t) + \sum P_n^i\lambda_i C_i(t) - DB_1^2\mathrm{v}n(t) - \Sigma_a\mathrm{v}n(t)\ , \\ &= (\bar{\nu}_p\Sigma_f - \Sigma_a - DB_1^2)n(t)\mathrm{v} + \sum P_n^i\lambda_i C_i(t)\ , \\ &= \mathrm{v}\Sigma_a(\bar{\nu}_p\Sigma_f/\Sigma_a - 1 - L^2B^2)n(t) + \sum P_n^i\lambda_i C_i(t)\end{aligned} \qquad (\mathrm{F}-18)$$

where $L^2 = D/\Sigma_a$

$$\frac{dn}{dt} = \mathrm{v}\Sigma_a\left(\bar{\nu}_p\Sigma_f/\Sigma_a - 1 - L^2B^2\right)\frac{(1+L^2B^2)}{(1+L^2B^2)}n(t) + \sum P_n^i\lambda_i C_i(t)\ .$$

Recall

$$\ell = \left[\mathrm{v}\Sigma_a(1+L^2B^2)\right]^{-1} \quad \text{is the mean lifetime of a reactor neutron}$$

Therefore

$$\frac{dn}{dt} = \frac{1}{\ell}\left(\frac{\bar{\nu}_p\Sigma_f/\Sigma_a - 1 - L^2B^2}{1+L^2B^2}\right)n(t) + \sum P_n^i\lambda_i C_i(t)\ .$$

Simplifying and substituting

$$\bar{\nu}_p = (1-\beta)\nu\ ,$$

yields

$$\frac{dn}{dt} = \frac{1}{\ell}\left(\frac{(1-\beta)\nu\Sigma_f/\Sigma_a}{1+L^2B^2} - 1\right) n(t) + \sum P_n^i \lambda_i C_i(t) \ .$$

Recall that

$$\nu\Sigma_f/\Sigma_a = \nu f = k_\infty$$

where f is the thermal utilization factor.

$$\text{Now } \frac{dn}{dt} = \frac{1}{\ell}\left(\frac{k_\infty(1-\beta)}{1+L^2B^2} - 1\right) n(t) + \sum P_n^i \lambda_i C_i(t) \ ,$$

and using

$$\frac{k_\infty}{1+L^2B^2} = k \ ,$$

gives

$$\frac{dn}{dt} = \frac{k(1-\beta)-1}{\ell} n(t) + \sum P_n^i \lambda_i C_i(t) \ . \qquad (\text{F}-19)$$

Substituting Eqns. (F-10) and (F-11) into Eqn. (F-9)

$$\frac{dC_i}{dt}\psi_1(\vec{r}) = y_i\Sigma_f \nu n(t)\psi_1(\vec{r}) + \sum_j BF_{j-i}\lambda_j C_j(t)\psi_1(\vec{r}) - \lambda_i C_i(t)\psi_1(\vec{r})$$

$$\frac{dC_i}{dt} = y_i\Sigma_f \nu n(t) + \sum_j BF_{j-i}\lambda_j C_j(t) - \lambda_i C_i \ . \qquad (\text{F}-20)$$

Again recalling that

$$\ell = \frac{1}{\nu\Sigma_a(1+L^2B^2)} \ ,$$

$$k = \frac{\nu\sum_f/\Sigma_a}{1+L^2B^2} \ , \text{ and}$$

$$\frac{k}{\ell} = \nu v \Sigma_f$$

gives

$$\frac{dC_i}{dt} = \frac{y_i}{\nu}\frac{k}{\ell} n(t) + \sum_j BF_{j-i}\lambda_j C_j(t) - \lambda_i C_i(t) \qquad (\text{F}-21)$$

Now define $\Lambda = \frac{\ell}{k}$ mean generation time between birth of a neutron and subsequent absorption inducing fission.

$$\frac{dn}{dt} = \left[\frac{1-\beta-\frac{1}{k}}{\Lambda}\right] n(t) + \sum_{\text{all } i} P_n^i \lambda_i C_i(t)$$

$$\frac{dC_i}{dt} = \frac{y_i}{\nu\Lambda} n(t) + \sum_j BF_{j-i}\lambda_j C_j(t) - \lambda_i C_i(t)$$

Recall the definition of reactivity

$$\rho(t) = \frac{k(t)-1}{k(t)} = 1 - \frac{1}{k} \ .$$

Therefore

$$\frac{dn}{dt} = \left[\frac{\rho(t)-\beta}{\Lambda}\right] n(t) + \sum_{\text{all } i} P_n^j \lambda_i C_i(t) \ , \qquad (\text{F}-22)$$

and

$$\frac{dC_i}{dt} = \frac{y_i}{\nu\Lambda} \ n(t) + \sum_j BF_{j-i}\lambda_j C_j(t) - \lambda_i C_i(t) \qquad (\text{F}-23)$$

are the resultant point kinetics equations using each individual precursor physically grouping delayed neutron precursors as given in Chapter 8.
Recall:

λ_i	–	decay constant for isotope i
P_n^i	–	probability of decayed neutron emission by precursor i
y_i	–	yield per fission of nuclide i
β	–	total delayed neutron fraction
Λ	–	mean generation time
BF_{j-i}	–	branching fraction for the production of nuclide i from nuclide j.

VITA

Michaele Clarice Brady was born at [redacted]

Ms. Brady completed her high school education at Seymour Rural High School, Seymour, Texas, in May 1977. She received a Bachelor of Science degree in Nuclear Engineering from Texas A&M University in May 1981. In December 1982 she earned a Master of Science degree in Nuclear Engineering also from Texas A&M. The title of her Master's thesis was "Radiation Field Measurements in the TAMU Nuclear Science Center Irradiation Cell."

After completing coursework for the degree of Doctor of Philosophy, Ms. Brady received an appointment in the Associated Western Universities Laboratory Participant Program to perform her doctoral research at Los Alamos National Laboratory (LANL). Her research in the area of delayed neutron data under the guidance of Dr. T. R. England of LANL and Dr. T. A. Parish of Texas A&M resulted in her Ph.D. dissertation entitled "Evaluation and Application of Delayed Neutron Precursor Data." Ms. Brady will receive the degree of Doctor of Philosophy in Nuclear Engineering from TAMU in December 1988.

Her areas of interest in the field of nuclear engineering include reactor fuel cycles, radiation shielding, reactor physics and nuclear data. Ms. Brady is currently employed by Martin Marietta Energy Systems, Inc., as a staff member in the Nuclear Engineering Applications Department at Oak Ridge National Laboratory. She may be reached at Oak Ridge National Laboratory, P. O. Box 2008, Oak Ridge, TN 37831-6370.

☆ U.S. GOVERNMENT PRINTING OFFICE: 1989-673-034/00114